



Chemical Characterization and Biological Activity of African Propolis

A Thesis Presented for the Degree of Doctor of Philosophy

Strathclyde Institute of Pharmacy and Biomedical Sciences

BY

Ruwida Mansour Elsnini

2016

DECLARATION

‘This thesis is the result of the author’s original research. It has been composed by the author and has not been previously submitted for examination which has led to the award of a degree.’

‘The copyright of this thesis belongs to the author under the terms of the United Kingdom Copyright Acts as qualified by University of Strathclyde Regulation 3.50. Due acknowledgement must always be made of the use of any material contained in, or derived from, this thesis.’

Signed:

DEDICATION

I dedicate this work to my beloved husband Ali gneiber, my lovely kids, mohamed ,Lamar, abdallah and dania, and my wonderful dad and mum in appreciation of their support and sacrifice in this accomplishment.

ACKNOWLEDGMENTS

My infinite appreciation and thanks goes to my supervisor Dr Dave Watson for his invaluable guidance and support, and endless effort in this project.

I offer my heartfelt thanks also to my second supervisor, Dr RuAn Edrada-Ebel, and to Dr Tong Zhang, Dr Carol Clements, and Dr Harry de Koning for their guidance and support.

I would like to express my sincere thanks to Prof. Alexander Gray and Dr John Igoli for their help with NMR experiments.

I am grateful to Mohamed Al Washih, Jonans Tusiimiri, Weam Elsihiri, and all my colleagues for their support and useful time as we shared experiences and information.

I want to express my gratitude to all my sisters Darren, Rania and Rehab, brothers Mohamed and Yousef, and my family in-law for their endless love.

Not to forget my lovely friends who made me feel at home in Glasgow Roua, Reza, my soul-mate Eman, Jehan, Salha, Ekram, Zena, Tagreed, Dima, Ahlam and Gzwa.

Finally, I would like to thank the Libyan embassy and Institute of Higher education in Libya for offering me a scholarship to pursue my studies at the University of Strathclyde.

TABLE OF CONTENTS

DECLARATION	i
DEDICATION	ii
ACKNOWLEDGMENTS	iii
TABLE OF CONTENTS	iv
LIST OF TABLES	ix
LIST OF FIGURES	xii
LIST OF ABBREVIATIONS	xvii
ABSTRACT	xx
PUBLISHED WORK FROM THIS RESEARCH	xxiii
1 GENERAL INTRODUCTION.....	2
1.1 Propolis.....	2
1.1.1 Origin	3
1.1.2 History.....	3
1.1.3 Physical characteristics of propolis.....	5
1.1.4 Chemical composition and how it is affected by geographic region	7
1.1.5 Pharmacological action, biological properties and toxicity of propolis	
18	
1.1.6 Bee Species and Propolis	24
1.2 Trypanosomes	26
1.2.1 Definition	26
1.2.2 Epidemiology of the disease	28
1.2.3 Treatment of Human African Trypanosomiasis (HAT).....	30
1.2.4 Previous studies on activity of propolis against Trypanosomiasis.....	38
1.3 Techniques used in propolis analysis	40
1.3.1 Introduction.....	40

1.3.2	Medium pressure liquid chromatography (MPLC).....	42
1.3.3	Gas chromatography with mass spectroscopy detection (GC-MS)	45
1.3.4	High performance liquid chromatography (HPLC)	47
1.3.5	Nuclear magnetic resonance (NMR) techniques.....	57
1.3.6	Data analysis	61
1.4	Aims of the study	63
2	MATERIALS AND GENERAL METHODS	65
2.1	General	65
2.1.1	Chemicals and reagents.....	65
2.1.2	Laboratory equipment and tools	65
2.1.3	Propolis sample collection and preparation	66
2.2	Extraction of propolis	66
2.3	General profiling of propolis samples.	68
2.3.1	High-performance liquid chromatography coupled with Ultraviolet detector and Evaporative Light Scattering Detector (HPLC-UV-ELSD).	68
2.3.2	High-performance liquid chromatography coupled with High- resolution Mass Spectrometry (LC-HRMS).....	69
2.3.3	Gas chromatography (GC-MS).....	71
2.3.4	NMR Methods.....	72
2.4	Fractionation work and isolation of compounds	72
2.4.1	Silica gel chromatography.....	72
2.4.2	Grace Reveleris® system.....	74
2.4.3	Gilson semi-preparative chromatography system.....	75
2.5	Identification of compounds.....	75
2.5.1	NMR spectroscopy.....	75
2.5.2	LC-MS ⁿ	76

2.5.3	Measurement of Optical Rotation	76
2.5.4	Melting point.....	77
2.6	Bioassay.....	77
2.6.1	In vitro trypanocidal bioassay	77
2.6.2	Screening against <i>Crithidia fasciculata</i>	79
3	CHEMICAL AND BIOLOGICAL PROFILING OF NIGERIAN PROPOLIS	
	SAMPLES.....	82
3.1	Introduction	82
3.2	Origin of the samples.	82
3.3	General biological screening of Nigerian propolis samples against <i>Trypanosoma brucei</i> and <i>Crithidia fasciculata</i>	84
3.3.1	Experimental	84
3.3.1	Results	84
3.4	Chemical profiling of samples	88
3.4.1	Profiling with HPLC-UV-ELSD.....	88
3.4.2	GC-MS analysis	89
3.4.3	¹ H-NMR of the Crudes Extracts	92
3.4.4	LC-HRMS Analysis of Crude Extracts from Nigerian Propolis Samples 94	
3.5	Prediction of the most active compounds in the crude propolis extracts from LC-MS data	99
3.6	Discussion	103
4	PURIFICATION OF ANTI TRYPANOSOMAL COMPOUNDS FROM	
	SOUTHERN NIGERIAN PROPOLIS	107
4.1	Introduction	107
4.2	Experimental	107
4.3	Results	108

4.3.1	Structure elucidation of compounds purified from Southern propolis samples	108
4.3.2	Bioassay results	121
4.4	Discussion	123
5	CHEMICAL CHARACTERIZATION OF NIGERIAN RED PROPOLIS AND ITS ACTIVITY AGAINST <i>Trypanosoma brucei</i>	125
5.1	Introduction	125
5.2	Experimental	126
5.2.1	Propolis sample collection and preparation	126
5.2.2	Preparative scale chromatography	127
5.3	Results	129
5.3.1	Structure Elucidation of Compounds Isolated From Nigerian Red Propolis	129
5.3.2	Structure elucidation of riverinol (6)	136
5.3.3	HPLC-UV-ELSD and HPLC- MS Profiling of RSN and BRN	144
5.3.4	Bioassay results	156
5.3.5	Chemometric modelling of RSN fractions with regard to anti-trypanosomal activity	162
5.4	Discussion	170
6	PROFILING AND PURIFICATION OF PROPOLIS FROM SOUTH AFRICA	173
6.1	Introduction	173
6.2	Profiling of crude propolis sample (D46SA)	174
6.3	Extraction and fractionation of propolis sample D46SA	183
6.3.1	Characterization of GMP13-8 and MPF11-12-2 as Pinocebrin	190
6.3.2	Characterization of MPF11-12-6 as Acetylimbricatolic acid (labdane type diterpene)	190

6.3.3	Characterization of MPF11-12-8 as (-)-Pimara-8(14), 15-dien-19-oic acid.	195
6.4	Anti-trypanosomal activity	200
6.5	Discussion	201
7	GENERAL DISCUSSION	204
8	CONCLUSION AND FUTURE WORK	210
9	References.....	212
10	Appendix	236

LIST OF TABLES

Table 1-1: Compounds responsible for the biological activity of different propolis types (Bankova, 2005).	23
Table 1-2 : An overview of trypanocidal drugs and the problems associated with them.....	32
Table 1-3 : Difference between various preparative column chromatographic techniques, SP: stationary phase, RP: reversed phase, atm: atmospheric (Hostettmann & Terreaux, 1996).....	43
Table 2-1: Propolis samples coding and collection areas and date of collection.	67
Table 2-2: Main parameters for the ESI mass spectral analysis.	70
Table 3-1: Codes, collection area and percentage of yield of ethanol extract (EEP) for the samples.	83
Table 3-2: Average of EC ₅₀ in µg/ mL for all crudes (n= 3) against three strains of <i>T.brucei</i> ; wild type (T b S427WD) standards drug sensitive control, and other two genetically modified types aqp2/aqp3 null and B48 adapted from Lister 427WT . Data were provided by Harry P. De Koning from Glasgow University. Samples were also tested against <i>C. fasciculata</i> . For (n= 4), data were provided by Tim Paget from, University of Sunderland, NA: not tested.	87
Table 3-3: Some compounds identified by GC-MS with similarity scores higher than 700 when searched against the NIST library.	91
Table 3-4: Putatively identified compounds responsible for the differences among propolis samples UDN, ION and CCN based on analysis by high resolution followed by PCA when searched in DNP.	98
Table 4-1: ¹ H- and ¹³ C- NMR data for the new xanthone.....	114
Table 4-2: Average of (EC ₅₀) for (n=3) for crudes and purified compounds against wild type <i>Trypanosome brucei</i> (T b S427WD) and two other genetically modified types (B48 and aqp2/aqp3 null). Averages and SEM are given for n=3. Resistance factor (RF) is the ratio of EC ₅₀ for resistant strain over WT. Unpaired ttest compared	

EC ₅₀ values of each resistant strain versus WT. Units are in μM except for crude ION and UDN where the EC ₅₀ value is given in μg/mL Data were provided by Harry P. De Koning from Glasgow University.	122
Table 5-1: ¹ H NMR (400 MHz) and ¹³ C NMR (100 MHz) data of new benzofuran in DMSO-d ₆ . Hd downfield and Hu=upfield partner of geminal proton pair.	143
Table 5-2: Anti-trypanosomal activity, of crude extracts, fractions obtained from reversed phase chromatography of EEP of RSN on Grace, fractions from CC of BRN, and purified compounds. Highlighted cells indicates high activity, * fractions were subjected for further purification. MIC expressed in μg/mL in case of crudes and fractions and in μM for pure compounds.	157
Table 5-3: EC ₅₀ values (n=3) against three strains of <i>T.brucie</i> ;Lister 427 wild-type,AQP2-KO and B48. Averages and SEM are given for n= 3. Resistance factor (RF) is the ratio of EC ₅₀ for resistant strain over WT. Unpaired t-test compared EC ₅₀ values of each resistant strain versus WT. Units are in μM except for crude RSN, BRN, where the EC ₅₀ value is given in μg/mL. Data were provided by Harry P. De Koning from Glasgow University.	160
Table 5-4: MIC and percentage of yields of fractions from Grace normal phase chromatography of EEP of RSN. Highlighted cells indicated high activity. GRP11 was chosen for further purification.MP (mobile phase). MIC in (μg/mL).	163
Table 5-5: List of potential anti-trypanosomal compounds extracted from the S-plot and searched in the DNP in house database.	167
Table 6-1: Compounds extracted from NIST library with Similarity score higher than 800.	177
Table 6-2: Putative identification of flavonols and other major components of the crude sample D46SA.	179
Table 6-3: Elemental compositions, exact mass and fragmentation of five abundant unknown compounds in the crude extract of D46SA. The chemical names in red are possible identities searched in DNP.	183
Table 6-4: Summary for the weights and anti-trypanosomal activity obtained from D46SA extracts. Highlighted cells indicate high activity.	184

Table 6-5: Summary of the weights and anti-trypanosomal activity of the fractions of D46SA-MF obtained from CC. Fractions in pink were isolated and identified. The highlighted cells indicate high activity.	186
Table 6-6: ¹ H (400 MHz) and ¹³ C NMR (100 MHz) data of MPF11-12-6 in DMSO-d ₆	193
Table 6-7: ¹ H (400 MHz) and ¹³ C NMR (100 MHz) data of MPF11-12-8 in DMSO-d ₆	198
Table 6-8: MIC values in μM of pure compounds when tested against <i>T. brucei brucei</i>	200

LIST OF FIGURES

Figure 1-1: Scientific research on propolis as judged by patents and publication numbers (Chemical abstract) cited from (Toreti <i>et al.</i> , 2013).....	6
Figure 1-2: Scientific production of Propolis by patents versus languages (Chemical abstract) cited from (Toreti <i>et al.</i> , 2013).....	6
Figure 1-3: Classification of flavonoids.....	12
Figure 1-4: Prenyl-Geranyl flavonoids.	13
Figure 1-5: Some representative terpenoids isolated from propolis.	14
Figure 1-6 : Some propolones isolated from Cuban propolis; 1 Propolone A, 2 Nemorosone, 3 Guttiferone, and 4 Xanthochynol.	16
Figure 1-7: The life cycle of <i>Trypanosome brucei</i> (www.dpd.cdc.gov/dpdx).....	27
Figure 1-8: Sleeping sickness national control programme, adapted from WHO annual country report in 2010.	29
Figure 1-9: Structures of drugs in current use against human African trypanosomiasis.....	33
Figure 1-10: The main components of medium pressure liquid chromatography system (Hostettmann & Terreaux , 1996).....	44
Figure 1-11: Schematic diagram showing the component of a GC-MS system.....	47
Figure 1-12: Schematic diagram shows the components of HPLC.	49
Figure 1-13: The major components of a HPLC-ELSD.	51
Figure 1-14: Schematics of the commercial LTQ-Orbitrap Classic model (Makarov <i>et al.</i> , 2006): (a) transfer octopole; (b) curved RF-only quadrupole (C-trap); (c) gate electrode; (d) trap electrode; (e) ion optics; (f) inner orbitrap electrode (central electrode); (g) outer orbitrap electrode.	55
Figure 1-15: The basic elements of a classical NMR spectrometer.....	58

Figure 3-1: Map of Nigeria showing collection sites for samples cited from (http://www.inecnigeria.org/page_id=373).....	84
Figure 3-2: General screening of propolis samples from different regions of Nigeria for activity against three strains of <i>T. brucei</i> and <i>C. fasciculata</i>	86
Figure 3-3 : ELSD-UV chromatograms of two samples AF2-3N and ION from Central and Southern Nigeria, blue indicates ELSD response. HPLC conditions in section 2.3.1.	89
Figure 3-4: Representative GC–MS chromatograms for three propolis samples BRN, AF2-3N, ION. Experimental condition in section 2.3.3	90
Figure 3-5: Structure of some common and volatile compounds identified by GC-MS in group I and II samples.....	92
Figure 3-6: Comparison of the ¹ H NMR spectra (400 MHz, in CDCl ₃) of two extracts ION and UDN with labelling the characteristic compounds, cyclotartanes in the ION sample and xanthenes in the UDN sample. Experimental conditions in section 2.3.4.	94
Figure 3-7: Score plot of PCA for duplicate analyses of crude extracts of Nigerian propolis samples, one outlier ION can be clearly observed. Samples from the central Nigeria were clustered together to some extent.	96
Figure 3-8: Hierarchical clustering generated from the PCA for the crude propolis extracts grouping them into three groups.....	97
Figure 3-9: Loading scatter plot of crude Nigerian samples showing the complexity of the data being modelled.	97
Figure 3-10: PLS model of predicted against measured anti-trypanosomal activity of Nigerian propolis extracts based on 180 features.	100
Figure 3-11: Loadings in the high activity region for the Nigerian propolis samples demonstrated the abundance of Denticulatain isomers in this region.....	101
Figure 3-12: Extracted ion traces for denticulatain (<i>m/z</i> 515.29-515.32) isomers in the high activity Nigerian propolis samples. Experimental condition in section 2.3.2	102

Figure 3-13: Extracted ion traces for isomers of guttiferone A in samples RSN, BRN, ION and CCN. Experimental condition in section 2.3.2.	102
Figure 4-1: Structures of prenylated xanthenes isolated from the UDN propolis sample.	110
Figure 4-2 : HR-ESIMS ion chromatogram and mass spectrum of three prenylated xanthenes isolated from sample UDN. Experimental conditions in section 2.3.2... ..	111
Figure 4-3: Numbered structure of the new xanthone.....	114
Figure 4-4: ¹ H NMR of Mudn10-51 (400 MHz, DMSO- d ₆), X denote for solvent peak.	116
Figure 4-5: ¹³ C NMR spectrum of Mudn10-51 (100 MHz, DMSO- d ₆).....	117
Figure 4-6: COSY spectrum (400 MHz) of Mudn10-51 in DMSO- d ₆	118
Figure 4-7: Expanded HMBC spectrum (400 MHz) of Mudn10-51 in DMSO-d ₆ . ..	118
Figure 4-8: LC-UV-ELSD chromatogram of purified triterpens from ION, all with ELSD only response. HPLC conditions in section 2.3.1.	119
Figure 4-9: The structure of the triterpenes isolated from the ION propolis sample Mion12-18 (ambonic acid) , Mion12-23 (mangiferonic acid), Mion13-25 (α amyryn).	121
Figure 5-1: Nigerian red propolis.....	127
Figure 5-2: Schematic representation of common fragmentation processes observed in the collision induced dissociation (CID) of flavonoid adapted from (Hughes <i>et al.</i> , 2001).	130
Figure 5-3: Structures of the flavonoids and isoflavonoids isolated from Nigerian red propolis.....	133
Figure 5-4: Structures of the prenylated flavonoids isolated from Nigerian red propolis.....	136
Figure 5-5: ¹ H NMR(400 MHz) of Riverinol in DMSO- d ₆ . The peaks denoted by X represent signals from solvent.....	139

Figure 5-6: DEPT 135 ¹³ C NMR spectrum (100 MHz) of Riverinol in DMSO- d ₆	140
Figure 5-7: COSY spectrum (400 MHz) of Riverinol in DMSO- d ₆	141
Figure 5-8: HMBC spectrum (400 MHz) of Riverinol in DMSO-d ₆	141
Figure 5-9: Numbered structure of Riverinol (6) for structure elucidation purposes, and a closely related dihydrobenzofuran previously isolated(Han <i>et al.</i> , 2008).....	142
Figure 5-10: Key HMBC (→) and COSY(—) correlation for Riverinol.....	142
Figure 5-11: A HPLC-ELSD-UV chromatogram of BRN; B is the negative LC-HR-ESIMS ion mode chromatogram for BRN and C is negative HR-ESIMS ion mode chromatogram for RSN.....	145
Figure 5-12: Extracted ion trace and negative ion spectra for Retusapurpurins.....	146
Figure 5-13: MS ² fragmentation of a polyprenylated benzophenone illustrated for oblongifolin A.....	153
Figure 5-14: Proposed MS ² and MS ³ fragmentation of denticulatain A.....	155
Figure 5-15: Hierarchical Clustering analysis (HCA), the dendrogram above shows observations clustered into three groups. X-axis fractions observations and y-axis hows similarity index. The higher the similarity index the more between-groups variability, and the smaller the similarity index the higher similarity within groups.	165
Figure 5-16: OPLS-DA score plot for fractions group1 (green) active fractions and group 2 (plum) inactive fractions.....	166
Figure 5-17: An S-plot showing putative biomarkers that were identified as contributing significantly to good activity.....	166
Figure 6-1: Map of South Africa and collection site of (D46SA) Propolis (http://bigpictureofthebible.com/south-africa-mission).	174
Figure 6-2: Chromatogram of HPLC-UV-ELSD of crude D46SA, red line ELSD response, blue and yellow are UV responses at 290 nm and 320 nm respectively. Experimental conditions in section 2.3.1	175

Figure 6-3: ^1H NMR spectrum (400 MHz, in CDCl_3) of crude D46SA showing mainly aliphatic protons, oleic acid and some phenolic compound(s) with lower intensities.	176
Figure 6-4: GC chromatogram of D46SA. Experimental condition in section 2.3.3.	177
Figure 6-5: TIC chromatogram of crude D46SA. Experimental condition as in section 2.5.2.	179
Figure 6-6: Structures of the previously reported South African propolis marker compounds were all identified except phenolic acids caffeic and <i>p</i> -Coumaric acid.	181
Figure 6-7: Extracted ion traces of the main unknown compounds in the crude D46SA extract.	182
Figure 6-8: Chromatogram of F13 on the Grace® system revealing the targeted UV absorbing compound (blue arrow).	187
Figure 6-9: Chromatogram of MPF11-12.6 on the analytical HPLC ELSD system.	191
Figure 6-10: A- Structure of acetylimbricatolic acid and B- Structure of 15-acetyl isocupressic acid.	192
Figure 6-11: A ^1H NMR spectrum (400 MHz) and B DEPT 135 ^{13}C NMR (100 MHz) of MPF11-12-6 in DMSO-d_6 , X denotes for solvnet.	194
Figure 6-12: ELSD Chromatogram of MPF11-12.8 on ELSD.	195
Figure 6-13: Structure of two isomers C pimaric acid, D (-)-pimara-8(14), 15-dien-19-oic acid.	196
Figure 6-14: E- ^1H NMR spectrum (400 MHz), F- DEPT 135 ^{13}C NMR spectrum (100 MHz) of MPF11-12-8 in DMSO-d_6 , X denotes the solvent peak.	199

LIST OF ABBREVIATIONS

μM	Micromolar
^{13}C NMR	Carbon nuclear magnetic resonance
2D NMR	Two dimensional nuclear magnetic resonance spectroscopy
API	Atmospheric pressure ionization
APCI	Atmospheric pressure chemical ionization
APPI	atmospheric pressure photo ionization
DESI	Desorption electrospray ionization
BBB	Blood brain barrier
Brs	Broad singlet
$^{\circ}\text{C}$	Celsius
CC	Column chromatography
CDCl_3	Deuterated Chloroform
CID	Collision induced dissociation
COSY	^1H - ^1H Correlation Spectroscopy
D	Doublet
Dd	Doublet of a doublet
DEPT	Distortionless Enhancement by Polarization Transfer
DMSO- d_6	Dimethyl sulphoxide
EC_{50}	Half maximal effective concentration

EEP	Ethanolic extract of propolis
EI	Electron impact
ELSD	Evaporative light scattering detection
ESI	Electrospray ionization
EtOAc	Ethyl acetate
FAB	Fast Atom Bombardment
H	Hour
¹ H NMR	Proton nuclear magnetic resonance
HAT	Human African Trypanosomiasis
HCA	Hierarchical Clustering analysis
HMBC	Heteronuclear Multiple Bond Coherence
HMQC	Heteronuclear Multiple Quantum Coherence
HPLC	High performance liquid chromatography
HR-ESIMS	High resolution electrospray ionisation mass spectrometry
HT-HRGC-MS	High temperature- high resolution gas chromatography-mass spectrometry
Hz	Hertz
LDL	Low density lipoprotein
LC-MS	Liquid chromatography mass spectrometry
M	Multiple
Mg	Milligram
MHz	Megahertz

MIC	Minimum inhibitory concentration
mL	Millilitre
MP	Mobile phase
MPLC	Medium pressure liquid chromatography
MS	Mass Spectroscopy
m/z	Mass to charge ratio
NMR	Nuclear Magnetic Resonance
No.	Number
NOESY	spectroscopyNuclear Overhauser effect
ODC	Ornithine decarboxylase
PCA	Principle component analysis
PLS	Partial least square
RDB	equivalent Ring and double bond
S	Singlet
SP	Stationary phase
T	Triplet
<i>T. brucei</i>	<i>Trypanosoma brucei</i>
TLC	Thin layer Chromatography
TMS	Tetramethylsilane
UV	Ultraviolet light
WHO	World Health Organization

ABSTRACT

Propolis or bee glue, is collected by bees and contains secondary metabolites largely derived from trees or shrubs; it has been used traditionally as a natural remedy with a wide range of biological activities. Its chemical composition is highly complex and variable, and it has been studied in detail worldwide except in Africa. This study investigated the chemical composition and activity of African propolis against blood stream form of *Trypanosoma brucei*, the causative agent for sleeping sickness that threatens a large population of both humans and animals in sub-Saharan Africa.

Extracts of propolis samples (n=12) collected from different regions in Nigeria and one sample collected from South Africa were chemically profiled by using various analytical techniques. These included high performance liquid chromatography (HPLC), coupled with different detection systems including evaporative light scattering detection (ELSD), ultraviolet detection (UV), and high resolution mass spectrometry (HRMS), along with gas chromatography- mass spectrometry (GC-MS) and proton-nuclear magnetic resonance ($^1\text{H-NMR}$).

Principal components analysis (PCA) of the processed LC-MS data collected was used in order to characterize samples according to their chemical composition. PCA demonstrated the uniqueness in chemical composition of some samples that were also active against *Trypanosoma brucei*. Therefore, the study proceeded to investigate in detail four samples collected mainly from the southern part of Nigeria. An optimized medium pressure chromatographic technique was used to isolate some of the component(s) responsible for the anti-trypanosomal activity.

Two samples collected from Rivers State Nigeria had a different appearance from the rest of the propolis samples, being red in colour and had the highest trypanocidal activity (EC_{50} =4.2 and 6.9 $\mu\text{g/mL}$) respectively. Their chemical composition was comparable to that of Brazilian red propolis. Fractionation work led to the isolation of ten phenolic compounds including calycosin, liquiritigenin, pinocembrin, vestitol, medicarpin, 8-prenylnaringenin, 6-prenylnaringenin, propolin D, macarangenin and a new benzofuran. All compounds structurally elucidated by 1D and 2D Nuclear Magnetic Resonance (NMR) spectroscopy and LC-MSⁿ. Some compounds showed strong inhibitory activity against trypanosomes such as medicarpin (MIC=11.5 μM) and propolin D (MIC=7.4 μM), macarangenin (EC_{50} =18.5 μM), 8-prenylnaringenin (EC_{50} = 17.9 μM), and vestitol (EC_{50} = 30.5 μM). The new benzofuran was moderately active with (EC_{50} =58.01 μM).

Fractionation of the propolis sample collected from the Ugelli/Delta sample led to isolation of three compounds 1,3,7-trihydroxy-2,8-di-(3-methylbut-2-enyl) xanthone, 1,3,7-trihydroxy-4,8-di-(3-methylbut-2-enyl) xanthone and a new xanthone. These compounds were tested against *T. brucei* and presented high activities of EC_{50} = 3.9, 11.04, 14.7 μM respectively.

Triterpenes were the main fingerprint compounds in a sample collected from Ijebu-Ode/Ogun; three compounds were isolated and elucidated as ambonic acid, mangiferonic acid and α -amyrin. These compounds had EC_{50} values against *T. brucei* of 39.5, 25.5 and 20.9 μM respectively.

Finally, sample D46SA from South Africa was found to contain mainly flavonols and diterpenic acids; three compounds pinocembrin, acetylimbricatolic acid and (-)-

pimara-8 (14), 15-dien-19-oic acid were isolated and tested. All were moderately active against *T. brucei*. with MIC ranging from 41.4-137.3 μM

In conclusion, this work has proved the variability of propolis collected even from the same region and the widespread activity of propolis against (blood stream form) *T. brucei*. It is likely that some of the propolis samples contain compounds with even higher activity that have not yet been isolated.

PUBLISHED WORK FROM THIS RESEARCH

1. Zhang, Tong, **Ruwida M. K. Omar**, Weam Siheri, Sultan Al Mutairi, Carol Clements, James Fearnley, RuAngelie Edrada-Ebel, and David Watson. "Chromatographic analysis with different detectors in the chemical characterisation and dereplication of African propolis." *Talanta*, 120 (2014): 181-190.
2. **Ruwida M. K. Omar**, John Igoli, Alexander I. Gray, Godwin Unekwuajo Ebiloma, Carol Clements, James Fearnley, RuAngeli Edrada Ebel, Tong Zhang, Harry P. De Koning and David G. Watson. "Chemical characterisation of Nigerian red propolis and its biological activity against *Trypanosoma Brucei*." *Phytochemical Analysis*, 27 (2016): 107-115.
3. **Ruwida Omar**, John Igoli, Tong Zhang, Alexander I. Gray, Godwin Unekwuajo Ebiloma, Carol Clements, James Fearnley, RuAngeli Edrada-Ebel, Tim Paget, Harry De-Koning and David G. Watson" The chemical characterization of Nigerian propolis samples and their activity against *Trypanosoma Brucei*."

Submitted to J.Pharmacy. Pharmacol.

CHAPTER ONE
GENERAL INTRODUCTION

1 GENERAL INTRODUCTION

1.1 Propolis

Bees have been in existence for 125 million years, and their evolutionary success has made them a unique species that can exploit virtually all habitats on the earth. This success is largely a result of their intelligence in chemistry, and wide applications of the six specific products that bees manufacture honey, beeswax, venom, propolis, pollen and royal jelly (Bankova, 2005).

Propolis or bee-glue is the third most important product of honey bees after honey and wax (Burdock, 1998). It is a strongly adhesive, resinous, multifunctional complex material. It is derived from secondary metabolites that are produced by trees to prevent infections of injured tree parts, retard bud development during frost, and to protect pollen from being infected by microbes (Assegid & Lamprecht, 1997). It is believed that honey bees process and alter the metabolites via their salivary enzymes (glucosidases), prior to its incorporation into beehives (Bankova *et al.*, 2000). Propolis is used by bee colonies in the construction and maintenance of their hives. Bees use propolis to smooth out the internal walls, protect the entrance against intruders, embalm dead intruders to their hives and as ‘glue to seal gaps between honeycombs. Additionally, propolis helps to keep the interior of the hive warm and humid free, and it presents the best defence against microbial contamination (Seidel *et al.*, 2008). Etymologically the term propolis derives from the Greek, pro (for ‘in front of’, ‘at the entrance to’) and polis (‘community’ or ‘city’) and means a substance in defence of the hive (Castaldo & Capasso, 2002).

1.1.1 Origin

Researchers have stated that propolis may originate either from an internal source; from the first phase digestion of pollen in a small organ placed between the sac and lower gut. It is then used to varnish cells, especially the newly built ones before the queen lays eggs on them (Hegazi, 1978). It has been observed that bees produce a detergent like secretion in order to remove propolis from the legs of bees that have collected it (Janko Botic, personal communication). Thus propolis may partly have an internal origin as well as an external origin like temperate propolis, which is harvested by the worker bees (*Apis mellifera*) (Burdock, 1998) from leaf buds, and cracks in the bark of numerous tree species, including poplar, fir, pine, horse chestnut, alder, willow and palm trees, and then incorporated in the hive. However, it has been found that bees can harvest propolis from other tree species since propolis has been found in hives in places where neither alders nor poplars are present. Its exact origin remains to be explained. Given the choice, bees may prefer poplar trees since components derived from poplar, have been observed in Brazilian propolis where poplar trees, as a non-native species, were planted near beehives (Alexandra Sawaya, personal communication).

1.1.2 History

Propolis is a natural remedy that has been employed extensively since ancient times, and its therapeutic characteristics have been well known for a very long time. Egyptian Pharaohs utilized the anti-putrefactive properties of propolis, and used it in antiquity to embalm cadavers, and in surgical procedures as an antiseptic agent (Castaldo & Capasso, 2002). The Greeks recognized propolis for its medicinal properties; this fact is demonstrated by its very Greek name.

Roman physicians, Dioscorides, Pliny and Galen, also used it although the harvesting methods that were used in the ancient world are not known. The Greek Historian Animalium referred to a substance ‘mitys’, which was probably propolis, as “a cure for bruises and suppurating sores” (Toreti *et al.*, 2013). Propolis was employed as an antiseptic and cicatrizant in wound treatment after mixing with petroleum jelly during the Anglo-Boer war in South Africa, with these uses being common in the Middle Ages and among Arab physicians. Abu Ali bin Sina (Avicenna) recognized two kinds of waxes in his work (The Canon of Medical Science), clean wax and black wax. Clean wax is the comb where the bees store the honey, and black wax is the dirt of the hive. It is clear that the black wax is propolis. He wrote that it has a strong smell and makes you sneeze (Hegazi, 1978). Propolis was also recognized by other peoples such as the Incas who employed it as an anti-pyretic agent. The London pharmacopoeias of the seventeenth century listed propolis as an official drug, and it became very popular in Europe between the seventeenth and twentieth century because of its anti-bacterial activity (Castaldo & Capasso, 2002). In folk medicine, it was claimed that propolis is efficient for the treatment of corns, as an inhalation for the treatment of respiratory tract infections, and finally it was also used in burns and angina.

However, there is a huge increase in global interest in propolis research. By searching the chemical abstracts Toreti *et al.* (2013) found that the number of publications on propolis had reached 3,880 in journals and 1697 in patents since the first publication and patent was launched in 1903 and 1904, respectively, as shown in **Figure 1-1**. This increase in interest may refer to its diverse biological properties and high added value, and its low price. Profiling of propolis patents showed that China,

Japan and Russia are those that hold most of the patents see **Figure 1-2** because they are the major producers of propolis. Japan ranks second and uses propolis extensively in foods and beverages, importing around 80% of their propolis from Brazil; this explains the increase in publications on Brazilian propolis.

1.1.3 *Physical characteristics of propolis*

The colour of Propolis ranges from yellow to dark brown depending on its origin and its age. Even transparent propolis has been reported by Cogshall and Morse (1984). Propolis usually starts softening between 25 °C to 45 °C and becomes flexible, and very sticky. When frozen at less than 15 °C it becomes hard and brittle and can remain brittle after freezing even at higher temperatures. Typically, Propolis will liquify at 60 °C to 70 °C, but for some samples the melting point may be as high as 100 °C.

The most commonly used solvents for commercial extraction of propolis are ethanol, ether, glycerol and water. For chemical analysis a large variety of solvents may be used in order to extract fractions containing various compounds of interest (Krell, 1996).

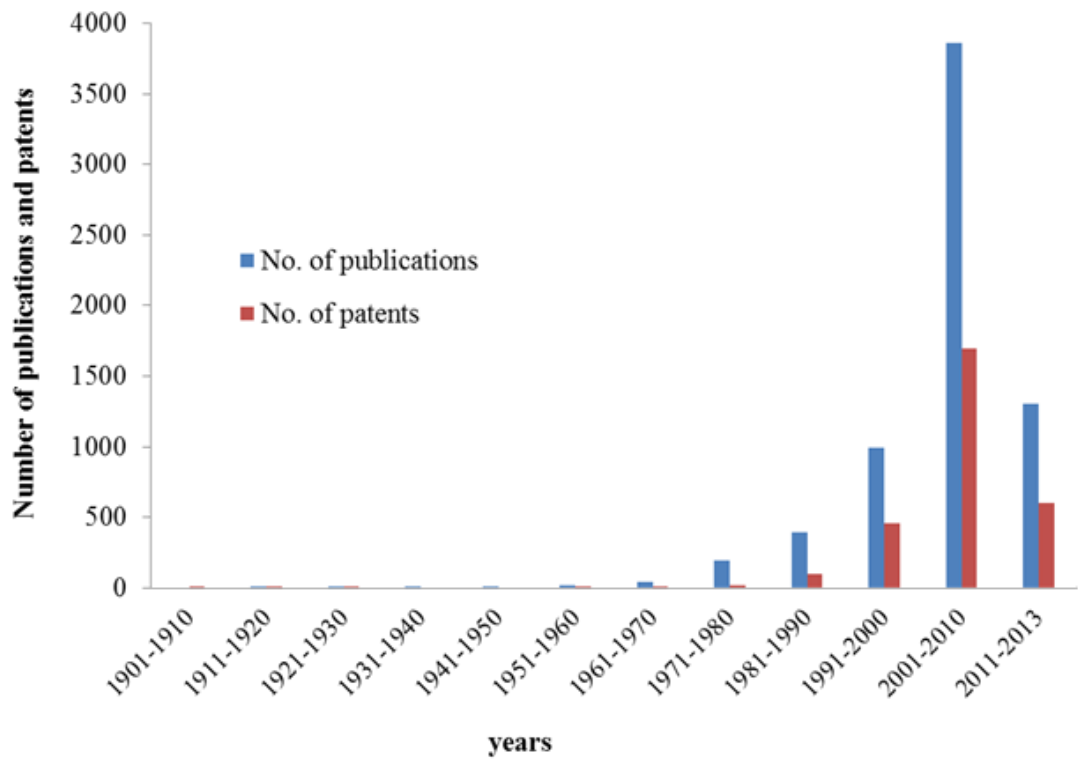


Figure 1-1: Scientific research on propolis as judged by patents and publication numbers (Chemical abstract) cited from (Toreti *et al.*, 2013).

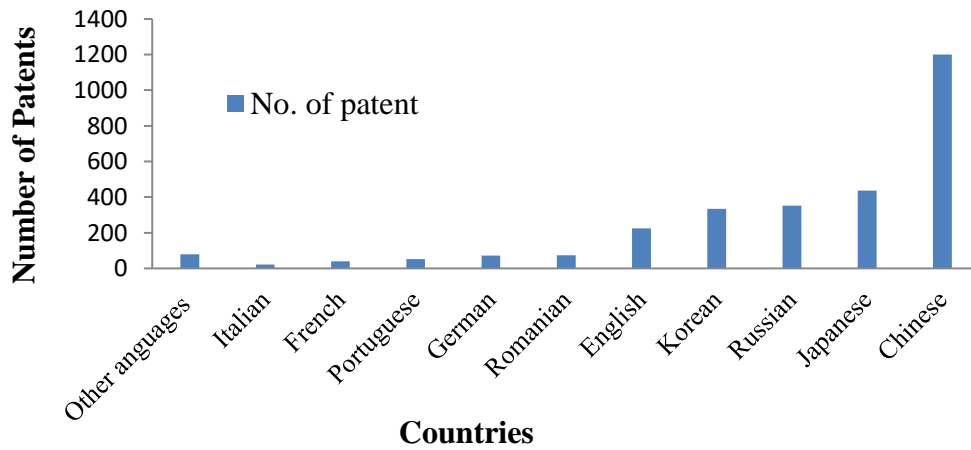


Figure 1-2: Scientific production of Propolis by patents versus languages (Chemical abstract) cited from (Toreti *et al.*, 2013).

1.1.4 Chemical composition and how it is affected by geographic region

Propolis has become an important subject of interest in pharmacological and chemical studies in the last few decades, and as a result, much useful knowledge has been gathered and more than 300 compounds have been isolated (Huang *et al.*, 2014). It is important to note that the paradigm concerning propolis chemistry has radically changed. In the 1960s, propolis was thought to be of very complex, but of more or less constant chemistry, like beeswax or bee venom, but analysis of numerous samples from different geographic regions led to the discovery that the chemical composition of bee glue is both highly variable and complex (Bankova, 2005).

The chemical composition of propolis varies depending on many factors, including the phytogeographic characteristic of collection site, the species responsible for collection, and the season of collection (Bankova *et al.*, 2000). Generally, propolis is composed of 50% resin and balsams, 30% wax, 10% essential and aromatic oils, 5% pollen grains, which are a rich source of essential elements such as magnesium, nickel iron and zinc, and 5% other organic substances (Pietta *et al.*, 2002). During processing the wax and organic debris are removed to produce a propolis tincture (Burdock, 1998).

In 2005, Bankova characterized propolis samples trying to understand the causes of the huge variability in their chemical composition, taking into consideration that bees use materials from different parts of plants; these are produced as a result of different botanical processes to produce propolis, and these substances have been either actively secreted by plants or exuded from wounds in plants. For example, lipophilic materials on leaves and leaf buds, gums, resins, latices, etc. (Crane, 1988). Hence,

Bankova broadly classified propolis into two large groups: propolis originating from tropical and subtropical zones, or from temperate zones (Bankova, 2005).

In case of temperate zones all over the world, such as in Europe, North America, New Zealand and Western Asia, the main source of propolis is the resinous exudates from poplar trees, mainly the black poplar *Populus nigra* (Toreti *et al.*, 2013). Therefore phenolics, including flavonoid aglycones, phenolic acids and their esters which are considered as typical ‘poplar bud’ components, are the dominant compounds in European propolis (Bankova *et al.*, 2002). However, in Northern parts of Russia analysis confirmed that the plant origin of propolis is birch buds *Betula verrucosa* (Bankova *et al.*, 2000).

Poplar and birch trees cannot grow in tropical and subtropical regions; therefore, bees have to find other plant sources instead of the poplar tree. As a result, propolis from tropical areas originates from different species such as leaf exudate of some *Cistus* spp. in Tunisian propolis (Martos *et al.*, 1997), while *Ambrosia deltoidea* and *Encelia farinose* are the plant sources in the Sonoran Desert propolis, as stated by Wollenweber and Buchmann (Wollenweber & Buchmann, 1997). Investigation of chemical composition of Australian propolis revealed that it originated from *Xanthorrhoea* spp the ‘grass trees’ endemic to Australia (Jefferies, 1978).

Chromatographic comparison of tropical samples collected from Venezuela proved that isolated polyprenylated benzophenones from propolis are the same as the main components of the resin exuded from the flowers of some *Clusia* species; *Clusia major* and *Clusia minor* (Guttiferae) (Word, 1993).

In Africa, the plant source of propolis has not yet been investigated thoroughly to trace the source of fatty acids, terpenoids, and flavonoids such as pinocembrin. Recent chemical profiling and chemometric studies on South African samples have shown that the majority of the samples from South Africa are rich in phenolic acids and flavonols, and the chemical profile of the majority of samples is similar to propolis produced in the temperate regions (Kasote *et al.*, 2014).

Brazilian propolis is the subject of increasing interest; widely investigated and studied, it has demonstrated a good example of how chemical composition can differ even within the same area. Since Brazil is a vast country with various types of climate and vegetation, accordingly Brazilian propolis has been physicochemically categorized into 12 different groups that differ in their botanical origin and chemical composition. Chemometric profiling suggested that *Baccharis* spp. is a significant source of tropical Brazilian propolis, in addition to *Araucaria heterophylla*, *Clusia major*, and *Clusia minor* (Banskota *et al.*, 1998).

Generally, the major and common chemical compounds that have been recognized in propolis are flavonoids, terpenoids, phenolic acids and their esters, and minor compounds such as aldehydes, ketones, fatty acids sugars and mineral elements. Common phytochemicals such as alkaloids and iridoids have not been reported (Kasote *et al.*, 2014).

1.1.4.1 Flavonoids

Flavonoids are considered to be the main contributors to the biological activity of propolis, and are the major constituents of temperate propolis, where they can be found without B-ring substitution, such as chrysin, galangin, pinocembrin, pinobanksin. These flavonoids are utilized as markers to standardize and evaluate the quality of propolis in these areas. Havsteen divided the mechanism of the action of flavonoids in animal systems into four categories including binding to biological polymers, binding to heavy metal ions, catalysis of electron transport, and ability to scavenge free radicals (Havsteen, 1983; Burdock, 1998)

Generally flavonoids can be classified into flavones, flavonols, flavanones, flavanonols, chalcones, dihydrochalcones, isoflavones, isodihydroflavones, flavans, isoflavans and neoflavonoids as shown in **Figure 1-3**, and in addition, flavonoid glycosides that were rarely isolated from propolis such as isorhamnetin 3-O-rutinoside (Popova *et al.* 2009) and narigenin 8-C-hexoside, which is the first reported flavone C-glycoside isolated from Brazilian red propolis (Righi *et al.*, 2011).

Geranylated flavonols such as 2'-Geranylquercetin, 8-(8''-Hydroxy-3'',8''-dimethyl-oct-2''-enyl)-quercetin and macarangin that were isolated from propolis samples from the Solomon Islands and Kenya suggest that the genus *Macaranga* is the main source of propolis in these samples (Nui *et al.*, 2012).

Unique open-chain neoflavonoids were isolated and identified from Nepalese propolis, and used as markers to recognize the plant source of propolis (Awale *et al.*, 2005).

Many prenylated and geranylated flavonones were identified in Pacific propolis collected from Japan, Thailand, and the Solomon Islands including propolins A to E; All of them exhibited a very strong antibacterial activity due to the presence of the lipophilic prenyl group which rapidly destroys the bacterial cell membrane (Raghukumar *et al.*, 2010) as illustrated in **Figure 1-4**.

Red Brazilian and Cuban propolis are considered as a new type of propolis that has attracted wide attention, due to them containing a wide range of flavonoids with various biological activities. They mainly originate from the resinous exudate of the leguminous plant *Dalbergia ecastophyllum* which includes flavanones such as alnustinol, dihydrooroxylin A, garbanzol, liquiritigenin and naringenin. Isoflavones also were identified in the exudate, including calycosin, isodihydroflavones such as biochanin A, daidzein, formononetin, (3S)-vestitone, violanone and xenognosin B and chalcones such as isoliquiritigenin, dihydrochalcones such as 2',4'-dihydroxychalcone and pterocarpins such as 6 α -ethoxymedicarpin, homopterocarpin and medicarpin were also characterized in red propolis (Li *et al.*, 2008).

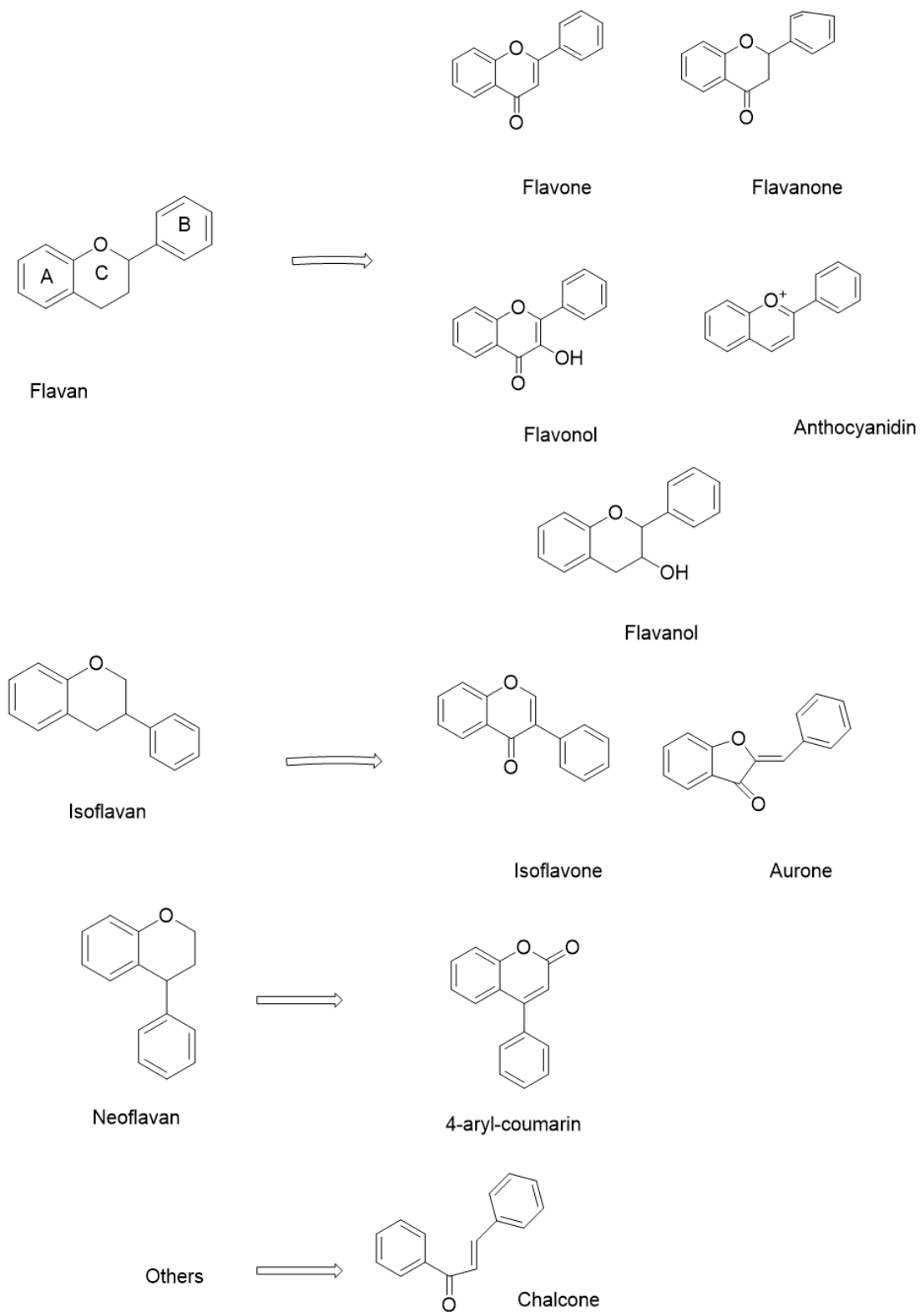


Figure 1-3: Classification of flavonoids.

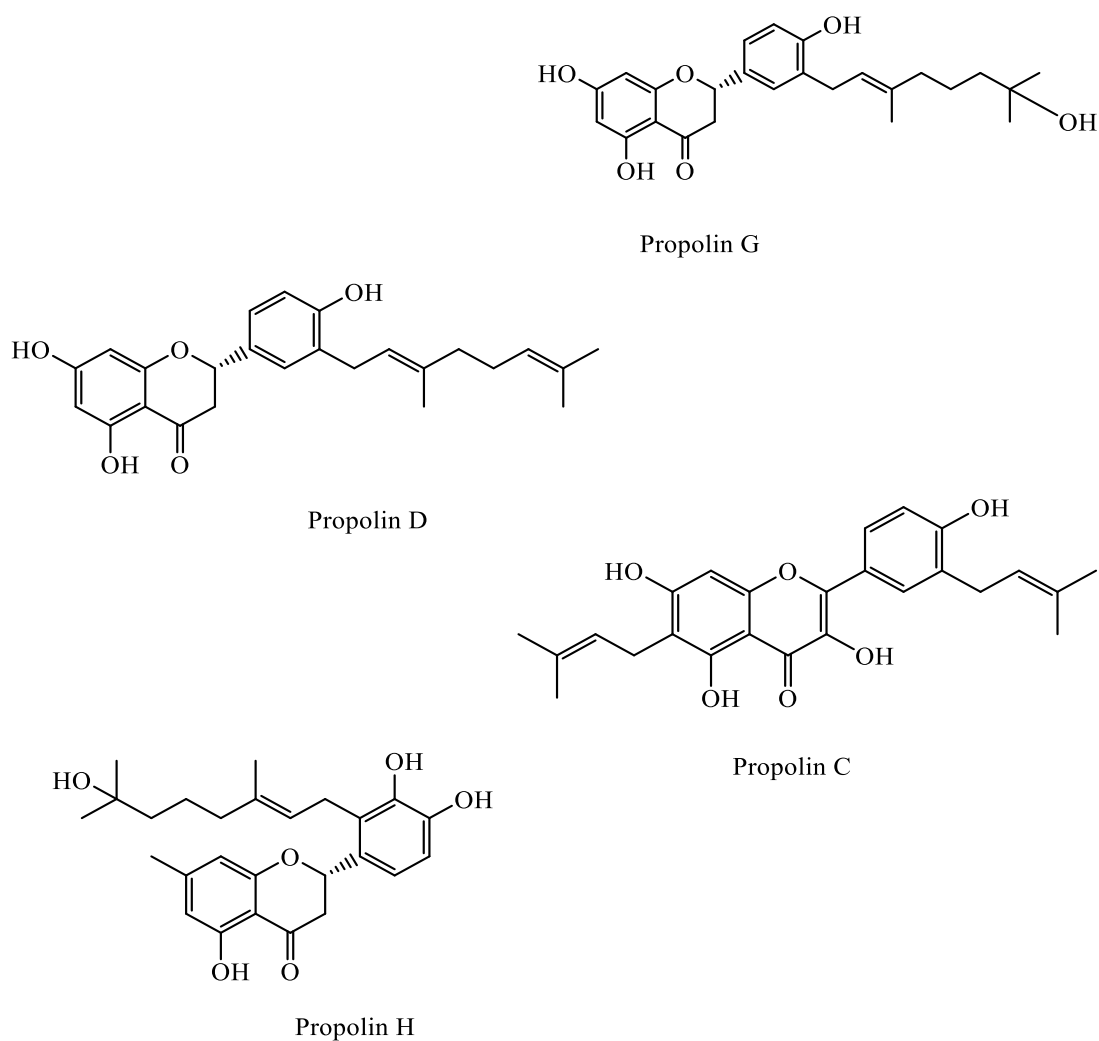


Figure 1-4: Prenyl-Geranyl flavonoids.

1.1.4.2 Terpenoids

Terpenoids represent about 10% of propolis constituents. They are responsible for the distinct resinous odour of propolis and play an important role in distinguishing between true and fake propolis. They contribute dramatically to the biological activity. Generally, they can be classified into monoterpenes (C_{10}) which are subdivided into acyclic, monocyclic, bicyclic monoterpenes, and their derivatives. Sesquiterpenes (C_{15}) are the most abundant chemical components in propolis,

according to their number of rings, sesquiterpenes, classified into acyclic, monocyclic, bicyclic and tricyclic. Diterpenes (C_{20}) include cembrane, labdane, abietane, pimarane, and totarane structures which are reported to be the major diterpenes in propolis, and some of these have been proven to have a broad spectrum of pharmacological properties. The tetracyclic triterpenes (C_{30}) found in propolis are lanostanes, cycloartane and the pentacyclic triterpenes are oleanane, ursane and lupane **Figure 1-5**. Propolis samples from Egypt and Brazil were found to contain a range of di- and triterpenes like pimaric and abietic acids, oleanane and ursane, lupeol and cycloartinol (Popova *et al.*, 2009).

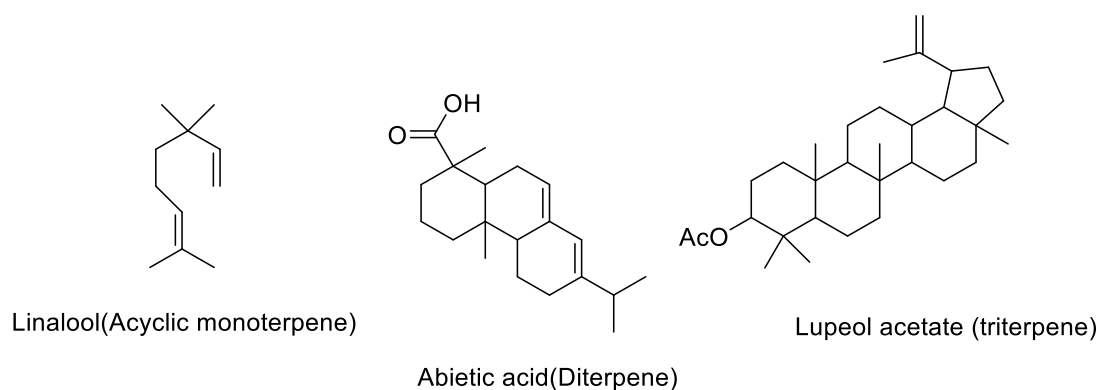


Figure 1-5: Some representative terpenoids isolated from propolis.

1.1.4.3 Phenolics and acids

Phenolics and acids occurring in propolis, including cinnamic acid, *p*-coumaric acid, caffeic acid, ferulic acid and their derivatives, have been isolated from green Brazilian propolis and demonstrate a wide range of biological activity (Salatino *et al.*, 2005).

Stilbenes, especially geranylated stilbenes, are not very common in plants, but were isolated from Kenya and Solomon Islands propolis due to the presence of *Macaranga* Sp. resins in the propolis. Prenylated stilbenes, were also reported in Australian Kangaroo Island propolis (Abu-Mellal *et al.*, 2012).

Lignans can be classified as phenolics and are the main components in the tropical propolis. They have been isolated from Kenyan and Brazilian propolis and include for example phyllamricin C, tetrahydrojusticidin, and 6-methoxydiphyllin (Petrova *et al.*, 2010).

Interestingly, in 1997 four new characteristic polyisoprenylatedbenzophenone compounds were isolated from Cuban brown propolis, named as propolone A, nemorosone, guttiferone E, and xanthochymol **Figure 1-6**, and in 2005 additional compounds belonging to the same family were isolated and were named propolones B-D, together with garcinielliptone I and hyperibone B. The plant source of these compounds was detected to be the floral resin of *Clusia rosea* (Hernández *et al.*, 2005).

1.1.4.4 Sugars

Glucose, fructose and sucrose have been isolated from propolis, although their origin is not known yet. It is not known whether they are from nectar and honey or from the hydrolysis of flavonoids glycosides. Many sugars, sugar alcohols and uronic acids were isolated from propolis collected from the Canary Islands, Malta and Egypt. Among these substances, galactitol, gluconic acid, galacturonic acid and 2-O-glycerylgalactose were identified for the first time in Egyptian propolis (Abd El Hady & Hegazi, 2002).

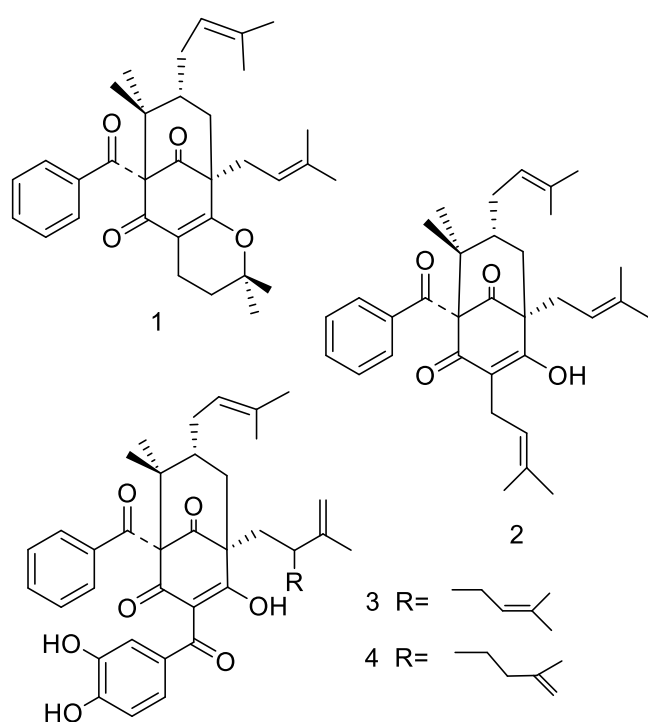


Figure 1-6 : Some propolones isolated from Cuban propolis; **1** Propolone A, **2** Nemorosone, **3** Guttiferone, and **4** Xanthochynol.

1.1.4.5 Hydrocarbons

Alkanes, alkenes, alkadienes, monoesters, diesters, aromatic esters, fatty acids and steroids have been identified in many types of propolis including Egyptian, Brazilian and Anatolian propolis. Studies showed that propolis waxes are secreted by bees, and this is affected by the genetic make-up of the bees not the plant source (Negri *et al.*, 1998).

1.1.4.6 Mineral Elements

The elements Calcium, Potassium, Magnesium, Sodium, Aluminium, Boron, Barium, Iron, Nickel and Zinc and toxic elements such as Arsenic, Cadmium, Mercury and Lead have been identified in Croatian and Argentinian propolis. These elements can be used as indicators for profiling and identification of propolis according to their location, and their identification is important for quality control since their presence can affect propolis nutritional use (Cantarelli *et al.*, 2011).

1.1.4.7 Summary

The chemical composition of the propolis is highly variable even within one geographical region. Chemical composition alone is not a characterizing factor for the standardization of propolis samples, where the biological efficacy is also an important factor in the determination of propolis quality. More than 300 compounds have been identified in propolis, however, they have not all been linked to biological activities. Therefore, propolis samples from various geographic regions with various biological activities have not been standardized. There is still a lot of work to be done to standardize propolis types to enable scientists to connect a particular chemical propolis type to a specific type of biological activity and formulate recommendations. Principal component analysis (PCA) or any other statistical tools

can be used to correlate the chemical composition to biological activity. However, in order for propolis to be accepted officially into the main stream of the healthcare system, it needs an accurate chemical standardization to guarantee its quality, safety, and efficacy.

1.1.5 *Pharmacological action, biological properties and toxicity of propolis*

Unlike many natural remedies, there is a massive database on the biological activity and toxicity of propolis indicating it has many antibiotic, antifungal, anti-inflammatory, antimycotic, antiseptic, antitumour, antiviral, anaesthetic, antioxidant, astringent, bacteriostatic and spasmolytic properties (Bankova *et al.*, 2000). Many studies have revealed that the observed effects might be the result of synergistic action of its complex constituents (Popova *et al.*, 2007). Although the composition of propolis collected from different geographic regions is diverse, there is not a wide variation in biological properties, although the diversity and difference in the compounds responsible for those activities is really surprising.

The most interesting recent trend in propolis research is the comparative study of biological properties of propolis from different geographic locations and different chemical composition, although the number of this type of studies is yet limited. A study by Kujumgiev *et al.* is a good example where the antifungal, antibacterial and antiviral activity in temperate zones is linked to flavonoids and esters of phenolic acids, while in tropical zones it is due to a different set of compounds (Kujumgiev *et al.*, 1999).

Trying to develop this comparative approach, Popova *et al.* used Analysis of variance (ANOVA) to investigate statistically significant correlation between biological activity and geographic origin of propolis samples. The antibacterial activity of three groups of propolis samples; European, Brazilian and Central American were compared, and results showed that despite the drastic differences in chemical composition propolis from Europe and Brazil had similar activity. Their antibacterial activity was significantly higher than that of Central American propolis. ANOVA was also applied to compare the toxicity of the same three propolis groups against *Artemia salina* (Crustaceae). In this case, there was no significant correlation between geographic origin and potential cytotoxicity (Popova *et al.*, 2004).

Sosa *et al.* (1997) observed that propolis samples inhibited the growth of some Gram-positive bacteria and *Candida albicans*, without affecting the growth of Gram-negative bacteria. Mirzoeva *et al.* (1997) tested propolis ethanolic extracts, and some of its active constituents such as flavonoids and cinnamic acid derivatives, on Gram positive *Bacillus subtilis* and Gram negative *Escherichia coli* and *Rhodobacter sphaeroides* and they found that the propolis had antimicrobial activity against both, but it was more active against Gram positive than Gram negative bacteria. In addition, the bactericidal effect of propolis is species dependent and exerts its activity by inhibition of bacterial motility and dissipation of the membrane potential.

(Bankova *et al.*, 2015) stated that regardless of the origin of propolis all types must have antibacterial activity because it is vital for the bee community. Moreover, the antibacterial activity of Brazilian propolis towards *Staphylococcus aureus*, which is used as an indicator strain, was correlated to volatile phenolic compounds and further

investigation revealed the activity of labdane type diterpenic acids such as isocupressic acid, acetylisocupressic acid, imbricatoloic acid and communic acid, together with syringaldehyde (Bankova *et al.*, 1996). In 2000, Sforcin *et al.* reported that the activity of Brazilian propolis is not affected significantly by season.

With regard to *Helicobacter pylori* the causative agent of gastric ulcer (Hashimoto *et al.*, 1998) found that phenolics such as *p*-coumaric acid, 3-prenyl-4-dihydrocinnamoyloxy cinnamic acid and artepillin C separated from Brazilian propolis showed significant activity against *H. pylori*.

(Valcic *et al.*, 1999) isolated 17 phenolic compounds that belong to the phenylpropane, benzaldehyde, dihydrobenzofuran or benzopyran classes from Chilean propolis; all were active against *Mycobacterium* species.

(Rubio *et al.*, 1999) isolated a novel polyisoprenylated benzophenone from an ethanol extract of Cuban propolis, which showed significant antimicrobial and antifungal activity against a variety of bacteria and yeasts. Moreover, antifungal activity against dermatophytes and *Candida* species was also reported (Ghaly *et al.*, 1998; Sawaya *et al.*, 2002).

Generally, the potency of the antimicrobial activity of propolis is highly dependent on the extraction solvents and extracts show a wide range of antimicrobial activities. Glycerine solutions show little inhibition of Gram-positive bacteria, whereas ethanol and propylene glycol solutions show good activity against yeasts (Tosi *et al.*, 1996).

Previous reports have also shown that both alcoholic and aqueous extracts of propolis have strong antioxidant and hepatoprotective activity. They reduced liver

damage induced either chemically or immunologically. This was attributed to their high content of flavonoids such as 3,5,7-trihydroxy-4'-methoxyflavanol, betuletol, kaempferide and ermanin, and phenolic constituents such as dicaffeoylquinic acid derivatives. The mechanism of hepatoprotection by labdane type diterpenoids isolated from Brazilian propolis such as isocupressic acid, agathic acid, 15-acetoxyisocupressic acid, and cupressic acid is not yet clear (Banskota *et al.*, 2001).

Propolis has also been reported to have antitumour activity and cytotoxicity since 1995. Matsuno isolated and tested a new clerodane type diterpene from Brazilian propolis, that has potent cytotoxic activity towards human hepatocellular carcinoma, human lung carcinoma, and reduced the incidence of skin tumours by inhibition of DNA synthesis in a *de novo* pathway (Matsuno, 1995). A small and simple molecule caffeic acid phenethyl ester (CAPE), which is isolated from many types of propolis, possessed significant antioxidant activity and cytotoxicity towards various tumour cell lines and antitumour activity against human leukaemia, and different oral tumours (Grunberger *et al.*, 1988).

One of the beneficial traditional medicinal properties of propolis is as an anti-inflammatory agent. (Krol *et al.*, 1996) studied the anti-inflammatory activity of ethanolic extract of propolis, and 19 phenolic compounds. They reported that caffeic acid phenylethyl ester (CAPE) was the most potent and was believed to be responsible for anti-inflammatory activity.

Three flavone derivatives galangin, kaempferol and kaempferide showed a strong but lesser anti-inflammatory activity (Krol *et al.*, 1996). The mechanism of action is thought to be through suppression of prostaglandin, leukotriene generation and the

lipxygenase pathway of arachidonic acid metabolism during inflammation (Mirzoeva & Calder, 1996).

Other biological activities have been reported such as the antihyperalgesic and analgesic effect of propolis collected in the southern part of Brazil and Bulgaria in rats and mice (de Campos *et al.*, 1998; Paulino *et al.*, 2003) through non-opioid mechanism. Significant anti-HIV activity of triterpenoid called moronic acid isolated from Brazilian propolis was reported by (Ito *et al.*, 2001).

Moreover, propolis has been found to lower blood pressure and cholesterol levels; however, more clinical studies are required to prove these claims. Due to the previously mentioned activities, propolis has been used in many over the counter pharmaceutical preparations, mainly topical creams, ointments, lotions, solutions, capsules, mouthwash and in powder form, it is also marketed as tablets, and chewing gum. In general, propolis is considered as relatively non toxic, but occasionally the bees may mix hazardous substances such as asphalt with the propolis from road construction sites (Alqarni *et al.*, 2015) or heavy metals that could accumulate and cause toxicity. Beekeeper's contact dermatitis has been reported and directly linked to poplar resins and it is believed to be caused by 1,1-dimethylallyl caffeic acid (Marcucci, 1995).

The fact that sometimes different chemistry leads to the same type of activity and in some cases even to an activity of the same order of magnitude is surprising (Bankova, 2005) **Table 1-1**. Nonetheless, it is important to have detailed and reliable comparative data on every type of biological activity, correlated with chemical data, in order to decide whether some specific areas of application of a particular propolis

type can be formulated as preferable for a particular indication. The biological tests have to be performed with chemically well characterized and, if possible, chemically standardized propolis. Such detailed comparative investigations are a challenge to propolis researchers. The most important recent developments in propolis research including studies based on bioassay-guided chemical analysis represent a promising trend in propolis research aimed at meeting this particular challenge.

Table 1-1: Compounds responsible for the biological activity of different propolis types (Bankova, 2005).

Activity	European (poplar)	Brazilian (Baccharis)	Cuban	Taiwanese
Antibacterial activity	Flavonone, flavones phenolic acids and esters	Prenylated <i>p</i> -coumaric acid, diterpenes	Prenylated benzophenones	Not tested
Anti-inflammatory Activity	Flavonone, Flavone, phenolic acid and esters	Unidentified	Not tested	Not tested
Antitumor activity	CAPE ester	Prenylated <i>p</i> -coumaric acid, diterpenes	Prenylated benzophenones	Prenylated flavonones
Hepatoprotective activity	CAPE ester, ferulic acid	Prenylated <i>p</i> -coumaric acid, flavonoids, lignans, caffeoyl quinic acid	unidentified	Not tested
Antioxidant activity	Flavonoids, phenolic acids and their esters	Prenylated <i>p</i> -coumaric acid, flavonoids	Prenylated benzophenones	Prenylated flavanones
Allergic activity	3,3-Dimethylallyl caffeate	Not tested	Not tested	Not tested

1.1.6 *Bee Species and Propolis*

As mentioned above, species, subspecies and varieties of bees have a major effect on chemical composition and quality of propolis. The genus *Apis* is subdivided into ten species, among them *Apis mellifera* (honeybee), the most common and widely studied species spread mainly through Europe, Africa and Asia. All other species are distributed in Asia. *A. mellifera* is subdivided into about 25 subspecies according to morphometry, behaviour, and biogeography (Arias & Sheppard, 2005).

Another important species is Meliponinae (Brazilian stingless bee species) which is restricted only to the tropics. Important examples are *Melipona scutellaris*, which produces geopropolis, which is rich in benzophenones but contains no flavonoids, and thus has a lower antibacterial activity than *Apis mellifera* propolis. *Melipona fasciulate* produces geopropolis containing high concentrations of polyphenols, flavonoids, triterpenoids, saponins, and even tannins (Dutra *et al.*, 2014)

Despite the fact that different species of honeybee prefer different plants, the chemical profile of propolis produced by the same species is not always the same. For example, Africanized *A. mellifera* produces both Brazilian green and red propolis and these types of propolis are largely different; the first is rich in prenylated phenylpropanoids, while the second's main components are isoflavonoids. The differences are due to the different plants from which the propolis is collected, namely *B. dracunculifolia* and *D. ecastophyllum* for green and red propolis,

respectively. Therefore, the variant chemical composition of propolis depends on the bees' preferences for different botanical sources and the species and varieties of bees.

1.2 Trypanosomes

1.2.1 Definition

Trypanosomatidae is a protozoan organism family of the order Kinetoplastida which includes six genera: *Herpetomonas*, *Leptomonas*, *Blastocrithidia*, *Crithidia*, *Trypanosoma* and *Leishmania* (Smyth, 1994). Among them, *Trypanosoma* and *Leishmania* are considered as the most relevant specimens for human and animal health while *Crithidia* is related to bees' infection. The genus *Trypanosoma* contains a large number of parasitic species that infect vertebrates, causing trypanosomiasis.

In humans, two types have been reported: Human African Trypanosomiasis (HAT) or sleeping sickness, which threatens millions of people in 36 countries in sub-Saharan Africa, caused by infection with *Trypanosoma brucei* transmitted to humans by the tsetse fly (*Glossina* genus), and Chagas disease (American trypanosomiasis) in Latin America caused by *Trypanosoma cruzi* carried by an insect vector, a triatomine bug. The latter occurs in 21 Latin American countries from Mexico to Argentina (Barrett *et al.*, 2003). The World Health Organisation (WHO) considers both of the diseases as neglected tropical diseases (Fairlamb, 2003).

Trypanosoma brucei has adopted a variety of strategies to evade elimination by the host immune system, by a process called antigenic variation, and its unique cell structure enables the parasite to invade and penetrate the host cells with little or no difficulty, resulting eventually in cell rupture, release of trypomastigotes, and their subsequent multiplication (Cross, 1978). *Trypanosoma cruzi* cells differ from

Trypanosoma brucei in that no replication occurs in the bloodstream, where cells are only able to replicate if another cell has been penetrated (Vickerman, 1985).

As shown in **Figure 1-7**, *Trypanosoma brucei* is able to survive in two markedly different environments: the tse-tse fly and the mammalian host, which have different nutrients and energy sources. Thus in blood stream the energy is generated using D-glucose through the glycolysis process, whereas in the procyclic (insect) stages energy is generated from L-proline (Coustou *et al.*, 2005).

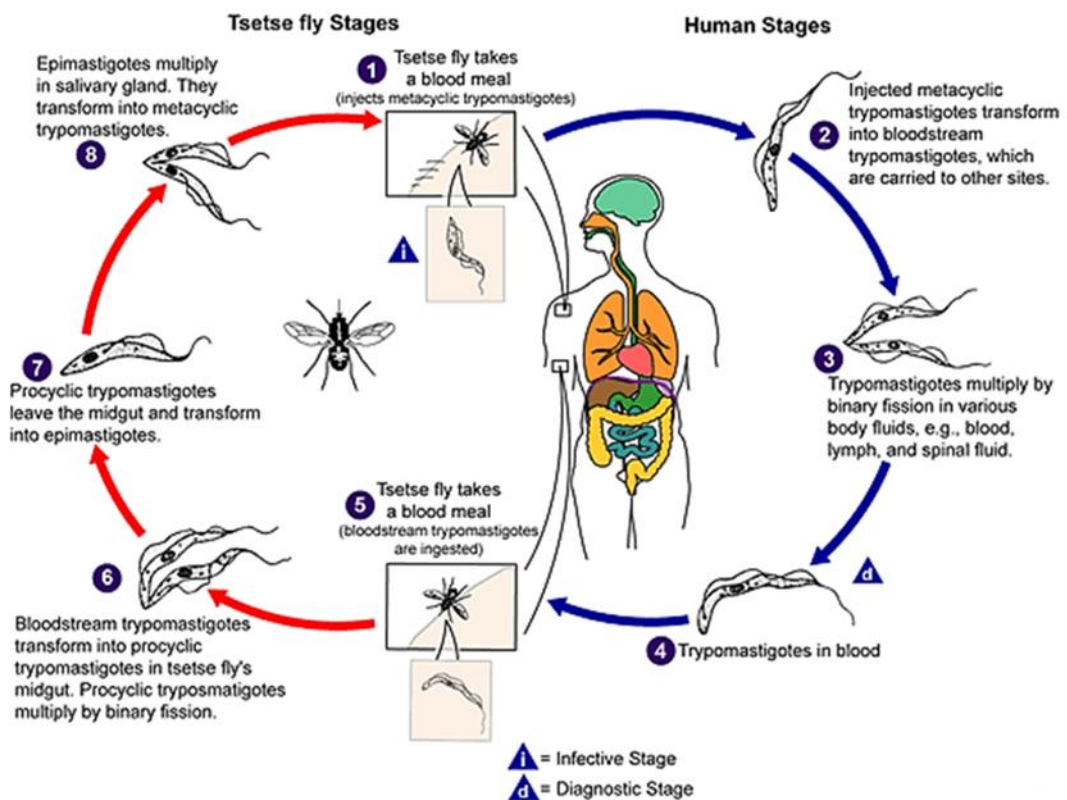


Figure 1-7: The life cycle of *Trypanosoma brucei* (www.dpd.cdc.gov/dpdx).

HAT is characterized by extracellular parasites in human blood serum and lymphatic fluid in the early stages of the disease, with cerebral fluid inclusion in the late stages. It is caused by two morphologically identical parasites. *Trypanosoma brucei gambiense* accounts for more than 98% of reported cases and is found in 24 countries in West and Central Africa, causing a more chronic condition with slow disease progression over several years. Eventually, when the central nervous system is affected more symptoms emerge. The other type is *Trypanosoma brucei rhodesiense* found in 13 countries in eastern and southern Africa which has a fast onset of acute disease with neurological impairment, leading to coma and death often within weeks. Only Uganda presents both forms of the disease, but in separate zones (WHO, 2016).

1.2.2 *Epidemiology of the disease*

Since many of the affected populations live in remote and rural areas with limited access to health services, this can cause delay of diagnosis and treatment; therefore, there is increased mortality in affected communities **Figure 1-8**.

According to WHO in 1998, the number of reported cases was 40,000. However, estimates suggest that 300,000 cases were undiagnosed and therefore untreated. The most recent reports indicate that the prevalence reached 50% in several villages in Angola, South Sudan, and the Democratic Republic of the Congo, which accounts for 89% of the cases reported in 2013. Sleeping sickness was the first or second greatest cause of mortality in those communities, even ahead of HIV/AIDS.

In 2009, after continued control efforts, the number of cases reported dropped below 10,000 for the first time in 50 years. This decline in the number of cases has

continued with 6,314 new cases reported in 2012. However, the estimated number of actual cases is about 20,000 and the estimated population at risk is 65 million people. Since the number of new human African trypanosomiasis cases reported between 2000 and 2012 dropped by 73%, the WHO Roadmap has targeted its elimination as a public health problem by 2020 (WHO, 2016).

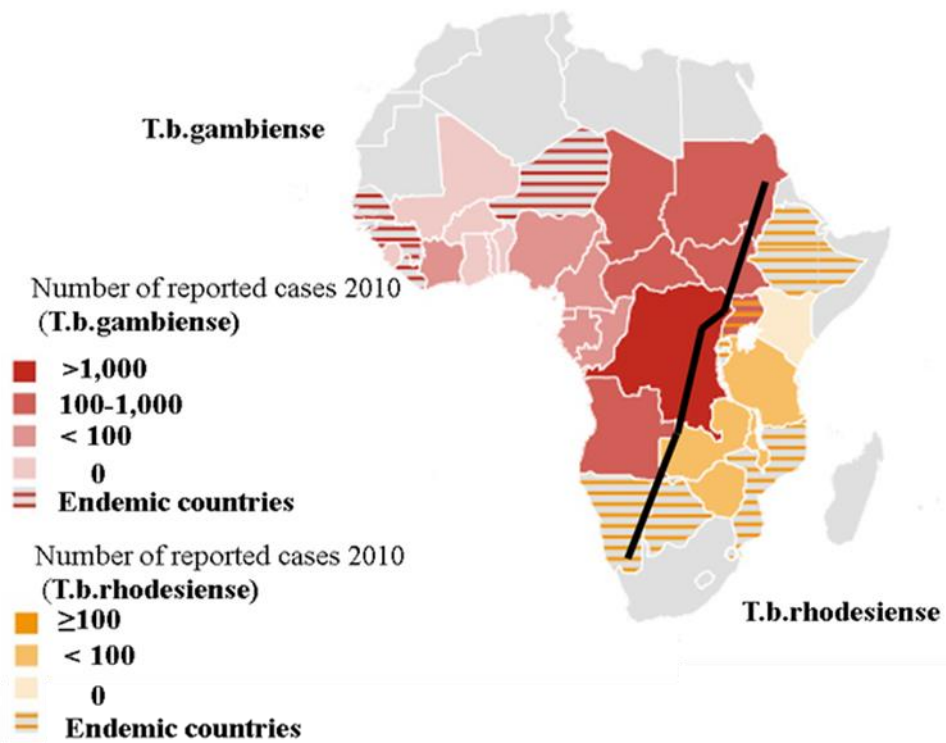


Figure 1-8: Sleeping sickness national control programme, adapted from WHO annual country report in 2010.

1.2.3 *Treatment of Human African Trypanosomiasis (HAT)*

HAT was one of the first diseases to be targeted by synthetic drugs, by Paul Erlich in the 1920s (Barrett *et al.*, 2007). It was a major hindrance for Europeans in the late 19th to the early 20th century, marring the colonization of Africa. Consequently, research was funded to develop drugs to cure the disease, but when Europe withdrew from Africa after the Second World War, it was no longer in the economic interests of the Western world to fund research into a disease that didn't affect their people, leading HAT to be one of today's more neglected diseases. New drugs for HAT are rare and the last compound to be available for treatment of HAT was brought out in the 1990s.

However, the choice of treatments of HAT is dependent on the subspecies involved, and the disease stage, which is divided into two pathological phases: early stage (Hemolymphatic stage), where symptoms begin with irregular fevers, headaches and joint pains, but can develop to generate other complications including enlarged lymph glands and spleen, local oedema and cardiac abnormalities. Then when parasites cross the blood–brain barrier, the disease enters the late stage (Encephalitic stage). Here, a series of neurologically related symptoms are observed, including severe headaches, alterations to sleeping patterns, personality change, mental function impairment, and weight loss. Without treatment, patients eventually fall into a coma and die (Barrett *et al.*, 2003).

There are numerous drawbacks with the drugs currently available for the treatment of HAT. They are old, highly toxic with severe side effects, which can make compliance difficult, leading to resistance development when a full treatment course

is not completed. Another reason for treatment failure could be due to inappropriate prescription. Not all drugs are suitable for late stage disease, as not all drugs can cross the blood–brain barrier (Hawking, 1940). Diagnosis of late stage disease is achieved through lumbar puncture and analysis of cerebral spinal fluid. This is often inaccurate; therefore, an unsuitable drug is prescribed.

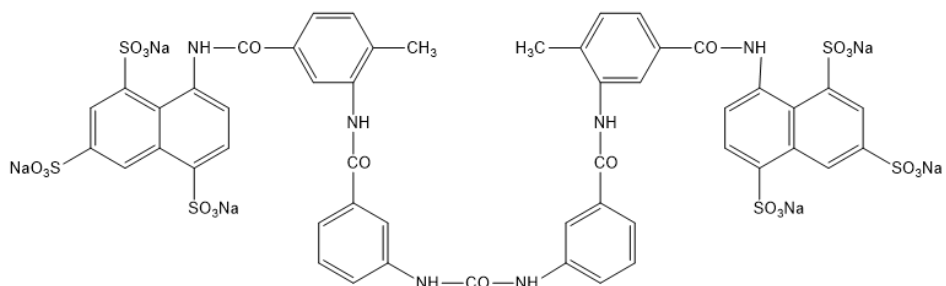
At the early stage drugs in current use include pentamidine (for *T. b. gambiense*), suramin (for *T. b. rhodesiense*), and neither compound can cross the blood–brain barrier and therefore cannot be used in late stages effectively. For late stages, melarsoprol (for both *T. b. gambiense* and *T. b. rhodesiense*), however, it is a highly toxic arsenical, and drug resistance is a major issue, eflornithine in contrast is relatively safe, but this compound is effective only against *T. b. gambiense* and the cost of treatment is problematic in underdeveloped countries **Table 1-2**.

Currently, Phase III clinical trials are evaluating the efficacy of a drug called Nifurtimox, which is a cheap and orally administered drug. It was registered in 1977 for the treatment of Chagas or American Trypanosomiasis. It showed promising contradictory results in the treatment of the cerebral stages of *T. b. gambiense* especially when combined with eflornithine. Recently, it was recommended by the WHO as a front-line treatment for infections with *T. b. gambiense*. But still there is a shortage of information regarding the toxicity of this combination and its activity against *T. b. rhodesiense* (Priotto *et al.*, 2009).

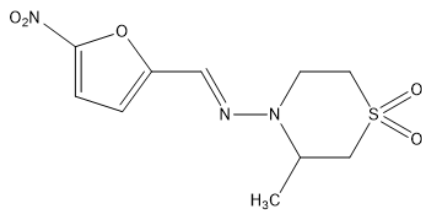
Table 1-2 : An overview of trypanocidal drugs and the problems associated with them.

Drugs	Activities	Limitations	Structure
Suramin Sodium (Early 1920s)	Effective against early stage of <i>T. b. rhodesiense</i>	Ineffective against early stage of <i>T. b. gambiense</i> and late stage of both HATs	Sulphonated naphthylamine
Pentamidine (1940)	Effective against early stage of <i>T. b. gambiense</i>	Ineffective against early stage of <i>T. b. rhodesiense</i> and late stage of both HATs	Aromatic diamine
Melarsoprol (1949)	Effective against late stage of both HATs	Toxic (kills up to 5% of patients), Resistance observed in field.	Trivalent organic arsenical
Eflornithine (1981)	Effective against late stage of <i>T. b. gambiense</i>	Ineffective against late stage of <i>T. b. rhodesiense</i> , difficult dosing scheme, and cost of hospitalization.	DL-alpha-difluoromethylornithine

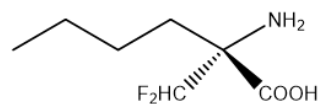
The most commonly used treatments for HAT are illustrated in **Figure 1-9** and a description of each drug is detailed below.



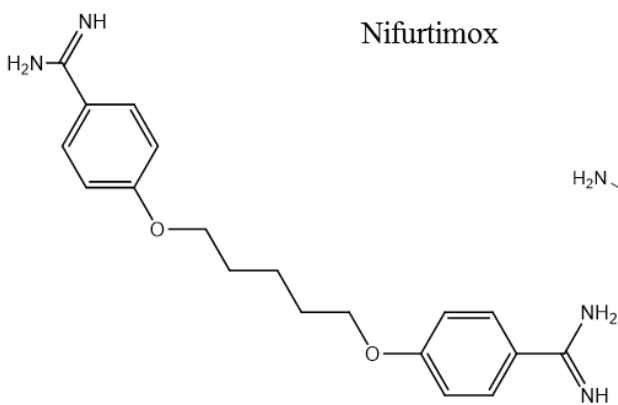
Suramin



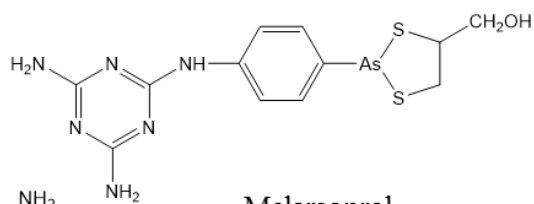
Nifurtimox



Eflornithine



Pentamidine



Melarsoprol

Figure 1-9: Structures of drugs in current use against human African trypanosomiasis.

1.2.3.1 Suramin

Suramin was the first drug used against HAT in 1922. Following observations that trypan dyes had trypanocidal activity. It is a symmetrical poly sulphonated naphthalene derivative of urea (Barrett *et al.*, 2007), discovered by Oskar Dressel and Richard Kothe at Bayer in 1916 (Haberkorn *et al.*, 2001). It is also effective against microfilariae and hormone refractory prostate cancer (Delespaux & de Koning, 2007). It is a large negatively charged polyanion, this appears to prevent it from freely crossing biological membranes, and hence hinders transport across the blood–brain barrier, and thus treating late stages of the disease, on the other hand it can promote binding to positively charged enzymes, such as those involved in glycolysis. Presumably the actions of suramin may be related to inhibition of Low density lipoprotein (LDL) uptake as the negative charge binds to the positively charged LDL receptor (Vansterkenburg *et al.*, 1993).

Some researchers, however, believe that suramin readily complexes with blood serum proteins such as albumin and enters *T. brucei* through receptor-mediated endocytosis (Delespaux & de Koning, 2007). Suramin is extremely stable in humans, not metabolized in the liver, and it is slowly excreted in the urine. These properties contribute to the relatively long half-life of 35–60 days. It has a low toxicity; this may explain why it has been used to treat early-stage *T. b. rhodesiense* for 90 years.

Limitations of suramin are that it cannot be used to treat *T. b. gambiense*, or late stage HAT. Another problem is the emergence of suramin-resistant strains of *T. brucei*, *in vitro*, but the resistance mechanisms underlying this phenotype have not been established yet (Scott *et al.*, 1996).

1.2.3.2 Pentamidine

Pentamidine is an aromatic diamidine and was first used against early stage of *T. b. gambiense* in 1940s (Delespaux & de Koning, 2007). It has been heavily used as a prophylactic as well as a curative agent as a second-line drug when suramin has failed (Pépin & Milord, 1994). Antimony resistant visceral and cutaneous leishmaniasis and *Pneumocystis carinii* infections also can be treated with pentamidine. As pentamidine is used on more than one parasitic infection, resistance has emerged and has been reported in *Leishmania donovani* (Sundar, 2001). Pentamidine cannot be used in late stages of the disease because it is positively charged and binds easily to blood serum proteins, as a result, it poorly crosses the blood brain barrier BBB. It is readily metabolized by the mammalian cytochrome P450 system, but not by the trypanosomal system, and excreted in urine. This explains its short half-life of 6.4–9.4 hours (Conte *et al.*, 1987).

The mode of action for pentamidine is not fully understood and seems to be multifactorial. It is believed that it exerts its effects via binding to negatively charged molecules such as DNA, so this may explain its wide range of effects (Simpson, 1986). It has also been proposed that pentamidine inhibits mitochondrial topoisomerase II activity, leading to the linearization of the kinetoplast DNA and the generation of dyskinetoplastic trypanosomes that will break down and eventually disappear (Shapiro & Englund, 1990). Other suggested mechanisms include inhibition of *T. brucei* S-adenosylmethionine decarboxylase or Ca^{2+} -ATPase activities, by affecting mitochondrial membrane potential, or by acting to uncouple oxidative phosphorylation. Uptake of pentamidine in *T. brucei* occurs through at

least three active transporters; the P2 aminopurine permease (TbAT1), the high affinity pentamidine transporter (HAPT1) and the low affinity pentamidine transporter transporters (LAPT1) (de Koning & Jarvis, 2001).

One of the major drawbacks of pentamidine is that it is not readily absorbed in the intestine, which makes administration difficult. Severe side effects have been reported, including anaphylactic shock, severe cutaneous reactions, neurotoxic signs, and cases of renal failure. Hypotension and hypoglycaemia are the most common side effects reported.

1.2.3.3 Melarsoprol (MelB)

Melarsoprol was introduced in 1949 by Ernst Friedheim (Bacchi, 1993) and is currently the only treatment used against the late stages of both forms of HAT. It is a trivalent melaminophenyl-based arsenical compound and is a prodrug where the active trivalent arsenic moiety is masked with 2,3-dimercaptopropanol which is metabolized in the body to form melarsen oxide, a trypanocidal agent (MelOx) (Delespaux & de Koning, 2007).

Melarsoprol appears to act by forming stable adducts with thiols, particularly with dihydrotrypanothione to form MelT which then acts as a competitive inhibitor for trypanothione reductase, an essential enzyme that protects *T. brucei* from oxidative stress (Bacchi, 1993). Adducts are also formed with lipoic acid (Barrett *et al.*, 2007). Another minor mode of action is through targeting glycolysis by inhibition of the pentose phosphate pathway enzymes such as the fructose-6- phosphate- 2-kinase enzyme (Bacchi, 1993). Melarsoprol is a highly toxic drug, infamously killing

around 5% of people treated, accompanied with serious side effects such as reactive encephalopathy, convulsions, fever, loss of consciousness, rashes, bloody stools, nausea and vomiting. It is administered intravenously but injections are very painful as the drug is dissolved in propylene glycol (Barrett *et al.*, 2007).

1.2.3.4 Eflornithine

DL- α -Difluoromethylornithine (DFMO) was originally developed in the 1970s as a treatment for cancer in humans (Heby *et al.*, 2007). It acts as an irreversible inhibitor of ornithine decarboxylase (ODC) by forming adducts in the active site of the enzyme (Poulin *et al.*, 1992). This inhibition leads to a decrease in putrescine and spermidine that conjugate with two molecules of glutathione to form trypanothione, a unique and vital antioxidant polyamine essential for trypanosomatid survival (Fairlamb *et al.*, 1987). Parasites treated with eflornithine are not actually killed by the drug directly, but are forced to differentiate to the non-replicative stumpy forms, which can be killed by the host immune system (Barrett *et al.*, 2007). Eflornithine has been in use since 1990 (World Health Organisation, 2006) and is effective against *T. b. gambiense* in both stages of the disease, although it is ineffective against *T. b. rhodesiense* for reasons that are not entirely clear, but may be due to faster ODC turnover rates in the latter parasite (Phillips *et al.*, 1987). The poor transport across the blood–brain barrier increases the dose required for treatment, making it difficult to administer, and it requires medical supervision to ensure compliance (Delespaux & de Koning, 2007). One other disadvantage with eflornithine use in sub-Saharan Africa is that a viable immune system is required to clear the parasite. With the increasing levels of the immunosuppressive disease such as HIV/AIDS, the drug is likely to become less useful in areas where HIV is more prevalent.

In conclusion, adequate vaccines against trypanosomatid infections have yet to be developed. The drugs currently available for chemotherapeutic intervention are mostly unsatisfactory mainly because of their lack of specificity, toxicity to humans, and, in many cases, developed parasite resistance. Thus, the priorities in tropical medicine research are the identification and characterization of parasite-specific biomolecules that play relevant physiological roles and thus might be exploited as selective agents. Thus there is still scope for the isolation of active natural products for treatment of HAT, and the success of artemisinin as a treatment for malaria provides an indication that a natural product can provide a useful new treatment (Mcintosh *et al.*, 2010).

1.2.4 Previous studies on activity of propolis against Trypanosomiasis

A number of previous studies have tested propolis against *Trypanosoma* species, but most of these studies have largely focused on the use of extracts rather than isolated compounds. (Salomão *et al.*, 2004) compared the microbiological activity of Brazilian and Bulgarian propolis and analysed their chemical composition by high temperature- high resolution gas chromatography-mass spectrometry (HT-HRGC-MS), and found that although they were of totally distinct compositions, they were both active against *Trypanozoma cruzi*, and some pathogenic fungi. As stated by (Salomão *et al.*, 2011), the Brazilian green propolis ethanolic extract was most effective against the intra cellular amastigote stage of the parasite, having an IC₅₀ value of 8.5 µg/mL with no damage to the host cells.

Extracts from two samples of Portuguese propolis collected from different areas and their potential floral sources were investigated against *Plasmodium falciparum*, *Leishmania infantum*, *Trypanosoma brucei* and *Trypanosoma cruzi* (Falcão *et al.*, 2014). IC₅₀ values were mainly <10 µg/mL and the greatest activity of 1.8 µg/mL being against *T. brucei*.

The effect of an extract of Brazilian propolis on *Trypanosoma evansi* *in vitro* and *in vivo* was investigated (Gressler *et al.*, 2012). The trypanocidal activity of propolis extract was dose-dependent, and IC₅₀ value for the extract *in vitro* was found to be 10 µg/mL, but although the propolis was ineffective in curing rats infected with *T. evansi* at the tested dose it was able to prolong the life of infected rats.

The activity of the 15 extracts of Brazilian propolis from *Apis mellifera* collected from different regions, extracted using ethanol, water, and a combination of both solvents, was assayed against blood stream trypomastigotes of *Trypanosoma cruzi*. Multivariate analysis was applied to evaluate the efficiency of the different extracts and the trypanocidal activity. The extracts prepared by reflux in a soxhlet using 100% ethanol showed lower content of bioactive compounds and consequently lower trypanocidal activity than other extracts (Barbosa *et al.*, 2004).

Two different extracts of Libyan propolis were investigated and demonstrated quite high activity against *Trypanosoma brucei*, further purification yielded three diterpenes, 13-epitorulosal, acetyl-13-epi-cupressic acid and 13-epi-cupressic acid, which were found to be highly active (Siheri *et al.*, 2014).

The chemical composition and biological activity of Saudi Arabian propolis was investigated. Four compounds were isolated, a diterpene propsiadin ((ent)-2-oxo-

kaur-16-en-6,18-diol) along with the flavonoids 3,4-dihydro-2-(3,4-dihydroxyphenyl)-2H-chromene-3,7-diol, psiadiarabin and the diterpene psiadin and all were found to exhibit a moderate activity against *Trypanosoma brucei* (Almutairi *et al.*, 2014).

Therefore, it is apparent that antiprotozoal activity of propolis is common to propolis samples from many regions and propolis could be a potential drug in the treatment of trypanosomiasis.

1.3 Techniques used in propolis analysis

1.3.1 Introduction

The composition of propolis is highly complex and variable, since it is composed of bees wax and secondary metabolites from plant origin, therefore, cannot be used as a raw material to get the maximum efficiency. In order to isolate individual compounds, it must undergo many processes: starting from extraction with suitable solvents to remove the inert materials, preserve the active compounds in fractions, ending with the identification and biological testing of the purified compounds. One of the most commonly used extraction methods is maceration, where propolis is soaked in the solvent of extraction in a closed container and left at normal temperatures. Maceration is usually used in combination with sonication by applying sound energy to agitate the particles in samples to accelerate the extraction. Other extraction techniques including hydro distillation and soxhlet extraction. They were not used in the current study due to involvement of high temperature and moisture to avoid any degradation or instability issues. Since there is not enough data regarding

thermal stability of propolis so far except for the flavonoids apigenin, chrysin and galangin, and propolis from Amaicha del Valle in Argentina which were found to be stable from room temperature to 120 °C (González *et al.*, 2009). In contrast, another study on green propolis from Brazil showed that the phenolic content decreased by 30% during exposure to heat during a spray-drying process (Da Silva *et al.*, 2011).

Many analytical techniques have been involved in the analysis of propolis and purification, ranging from simple traditional phytochemical methods such as column chromatography to advanced and modern methods including preparative or semipreparative chromatography in order to fractionate and isolate components; to even more advanced spectrometric methods including high performance liquid chromatography (HPLC) coupled to different detectors such as evaporative light scattering detector (ELSD), ultraviolet (UV), and high resolution mass spectrometry (HRMS). In addition to gas chromatography- mass spectrometry (GC-MS), and finally nuclear magnetic resonance spectroscopy (NMR), which is mainly employed to structurally elucidate the isolated components, have also been widely used.

Generally, all chromatographic techniques aim to separate compounds based on their size, shape or charge and their ability to interact with a surface or stationary phase (Heftmann, 1992). The separation is based on the interactions between the analyte and two phases (mobile phase: MP, and stationary phase: SP). Separation of the sample is based on the polarity of components and their partitioning between the active sites on SP and MP (Salituro and Duresne, 1998). The choice of technique depends generally on physicochemical properties like solubility, volatilities and ionizability of the compounds to be separated. Therefore, selectivity is achieved by varying either the MP or SP or both.

In this research, many chromatographic techniques were employed in order to either detect or separate the compounds in the crude extracts of propolis.

1.3.2 *Medium pressure liquid chromatography (MPLC)*

MPLC is one of the various preparative column chromatography techniques that can be used on a large scale to separate compounds in a mixture. It is widely used for purification of naturally occurring compounds that are the basis of many commonly used pharmaceuticals, which are the backbone of the growing nutraceutical market (Hans jorg Part, 2011). It is performed under pressure ranging from 5–20 bars with an adjustable flow rate that allows the elution of the sample at a faster rate than other techniques such as open-column chromatography (CC), low-pressure liquid chromatography (LPLC). It is considered as flexible technique where different types of stationary phases either normal phase, where the columns are packed with silica with variable particle sizes, or reversed phase (C18) can be employed. This separation method can be effectively used in combination with other preparative methods such as CC, LPLC or preparative high performance liquid chromatography in order to get higher purity compounds.

More details about the experimental differences between chromatographic methods are given below in **Table 1-3**.

Table 1-3 : Difference between various preparative column chromatographic techniques, SP: stationary phase, RP: reversed phase, atm: atmospheric (Hostettmann & Terreaux, 1996).

Technique	SP particle size (μm)	Pressure (bar)	Flow rate (mL/mi)	Sample amount (g)	Solvent	General
Open-column chromatography	63-200	atm	1-5	0.01-100	General solvent used	Frequent packing; RP not possible
Flash chromatography	40-63	1-2	2-10	0.01-100	General solvent used	Frequent packing
Low pressure LC	40-63	1-5	1-4	1-5	More solvent required	Prefilled columns
Medium pressure LC	15-40	5-20	3-16	0.05-100	More solvent required	Infrequent packing
Preparative HPLC	5-30	>20	2-20	0.01-1	High purity solvent required	Higher resolution

MPLC is reliable and effective in the separation of compounds with different polarities from crude extracts or semi-purified fractions with varying amounts in a relatively short time. It is widely used in many applications due to simplicity and availability of the instrumentation, together with ease of recycling of packing

materials and low maintenance costs (Loibner & Seidl, 1997). Researchers usually develop a method to optimize the conditions before it is transferred to MPLC. Therefore, in case of normal phase it is fairly typical to first run TLC plate experiments, while in reversed phase flash chromatography this could be problematic due to the generation of non-representative retention factor (R_f) data from commercially available reversed phase TLC plates; therefore, analytical reversed phase HPLC could be used, then scaled up to be transferred to MPLC.

The main components of an MPLC system are shown in the schematic diagram below

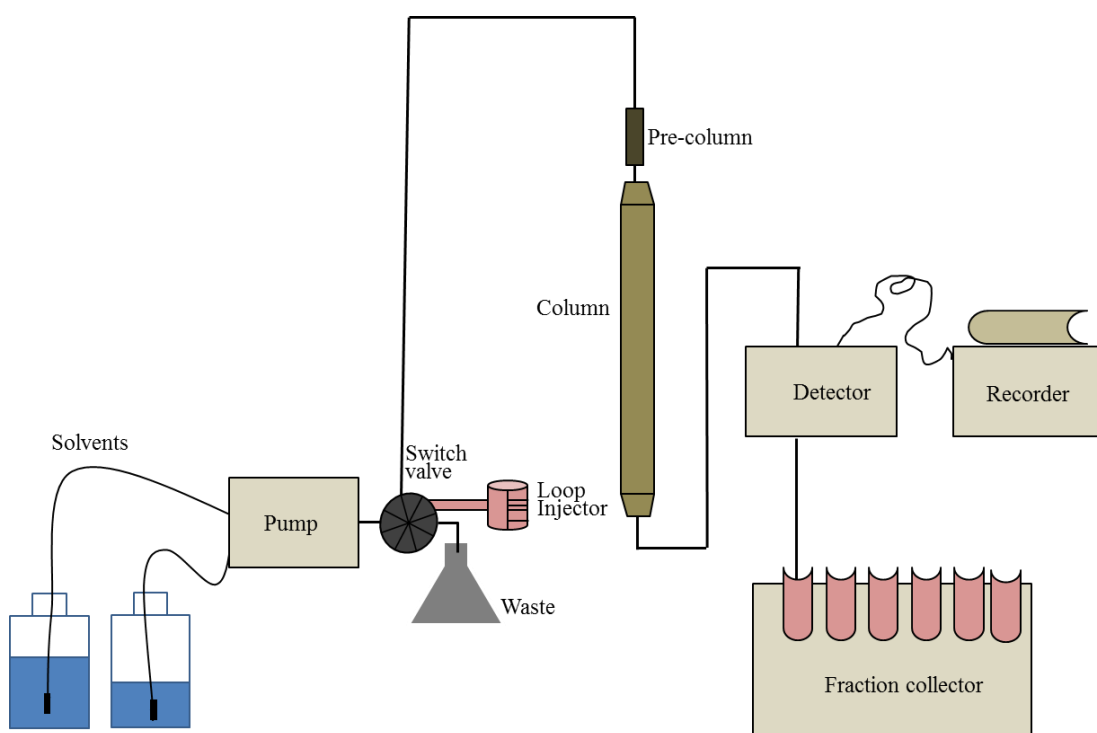


Figure 1-10: The main components of medium pressure liquid chromatography system (Hostettmann & Terreaux , 1996).

In this research, for purification purposes, two systems were employed: A Grace Reveleris® flash chromatography system equipped with UV/VIS and ELSD detectors which will be described in detail in the methodology chapter. The other system is the Gilson Semi-preparative chromatography system which is part way between an analytical HPLC and preparative LC, it was useful when the quantity of sample was too small to be purified using the Grace MPLC system. The Gilson HPLC system is an automated system connected to a UV detector, which can be adjusted to five channels. It performs sample injection, peak detection, fraction collection and can perform re-injection of collected fractions for more purification.

It has the advantages of automated as well as manual fraction collection, displays of a chromatogram, and uses up to five UV channels detectors, but it lacks an ELSD detector which is very important in some samples that do not have UV absorbing compounds.

1.3.3 *Gas chromatography with mass spectroscopy detection (GC-MS)*

Gas chromatography was first developed in the 1950s and, shortly after this, it was combined with mass spectrometry (GC-MS). It is a powerful, and highly sensitive technique that can effectively analyse volatile and semi volatile thermally stable compounds, such as terpenoids, hydrocarbons, short chain fatty acids and fatty acid esters.

It is used to profile and hence provide an overall view of propolis composition and (Greenaway *et al.*, 1991) were able to analyse 150 compounds of which 28 were identified for the first time in propolis by using GC-MS.

The sample is dissolved in volatile organic solvent, then injected into the GC inlet, where it is vaporized and swept into the column by the carrier gas which is usually helium. The compounds separate depending on their interactions with the stationary phase and the carrier gas. The column passes into a heated transfer line to the ion source and here ions are generated using the electron impact ionization technique (EI), in which components will collide with high-speed electrons resulting in positively charged ions that can be detected. EI is operated at high energy (70eV) which enhances sensitivity, and spectra obtained at this energy level are comparable between instruments (Hübschmann, 2008); components of a GC-MS system are shown in **Figure 1-11**. The identification of components is based on the molecular weight of the fragments obtained, which are compared with a GC library such as the NIST (National Institute of Standards and Technology) library that will give the approximate chemical structures of the components. The technique has the disadvantage of a requirement for derivatization in order to analyse relatively polar compounds such as flavonoids, phenolic acids and their esters due to their low volatility in GC-MS. Additionally, high molecular weight compounds do not transmit well through a GC column, therefore their percentage occurrence may be seriously underestimated.

In propolis though, there are several compounds that are not volatile enough even after derivatization, such as some flavonoids and polyphenols for analysis by GC-MS. Therefore, HPLC is a popular method that can be used to analyse these compounds.

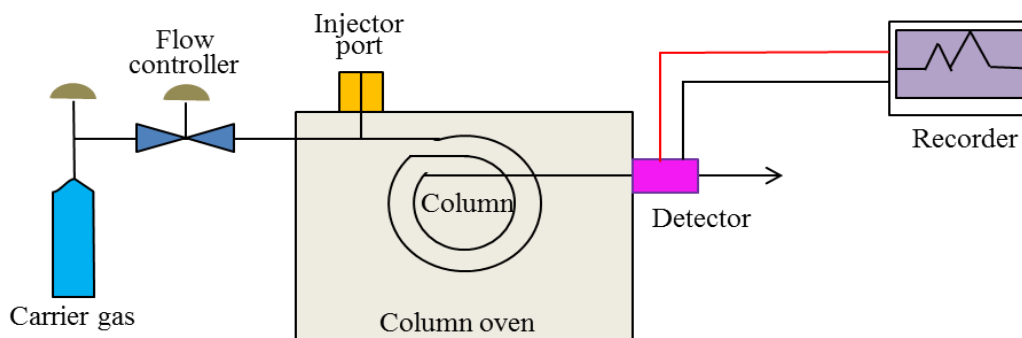


Figure 1-11: Schematic diagram showing the component of a GC-MS system.

1.3.4 High performance liquid chromatography (HPLC)

HPLC has become the most popular chromatographic technique used nowadays, because it is not limited by the volatility or stability of the compounds in the sample. Separation in HPLC is asample with the MP, which determines the degree of migration and separation of the components contained in the sample. For example, samples that have stronger interactions with the SP than with the MP elute from the column less quickly and thus have a longer retention time, while those samples that have stronger interactions with the MP than with the SP elute from the column faster and thus have a shorter retention time. The mechanism of separation depends on the MP composition and the type of SP. The mechanism of retention involved depends on whether the type of SP is liquid–solid adsorption, liquid–liquid partition, size exclusion, or ion exchange.

In adsorption chromatography, the interaction between the analyte and the SP operates on the basis of polarity. For example, normal phase HPLC compounds that possess functional groups capable of strong hydrogen bonding will adhere more

tightly to the SP than less polar compounds. Thus, less polar compounds elute from the column faster than compounds that are highly polar.

In size exclusion chromatography, compounds are separated on the basis of their molecular size. The SP consists of porous beads. The larger compounds are excluded from the interior of the bead and are eluted first. The smaller compounds enter the beads and elute according to their ability to exit from the same sized pores into which they were internalized. The column can be either silica or non-silica based.

Ion-exchange operates on the basis of the selective exchange of ions in the sample with counterions in the SP. It is performed with columns containing charge-bearing functional groups attached to a polymer matrix. The functional ions with counterions are permanently bonded to the SP. The sample is retained by replacing the counterions of the stationary phase with its own ions.

Finally, reversed-phased HPLC is the most commonly used form of HPLC. It is performed with a column that is the same size as for the other techniques, but the silica is modified to make the surface non-polar by attaching long hydrocarbon chains C8 or C18. Reversed-phase chromatography employs a polar (aqueous) mobile phase. As a result, hydrophobic molecules in the polar mobile phase tend to be adsorbed to the hydrophobic stationary phase, and hydrophilic molecules in the mobile phase will pass through the column and are eluted first. Generally, most applications in natural products chemistry have used the reversed phase with gradient elution, which enables separation of compounds of ranging polarities, thus making it convenient for analysis of most of propolis compounds.

HPLC has the advantage that it can be connected to various detectors depending on the nature of the compounds present. The most commonly used ones include Refractive Index (RI), Fluorescent, Radiochemical, Electrochemical, Near-Infra Red (Near-IR), evaporative light scattering detector (ELSD), ultra violet (UV), Nuclear Magnetic Resonance (NMR), and Mass spectrometer (MS).

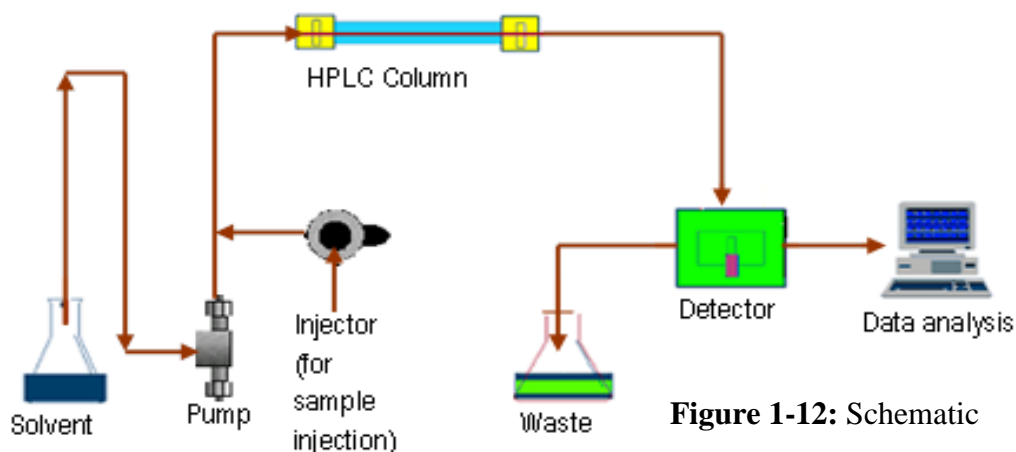


Figure 1-12: Schematic

diagram shows the components of HPLC.

Many spectrophotometric methods were previously developed and validated for analysis of (flavones and flavonols, flavanones and dihydroflavonols, and total phenolics) in poplar-type propolis for measuring the total flavonoid content, using markers compounds as standards (Popova *et al.*, 2007). But there is still a lot of work to be done by researchers to achieve a reliable standardization of propolis types other than the poplar type. In the current research HPLC-UV-ELSD, and HPLC-HRMS were used and are discussed in detail below.

1.3.4.1 HPLC with evaporative light scattering (ELSD), and ultraviolet (UV) detection.

Ultraviolet/ visible (UV/VIS) are the most widely used detectors in modern HPLC, and with photodiode array (PDA); it has become easier to obtain the spectra for an unknown natural product. UV/VIS detectors are very sensitive and are able to detect a wide range of compounds but they are not very specific and restricted only to chromophore containing compounds. On the other hand, the evaporative light scattering detector (ELSD) can be considered as a universal detector. It is useful to detect compounds that lack chromophores in their structure and have poor UV absorption, such as terpenoids, fatty acids and glycosides. Its response is independent of the solvent, although the solvent should be volatile and free of nonvolatile additives. An additional benefit of ELSD is the ability to employ mobile phases that absorb light at the same wavelength as the compound(s) of interest. Due to its linear response it can be used quantitatively over a wide range of analyte concentration, since the amount of scattered light is directly proportional to the concentration of target components in a sample.

The disadvantage of ELSD is that it is a destructive technique and there is the possibility of decreased sensitivity as the volatility of the analyte increases. ELSD is based on evaporation of the mobile phase followed by measuring the light scattered from analyte particles. As shown in **Figure 1-13** the effluent from the column is nebulized under a stream of nitrogen gas and the mobile phase is evaporated in a drift tube, leaving the non-volatile particles of analyte suspended. Then the light scattered by these particles will be detected by a photodetector mounted at a fixed angle from the incident beam (Snyder *et al.*, 2010).

In the current research, the HPLC system used was connected to both UV (five channels) and to an ELSD in order to detect most compounds regardless of their nature. It was also useful in testing purity and in method development for the purification of either crude extracts or fractions collected from the open column chromatography before being transferred to the Gilson or Grace chromatography systems.

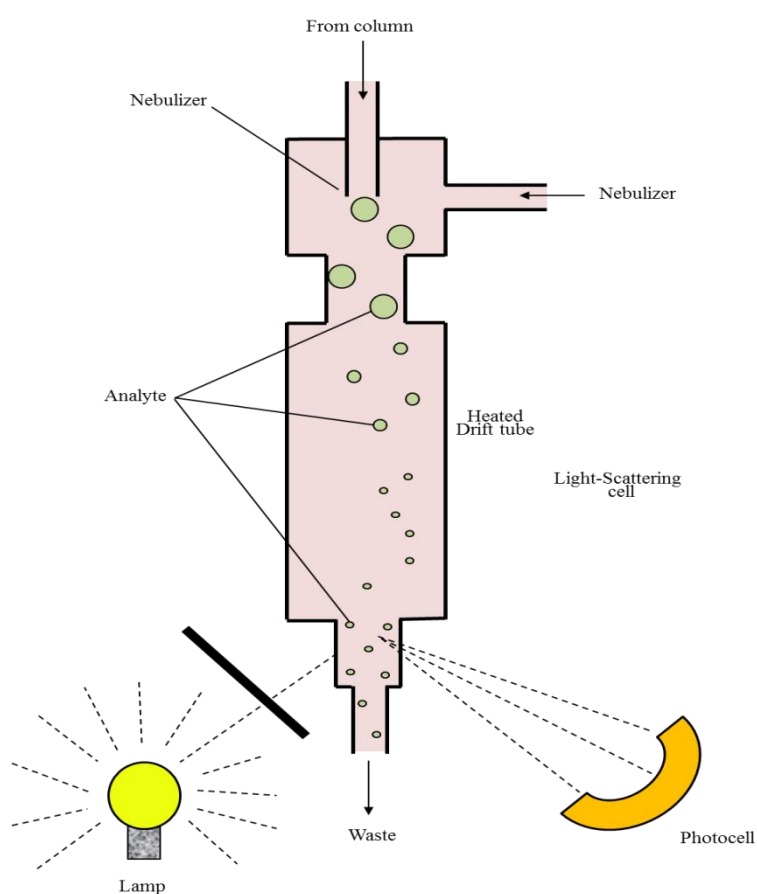


Figure 1-13: The major components of a HPLC-ELSD.

1.3.4.2 LC with high resolution mass spectrometry (HRMS)

HRMS is the most commonly used technique in the dereplication of natural products; largely as a result of the widespread availability of the technique, its accuracy and high sensitivity. It permits characterization based on molecular weight and elemental composition and/or fragmentation patterns. Briefly, LC-MS is composed of an ion source, a mass analyser, detector and computer. The sample is dissolved in a polar volatile solvent, then transported through a needle of high potential. The mobile phase will evaporate under the effect of a warm nitrogen flow and the ions will be produced then transferred to the high vacuum region of a mass analyser, that can separate the given ions based on their mass to charge ratio (m/z). The resulting data are then collected by the detector which then converts them to signals that can be displayed on a computer monitor.

In LC-MS various ionization techniques can be applied:

Ionization methods

The different ionization methods work by either ionizing a neutral molecule through electron ejection, electron capture, protonation, cationization, or deprotonation, or by transferring a charged molecule from a condensed phase to the gas phase (Watson and Sparkman, 2007).

Several types of ionization methods exist. Commonly utilized techniques for small molecule profiling include the atmospheric pressure ionization (API) techniques such as electrospray ionization (ESI), desorption electrospray ionization (DESI), in addition to atmospheric pressure chemical ionization (APCI) and atmospheric pressure photo ionization (APPI). APCI and APPI induce little or no fragmentation

and they are robust, tolerant to high buffer concentration, and they are efficient for non polar and thermally stable compounds such as lipids (Bagag *et al.*, 2008). Other ionization techniques that are also used for specific applications include matrix-assisted laser desorption/ionization (MALDI), chemical ionization (CI), and fast atom bombardment (FAB). All the above mentioned techniques are considered as soft ionization techniques, while electron ionization (EI) is considered as hard ionization due to its ability to fragment the analyte.

Electrospray (ESI) is the most commonly used soft ionization technique, since it can ionize compounds over a large mass range detection. With capabilities ranging from the picomole (10^{-12}) to the zeptomole (10^{-21}) level, it can be applied to more polar, non volatile, and higher molecular weight compounds. In contrast to other ionization techniques such as electron impact (EI) or chemical ionization (CI), it can be used either in the positive mode or negative mode. The disadvantage is that it is sensitive to matrix effects such as pH, solvent composition and salt concentration, which might lead to signal suppression. Fragmentation pattern is important in structure determination. Collision induced dissociation (CID) MS/MS is often performed to generate fragmentation patterns following ESI.

Ion separation and mass analysis

After ions are produced, they are separated by the mass analyser. The ability of a mass spectrometer to distinguish very closely related masses determines its resolving power. Many techniques are now available for mass analysis interfaced with HPLC, the main systems are discussed below.

Time of flight (TOF)

In TOF the velocity of the ions depends on their masses and the lighter the ions, the shorter the flight time. TOF has a relatively low resolution as a result of difference in kinetic energies of ions giving poor mass focusing, but now instruments are provided with reflectrons for focusing ions. TOF can be used with MALDI ionization or QTOF-MS where the TOF is coupled with quadrupole, which is now widely used due to increased sensitivity and resolution.

Quadrupole-tandem MS

Composed of four parallel rods, each pair has the same and opposite charge potential. Therefore, only ions that have m/z within a specified range will be transported through the quadrupoles and reach the detector. The quadrupole provides more sensitive analysis and fragmentation ion formation, allowing experiments such as neutral loss, product ion spectra and selected reaction monitoring to be carried out when a triple quadrupole set up is employed.

Fourier transform ion cyclotron FT-ICR

FT-ICR provides the highest resolving power and accurate mass among all mass spectrometry ion separation techniques. It is based on the measurement of the frequency of oscillation of ions. Its performance is time dependent. Ion-ion interactions decrease the dynamic range of measurement and this is regarded as serious disadvantage of this technique.

The Orbitrap mass spectrometer

The Orbitrap was invented by Alexander Makarov in 1990's and introduced in 2005 by Thermo Fisher Scientific as a part of hybrid LTQ Orbitrap instrument. The ion separation is carried out by trapping the ions injected into the trap between an outer barrel-like electrode (C-Trap) and an inner spindle-like electrode. The frequency of harmonic oscillation along the axis of the electric field is directly proportional to m/z . It uses either ESI or APCI as the ionization method. The main components of the instrument are shown in **Figure 1-14**.

The Orbitrap analyser can be interfaced to a linear ion trap (LTQ Orbitrap family of instruments), quadrupole mass filter (Q Exactive family) or directly to an ion source (Exactive instrument).

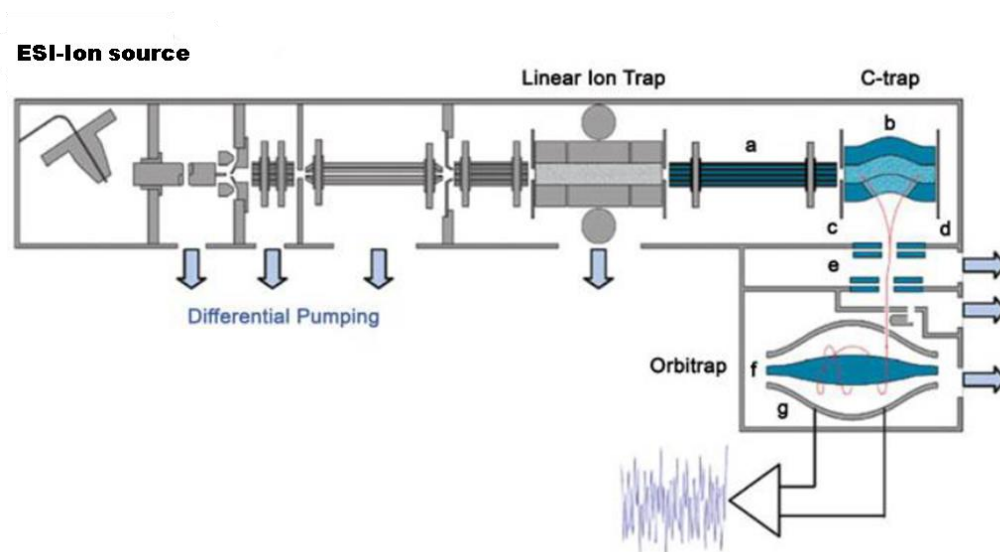


Figure 1-14: Schematics of the commercial LTQ-Orbitrap Classic model (Makarov *et al.*, 2006): (a) transfer octopole; (b) curved RF-only quadrupole (C-trap); (c) gate electrode; (d) trap electrode; (e) ion optics; (f) inner orbitrap electrode (central electrode); (g) outer orbitrap electrode.

In LTQ Orbitrap the ions are produced by the ESI source at the extreme left. Then the ions are directed through the source, collision quadrupole, selection quadrupole and then pass into the storage quadrupole. After accumulation and bunching in the storage

quadrupole, the application of a voltage causes ions in the C-trap to accelerate towards the inner spindle-shaped electrode where a specially applied voltage causes them to circulate round the electrode, thereby getting trapped in their motion. Balance between electrostatic attraction and centrifugal forces will keep the ions trapped. Mass measurement is only dependent on the frequency of transients generated by vibrating ions and is independent of both the spatial spread of the ions and the energy of the ions themselves. The performance parameters used to characterize the Orbitrap are resolution, resolving power up to 150,000, mass accuracy (0.5–2 ppm), high m/z range around 6000, and dynamic range around 10^4 (Hu *et al.*, 2005).

LTQ Exactive Mass Analyser

The Exactive is a bench-top Orbitrap instrument that is ideal for high throughput screening and compound identification characterized by fast polarity; switching can be used allowing acquisition of positive and negative ion data in a single experiment. One scan is obtained in positive and one in negative ion modes per second, without compromising mass accuracy. It has high resolution of up to 100,000, accurate mass, and wide dynamic range, making it ideal for a variety of experiments.

Samples are introduced through the atmospheric pressure ionization source by direct infusion or through HPLC. Thus the instrument has a variety of applications

including high throughput screening of natural products, biomarker discovery, metabolomics, quantitative analysis and for exact mass measurements during organic synthesis.

1.3.5 Nuclear magnetic resonance (NMR) techniques

NMR is a physical phenomenon in which nuclei are excited by a magnetic field and re-emitted electromagnetic radiation is measured. The resonance frequency of the energy is dependent on the strength of the magnetic field applied and the magnetic properties of the isotope of the atoms.

All isotopes that contain an odd number of protons and/or of neutrons have an intrinsic magnetic moment and angular momentum, a nonzero spin, while all nucleotides with even numbers of both have a total spin of zero. The most commonly studied nuclei are ^1H and ^{13}C . The components of the NMR instrument are shown in

Figure 1-15.

NMR is considered the most effective technique that can simultaneously elucidate compounds from various categories of natural product. This includes waxes, terpenoids and phenolics that range through different polarities, without being limited by ionizability or chromophore requirement, or thermal stability like the previously mentioned techniques. NMR is capable of detecting any compound containing spin-active nuclei and is especially applicable to the analysis of organic compounds. Its main limitation is resolution and sensitivity but this can be solved by increasing the magnet power.

NMR is widely used in phytochemical analysis mainly in structure elucidation for identification and conformation of the structure of chemical compounds, by

comparing the NMR spectra obtained with spectra of standard samples or with previously published spectral data. Interpretation of the resultant data from NMR is not easy especially when applied to non-pure propolis samples. Therefore, many recent studies have used Chemometric techniques such as principal component analysis (PCA) and partial least squares (PLS) to generate a meaningful data for profiling and correlation of composition to biological activity or geographic distribution of different propolis samples (Stoyanova & Brown, 2001; Gavaghan *et al.*, 2002).

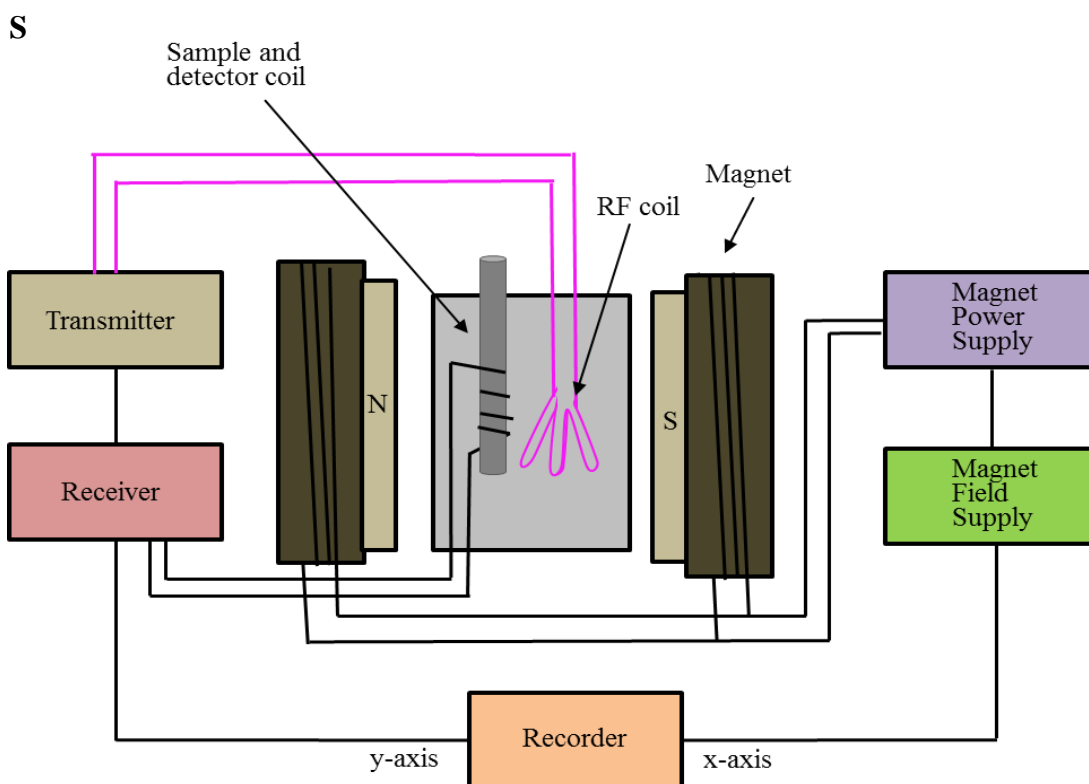


Figure 1-15: The basic elements of a classical NMR spectrometer.

In the current research, identification of pure compounds was carried out by utilizing one-dimensional ^1H and ^{13}C NMR spectroscopy. Identification of known compounds enabled following comparison Spectra obtained with published spectral data. Further 2D experiments were carried out when necessary to accurately assign proton and carbon chemical shifts to novel or previously undescribed compounds.

1.3.5.1 ^1H NMR

^1H NMR provided information on the protons present in the molecule, their chemical shifts, multiplicity (coupling information) and estimated proton numbers from the integration. In the current research, it was carried out for all compounds isolated and was used even on crude extracts and fractions as a primary means for structural identification. The spectra obtained were also used to assess the purity of any isolated compounds (Breitmaier, 2002).

1.3.5.2 ^{13}C NMR

^{13}C NMR gives information on the number and type of carbons present in an isolated compound. The spectra obtained were either broad band-decoupled or J-modulated. In broad band-decoupled spectra, the ^1H nuclei are irradiated during the ^{13}C acquisition so all protons are fully decoupled from the ^{13}C nuclei. When this is done each distinct ^{13}C environment in the molecule gives rise to a separate singlet signal.

The J-modulated experiment helps distinguish the carbons according to the extent of their proton attachments (C, CH, CH_2 and CH_3). DEPT (Distortionless Enhancement by Polarization Transfer) spectrum is a pulse sequenced experiment that transforms the information of CH signal multiplicity and spin–spin coupling into a phase relationship. In a DEPT 135 spectrum, CH_3 and CH are directed towards the positive

phase of the spectrum while CH₂ is facing the negative phase. The obvious advantage of the DEPT 135 spectrum over a standard broad band-decoupled carbon spectrum is that using this technique it is possible to distinguish C/CH₂ carbons from CH/CH₃ carbons in one experiment. The other advantage is that it is four times more sensitive as it uses ¹H–¹³C polarization transfer (Breitmaier, 2002; Friebolin, 2011).

1.3.5.3 Correlation spectroscopy (COSY)

This 2D experiment gives ¹H–¹H coupling in a molecule and it is possible to reveal all coupling relationships in one experiment using a suitable pulse sequence. The proton shifts are plotted on both axes with the contour plot along the diagonal of the square, and the correlations are shown as cross peaks with the diagonal corresponding to the ordinary ¹H spectrum. Thus, the cross peaks refer to the spin–spin coupled protons. The correlations observed are due to geminal (*2J*) and vicinal (*3J*) protons. *4J* and *5J* couplings or allylic couplings can also be observed in a COSY spectrum (Breitmaier, 2002).

1.3.5.4 Heteronuclear Single Quantum Correlation (HSQC)

This 2D ¹H–¹³C experiment shows one-bond (*1J*) direct correlations. In an HSQC spectrum, the ¹H and ¹³C (or DEPT) spectrum is plotted along the abscissa and ordinate, respectively (or vice versa). Cross-peaks indicate proton and carbons that are directly connected to each other (Claridge, 2006).

1.3.5.5 Heteronuclear Multiple Bond Correlation (HMBC)

The spectra obtained from this experiment reveal heteronuclear shift correlations via long-range couplings (*2J* CH and *3J* CH). The proton spectrum is arranged on one

axis and the carbon on the other, and the correlations are displayed, as cross peaks (Breitmaier, 2002; Claridge, 2006).

1.3.6 Data analysis

1.3.6.1 Data processing

LC-MS analysis of samples generates a large amount of data of a two-dimensional nature chromatogram / mass spectrum. These should be pre-processed using software by first elimination of noise and extraction of relevant information usually by using curve resolution or deconvolution methods. Retention time variation due to variation in mobile phase composition, temperature variation or column variability can cause problems in statistical modelling. Therefore, they should be aligned. Much software has been developed to perform this, such as MZmatch, or Sieve software, which uses a Novel algorithm called Chrom-Align for chromatographic alignment. This software has disadvantages of interferences of background, which includes false peaks originating from the mobile phase, sample preparation, column leaching, and plastic tubing, especially when using high temperature. So manual checking is usually needed to be more confident about the resultant peaks.

Another software that is extensively used is MZ-mine 2.10 project which was first initiated by Matej Orešič from the Quantitative Biology and Bioinformatics group at VTT Technical Research Centre of Finland, and Mikko Katajamaa from the Computational Systems Biology Research group at Turku Centre for Biotechnology in 2004 (Katajamaa & Orešič, 2005). It was first released in 2005 allowing processing of LC-MS data from different mass spectrometry platforms for

differential profiling and data visualization through performing different stages, including spectral filtering, peak detection, alignment and normalization.

Finally, the peaks-lists generated can be exported to any statistical program for analysis. Recently a new important function of prediction of the molecular formula has been introduced.

1.3.6.2 Pattern recognition

Principal component analysis (PCA) is one of the most widely used unsupervised chemometrics methods. PCA is utilized to discriminate different groups and helps to reduce the complexity or dimensionality of datasets and to provide better visualization. PCA allows visual detection of sample patterns and analysis of differences among samples and identifying the main contributors to such differences. In addition, it reveals relationships between datasets (Bro & Smilde, 2014). There are various types of software that can be used to perform PCA and in the current work SIMCA-P 14 was used for PCA modelling and partial least squares (PLS) modelling.

1.3.6.3 Databases

At present there is no comprehensive tool for researchers for identification for all metabolites, or secondary metabolites based on their accurate m/z . MS data are identified from online or in house databases like MarinLit, which is a databases used for marine natural products; AntiBase, a database of microbial secondary metabolites; and KEGG, a collection of online databases dealing with genomes, enzymatic pathways, and biological chemicals. NIST (National institute of standards and technology) and dictionary of natural products (DNP) are the most widely used databases for identifying secondary metabolites present in propolis.

1.4 Aims of the study

- To chemically characterize and profile propolis samples collected from different regions within Nigeria, and one South African sample. By using HPLC connected to HRMS and UV-ELSD detectors, GC-MS and NMR, in addition to screening biological activity against *Trypanosoma brucei* and *Crithidia fasciculata*.

- To develop a quick and reproducible chromatographic method for the extraction and purification of the targeted component (s) and to test activity against *Trypanosoma brucei*. In addition, to correlate the chemical structure to activity.

- To elucidate the structures of the isolated compounds using 1D-2D NMR, and LC-MSⁿ.

CHAPTER TWO

MATERIALS AND GENERAL METHODS

2 MATERIALS AND GENERAL METHODS

2.1 General

2.1.1 *Chemicals and reagents*

Davisil grade 633 amorphous precipitated silica pore size 60 A, mesh size 200–425 μm , for column chromatography, Celite filter agent for sample dry loading onto Grace and deuterated solvents CDCl_3 , $\text{DMSO-}d_6$ for the NMR analysis were all purchased from Sigma-Aldrich (Dorset UK). Davisil grade 636 column grade silica gel pore size 60 A, mesh size 35–60 mesh, for sample loading onto glass column was purchased from Merck (Germany).

HPLC grade solvents including: ethyl acetate, methanol, acetonitrile, hexane, and absolute ethanol which was used for extraction purposes were all supplied by Fisher Scientific (Loughborough, UK). AnalaR grade of formic acid (98%) was obtained from BDH-Merck (Dorset UK). Water was produced in house using a MiliQ water filter.

2.1.2 *Laboratory equipment and tools*

The syringes and Acrodisc filters, rotary evaporator (Buchi, Switzerland), and ultrasonic Bath (Scientific Laboratory Supplies, Ltd) were obtained from Fisher Scientific (Loughborough, UK). Gilson automatic pipettes were from (Anachem, UK) and NMR tubes (5 mm 300 MHz, 187 mm L, from (Norell USA). were obtained from Sigma Aldrich, (Dorset, UK) Erlenmeyer flasks, beakers, vials were from Fisher Scientific (Loughborough, UK). Glass columns for column chromatography were from (Rotaflo UK). Empty dry-loader cartridges for samples packing to be

loaded onto the Grace Revelreis system, C18 (12 g) cartridge, and silica cartridge (24 g) were all purchased from Alltech (Carnforth, Lancs, UK).

2.1.3 Propolis sample collection and preparation

Nigerian propolis samples (n=12) were supplied either by James Fearnley from BeeVital Company (Whitby, UK) or were collected by Dr John Igoli from different regions within Nigeria as shown in **Table 2-1**. One South African sample coded (D46SA) that previously showed interestingly very high anti-trypanosomal activity (Zhang *et al.*, 2014) was also studied. All samples were stored at room temperature in a dark and dry place until the time of analysis. All samples had the same appearance, being dark brown and sticky except for the River State and Calabar State samples, which were red in colour.

2.2 Extraction of propolis

Propolis samples were either cut off or coarsely ground into small pieces using a mortar and pestle. For profiling purposes approximately, 50 mg of each sample was extracted with 5 mL ethanol three times by sonication with heat at 40 °C for 3 hours each. The samples were filtered using syringe filter (Acrodisc 0.45 µm). The filtered solution was dried using a nitrogen flow and the amount of residue was measured by subtracting the weight of empty vial from the total weight, and then stored at –20 °C until required.

Bioassay guided extraction was performed for most active samples in order to isolate the active constituents in fractions. Five biologically active propolis samples coded RSN, BRN, UDN, ION, and D46SA were extracted with proper amount of ethanol (exact amount will be mentioned separately in following chapters 4, 5, 6) three times,

by sonication with heating at 40 °C for three hours each, and then macerated over night with ethanol. Each extract was filtered through filter paper, then the extracts were combined and the solvent was evaporated using a rotatory evaporator in Pre-weighed round-bottomed flask so that we could weigh the dry ethanolic crude extracts. All extracts were stored at –20 °C until required.

Table 2-1: Propolis samples coding and collection areas and date of collection.

Origin (town/State)	Code	Collection date	Colour
Bonny/River State Nigeria	RS-N BRN	2003 July/2013	Red
Kaduna/Kaduna State Nigeria	KAP-N P3N KK-N	Unknown October/2007 July/2013	Brown
Jos/Plateau Nigeria	S97 N	February/2005	Brown
Ijebu-Ode/Ogun State	IO-N	July/2013	Brown
Ugelli/Delta State	UD-N	July/2013	Brown
Calabar/Cross River State	CC-N	July/2013	Red
Plateau State	S95N	February/2005	Brown
Zaria / Kaduna State	AF2-3N	Unknown	Brown
Unknown location	S96-N	February/2005	Brown
Kwa Zulu Natal, S. Africa	D46 SA	Unknown	Brown

2.3 General profiling of propolis samples.

All crude extracts were dissolved in methanol to prepare 2 mg/mL to perform LC-MS analysis and HPLC-UV-ELSD analysis. In the case of more hydrophobic, poorly soluble samples, a few drops of ethyl acetate were added to improve solubility.

2.3.1 *High-performance liquid chromatography coupled with Ultraviolet detector and Evaporative Light Scattering Detector (HPLC-UV-ELSD).*

LC-UV-ELSD analysis was performed on an Agilent 1100 system, consisting of a quaternary pump, an auto sampler and a degasser, and UV channels were set to monitor at 290 and 320 nm and ELSD (model: SEDEX75, SEDERE France) at 30 °C. The column used was an ACE C18 column (150×3 mm, 3 µm) supplied by HiChrom (Reading, UK), and the mobile phase used was A: water and B: Acetonitrile at flow rate of 300 µl/min. The formic acid was omitted from A and B when the ELSD detector was used in order to reduce the background noise.

The gradient elution was programmed as follows: linear gradient from 30% B to 50% B over 15 minutes, then the gradient was held at 50% of B for 10 min. and this was followed by a gradient from 50% to 80% of B from 25–40 min, and followed by holding at 80% of B for 10 min, then a 1 min to increase to 100% of B and then composition was held for 9 min at 100% of B with the flow rate increasing to 500 µl/min in order to wash the column. The system was then returned back to 30% of B to re-equilibrate the system for 10 min. This gave a total run time of 70 min. The Injection volume used was 10 µl. The data was collected and processed using Clarity software from Data Apex.

2.3.2 High-performance liquid chromatography coupled with High-resolution Mass Spectrometry (LC-HRMS).

The same samples in duplicate, injection volume and chromatographic conditions were used as for HPLC-UV-ELSD except with the addition of 0.1% formic acid to both A and B mobile phases to induce the ionization under ESI conditions, in order to correlate the peaks obtained above in 2.3.1 with the accurate masses from LC-MS.

HRMS was performed on an Accela 600 HPLC system combined with an Exactive (Orbitrap) mass spectrometer from Thermo Fisher Scientific (Hemel Hempstead, UK). The MS detection range was from m/z 100 to 1500 and the scanning was performed under ESI polarity switching mode.

The LC-MS system was controlled by Xcalibur version 2.2 (Thermo Fisher Corporation). The mass axis of the instrument was externally calibrated according to the manufacturer's instructions just before commencing the experiment, using the standard Thermo Calmix solution, and was internally calibrated during the experiment by appropriate lock masses which were m/z 83.06037 in positive mode (acetonitrile dimer) and 91.00368 in negative ion mode (formic acid dimer). The Main parameters for the ESI mass spectral analysis are listed in **Table2-2**.

Table 2-2: Main parameters for the ESI mass spectral analysis.

Attribute	Positive mode	Negative mode
Capillary temperature (°C)	275.0	
Sheath gas flow (bar)	50.0	
Auxiliary gas flow (bar)	17.0	
Spray voltage (kV)	4.5	- 4.0
Source current (µA)	100.0	
Capillary voltage (V)	35.5	- 48.0
Tube lens (V)	90.0	-145.0

2.3.2.1 Data Extraction and Database Searching

Since the Exactive HRMS works in dual polarity mode, the peak lists needed to be split into negative and positive file before transfer to MZ-mine2.14 to be processed (Pluskal *et al.*, 2010); this was carried out using ProteoWizard. The generated peak lists from both ESI positive and negative modes were imported separately into SIMCA-P 14 (Umetrics, Sweden) for Principal Component Analysis (PCA) for chemical characterization, classification of the Nigerian propolis samples, and targeting of the major characteristic components that cause the differences in the PCA plots.

The parameters that were used in extraction of the data in MZmine 2.10 software were as follows: Mass detection with centroid peaks, noise level 1×10^5 , m/z tolerance 0.001 -5.0 ppm, minimum peak height 5×10^5 , and mass range 100–1500 m/z ; for deisotoping with retention time (t_R) tolerance 0.2 min and a maximum charge of 2, and most intense isotope is filtered out. For alignment join aligner was used with weight function in relation to m/z and retention time (20:20); this means t_R and m/z both have the same importance, t_R tolerance of 5%. After that gap filling was used to detect missing peaks at an intensity tolerance of 1%, m/z tolerance 0.001–5ppm and t_R tolerance of 0.5 min, after gap filling all solvent peaks were removed from the data and adducts and complexes peaks were identified. The formula prediction function was performed within the setting for only C, H, O containing compounds since no compounds containing other elemental compositions were isolated before from propolis. The data were exported as CSV files included MZ-Mine ID, m/z , retention time, name (if available) and peak area.

The first 2000 LC-HRMS features from each sample were selected based on the mean peak area and putatively identified by searching for the accurate masses against the Dictionary of Natural Products (DNP 2013 version). Moreover, these negative ion data were univariate scaled and log transformed prior to PCA modelling.

2.3.3 Gas chromatography (GC-MS)

Around 2 mg of the sample was reconstituted in 1 mL ethyl acetate to be injected in GC-MS in splitless mode. 1 μ l of each prepared sample was injected at 280 °C into the GC-MS from Thermo Scientific Focus (GC-DSQ2) system from Thermo Fisher Scientific (Hemel Hempstead, UK); equipped with a 30 m long, 0.25 mm i.d., and 0.25 μ m film thickness InertCap 1MS capillary column (GL Sciences, Japan). An

AS3000 autosampler was used, mass spectrometer (DSQ 2) is connected to GC, positive Ion generated at 250 °C, the full scan was performed in mass range of 50–800 amu. Total scan time was 0.2 second, scan rate of 4.926. The temperature gradient was programmed as follows: initially holding at 80 °C for 1 min, linearly increasing to 200 °C at the rate of 15 °C/min, holding at 200 °C for 15 mins and linearly increasing to 320 °C at the rate of 5 °C/min and holding for 10 mins. The ionization voltage was 70 eV for EI–MS in positive polarity mode.

2.3.4 NMR Methods

For profiling, 15 mg of each crude sample was dissolved in 0.6 mL of D-Chloroform, prepared into the standard NMR tubes (5 mm x 187 mm L). ¹H NMR data was acquired on a JEOL-LA400-MMR (JEOL Ltd, UK) spectrometer system at 400 MHz. All spectra were referenced to the residual solvent peaks using TMS as internal standard; chemical shifts are given in ppm and coupling constants are in Hz. MestReNova 8.1.2 software (Mestrelab Research SL, Spain) was used to process the NMR spectroscopic data.

2.4 Fractionation work and isolation of compounds

The bulk biologically active propolis resins were subjected to further investigation in order to isolate the compounds responsible for activity. Several chromatographic techniques were used for the isolation and purification of compounds from crude extracts, which have activity against *Trypanosoma brucei*.

2.4.1 Silica gel chromatography

The classical system column chromatography (CC) is a common and useful purification technique that allows one to isolate and collect the compounds

individually from a crude extract or fractions. Column Chromatography was performed on silica gel 60 (mesh size 200–425 μm). The column was packed using the wet packing technique, slurry of silica (around 50 g) and least polar solvent in eluting system (Hexane) was made and then poured and packed in a glass column of appropriate size (55 x 3 cm). The column was tapped to remove the air bubbles. Excess solvent was allowed to run through and the column was left to settle down. A portion of propolis extract was dissolved in minimum quantity of solvent, usually ethyl acetate, and mixed with coarse silica, then left to dry completely under a vacuum hood. The dried extract was then loaded onto the top of the column. A small amount of coarse silica or cotton wool was applied over the sample to prevent any disturbance of interface between sample and solvent when applying the solvent, and then elution was carried out sequentially using different solvent systems containing varying proportions of polar and nonpolar solvents (Braithwaite & Smith 1996).

Elution was carried out using a stepwise gradient of polarity with hexane-ethyl acetate-methanol using 200 mL of mobile phase at each step starting with 100% hexane then stepwise increments of ethyl acetate as follows: 90:10 – 80:20 – 60:40 – 40:60 – 20:80 – 100% ethyl acetate and then continuing with increasing amounts of methanol in presence of ethyl acetate as follows: 90:10 – 70:30 – 60:40 – 50:50 – 100% methanol. Fractions of (50 mL) were collected and concentrated on rotatory evaporator and were pooled based on HPLC-UV-ELSD analysis according to similarity in chemical profiles. They all were weighed and kept at $-20\text{ }^{\circ}\text{C}$ for further purification. All fractions were tested against *T. brucei* in order to target active fractions.

2.4.2 *Grace Reveleris® system.*

A Grace Reveleris® iES Chromatography System (Alltech, Carnforth, Lancs, UK) was used in this project either on crude extracts, or on fractions obtained from column chromatography for purification purposes. The samples to be purified on the Reveleris system were dissolved in a minimum amount of appropriate solvent usually (EtOAc) and mixed with celite (1:2) by weight, then the mixture was left under a vacuum hood until completely dried and was then dry loaded into special cartridges. Fractionation can be performed either on normal phase using a silica gel column (GraceResolv Silica 24 g/32 mL) or reversed system using a C18 (12 g) cartridge. In the latter case, HPLC-ELSD-UV was used to optimize a method with suitable isocratic conditions that gave a better peak resolution to be transferred to the Grace system.

The Grace system was equipped with detection System using two UV channels adjusted to (290, 320 nm) in all experiments, and ELSD that can detect both non-chromophoric and chromophoric compounds in complex extracts during a single run. An automatic fraction collector that collected peaks according to either slope or threshold detection was employed. The sensitivity level was adjusted to medium in all experiments which gave reasonable compromise for most cases, and less noisy chromatograms. Data were collected and processed using Reveleris® Navigator™ Windows and exported as a pdf file.

Fractions were collected in numbered test tubes and they are named accordingly, then according to the chromatograms produced by the instrument the tubes representing one peak were collected in the same tube, dried, and weighed individually. The purity of each fraction was tested by HLC-UV-ELSD and, in the

case of fractions having purity higher than 80–90%, structures were elucidated by NMR and further confirmation of structure was obtained by LC-MSⁿ.

2.4.3 *Gilson semi-preparative chromatography system*

The system consists of a Gilson two pumps (model 306) connected to manometric module (model 806), diode array detector (model 1100 from Hewlett Packard), and a fraction collector (model FC 204). The column used was an ACE5-C18 column (250 x 10 mm i.d.) supplied by Hichrom (Reading, UK). All components were interfaced to Gilson Unipoint system Software. Semi pure CC fractions or the Grace fraction to be purified by the Gilson was dissolved in methanol to make concentration of 25–50 mg/mL and injected automatically. The elution conditions used were optimized first by using HPLC-UV-ELSD. The fraction purified on the Gilson was the Grace fraction from silica gel fraction of D46SA. Conditions used were as follows: isocratic elution of 50:50 acetonitrile: water, and a flow rate of 4.5 mL/min for 30 min. The detection wavelength was set to 290 nm and 320 nm. Data were acquired and processed by using Unipoint software.

2.5 Identification of compounds

After testing the purity of the isolated compounds with HPLC-UV-ELSD, the fractions with high purity were elucidated by NMR and confirmed by LC-MSⁿ.

2.5.1 *NMR spectroscopy*

The identification of pure compounds was first carried out by one dimensional ¹H and ¹³C NMR spectroscopy, both NMR experiments were carried out on a JEOL (JNM LA400) 400 MHz. For structural elucidation, spectra obtained for known compounds were identified following comparison with published spectral data. 1D-

^1H and ^{13}C NMR, DEPT 135 and 2D: ^1H - ^1H -COSY, HSQC, HMBC were acquired on Bruker Avance 600 when necessary to accurately assign proton and carbon chemical shifts for samples of small amounts or previously undescribed compound. Samples to be tested were dissolved in about 0.6 mL of a suitable deuterated solvent either D-Chloroform or DMSO- d_6 according to their solubility, in NMR tubes.

2.5.2 *LC-MSⁿ*

Sample of 2 mg was dissolved in 1 mL of methanol and run on the Orbitrap using the same column and chromatographic conditions were used in the profiling section 2.3.2.

The system employed for MS^n experiments was an LTQ-Orbitrap which consists of a Surveyor HPLC pump hyphenated to an LTQ Orbitrap mass spectrometer (Thermo Fisher Scientific, Hemel Hempstead, UK). The instrument works in single polarity at a time but can perform MS^n . The fragmentation data collected from MS^n was not included in general profiling, but was carried out for either elucidation or confirmation of the structure of the purified compounds, by comparing the fragmentation patterns produced with the literature, for trying to build a library of the pure compounds isolated from propolis and their fragments. MS^n analysis was carried out by using Collision Induced Dissociation (CID) negative mode at 35 V on a LTQ-Orbitrap, where the most intense signal on MS full scan was chosen to be fragmented.

2.5.3 *Measurement of Optical Rotation*

The specific rotation for optically active compounds was measured using a Perkin–Elmer 241 polarimeter with a sodium lamp at 20 °C (PerkinElmer Inc., USA) to

measure their optical rotation. 1 mg of each of the compounds was dissolved in chloroform or methanol to get 1 mg/mL. The average ten readings were taken and then optical rotation was calculated using the equation:

$$[\alpha]_{\lambda}^T = \frac{100 \times \alpha}{l \times c}$$

Where $[\alpha]$ is the specific rotation at wavelength λ , T is the temperature at 20 °C, α is the average of the measured rotation (°), l is the path length in decimetres, and c is the concentration of the solution in g/100 mL.

2.5.4 Melting point

For the two new compounds isolated, the melting points were measured using a Stuart Scientific melting point apparatus (Bibby, UK).

2.6 Bioassay

2.6.1 *In vitro* trypanocidal bioassay

2.6.1.1 First stage testing

Crude extracts, fractions and isolated compounds underwent preliminary testing against the blood stream form of *Trypanosoma brucei brucei* (S427) *in vitro*. Anti-trypanosomal tests was carried out by using an Alamar Blue assay according to a standard protocol as described in (Rüz *et al.*, 1997). This assay is based on viable cells metabolizing the blue resazurin dye to resorufin, which is pink and fluorescent. It was performed using *Trypanosoma brucei* S427 at concentration of $2-3 \times 10^4$ trypanosomes/mL and stock solutions of the samples prepared with a concentration of 10 mg/mL in 100% DMSO and diluted with HMI-9 medium to a concentration of

1 mg/mL and. The 20 µg/mL conc. Of these test solutions were prepared by pipetting 4µl of test stock solution into the flat bottomed and transparent microtitre 96-well plates followed by adding 96 µl of HMI-9 medium into each well. Suramin with different conc. ranging from 0.008 µM-1.00 µM act as a positive control was added to the last column to act as the positive control. A 100 µl of trypanosome suspension was eventually added to each well except the first column which is used for (sterility check) followed by an incubation period of 48 hours at 37 °C in a 5% CO₂ humidified incubator. After incubation, 20 µl of Alamar-Blue was added and the plate was incubated under the same conditions for further 24 hours; the fluorescence values for the test plates are measured using a microplate reader (Wallace Victor Spectrofluorimeter) in fluorescence mode with excitation and emission wavelengths of 560 and 590 nm respectively. The test samples are initially screened at a single concentration and the results were calculated as % of the DMSO control value. Finally, MIC (Minimum inhibitory concentration) values were determined for active samples (which showed < 10% of control values) at n= 2 or n= 3. And this was performed in duplicate where 200 µg/mL test solutions were prepared in second column by pipetting 4 µL of (10 mg/mL) test stock solution and 196 µL HMI-9 medium into each well. 100 µl HMI-9 medium was pipetted into all columns except the second column . 1:1 serial dilutions were carried out from columns 2 to column 11. A 80µl of HMI-9 medium was added to the last column and 20µl of x10 concentrations of suramin to give a final concentration range of 0.008 to 1.0µM. An inoculum of 100µl of trypanosomes at a concentration of 2-3x10⁴/ ml was added to each well except the first column, and the procedure continued as previously described.

sample preparation: samples to be tested were prepared as 2 mg/200 µl in 100% DMSO, the original crude extracts of propolis, fractions from open columns or from the Grace MPLC along with pure compounds isolated were all tested.

2.6.1.2 Second stage testing

More detailed screening of all crude extracts as well as the more active compounds was carried out in Glasgow University, using a previously described variant of the assay described in 2.6.1.1 (Wallace *et al.*, 2002; Rodenko *et al.*, 2007). The assays were performed using serial dilutions in 96-wells, with each compound or mixture doubling diluted over two rows of the plate, ensuring an optimally defined 50% Effective Concentration (EC₅₀) after plotting of the reading to a sigmoid curve with variable slope (GraphPad Prism 5.0). Three distinct, clonal lines of *T. b. brucei* were utilized: Lister strain 427 (s427), the standard drug-sensitive control strain, the B48 clone that was derived by *in vitro* adaptation to pentamidine (Bridges *et al.*, 2007) and the aqp2/aqp3 null strain (Baker *et al.*, 2012), from which the gene encoding the High Affinity Pentamidine Transporter (HAPT1) has been deleted. For each strain, the seeding density at the start of the assay was 2×10^4 cells/well, and the cells were exposed for 48 h to the test compounds, at 37 °C/ 5% CO₂, before the addition of the resazurin dye and a further incubation of 24 h under the same conditions. Fluorescence was determined in a FLUOstar Optima (BMG Labtech) at wavelengths of 544 nm and 620 nm for excitation and emission, respectively.

2.6.2 Screening against *Crithidia fasciculata*

All Nigerian crudes were tested against *Crithidia fasciculata* (ATCC 50083) at the University of Sunderland by Dr Tim Paget. *C. fasciculata* is a close relative to trypanosomes that infect bees. It was grown in in RPMI 1640 medium supplemented

with L-glutamine and 10% v/v heat inactivated foetal bovine serum for 24 h with shaking prior to use (Alcolea *et al.*, 2014). These cells were then used to inoculate wells of a 96 well plate with 1×10^5 cells per well in total of 100 μ l of medium, stock extracts were made for each concentration so that there was a constant percentage of DMSO-d₆ (2.5% v/v) per well. The absorbance of plates was determined at 620 nm (T_0) using a Bio Rad xMark Microplate Spectrophotometer (Hemel Hempstead, UK) and these plates were then incubated for 48 h at 25°C. The absorbance of the wells was then determined again at 620 nm (T_{48}). For extracts showing total inhibition of growth and no change in absorbance, terminal subculture of cells taken from wells. Growth determined by microscope and absorbance changes. Pentamidine was included as a control drug in all assays but it shows variable activity against *C. fasciculata* (Bacchi *et al.*, 1974), thus menadione was used as an additional control drug.

CHAPTER THREE

CHEMICAL AND BIOLOGICAL PROFILING OF

NIGERIAN PROPOLIS SAMPLES

3 CHEMICAL AND BIOLOGICAL PROFILING OF NIGERIAN PROPOLIS SAMPLES

3.1 Introduction

Twelve ethanolic extracts of propolis samples collected from eight different regions in Nigeria were subjected to detailed screening against *Trypanosoma brucei*, and two other genetically modified types using pentamidine as the control drug. The samples were also tested against *Crithidia fasciculata*, using menadione as control drug. Extracts were also chemically profiled by using different analytical techniques.

3.2 Origin of the samples.

Propolis samples were extracted according to the procedure in section 2.2 and the yields of the ethanolic extracts are shown in **Table 3-1**. The map in **Figure 3-1** shows the exact collection sites of samples.

Table 3-1: Codes, collection area and percentage of yield of ethanol extract (EEP) for the samples.

Code	Origin (town/State) Geographical co-ordinates	Collection date	% Yield from 50mg
RSN BRN	Bonny/River State Nigeria 4°26' N 7°10'E	2003 and July 2013	76.0 70.6
KAPN P3N KKN	Kaduna/Kaduna State Nigeria 10°31'N 7°26'E	Unknown, October 2007, July 2013	73.6 40.0 53.3
S97N	Jos, Plateau State Nigeria 9°56'N 8°53'E	February 2005	51.0
ION	Ijebu-Ode, Ogun State 6°49'N 3°55'E	July 2013	38.9
UDN	Ugelli, Delta State 5°30'N 5°59'E	July 2013	60.2
CCN	Calabar, Cross River State 4°57' 8°19'E	July 2013	42.4
S95N	Jos Plateau State 9°56'N 8°53'E	February 2005	73.0
AF23N	Zaria, Kaduna State 11°04'N 7°42'E	NA	58.4
S96N	Unknown location in Nigeria	February 2005	52.4



Figure 3-1: Map of Nigeria showing collection sites for samples cited from (http://www.inecnigeria.org/page_id=373).

3.3 General biological screening of Nigerian propolis samples against *Trypanosoma brucei* and *Crithidia fasciculata*.

3.3.1 Experimental

The general materials and methods are described in section 2.6.

3.3.1 Results

The results indicated variable activity of samples collected from different regions as shown in **Figure 3-2**. Samples collected from Southern regions (coded: RSN, BRN, CCN, ION and UDN) demonstrated the highest activity with average EC_{50} values of 4.2, 6.9, 9.1, 5.9 and 12.1 $\mu\text{g/mL}$ respectively, while samples collected from the central part of Nigeria were generally less active ranging from highly active such as

KAP-N with an EC_{50} value of 7.8 $\mu\text{g/mL}$ collected from Kadua state in central Nigeria to moderately active (P3N, KKN, S97N, S95N and S96N) and last a non-active sample AF2-3N. The same pattern with the other two strains of pentamidine resistant trypanosomes was observed as shown in **Table 3-2**. Regarding activity against *Crithidia fasciculata*, RSN, UDN and KAP-N were the most active among others with EC_{50} 1.2, 7.6, and 9.5 $\mu\text{g/mL}$ respectively. This activity against *C. fasciculata* supports the idea that the bees may collect propolis to protect from infection by Crithidia species which are known to be pathogens of bees (Schluns *et al.*,2010), and are quite closely related to *T. brucei*.

The samples that presented stronger antitrypanosomal activities were subjected to further investigation.

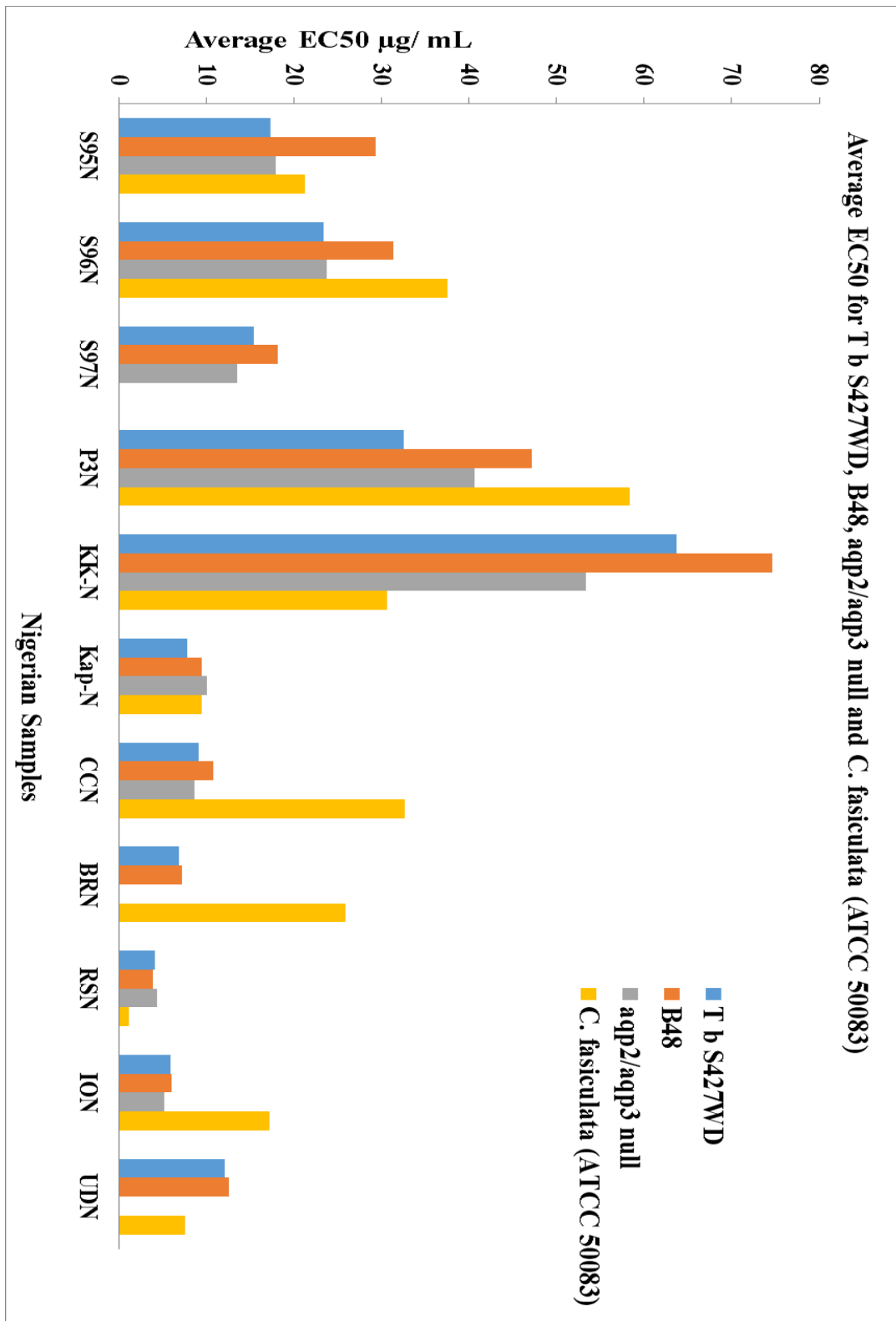


Figure 3-2: General screening of propolis samples from different regions of Nigeria for activity against three strains of *T. brucei* and *C. fasciculata*.

Table 3-2: Average of EC₅₀ in µg/ mL for all crudes (n= 3) against three strains of *T.brucei*; wild type (T b S427WD) standards drug sensitive control, and other two genetically modified types aqp2/aqp3 null and B48 adapted from Lister 427WT . Data were provided by Harry P. De Koning from Glasgow University. Samples were also tested against *C. fasciculata*. For (n= 4), data were provided by Tim Paget from, University of Sunderland, NA: not tested.

Samples	T b S427WD			B48			aqp2/aqp3 null					<i>C. fasciculata</i> (ATCC 50083)				
	EC ₅₀	SEM	EC ₅₀	SEM	RF	t-Test	EC ₅₀	SEM	RF	t-Test	EC ₅₀	SEM	RF	t-Test	EC ₅₀	SD
S95N	17.3	0.24	29.3	1.46	1.69	0.00	17.9	0.12	1.03	0.10	21.3	0.12	1.03	0.10	21.3	3.2
S96N	23.4	0.77	31.4	1.09	1.34	0.00	23.8	0.56	1.02	0.68	37.5	0.56	1.02	0.68	37.5	4
S97N	15.5	0.20	18.2	1.81	1.18	0.21	13.5	0.27	0.87	0.00	NA	0.27	0.87	0.00	NA	NA
P3N	32.6	0.33	47.2	3.91	1.45	0.02	40.6	2.48	1.25	0.03	58.4	2.48	1.25	0.03	58.4	4.7
KK-N	63.7	0.51	74.7	2.68	1.17	0.02	53.4	3.20	0.84	0.03	30.6	3.20	0.84	0.03	30.6	3.7
Kap-N	7.8	0.41	9.5	0.77	1.21	0.14	10.1	0.31	1.28	0.01	9.5	0.31	1.28	0.01	9.5	0.8
AF2-3N	>400 Inactive		>400 Inactive				>400 Inactive				>400 Inactive				>200 Inactive	
CCN	9.1	0.17	10.8	0.80	1.19	0.10	8.7	0.20	0.95	0.19	32.7	0.20	0.95	0.19	32.7	1.9
BRN	6.9	0.30	7.2	0.28	1.04	0.58		NA			25.9				25.9	1.1
RSN	4.2	0.04	3.9	0.16	0.92	0.13	4.4	0.26	1.05	0.46	1.2	0.26	1.05	0.46	1.2	0.2
ION	5.9	0.02	6.0	0.21	1.01	0.73	5.2	0.10	0.88	0.00	17.2	0.10	0.88	0.00	17.2	1.5
UDN	12.1	0.32	12.6	0.08	1.04	0.35		NA			7.6				7.6	1.3
Pentamidine	0.0023	0.0002	0.5	0.04	224.78	<0.001	0.1	0.002	31.08	<0.001	18.3	0.002	31.08	<0.001	18.3	3.8
Menadione	-	-	-	-	-	-	-	-	-	-	-	-	-	-	0.8	0.2

In **Table 3-2** aqp2/aqp3 null is the same strain as WT, but with the TbAQP2 gene, coding for the important drug transporter HAPT1, deleted by targeted gene deletion; resistant to pentamidine and melarsoprol, and strain B48 adapted from Lister 427WT by *in vitro* exposure to pentamidine; lost both main drug transporters, HAPT1 and TbAT1, and is highly resistant to pentamidine. Averages EC_{50} and the standard error of the mean (SEM) are given for $n=3$. Resistance factor (RF) is the ratio of EC_{50} for resistant strain over WT. Unpaired t-test compared EC_{50} values of each resistant strain versus WT. Units are in $\mu\text{g/mL}$ except for pentamidine, where the EC_{50} value is given in μM .

3.4 Chemical profiling of samples

Chemical profiling was performed using various techniques as described in section 2.3.

3.4.1 Profiling with HPLC-UV-ELSD

The chromatograms of the crude samples run on HPLC-UV-ELSD suggested a wide diversity in the chemical composition for the Nigerian samples. The samples could be divided into two groups. Group **I** was comprised of samples that were collected from the central part of Nigeria (AF2N3, P3N, KKN, S97N, S95N, KAPN, S96N), which mostly demonstrated an intense ELSD only response, with weak or absent UV peaks, suggesting a high content of terpenoids and/or fats, and the absence of any chromophore containing compounds such as flavonoids, lignans or any other phenolic compounds. All of these samples were also noted to have at most weak activity against trypanosomes. In contrast, samples in group **II** were collected from Southern areas and showed strong UV-ELSD responses and high activity against *T. brucei*.

Figure 3-3 shows a comparison of the chromatograms obtained for a Southern and a Central Nigerian sample confirmed the variability in of chemical composition.

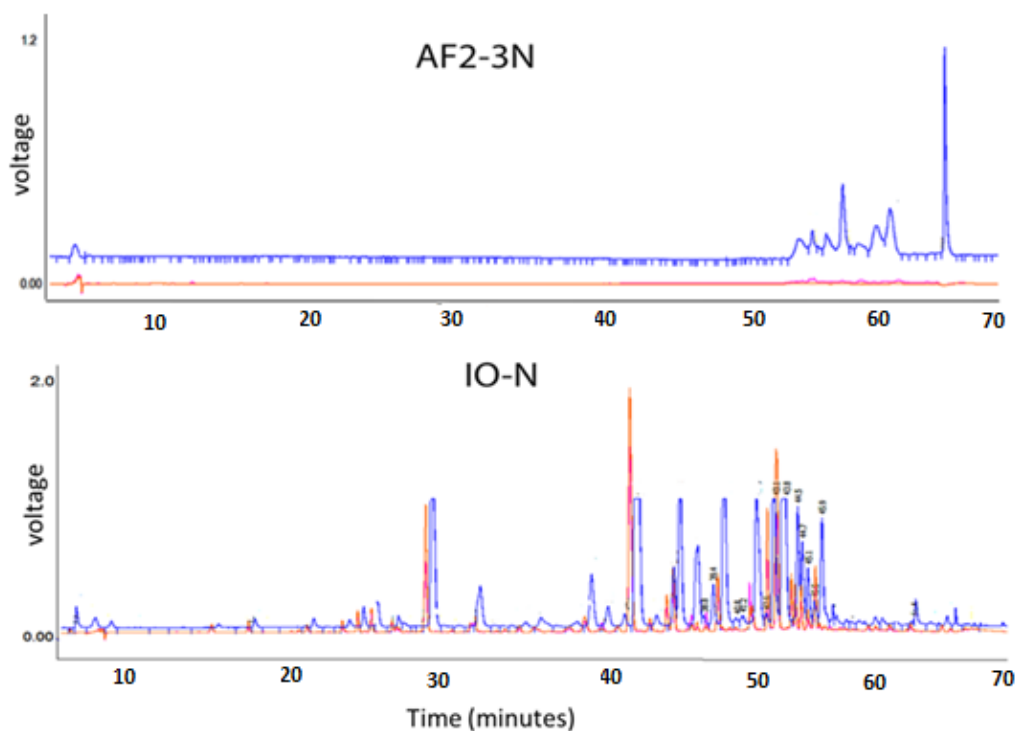


Figure 3-3 : ELSD-UV chromatograms of two samples AF2-3N and ION from Central and Southern Nigeria, blue indicates ELSD response. HPLC conditions in section 2.3.1.

3.4.2 GC-MS analysis

Profiling of the crude samples by GC-MS showed that group I samples demonstrated relatively similar chromatograms showing a group of intense peaks in the range of 41.0–43.0 min. The fragmentations of these intense peaks were searched against the

NIST library and identified as various triterpenoids, waxes and long chain fatty acids, with similarity scores of more than 700, which appeared to be the major chemical components in these samples; this explained the high responses in ELSD only. **Table 3-3** shows some of the compounds identified by GC-MS in the group I samples according to matching against the NIST library. Most of the components in the group I samples had retention times > 40.0 min.

Figure 3-4 shows a comparison of the GC-MS chromatograms for three representative samples. The structures for the triterpenes identified by a library search are shown in **Figure 3-5**.

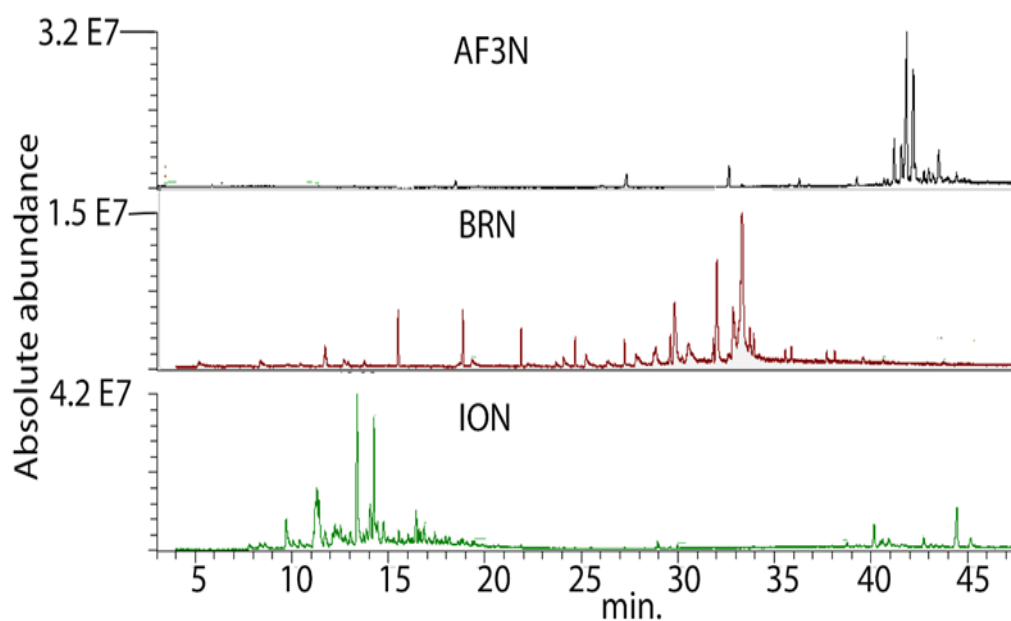


Figure 3-4: Representative GC-MS chromatograms for three propolis samples BRN, AF2-3N, ION. Experimental condition in section 2.3.3

Table 3-3: Some compounds identified by GC-MS with similarity scores higher than 700 when searched against the NIST library.

Name	Elemental composition	t _R (min.)
2-Methyloctadecane	C ₁₉ H ₄₀	40.0
Ursenol	C ₃₀ H ₅₀ O	41.2
Cholestan-3ol-2methylene	C ₂₈ H ₄₈ O	41.5
Lupeol	C ₃₀ H ₅₀ O	43.5
α and β-Amyrin	C ₃₀ H ₅₀ O	43.6
Lupenol acetate	C ₃₂ H ₅₂ O ₂	43.9

In the case of group **II** samples from Rivers State Nigerian, e.g. BRN and RSN, most of the GC-MS peaks eluted before 35.0 min. and these peaks referred to flavonoids that were confirmed on LC-HRMS and in GC-MS as 7-O methylvestitol and neovestitol which were identified as major components in these samples. However, for the ION sample the retention times were mainly less than 20.0 min. referring to diterpenoid acids and sesquiterpene alcohols such as nerolidol, and cubebol but with lower similarity scores. The peaks between 39.0 and 43.0 min. are the same as in group I samples and the main peak is due to Lupenol. The pattern of peaks in CCN was close to that of the group I samples.

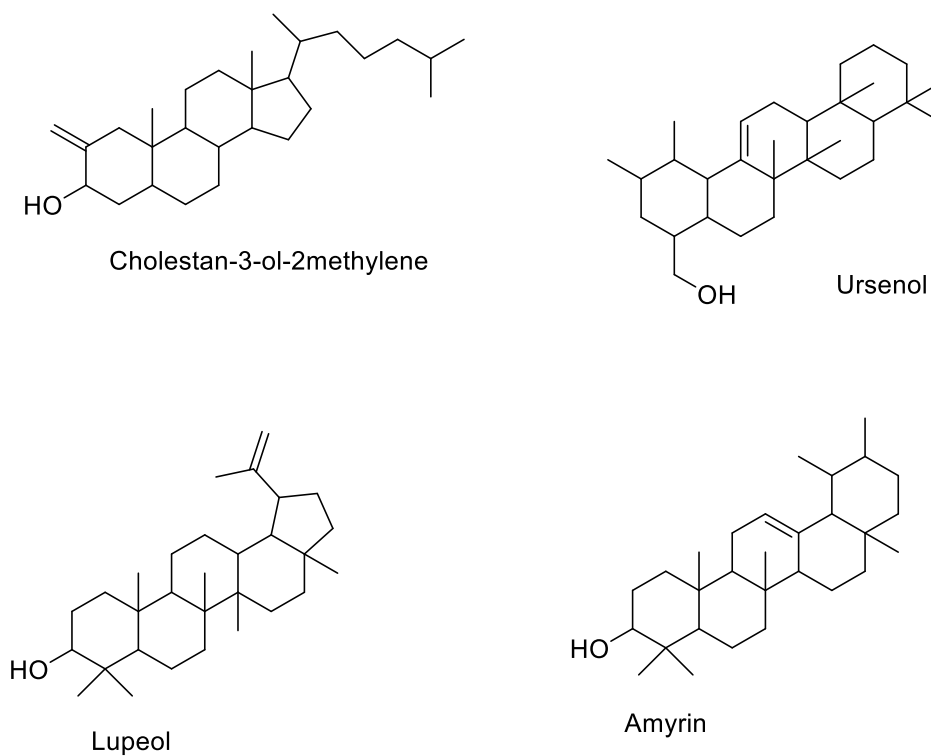


Figure 3-5: Structure of some common and volatile compounds identified by GC-MS in group I and II samples.

3.4.3 $^1\text{H-NMR}$ of the Crudes Extracts

$^1\text{H-NMR}$ provided global information about nature and fingerprint of these complex samples. It is also effective for compounds that have a poor ionizability or lack chromophores. In the group I samples the $^1\text{H-NMR}$ spectra showed that the main signals were almost exclusively in the aliphatic region (δ_{H} 0.75- 2.4). Downfield signals of variable intensities between 3.0 and 5.6 ppm were present in all samples, while signals in the aromatic region over 7.0 ppm were absent or very weak. The data suggested the presence of aliphatic compounds such as terpenoids, sterols and fats as the main constituents of this propolis group.

While in group II which included the red samples BRN-RSN and CCN the NMR pattern was quite different. These propolis samples displayed characteristic signals of flavonoids and a strong aliphatic region between 1.5 and 4.3 ppm. In addition to clear triplets around 5.26–5.31 ppm corresponded to protons within prenyl or geranyl groups and singlets over 12.0 ppm which are usually related to the flavonoid -OH group. The principle differences with respect to group I were the clear aromatic methoxyl signals (δ_{H} 3.71-3.76) and a wide and complex aromatic region (δ_{H} 6.34-8.1). The NMR signals of the main compounds in these extracts were assigned to isoflavonoids.

The protons of the C ring of isoflavans that usually appear in the ranges of δ_{H} 2.70–3.0, 3.5 and 4.04–4.35 were clearly visible in all ^1H NMR spectra. Doublets near 5.51 ppm typical of pterocarpans (H-11a), were also found to be characteristic ^1H NMR signals of this propolis type. In case of CCN red propolis the spectrum was a mixture between group I and River state Nigerian containing strong response in aliphatic regions referring to triterpenes and weaker aromatic signals. In group II UDN showed an interesting signal at 13.5 ppm suggesting the presence of a xanthenes type of phenolics. While in ION two clear doublets at 0.80, 0.60 ppm suggested cycloartane type compounds, which seems to be a major component in this sample, in addition to a complex mixture of phenolic compounds. **Figure 3- 6** shows comparison of the ^1H NMR spectra of two samples; ION and UDN, demonstrating two characteristic classes of cycloartane and xanthenes type of compounds.

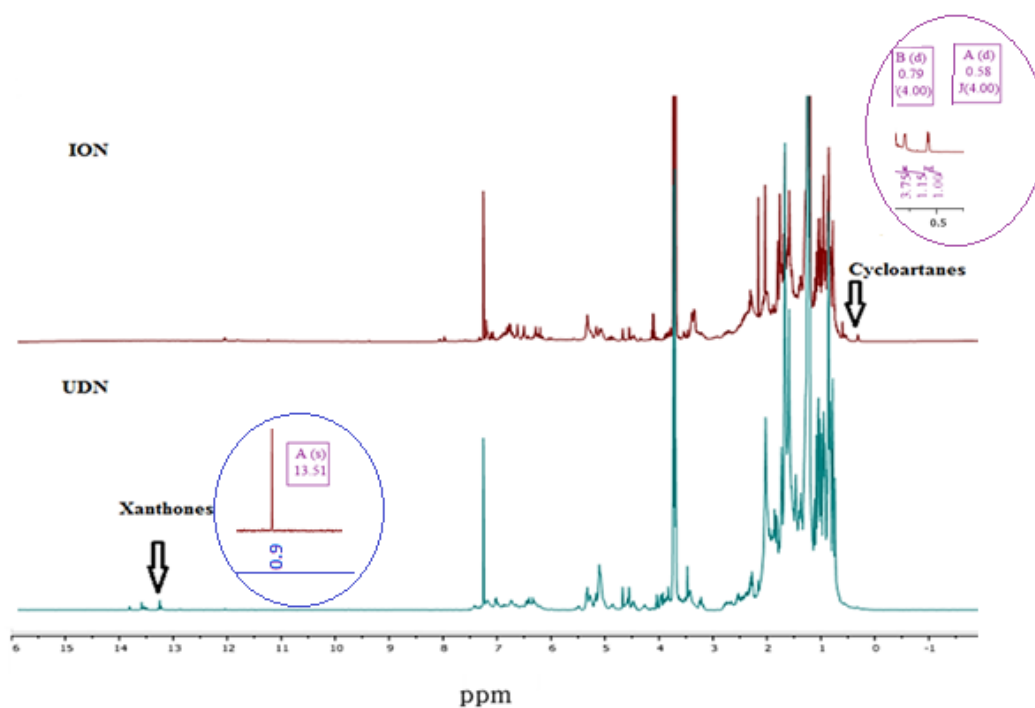


Figure 3-6: Comparison of the ^1H NMR spectra (400 MHz, in CDCl_3) of two extracts ION and UDN with labelling the characteristic compounds, cycloartanes in the ION sample and xanthenes in the UDN sample. Experimental conditions in section 2.3.4.

3.4.4 LC-HRMS Analysis of Crude Extracts from Nigerian Propolis Samples

All samples were run in duplicate in order to verify the instrumental precision and reproducibility. The data collected from the LC-MS were complex and difficult to process manually, and were split into positive and negative ion data, and then processed by MZ-mine 2.14, and the extracted features were searched against the Dictionary of Natural Products database. The 2000 most intense features with the highest mean peak areas across the 12 samples, selected by m/z mine from the negative ion data, were used to build a PCA model. The data was univariate (uv)

scaled and log transformed prior to PCA modelling, the score plot **Figure 3-7** showed that most of the samples collected from central Nigeria were clustered near the centre due to the absence of LC–HRMS features with a high MS response. The locations of the rest of the samples, even for samples that were collected from the same area such as BRN and RSN (both of which were collected from River state, Nigeria), were not identical. Samples UDN and CCN were also from the South of the country and were intermediate in composition between the samples from central Nigeria and those from Rivers State. The ION samples lay slightly outside the ellipse demonstrating more unique chemical composition. Hierarchical cluster analysis (HCA) was used to divide the samples into three groups **Figure 3-8** according to similarity in chemical composition.

Figure 3-9 shows the loadings (metabolites) on which the PCA separation was based.; from the loading plot characteristic chemical compounds responsible for variation among samples could be assigned exclusively to single chemical formulas within a 3 ppm mass error window. Each elemental composition generally corresponded to a large number of isomers within the DNP database. **Table 3-4** shows some of the most responsible compounds for producing the PCA separation in samples; UDN, ION, CCN. Samples collected from River state Nigeria will be discussed in details in Chapter 5.

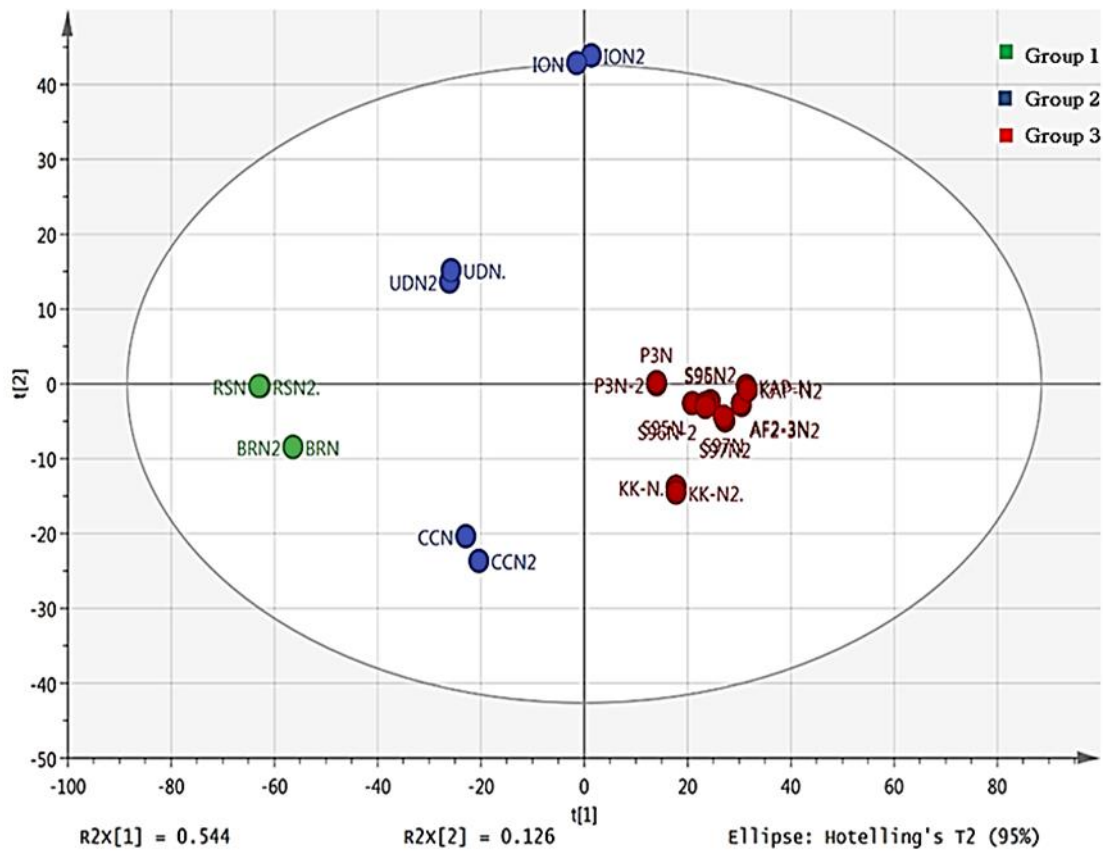


Figure 3-7: Score plot of PCA for duplicate analyses of crude extracts of Nigerian propolis samples, one outlier ION can be clearly observed. Samples from the central Nigeria were clustered together to some extent.

Table 3-4: Putatively identified compounds responsible for the differences among propolis samples UDN, ION and CCN based on analysis by high resolution followed by PCA when searched in DNP.

Propolis sample UDN				
<i>m/z</i>	<i>t_R</i> (min.)	Formula	Compound name	Botanical source
379.156	40.3	C ₂₃ H ₂₄ O ₅ 38 isomers	Prenyl xanthone	<i>Garcinia mangostana</i> (mangosteen), <i>Garcinia parvifolia</i>
395.15	35.3	C ₂₃ H ₂₄ O ₆ 81 isomers	Tetrahydroxy-2 diprenylxanthone	<i>Garcinia</i> <i>smeathmannii</i> , <i>Garcinia buchananii</i>
531.276	40.0	C ₃₃ H ₄₀ O ₆ 3 isomers	Garcimultiflorone I	<i>Garcinia multiflor</i>
601.354	49.6	C ₃₈ H ₅₀ O ₆ 26 isomers	Guttiferone A	<i>Symphonia</i> <i>globulifera</i> , <i>Garcinia</i> <i>livingstonei</i> , <i>Garcinia</i> <i>macrophylla</i>
Propolis sample ION				
<i>m/z</i>	<i>t_R</i> (min.)	Formula	Name	Botanical source
383.114	21.9	C ₂₁ H ₂₀ O ₇ 88 isomers	4',5,7-Trihydroxy-6-methoxy-flavone	Many
407.187	30.7	C ₂₅ H ₂₈ O ₅ 99 isomers	Geranylated or diprenylated flavanoid	Many
421.166	31.8	C ₂₅ H ₂₆ O ₆ 127 Isomers	Prenyl flavonoid	Many
423.182	25.3	C ₂₅ H ₂₈ O ₆ 94 isomers	Geranylated or diprenylated flavanoid	Many
437.161	28.7	C ₂₅ H ₂₆ O ₇ 57 isomers	1,3,6,Tetrahydroxy2,diprenylxanthone	<i>Garcinia mangostana</i> (mangosteen)

Propolis sample CCN				
<i>m/z</i>	<i>t_R</i> (min.)	Formula	Name	Botanical source
461.198	48.8	C ₂₈ H ₃₀ O ₆ 20 isomers	1,3,6-Trihydroxy-2,5-diprenyl-6',6'-dimethylpyrano(2',3':7,8) xanthone (tovophyllin A)	<i>Garcinia mangostana</i>
465.338	48.6	C ₃₁ H ₄₆ O ₃ 9 isomers	Enervosanone (polyisoprenylated ketone)	Clusiaceae (Guttiferae)
569.364	49.0	C ₃₈ H ₅₀ O ₄ 9 isomers	hypersampsone G (Geranyl Bearing Polyisoprenylated Benzoylphloroglucinol)	<i>Hypericum sampsonii</i>
599.338	47.9	C ₃₈ H ₄₈ O ₆ 10 isomers	Oblongifolin F	<i>Garcinia oblongifolia</i>
601.354	43.8	C ₃₈ H ₅₀ O ₆ 26 isomers	polyisoprenylated benzophenone isomer of guttiferone A	<i>Symphonia globulifera</i> , <i>Garcinia livingstonei</i> , <i>Garcinia macrophylla</i>

3.5 Prediction of the most active compounds in the crude propolis extracts from LC-MS data

The extracted LC-MS data was used to build a partial least square (PLS) model for predicted against measured EC₅₀ values against wild type *T. brucei* **Figure 3-10**. Two of the low activity samples AF2-3N and KKN were omitted from the model. The model was edited to remove variables having less impact in the prediction of anti-trypanosomal activity and Figure 3-10 was based on 180 features.

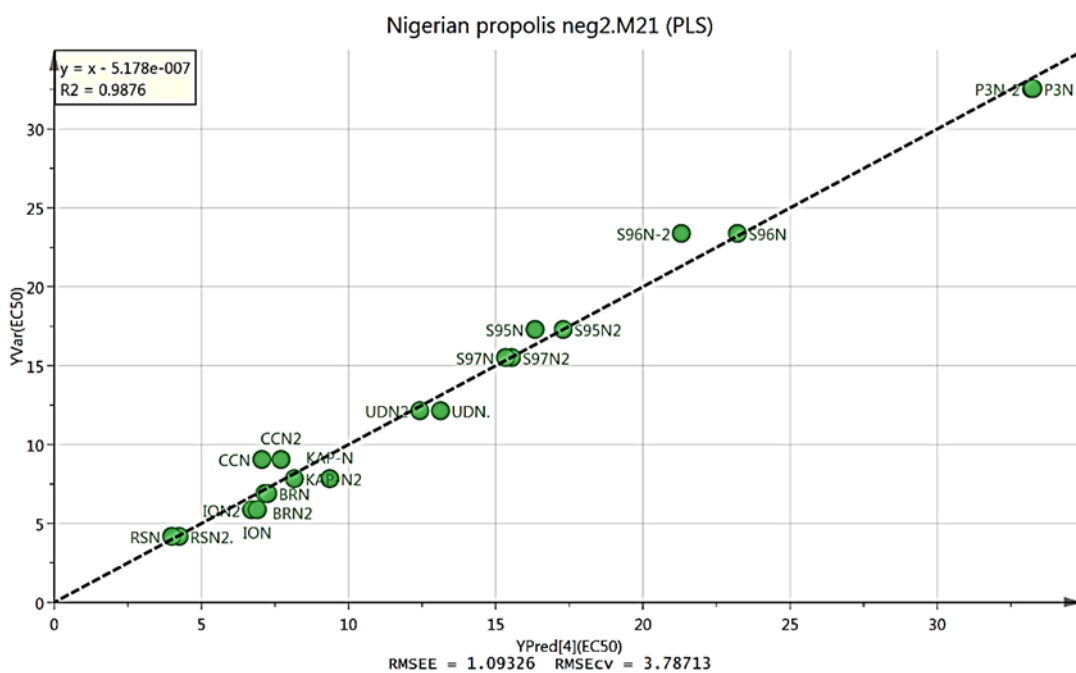


Figure 3-10: PLS model of predicted against measured anti-trypanosomal activity of Nigerian propolis extracts based on 180 features.

When the loadings plot for the model **Figure 3-11** was examined it was clear that the compounds predicted to be most responsible for anti-trypanosomal activity were isomers of denticulatain , and most of the isomers had a characteristic fragment ion at m/z 241.05 as described in detailed elucidation of the MS² spectra in chapter 5 page 151. These compounds are probably obtained from macaranga species.

When data processed manually for m/z 515.3158, **Figure 3-12** shows an extracted ion trace for the denticulatain isomers in four high activity samples indicating that the abundance of these isomers correlates with activity against *T. brucei*. We were interested in the occurrence of guttiferone isomers which we had observed in Rivers State propolis samples in our earlier study, and speculated that these might be

responsible for the high anti-trypanosomal activity of the of the samples since we had previously observed very high activity for a phlorogucinone compound isolated from Cameroonian propolis (Almutairi *et al.*, 2014). However, as can be seen in the extracted ion traces shown in **Figure 3-13** for guttiferone isomers sample CCN, which has lower anti-trypanosomal activity than sample RSN, there are much higher levels of these isomers than sample RSN. Thus, it would appear that levels of denticulatain isomers correlate more closely with observed anti-trypanosomal activity. Therefore, these compounds should be targeted for isolation and testing.

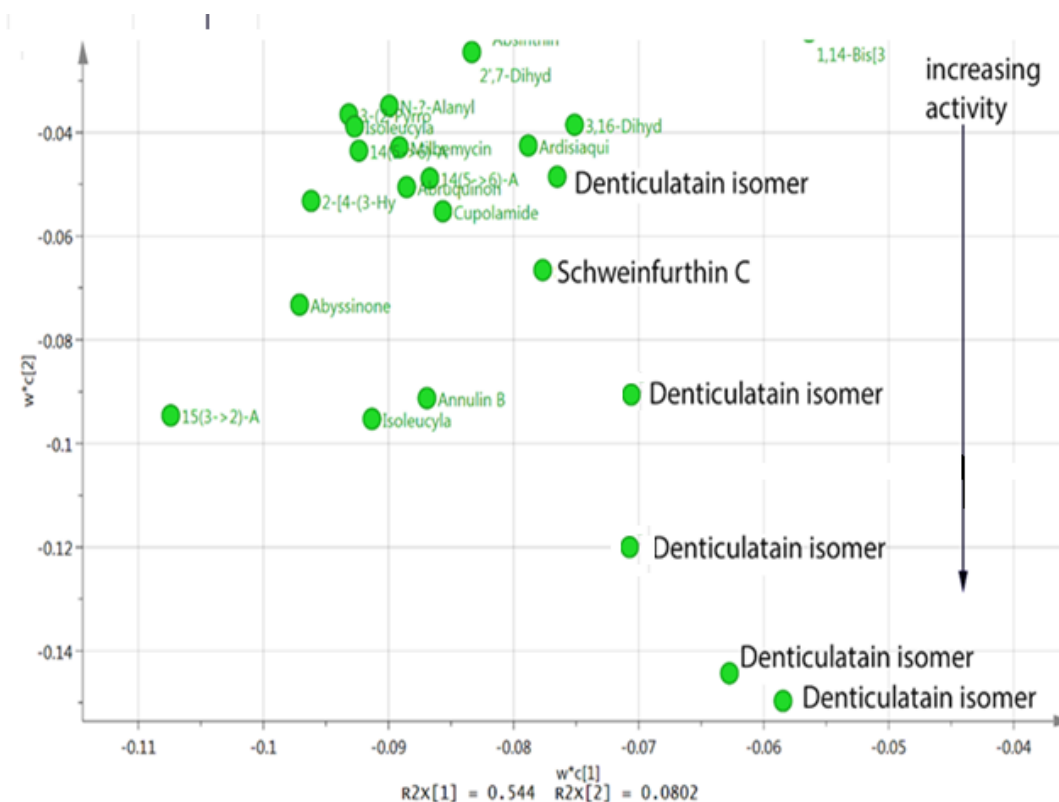


Figure 3-11: Loadings in the high activity region for the Nigerian propolis samples demonstrated the abundance of Denticulatain isomers in this region.

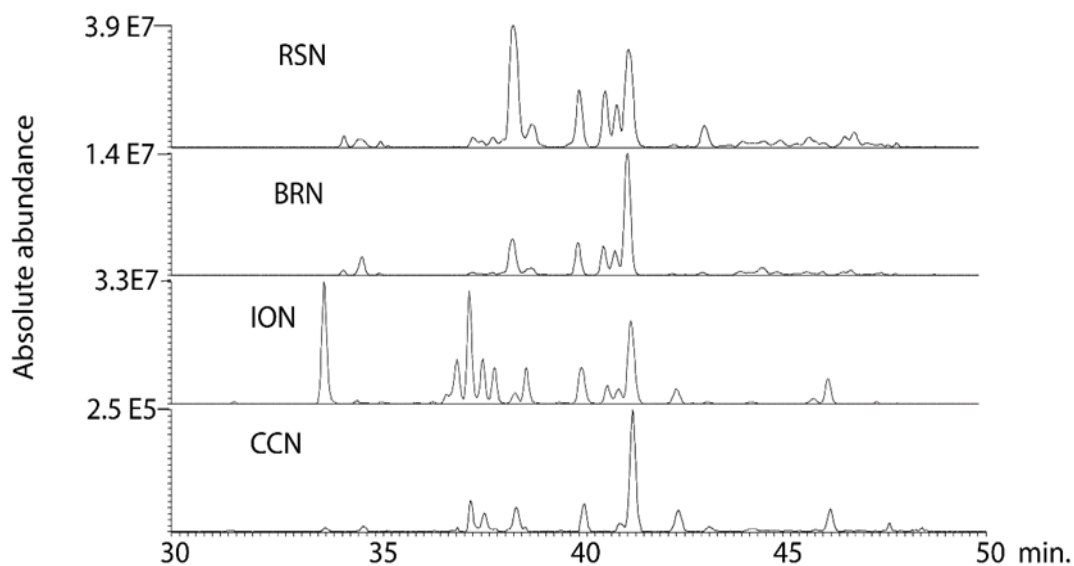


Figure 3-12: Extracted ion traces for denticulatatin (m/z 515.29-515.32) isomers in the high activity Nigerian propolis samples. Experimental condition in section 2.3.2

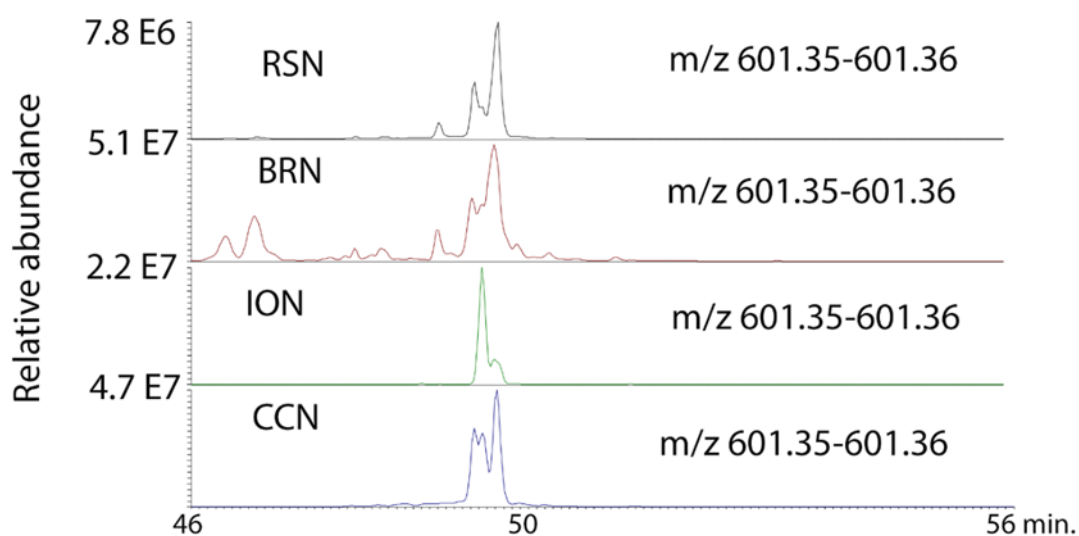


Figure 3-13: Extracted ion traces for isomers of guttiferone A in samples RSN, BRN, ION and CCN. Experimental condition in section 2.3.2.

3.6 Discussion

A range of analytical methods has been used to profile propolis qualitatively and quantitatively, including spectrophotometry HPLC, ESI/MS capillary electrophoresis, GC-MS, TLC and NMR. Although most of them have not been validated in agreement with ICH guidelines, and they focus on marker compounds, it would be advantageous to be able to treat the samples as a whole rather than rely solely on the commonly used marker compounds. To do this effectively, chemometric methods are being increasingly applied to complex sets of data and have recently been applied to MS data obtained from propolis (Araújo *et al.*, 2005; Zhang *et al.*, 2014). Since propolis consists of a wide range of organic compounds of varying polarity and ionizability, complementary techniques were used in parallel to get the whole picture. Techniques that can simultaneously examine waxes, terpenoids and phenolics are NMR spectroscopy and GC-MS while HPLC-ELSD typically reveals compounds with UV-absorbing and non UV-absorbing chromophores, since ESI/MS can only detect compounds that ionize under the conditions used.

Based on a previous study performed on African propolis collected from different regions of Africa (Zhang *et al.*, 2014), and no clear geographic delineation for the classification of these African propolis samples having been observed, interestingly one sample from Nigeria stood out with unique chemical composition and strong anti-trypanosomal activity. This study investigated the chemical characterization of propolis samples from widespread regions within Nigeria, which is considered as wet Savannah. The biological activity against *Crithidia fasciculata* and *Trypanosoma brucei* which is a health threat to cattle and humans in the Savannah was also

studied. As the existing drugs are old, in many cases quite toxic, not completely effective and the rate of drug development against this disease is very slow.

Nigerian samples (n=12) were chemically profiled using different complementary analytical techniques including NMR, GC-MS, HPLC-UV-ELSD and LC-HRMS which have been used in parallel to try to get the overall picture and fingerprints of chemical components in these complex samples. They work together to detect all components and target characteristic compounds to be purified by optimized conditions and tested.

The composition of Nigerian propolis samples varies widely and can be divided into two groups according to geographical origin; either were Southern propolis samples rich in UV absorbing phenolic compounds or central propolis containing mainly non-UV absorbing triterpenoids.

PCA results of the processed LC-MS data collected, demonstrated that the chemical composition was highly diverse; samples collected from the central Nigeria were clustered together near the centre **Figure 3-7**, while the samples from Southern Nigeria were quite different from each other, even with samples collected from same area such as BRN, and RSN collected from River state Nigeria. The compounds responsible for differences among Southern samples were putatively identified from DNP, and these samples were subjected for further purification and investigation.

Samples coded RSN, BRN, CCN, ION and UDN from Southern Nigeria demonstrated the highest activity against *T.brucei* and *C.fasiculata* **Table 3-2**. The activity against *C.fasiculata* supports the idea that the bees may collect propolis to protect from infection by *Crithidia* species, which are known to be pathogens of

bees, and are quite closely related to *T.brucei*. The extracts were active against both the standard strain of *T.brucei* and two isolates which displayed a degree of resistance against pentamidine.

In order to determine what are the most active components in the extracts, PLS modelling was carried out using high-resolution mass spectrometry data from the extracts. The loadings plot for a PLS model pointed towards denticulatain isomers as being most strongly associated with the anti-trypanosomal activities and these could be a target for isolation and testing.

CHAPTER FOUR

PURIFICATION OF ANTI-TRYPANOSOMAL

COMPOUNDS FROM SOUTHERN NIGERIAN

PROPOLIS

4 PURIFICATION OF ANTI TRYPANOSOMAL COMPOUNDS FROM SOUTHERN NIGERIAN PROPOLIS

4.1 Introduction

The study proceeded to examine in more detail the samples that were most active against *Trypanosoma brucei* by trying to purify the component(s) responsible for the activity, by using an optimized medium pressure chromatographic technique. In this chapter, sample ION collected from Ijebu-Ode/Ogun State and sample UDN collected from Ugelli/Delta State were fractionated and isolated compounds were tested. The other active samples collected from River state Nigeria will be discussed in detail in Chapter 5.

4.2 Experimental

Two active samples coded ION, UDN were fractionated further; 100 g of each sample was extracted with 500 mL ethanol as described in section 2.2 and yielding 40 g and 61 g of ethanolic extract of propolis (EEP) of ION and UDN respectively. 10 g of EEP of sample ION and 7 g of UDN were fractionated by silica column as described in section 2.4.1 resulting in 52 fractions (50 mL) each. In the case of UDN, two fractions UDN10 (265.0 mg) collected at 40:60 ethyl acetate: hexane, and UDN14 (130.0 mg) eluted at 50:50 ethyl acetate: hexane were chosen because they contained characteristic xanthenes at m/z 379.154 according to LC-MS profiling.

The fractions were purified using the Grace Davison Reveleris® flash chromatography system. After method development with the analytical LC-UV-ELSD system, both were re-chromatographed using the Grace system in reversed phase mode using a 12

g (C18) cartridge and a flow rate of 12 mL/min, and isocratic conditions of 30:70 ACN: water for 30 min. then increasing to 100% ACN over 30 min. and holding for 5 min., then back to 30% ACN in 1 min., holding it for 5 min.; yielding three compounds **Mudn14-40** (8.6 mg), **Mudn10-242526** (11.0 mg) and **Mudn10-51** (7.0 mg). All were as fine yellow powders.

In the case of ION, NMR profiling revealed that it contained a characteristic cycloartane class of triterpene as a major component, while LC-MS proved the presence of denticulatain isomers phenolic compounds strongly associated with the anti-trypanosomal activities and thus targeted for isolation and testing. In the case of the open column fractions of the ION sample, fractions ION12 (165.0 mg) and ION13 (160.0 mg) both eluted at 60:40 hexane: EtOAc. They were purified by using the reversed phase C18 (12 g) cartridge. The elution method used isocratic conditions with 90:10 ACN: water for 30 min. with a flow rate of 9 mL/min. yielding compounds **Mion12-18** (13.0 mg), **Mion12-23** (6.0 mg) and **Mion13-25** (12.2 mg). All were white amorphous solids.

4.3 Results

4.3.1 *Structure elucidation of compounds purified from Southern propolis samples*

4.3.1.1 **Characterization of compounds isolated from UDN sample.**

Sample UDN showed characteristic peak at m/z 379.154 in negative ion ESI $[M - H]^-$ corresponding to the formula $C_{23}H_{24}O_5$, which was targeted and purified to give three isomers of prenylated xanthenes with different retention time on LC-MS as shown in **Figure 4-2**. Two of them **Mudn14-40** and **Mudn10-242526** were first isolated

from *Cudrania cochinchinensis* and *Cudrania tricuspidata* (Hou *et al.*, 2001; Uksamrarn *et al.*, 2006) and the NMR current spectra were thus compared to the literature. While the third **Mudn10-51** was not described before, and was elucidated by 1D and 2D NMR as shown in **Table 4-1**. The fragments from LC-MSⁿ analysis were different from the each other especially for the new xanthone.

Closely related xanthone compounds were found for the first time in Thai propolis collected by *Tetragonula laeviceps* species of stingless bee. *Garcinia mangostana* (Mangosteen) was the most probable plant source (Sanpa *et al.*, 2015). The chemical structures of isolated compounds are shown in **Figure 4-1**.

Compound (Mudn14-40) 1,3,7-trihydroxy-2,8-di-(3-methylbut-2-enyl)xanthone:

Fine yellow powder ; HR-EIMS t_R 47.8 min m/z (% rel. int.) 379.1544 (100) [M-H]⁻ calculated for C₂₃H₂₄O₅, MS² 356.0894(40) (C₁₉H₁₆O₇, Δ -2.05 ppm), 323.0920 (30) (C₁₉H₁₅O₅, Δ -1.35 ppm), 281.0452 (30) (C₁₆H₁₀O₅, Δ -1.13 ppm), 335.0918 (20) (C₂₀H₁₆O₅, Δ -2.08 ppm), 309.0764 (10) (C₁₈H₁₄O₅, Δ -1.41 ppm); ¹H NMR (DMSO-d₆, 400 MHz) and ¹³C NMR(DMSO-d₆, 100 MHz) spectra are shown in **appendix 1**, data were comparable to the data in the literature (Mahabusarakam, 1987), values of the chemical shifts are given in **Table S1** in the appendix.

Compound(Mudn10-242526)1,3,7-trihydroxy-4,8-di-(3-methylbut-2-enyl)
xanthone:

Fine yellow powder ; HR-EIMS t_R 41.9 min m/z (% rel. int.) 379.1550[M-H]⁻(100) calculated for C₂₃H₂₄O₅, MS² 356.0904 (60) (C₁₉H₁₇O₇, Δ 0.5 ppm), 324.1005 (40) (C₁₉H₁₇O₅, Δ 0.4 ppm), 310.0847 (30) (C₁₈H₁₅O₅, Δ 0.155 ppm), 267.0300 (20) (C₁₅H₈O₅, Δ 0.5 ppm), 255.0300 (20) (C₁₄H₈O₅, Δ 0.3 ppm); ¹H NMR (DMSO-d₆,

400MHz) and ^{13}C NMR(DMSO- d_6 , 100 MHz) spectra are shown in **appendix 2**, data were comparable to the data in the literature and the chemical shifts are given in **Table S2** in appendix.

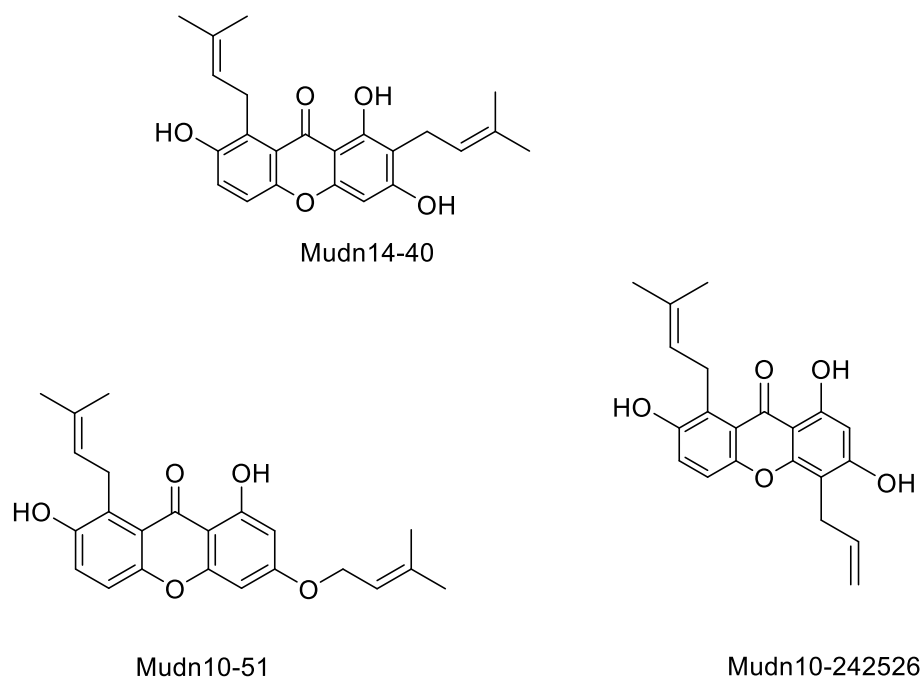


Figure 4-1: Structures of prenylated xanthenes isolated from the UDN propolis sample.

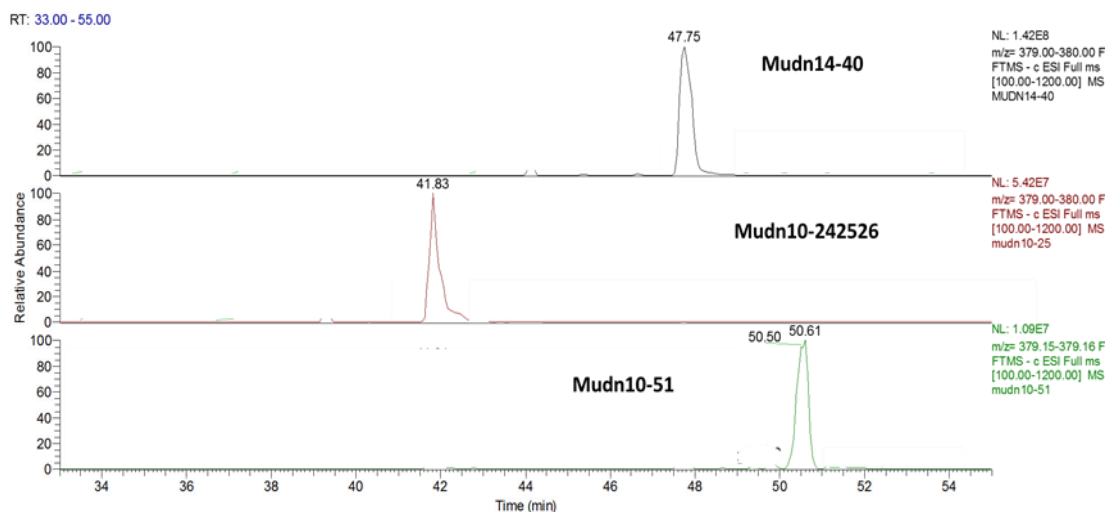


Figure 4-2 : HR-ESIMS ion chromatogram and mass spectrum of three prenylated xanthenes isolated from sample UDN. Experimental conditions in section 2.3.2.

Compound Mudn10-51 (previously undescribed prenylated xanthone):

Fine yellow powder; HR-EIMS t_R 50.6 min m/z (% rel. int.) 379.1551[M-H]⁻ calculated for C₂₃H₂₄O₅, MS² 310.0844 (100) (C₁₈H₁₅O₅, Δ -1.070 ppm), MS³ 295.0612(100) (C₁₇H₁₂O₅, Δ 0.023 ppm), 242.0220(60) (C₁₃H₁₇O₅, Δ 0.130 ppm) 267.0299(20) (C₁₅H₈O₅, Δ 0.162 ppm). Melting point (179–181 °C) 1-2D NMR was performed (DMSO- d₆, 400 MHz) and the data used for elucidation are shown below in **Table 4.1**.

The NMR data for the new xanthone were compared with calothwaiteaxanthone (Dharmaratne *et al.*, 1986). The ¹HNMR spectrum showed signal for one hydroxyl group δ 13.19 (1H, s). The compound contained four protons in the aromatic region, which formed two AB systems. The more shielded pair aromatic protons δ 6.36 (1H, d, $J = 2.3$ Hz) and 6.57 (1H, d, $J = 2.3$ Hz), H-2 and H-4 exhibited meta-coupling to

each other. For the other two protons, the HMBC spectrum indicated that both of these protons coupled to C-3 at (δ 156.8) that was attached to an oxygen atom. The other two protons were ortho-coupled aromatic protons δ 7.03 (1H, d, $J=8.2$ Hz) and 7.23 (1H, d, $J=8.2$ Hz), the chemical shifts for methylene H-11 and H-16 of two prenyl groups where the different one was more deshielded due to attachment of oxygen at H-16 δ 4.69, (2H, brd, $J=6.8$ Hz) while H-11 δ 3.90, (2H, brd, $J=7.2$ Hz). Two prenyl group multiplets (m) appeared at δ 5.33, δ 5.47 corresponding to 1H referred to H-12, H-17 respectively, the latter was higher due to the presence of the oxygen attached. Four methyls appeared at δ 1.68, 1.71, 1.78, and 1.74, all were 3H (brd, $J=1.3$) analysis of their HMQC and HMBC spectra allowed the unambiguous assignments of all proton and carbon signals which also clarified the position of these substituents. Several HMBC couplings, including correlations of the OH-1 proton with C-1 (δ 162.5), C-2 (δ 97.9), and C-9a (δ 103.9). The two methyl groups at δ 1.68 (H-14), and 1.71 (H-15) with C-12 (δ 124.0), the other two methyls at δ 1.78 (H-19) and 1.74 (H-20) correlate with C-17 (δ 119.6). The aromatic doublet protons at δ 6.36 (H-2) and δ 6.57 (H-4) with C-9a (δ 103.9), revealed a partial structure of compound 1, 7-dihydroxy-8(3-methylbut-2-enyl)-3(methylbut-2-enyloxy) xanthone.

The positions of the prenyloxy and hydroxyl groups on A ring were deduced by following HMBC correlation peaks: Cross-peaks between the oxygen-bearing methylene at δ 4.69 (H-16) with C-3 (δ 156.3), and the doublet at δ 6.36 (H-2) with C-9a (δ 103.9) and the doublet at δ 6.57 (H-4) with C-9a (δ 103.9), and C-2 (δ 97.9) were also observed in the spectrum. Accordingly, the two hydroxyls were at C-1, C-7 and the oxygenated prenyl groups were located at C-3 and prenyl at C-8,

respectively. Thus, the structure of this xanthone was concluded to be as shown in **Figure 4-3**.

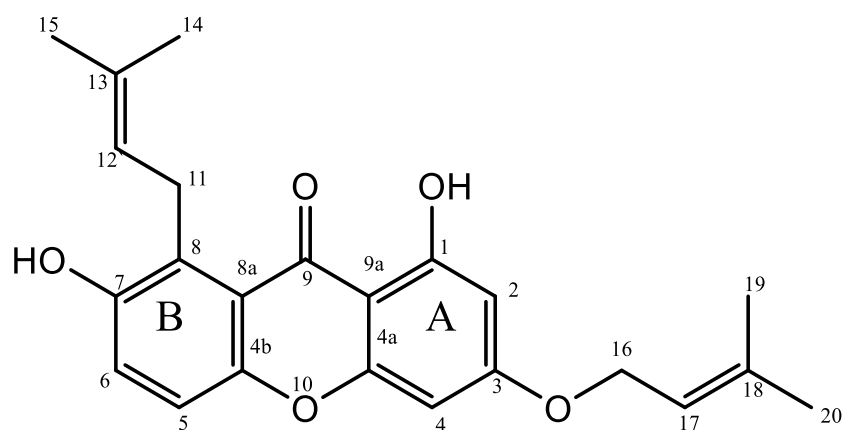


Figure 4-3: Numbered structure of the new xanthone.

Table 4-1: ^1H - and ^{13}C - NMR data for the new xanthone.

Position	Chemical shift δ ppm ^1H (mult, J Hz)	Chemical shift δ ppm ^{13}C	COSY ($^1\text{H} - ^1\text{H}$)	HMBC ($^1\text{H} - ^{13}\text{C}$)
1	-	162.5 (C)	NA	-
2	6.36 (d, 2.3)	97.9 (CH)	H4	C3,C4, C9a
3	-	156.8 (C)	NA	-
4	6.57 (d, 2.3)	93.0 (CH)	H2	C2, C3,C9a,C4a
4a	-	154.3 (C)	NA	-
4b	-	146.4 (C)	NA	-
5	7.03 (d, 8.2)	125.7 (CH)	H6	C6, C7, C8a
6	7.23 (d, 8.2)	120.7 (CH)	H5	C4b,C5, C8
7	-	144.5 (C)	NA	-
8	-	132.9 (C)	NA	-
8a	-	118.3(C)	NA	-

9	-	183.0 (C)	NA	-
9a	-	103.9 (C)	NA	-
10	-	-	-	-
11	3.90, 2H (brd,7.2)	32.8 (CH ₂)	H12, H14,H15	C7, C8, C8a,C12, C13
12	5.33 , 1H (m)	124.0 (CH)	H11,H14,H15	C11, C14,C15
13	-	131.6(C)	-	-
14	1.68, 3H (brd,1.3)	26.1 (CH ₃)	H11,H12,H15	C12, C13, C15
15	1.71, 3H (brd,1.3)	18.3 (CH ₃)	H11,H12,H14	C12, C13, C14
16	4.69, 2H(brd, 6.8)	65.9 (CH ₂)	H17,H19,H20	C17
17	5.47, 1H (m)	119.6 (CH)	H15,H19,H20	C18, C19, C20
18	-	138.7 (C)	NA	-
19	1.78, 3H (brd,1.3)	25.9 (CH ₃)	H16,H17,H20	C17,C18,C20
20	1.74, 3H (brd,1.3)	18.6 (CH ₃)	H16,H17,H19	C17,C18,C19
1-OH	13.19, 1H (s)	-	NA	C1

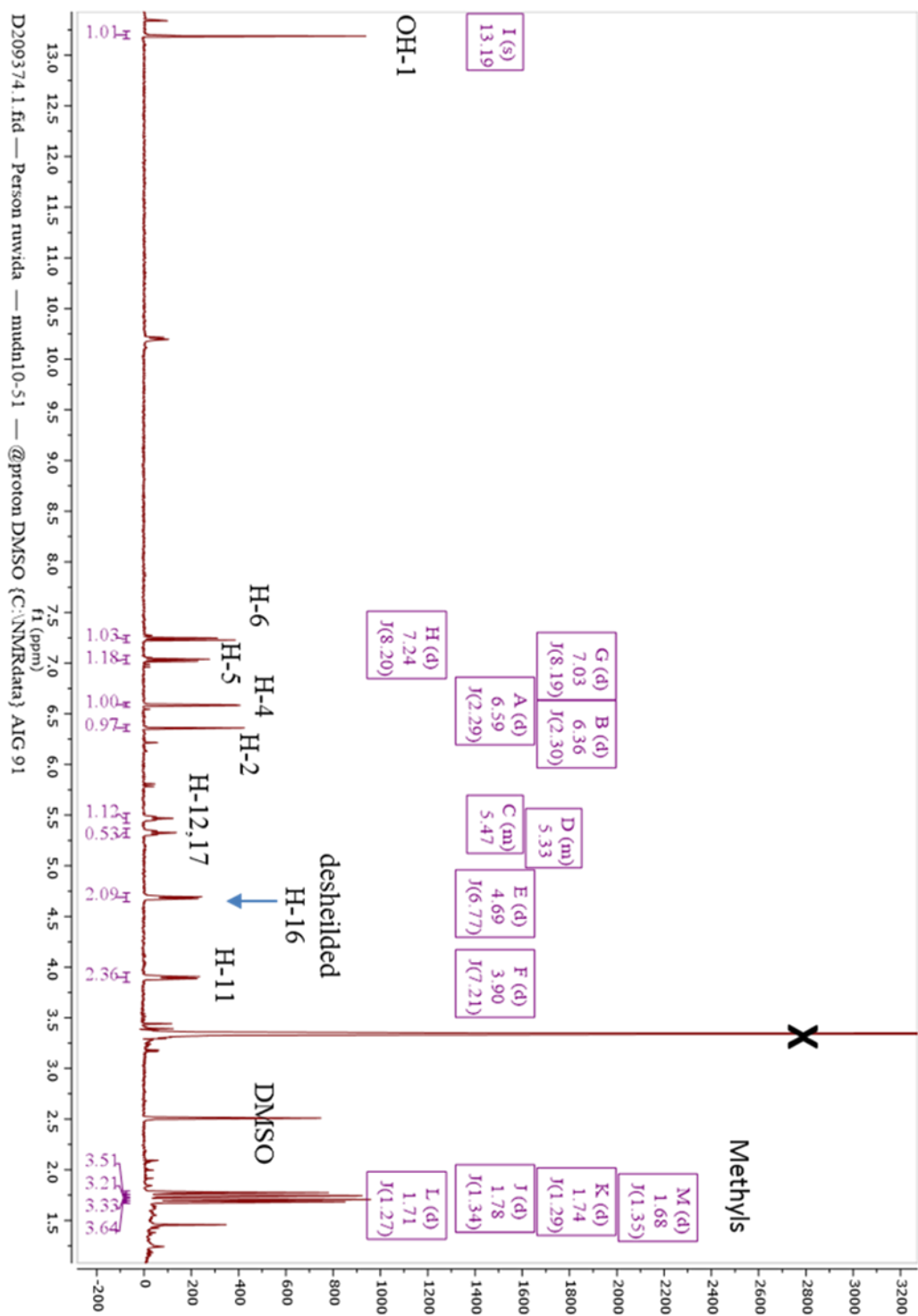


Figure 4-4: ^1H NMR of Mudn10-51 (400 MHz, DMSO-d_6), X denote for solvent peak.

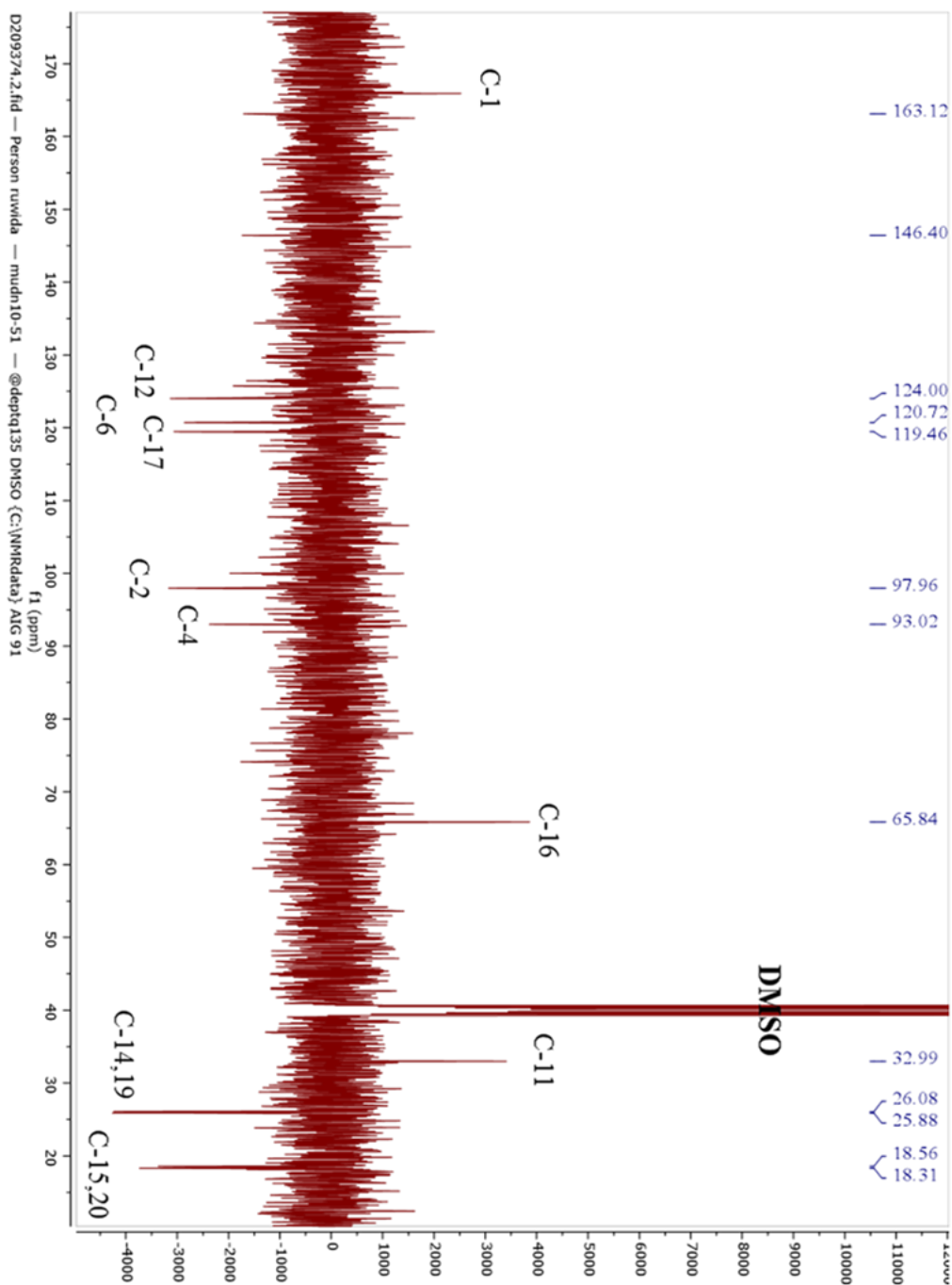


Figure 4-5: ^{13}C NMR spectrum of Mudn10-51 (100 MHz, DMSO- d_6).

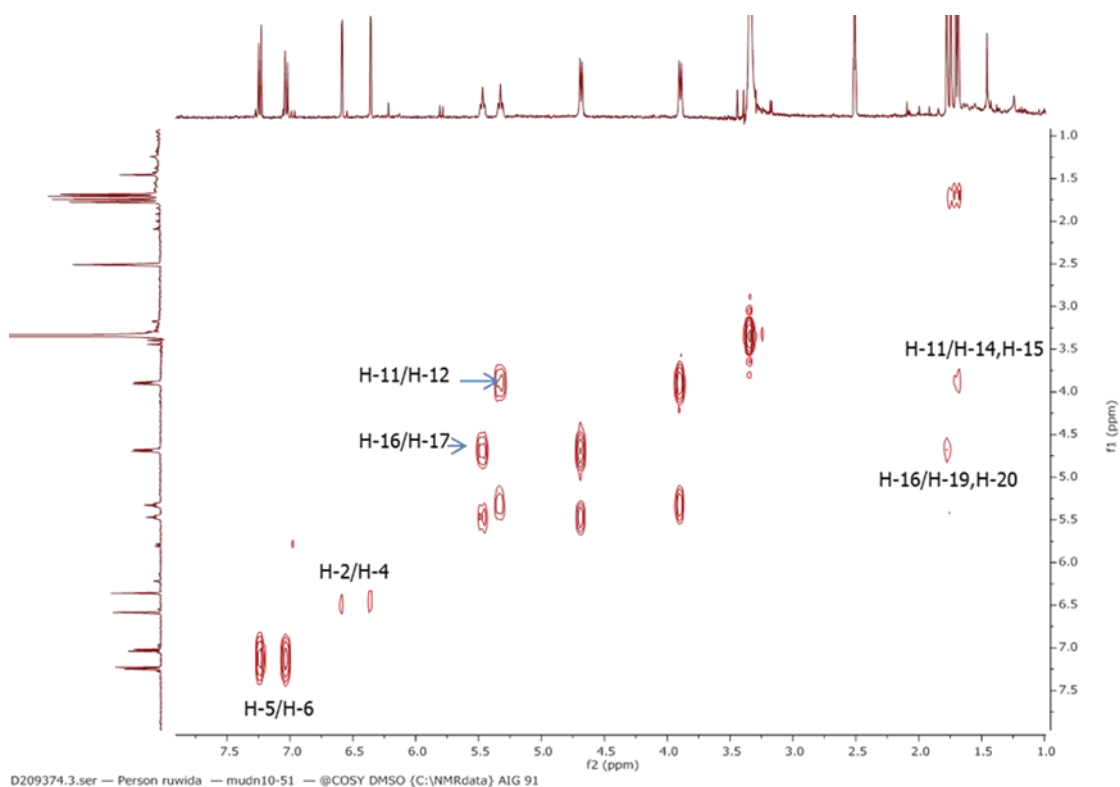


Figure 4-6: COSY spectrum (400 MHz) of Mudn10-51 in DMSO- d_6 .

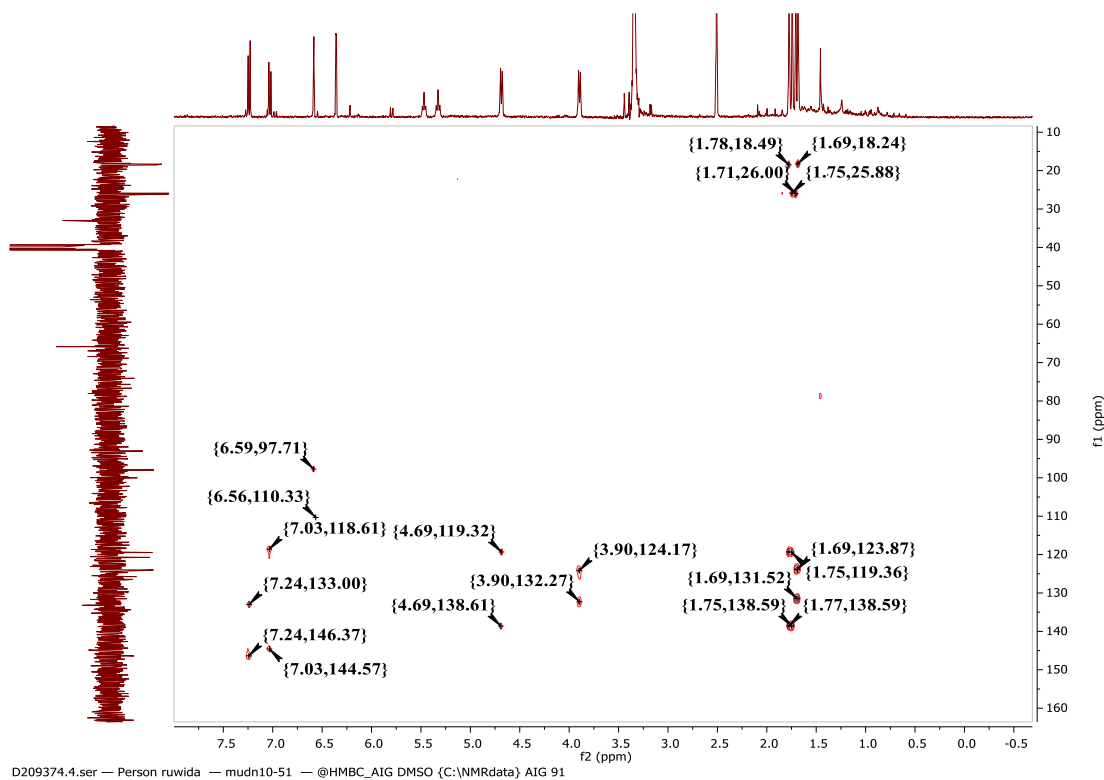


Figure 4-7: Expanded HMBC spectrum (400 MHz) of Mudn10-51 in DMSO- d_6 .

4.3.1.2 Characterization of compounds isolated from ION sample

With regard to the ION sample two cycloartanes, ambonic and mangiferonic acids, were separated and their NMR spectra were compared with the literature, and also a mixture of α Amyrin with mangiferonic acid as (1:3) as interpreted by NMR integration. MSⁿ fragmentation of these compounds were not obtained since they had a poor ionizability. Although all of them gave good ELSD responses from LC-UV-ELSD **Figure 4.7**.

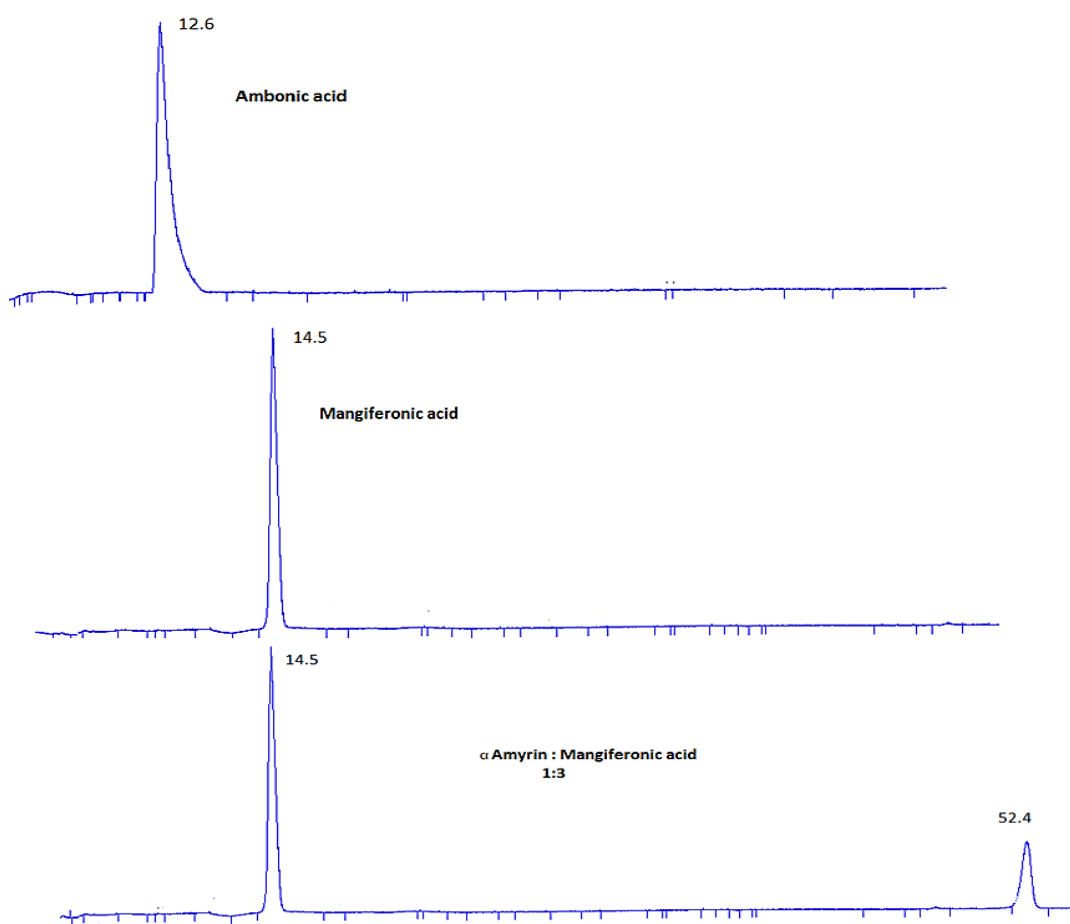


Figure 4-8: LC-UV-ELSD chromatogram of purified triterpens from ION, all with ELSD only response. HPLC conditions in section 2.3.1.

These compounds were isolated before from Cameroonian propolis, and mango (*Mangifera indica*) Anacardiaceae; it seems that this plant may be the source of the resin since it is widely used in honey production in Cameroon and throughout tropical Africa (Kardar *et al.*, 2014). α Amyrin and Mangiferonic acid were also found in Brazilian propolis (Silva *et al.*, 2005; Silva *et al.*, 2008), and the latter has been isolated from propolis from Myanmar and showed strong cytotoxic properties (Li *et al.*, 2009). The data for the isolated triterpenes is summarized below.

Compound (Mion12-18) ambonic acid:

White amorphous solid, $[M-H]^-$ m/z 467.3531 (calculated for $C_{31}H_{48}O_3$) 1H NMR ($CDCl_3$, 400 MHz) and ^{13}C NMR ($CDCl_3$, 100 MHz) spectra are shown in **appendix 3**; data were comparable to the literature, and the values of chemical shifts are given in **Table S3** in the appendix.

Compound (Mion12-23) mangiferonic acid:

White amorphous solid, $[M-H]^-$ m/z 453.3378 (calculated for $C_{30}H_{46}O_3$) 1H NMR ($CDCl_3$, 400 MHz) and ^{13}C NMR ($CDCl_3$, 100 MHz) spectra are shown in **appendix 4**; data were comparable to the literature, and the values of chemical shifts are given in **Table S4** in the appendix.

Compound (Mion13-25) α amyryl in mixture:

White amorphous solid, $[M-H]^-$ m/z 425.2460 (calculated for $C_{30}H_{50}O$) 1H NMR ($CDCl_3$, 400 MHz) and ^{13}C NMR ($CDCl_3$, 100 MHz), spectra are shown in **appendix 5**; data were comparable to the literature, and the values of chemical shifts are given in **Table S5** in the appendix.

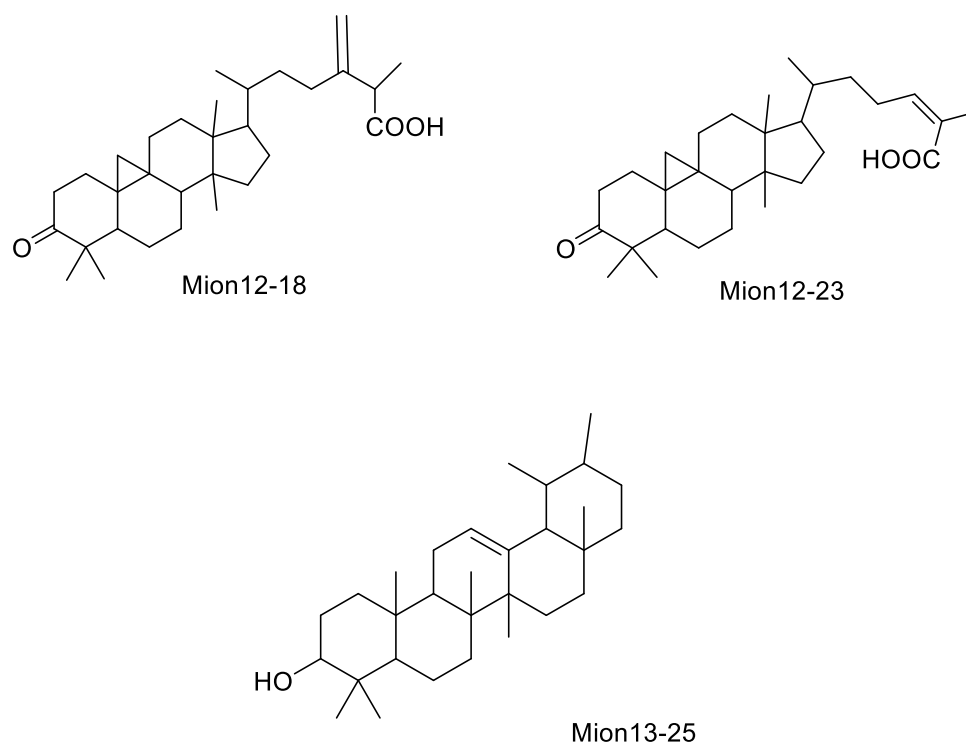


Figure 4-9: The structure of the triterpenes isolated from the ION propolis sample Mion12-18 (ambonic acid) , Mion12-23 (mangiferonic acid), Mion13-25 (α amyryrin).

4.3.2 Bioassay results

All isolated compounds from ION and UDN propolis samples were tested and activity evaluated against *Trypanosome brucei*. The highest activity observed was for the three xanthenes but all the compounds isolated from the resins were to some degree active as shown in **Table 4-2**.

Table 4-2: Average of (EC₅₀) for (n=3) for crudes and purified compounds against wild type *Trypanosome brucei* (T b S427WD) and two other genetically modified types (B48 and aqp2/aqp3 null). Averages and SEM are given for n=3. Resistance factor (RF) is the ratio of EC₅₀ for resistant strain over WT. Unpaired ttest compared EC₅₀ values of each resistant strain versus WT. Units are in μM except for crude ION and UDN where the EC₅₀ value is given in μg/mL Data were provided by Harry P. De Koning from Glasgow University.

Samples	T b S427WD		B48				aqp2/aqp3 null			
	EC ₅₀	SEM	EC ₅₀	SEM	RF	<i>t</i> -Test	EC ₅₀	SEM	RF	<i>t</i> -Test
ION crude	5.9	0.02	6.0	0.21	1.01	0.73	5.2	0.10	0.88	0.00
Mangiferonic acid	25.5	0.30	31.0	0.68	1.22	0.03	20.0	0.13	0.78	0.00
Ambonic acid	39.5	1.19	52.0	1.08	1.32	0.02	27.1	2.71	0.68	0.12
α-Amyrin mix.	20.9	0.88	24.8	0.81	1.20	0.22	19.2	0.23	0.93	0.52
UDN crude	12.1	0.32	12.6	0.08	1.04	0.35	NA	NA	NA	NA
Mudn 14-40	3.9	0.03	6.1	0.14	1.58	0.00	2.1	0.02	0.54	0.00
Mudn 10-242526	11.3	0.08	16.8	0.30	1.48	0.00	11.3	0.05	0.99	0.75
Mudn 10-51	14.7	0.20	17.9	0.39	1.21	0.05	16.8	0.22	1.15	0.05
Pentamidine	0.0023	0.0002	0.5	0.04	224.78	<0.001	0.1	0.002	31.08	<0.001

4.4 Discussion.

Xanthenes which are the characteristic compounds in propolis samples collected from Ugelli/Delta State coded UDN were targeted for fractionation. The method developed on HPLC-ELSD-UV and transferred to MPLC led to isolation of three xanthenes isomers 1,3,7-trihydroxy-2,8-di-(3-methylbut-2-enyl) xanthone, 1,3,7-trihydroxy-4,8-di-(3-methylbut-2-enyl) xanthone and a previously undescribed xanthone. They were structurally elucidated by 1D-2D NMR and LC-MSⁿ. All of them were more active than the crude extract and the activity varies with changing the position of the substituents.

Closely related prenylated compounds have been isolated before from *Garcinia mangostana* (Mangosteen) and showed *in vitro* antileishmanial, antiplasmodial and antitrypanosomal activity, although they were non-selective ie. being toxic to human to some extent (Al-Massarani *et al.*, 2013).

Three triterpenes ambonic acid, mangiferonic acid and (inseparable mixture) α amyryl with mangiferonic acid 1:3 were isolated from a propolis sample collected from Ogun State. The isolated compounds were structurally elucidated by NMR. Bioassay tests demonstrated a moderate inhibitory activity against trypanosomes to a lesser extent than the crude itself. According to a previous comparative study on the antitrypanosomal activity of 15 isolated triterpenoids and sterols and some related compounds Hoet *et al.* has indicated that the presence of an oxygenated function group at C-28 or an oxygenated side chain at C-17 seems to be important for the antitrypanosomal activity of triterpenoids and sterols, respectively. All isolated compounds lack of these oxygenated functional group at specified location, this might explain the weakness of the activity (Hoet *et al.*, 2007).

CHAPTER FIVE

CHEMICAL CHARACTERIZATION OF

NIGERIAN RED PROPOLIS AND ITS ACTIVITY

AGAINST *Trypanosoma brucei*

5 CHEMICAL CHARACTERIZATION OF NIGERIAN RED PROPOLIS AND ITS ACTIVITY AGAINST *Trypanosoma brucei*

5.1 Introduction

In a previous study (Zhang *et al.*, 2014), 22 samples of propolis collected from nine different sub-Saharan countries were profiled and found to present a high diversity in chemical composition but no clear geographic delineation was observed for the classification of these samples. By comparative chemical profiling, a sample from Rivers State (coded: RSN) in Southern Nigeria showed a significant chemical diversity it also demonstrated relatively high activity against *Trypanosoma brucei* (MIC: 1.56 µg /mL, and EC₅₀: 4.2 µg /mL). In the current study, this sample of propolis was subjected to further investigation and compared to Brazilian propolis which is generally used as the “golden standard” for all commercially produced propolis from tropical regions.

A second sample of this propolis from Rivers State Nigeria was collected at a different time in order to compare and chemically characterize the ethanolic extracts of the two samples. A quick and reproducible isocratic method was developed using analytical HPLC-UV-ELSD. This method was then transferred to a flash chromatographic system for the isolation and purification of target common component(s).

As a result, ten phenolic compounds were isolated or partially purified. NMR and mass spectroscopic data for nine of these matched literature reports of known compounds as follows: One isoflavone, Calycosin (**1**); two flavanones, liquiritigenin

(2) and pinocembrin (3); an isoflavan, vestitol (4); a pterocarpan, medicarpin (5); two prenylflavanones, 6-prenylnaringenin(7) and 8-prenylnaringenin (8) and two geranyl flavonoids, propolin D (9) and macarangin (10). The tenth component was characterized as a previously undescribed dihydrobenzofuran (6). The isolated compounds were tested against *Trypanosoma brucei* and displayed moderate to high activity. Some of the compounds tested had similar activity against wild type *T. brucei* and two strains displaying pentamidine resistance.

5.2 Experimental

5.2.1 Propolis sample collection and preparation

The propolis sample coded RSN was collected in 2003 (exact location of collection unknown) in Rivers State Nigeria and was supplied by BeeVital (Whitby, UK). The second, coded BRN, was collected by Dr John Igoli from Bonny, a riverine town in Rivers State, Nigeria in July 2013. Both samples were reddish and had a very sticky texture. The propolis samples RSN (.3 g) and BRN (140.0 g) were extracted three times with fresh ethanol (50 mL and 500 mL respectively) by sonication at 40 °C for 3 hours each, and the final residue was macerated overnight with ethanol (50 mL and 500 mL respectively). Each of the four extracts per sample was filtered through filter paper, combined and the solvent evaporated by using a rotatory evaporator to yield the ethanolic extracts of RSN (2.5 g, of a red gum) and (110.1 g of a red gum). These ethanolic crude extracts of each sample were prepared at the same time and stored at –20 °C until required.



Figure 5-1: Nigerian red propolis.

5.2.2 Preparative scale chromatography

For reversed phase chromatography, the ethanolic extract EEP of RSN (500 mg) was dissolved in ethyl acetate (5 mL) and was mixed with celite (1 g), dried in a fume cupboard and the sample was packed into an empty “dryloader” cartridge to be transferred onto a Grace Davison Reveleris® flash chromatography system. The gradient elution method used was the same as in the analytical profiling section 2.3.1, but with a flow rate of 12 mL/min and a C18 (12g) cartridge. Fractions were monitored using HPLC-UV-ELSD to yield compounds **6** (17.1 mg), **9** (6.6 mg) **10** (8.3 mg) and a mixture of **1** and **2** (10.6 mg).

For normal phase chromatography, the EEP of RSN (800 mg) was redissolved in ethyl acetate (5 mL) and mixed with celite (1.6 g), blown dry and the sample was packed

into an empty “dryloader” cartridge allowing it to be eluted onto the Revelris MPLC system which was fitted with a pre-packed 24 g silica column. By using hexane:ethyl acetate ranging from 0–100% over a 57 min linear gradient, 26 fractions of varying volumes were collected. Fraction GRP11 (188.3 mg) was the largest in weight, has high antitrypanosomal activity, and was collected at around 60:40 hexane:ethyl acetate. This fraction was re-chromatographed using a Reveleris® flash chromatography system fitted with a Grace C18 cartridge (12 g). Compounds were eluted with acetonitrile: water 40:60 at 9 mL/min over 30 min followed by linearly increasing acetonitrile to 100% over 30 min. This resulted in the separation of compounds **4** (6.5 mg), **7** (5.0 mg) and **8** (4.0 mg).

The EEP of sample BRN (7 g) was fractionated using open column chromatography (CC) as shown in section 2.4.1. Fractions (50 mL) each were collected and pooled, based on HPLC-UV-ELSD analysis, to yield 14 fractions. Fraction BRN5 (163 mg), which was eluted with ethyl acetate: hexane 60:40 and fraction BRN9, which was eluted from the open column with 100% ethyl acetate were re-chromatographed isocratically with ACN: water 50:50 and ACN: water 30:70 respectively at 12 mL/min over 30 min using the Grace Revelris™ system fitted with a Grace C18 cartridge (12 g). Fraction BRN5 yielded compounds **3** (8.6 mg), **5** (22.4 mg) and **6** (8.0 mg), and fraction BRN9 yielded compound **1** (17.6 mg).

5.3 Results

5.3.1 *Structure Elucidation of Compounds Isolated From Nigerian Red Propolis*

Nine compounds were isolated from the Nigerian red propolis and their structures were determined by NMR.

In addition, the structure of liquiritigenin (**2**) was determined although it was part of a mixture containing calycosin (**1**) (also isolated in pure form) in approximately equal amounts. The NMR spectra of nine of the compounds were consistent with the literature data for known compounds (full NMR details are given in appendix 6-14). For the compounds derived from flavanoids the typical fragmentations across the C ring giving the substitutions in rings A and B as shown in **Figure 5-2** proposed previously were useful for structure elucidation (Hughes *et al.*, 2001). The mass spectrometry and retention time data for the isolated compounds is summarized briefly below; the structure is shown in **Figures 5-3, 5-4**.

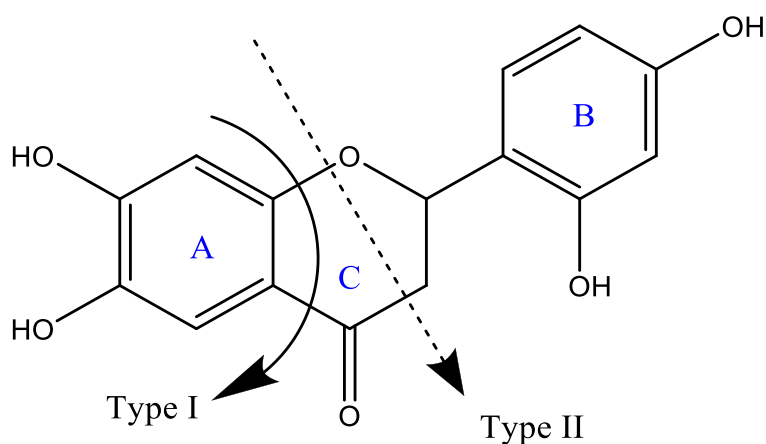


Figure 5-2: Schematic representation of common fragmentation processes observed in the collision induced dissociation (CID) of flavonoid adapted from (Hughes *et al.*, 2001).

Calycosin (1) white powder, t_R 8.0 min. Ratio BRN/RSN 0.976. 1H , ^{13}C NMR data in DMSO- d_6 , were consistent with those previously reported (Du *et al.*, 2006) 1H and ^{13}C NMR (DMSO- d_6) spectra are shown in **appendix- 6** and values of the chemical

shifts are given in **Table- S6** in the appendix. ESI-MS (negative mode), $[M - H]^-$ m/z 283.0614 ($C_{16}H_{11}O_5$, Δ -0.024 ppm). MS^2 m/z 268.0378 (100) ($C_{15}H_8O_5$, Δ -0.454 ppm), MS^3 m/z 240.0430 (100) ($C_{14}H_8O_4$, Δ 0.096 ppm), m/z 239.0352 (50), m/z 224.0482 (50), m/z 211.0403 (60), m/z 195.0454 (30) none of these fragments were indicative of structure. However, in addition there was a small A ring fragment at m/z 135.0090 (4) ($C_7H_3O_3$, Δ 1.5 ppm) indicating one hydroxyl group in ring A.

Liquiritigenin (2) white powder, t_R 8.0 min. Ratio BRN/RSN 0.807 1H , ^{13}C NMR data in d_6 DMSO- d_6 were consistent with those previously reported (Ma *et al.*, 2005), 1H and ^{13}C NMR (DMSO- d_6) spectra are shown in **appendix-7** and values of the chemical shifts are given in **Table- S7** in the appendix.

ESI-MS (negative mode), $[M - H]^-$ m/z 255.0664 ($C_{15}H_{11}O_4$, Δ 1.67 ppm). MS^2 , m/z 237.0559(20), m/z 153.0194(30), m/z 135.0087 (100) ($C_7H_3O_3$, Δ -0.424 ppm), m/z 119.0502 (20) (C_8H_7O , Δ 0.706 ppm). The ion at m/z 135.0087 indicates a single hydroxyl in ring A and there is a corresponding ion at m/z 119.0502 which contains the B ring and indicates a single oxygen in the B ring.

Pinocembrin (3) white needle, t_R 11.5 min. Ratio BRN/RSN 0.724. 1H , ^{13}C NMR data were consistent with those previously reported (Jung *et al.*, 1990), 1H and ^{13}C NMR (DMSO- d_6) spectra are shown in **appendix-8** and values of the chemical shifts are given in **Table- S8** in the appendix.

ESI-MS (negative mode), $[M - H]^-$ m/z 255.0665 ($C_{15}H_{11}O_4$, Δ 1.24 ppm) MS^2 m/z 213.0560(80), m/z 211.0767 (30), m/z 187.0786 (11), m/z 151.0038 (30) ($C_7H_3O_4$, Δ 0.583 ppm), m/z 169.0661(10). The fragment ion at m/z 151.0038 indicates the presence of two hydroxyl groups in ring A. $[\alpha]_D + 108$ (C 1.00, methanol).

Vestitol (4) colourless needles, t_R 13.3 min. Ratio BRN/RSN 0.741 1H , ^{13}C NMR data were consistent with those previously reported (Piccinelli *et al.*, 2005), 1H and ^{13}C NMR in ($CDCl_3$) spectra are shown in **appendix -9** and values of the chemical shifts are given in **Table- S9** in the appendix.

ESI-MS (negative mode), $[M - H]^-$, m/z 271.0977 ($C_{16}H_{15}O_4$, Δ -0.082 ppm). MS^2 m/z 109.0295(70) ($C_6H_5O_2$, Δ -0.117), m/z 135.0451 (100) ($C_8H_7O_2$, Δ 0.646 ppm), m/z 147.0452(70) ($C_9H_7O_2$, Δ 1.55 ppm). The fragment at m/z 135.0451 is consistent with a fragment containing the B ring while the fragment at m/z 109.0295 derives from the A ring. Specific optical rotation $[\alpha]_D +3.6^\circ$ (c 1.00, Methanol).

Medicarpin (5) dark orange powders, t_R 14.0 min. Ratio BRN/RSN 0.325. 1H , ^{13}C NMR data were consistent with those previously reported (Piccinelli *et al.*, 2005), 1H and ^{13}C NMR in ($CDCl_3$) spectra are shown in **appendix -10** and values of the chemical shifts are given in **Table- S10** in the appendix.

ESI-MS (negative mode), $[M - H]^-$ m/z 269.0822 ($C_{16}H_{13}O_4$, 1.51 ppm) MS^2 m/z 254.0587 (78) ($C_{15}H_{10}O_4$, Δ 0.602 ppm), m/z 237.0560 (83) ($C_{15}H_9O_3$, Δ 1.40 ppm), m/z 145.0296 (100) ($C_9H_5O_2$, Δ 1.02 ppm). $[\alpha]_D +117.9^\circ$ (c 1.00, Methanol).

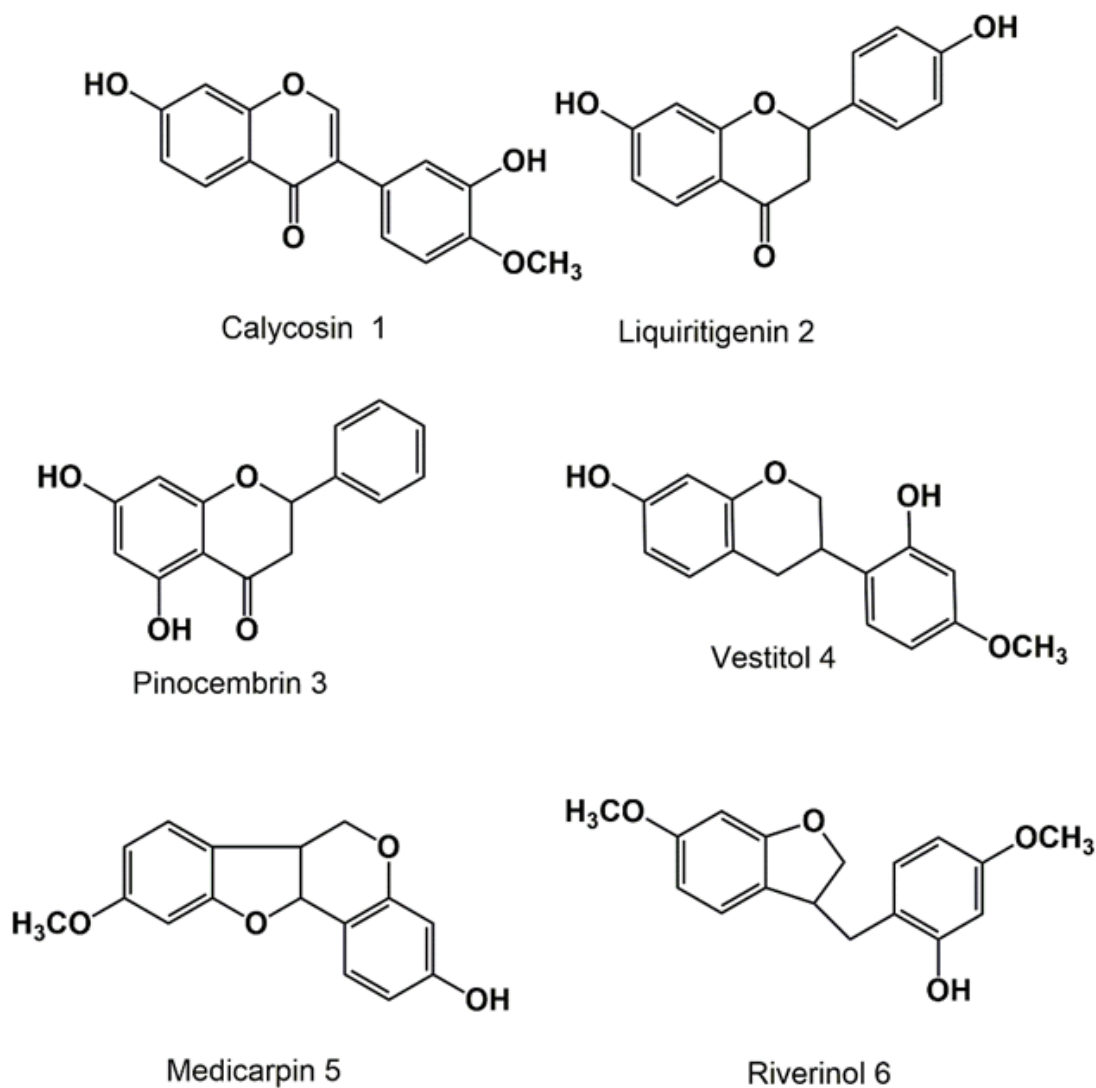


Figure 5-3: Structures of the flavonoids and isoflavonoids isolated from Nigerian red propolis.

6-prenylnaringenin (7) pale yellow solid, t_R 23.9 min. Ratio BRN/RSN 0.208. 1H , ^{13}C NMR data were consistent with those previously reported (Stevens *et al.*, 1997; Nakahara *et al.*, 2003), 1H and ^{13}C NMR in (DMSO- d_6) spectra are shown in **appendix -11** and values of the chemical shifts are given in **Table- S11** in the appendix.

ESI-MS (negative mode), $[M - H]^-$ m/z 339.1236 ($C_{20}H_{19}O_5$, Δ 0.82 ppm), MS^2 m/z 219.0663 ($C_{12}H_{11}O_4$, Δ 0.127 ppm) (100), m/z 119.0503 (4) (C_8H_7O , Δ 0.435 ppm), MS^3 m/z 175.07669(100) ($C_{11}H_{11}O_2$, Δ 0.897 ppm), m/z 151.07656(50) ($C_9H_{11}O_2$, Δ 0.444 ppm), m/z 133.06593(85) (C_9H_9O , Δ 0.238 ppm). The fragment at m/z 219.0663 is consistent with a prenyl group in ring A along with two hydroxyl groups and the small fragment at m/z 119.0503 contains the B ring indicating one hydroxyl group in the B ring. A longer retention time in reversed phase mode in comparison with 8-prenylnaringenin is probably due its higher surface area (298.3 \AA^2 for 8-prenylnaringenin compared to 311.2 \AA^2 for 6-prenylnaringenin as computed by Chem 3D, CambridgeSoft, Boston, USA). $[\alpha]_D -12^\circ$ (c 1.00, Methanol).

8-prenylnaringenin (8) pale yellow solid, t_R 16.1 min. Ratio BRN/RSN 0.086. 1H , ^{13}C NMR data were consistent with those previously reported (*Stevens et al.*, 1997), 1H and ^{13}C NMR in (DMSO- d_6) spectra are shown in **appendix -12** and values of the chemical shifts are given in **Table- S12** in the appendix.

ESI-MS (negative mode), $[M - H]^-$ m/z 339.1236 ($C_{20}H_{19}O_5$, Δ 1.39 ppm), MS^2 m/z 219.0663 (100) ($C_{12}H_{11}O_4$, Δ 0.335 ppm), m/z 119.0503 (3) (C_8H_7O , Δ 0.351 ppm), MS^3 m/z 175.07669(100) ($C_{11}H_{11}O_2$, Δ 1.61 ppm), m/z 151.0766 (50) ($C_9H_{11}O_2$, Δ 1.17 ppm), m/z 133.0659 (90) (C_9H_9O , Δ 1.37 ppm). The fragment at m/z 219.0663 is consistent with a prenyl group in ring A along with two hydroxyl groups and the small fragment at m/z 119.0503 contains the B ring indicating one hydroxyl group in the B ring. $[\alpha]_D -18.3^\circ$ (c 1.00, Methanol).

Propolin D (9) brown powder, t_R 28.6 min. Ratio BRN/RSN 0.293. 1H , ^{13}C NMR data were consistent with those previously reported (*Chen et al.*, 2004), 1H and ^{13}C

NMR in (CDCl₃) spectra are shown in **appendix -13** and values of the chemical shifts are given in **Table- S13** in the appendix.

ESI-MS (negative mode), [M - H]⁻ *m/z* 423.1819 (C₂₅H₂₇O₆, Δ 0.208 ppm), MS² 151.0035 (100) (C₇H₃O₄, -Δ 0.807 ppm), *m/z* 405.1701(70) (C₂₅H₂₅O₅, Δ -1.81 ppm), *m/z* 271.1703 (20) (C₁₈H₂₃O₂, Δ 0.762 ppm), 297.1496 (10) (C₁₉H₂₃O₃, Δ -1.60 ppm). The ion at *m/z* 151.0035 indicates two hydroxyl groups in ring A and the ion at *m/z* 271.1703 indicates that the geranyl chain is in the B ring. [α]_D +3.6° (c 1.00, Methanol).

Macarangin(10) red brown powder, *t_R* 35.4 min. Ratio BRN/RSN 0.371 ¹H, ¹³C NMR data were consistent with those previously reported (Hnawia *et al.*, 1990), ¹H and ¹³C NMR in (CDCl₃) spectra are shown in **appendix -14** and values of the chemical shifts are given in **Table- S14** in the appendix.

ESI-MS (negative mode), [M - H]⁻ *m/z* 421.1654 (C₂₅H₂₅O₆, Δ -1.05 ppm) MS² *m/z* 352.09533 (80) (C₂₀H₁₆O₆, Δ -1.35 ppm), *m/z* 335.09236 (28) (C₂₀H₁₅O₅, Δ 1.18 ppm), *m/z* 309.0404 (100) (C₁₇H₉O₆, Δ -1.26 ppm), *m/z* 297.0405 (70) (C₁₆H₉O₆, Δ -0.913 ppm). In this case the MS² fragments result from losses of portions on the geranyl chain. [α]_D +4.8° (c 1.00, Methanol).

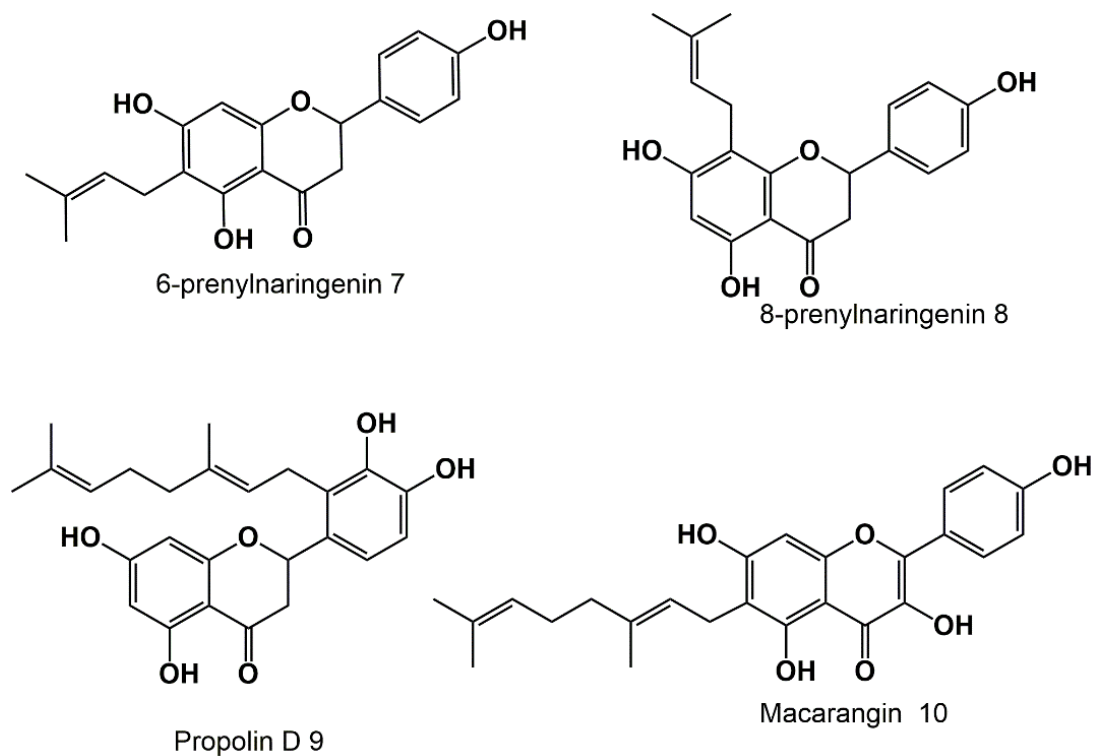


Figure 5-4: Structures of the prenylated flavonoids isolated from Nigerian red propolis.

5.3.2 Structure elucidation of riverinol (6)

Of the 10 compounds chromatographically isolated from Nigerian red propolis in this study, compound **6**, red brown solid eluted at t_R 20.9 min. (mp. 137 – 142 °C), $[\alpha]_D - 10^\circ$ (c 1.00, Chloroform), did not correspond to previously described compounds. ESI-MS (negative mode), $[M - H]^-$ m/z 285.1134 ($C_{17}H_{17}O_4$, $\Delta = 0.6$ ppm) indicating a molecular formula $C_{17}H_{18}O_4$.

The 1H and ^{13}C NMR data for compound **6**, **Figures 5-5, 5-6, 5-7, 5-8, Table 5-1** indicated two similar aromatic systems each containing three protons with two protons ortho to each other and one meta-coupled proton. The DEPT 135 spectrum showed 17 carbons; six quaternary aromatic carbons, four of which were attached to

oxygens; six aromatic methine carbons; and five aliphatic carbons, two of which corresponded to methoxy groups, two methylene carbons bearing and one methine carbon. A careful analysis of the 1D and 2D NMR spectroscopy data allowed elucidation of **6** as a previously undescribed dihydrobenzofuran herein given the trivial name riverinol.

For ease of structure elucidation, an idiosyncratic numbering system was used **Figure 5-9**. In the HMBC spectrum, the most useful carbons for connecting the structure were the 4 and 4' carbons which showed couplings to the aromatic protons within their rings and to the aliphatic protons (i.e., C4 to H6, H8, H10_d, H10_u and C-4' to H10_u, H10_d, H3, H2', 3'-OH, H6'). It was possible to assign the position of the hydroxyl group to the 3' position on the basis of a weak four bond coupling of C3' to the C3 proton; this would not be possible for the alternative C1' position for this substituent. **Figure 5-10** summarizes the HMBC and COSY correlations observed in the spectrum of riverinol. Thus the data are consistent with riverinol being 3-(2-hydroxy-4-methoxybenzyl)-6-methoxy-2,3-dihydrobenzofuran (**6**).

A literature search revealed a closely related dihydrobenzofuran isolated from *Campyloctropis hirtella* (Franch.) Schindl. (Han *et al.*, 2008) that presented very similar and supporting NMR data. Further support for the structure of riverinol was derived from the MS data. MS² m/z 270.0902 (C₁₆H₁₄O₄, Δ 1.56 ppm), m/z 255.0667 (C₁₅H₁₁O₄, Δ 1.56 ppm), m/z 149.0609 (34) (C₉H₉O₂, Δ 0.853 ppm), m/z 123.0452 (100) (C₇H₇O₂, Δ 0.384 ppm), m/z 108.0217 (13) (C₆H₄O₂, Δ 0.577 ppm).

The ion at m/z 149.0609 corresponds to cleavage between C10 and C3 with retention of charge on the dihydrobenzofuran portion of the molecule. The ion at m/z 123.0452 corresponds to cleavage across the furan ring between the oxygen and C3 and C2 and the aromatic ring and the ion at m/z 108.0217 corresponds to loss of methyl from the fragment at m/z 123.0452.

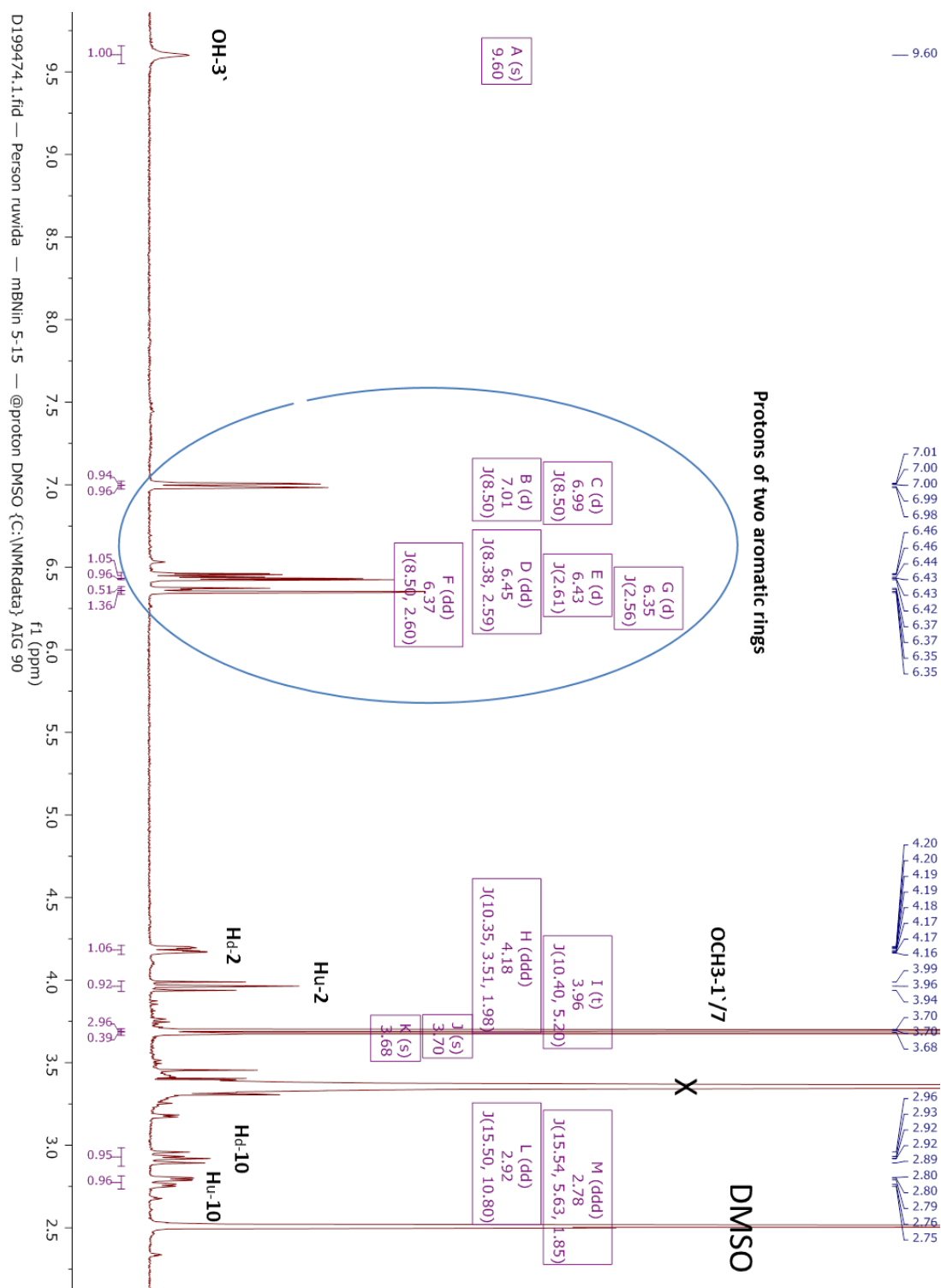


Figure 5-5: ^1H NMR(400 MHz) of Riverinol in $\text{DMSO}-d_6$. The peaks denoted by X represent signals from solvent.

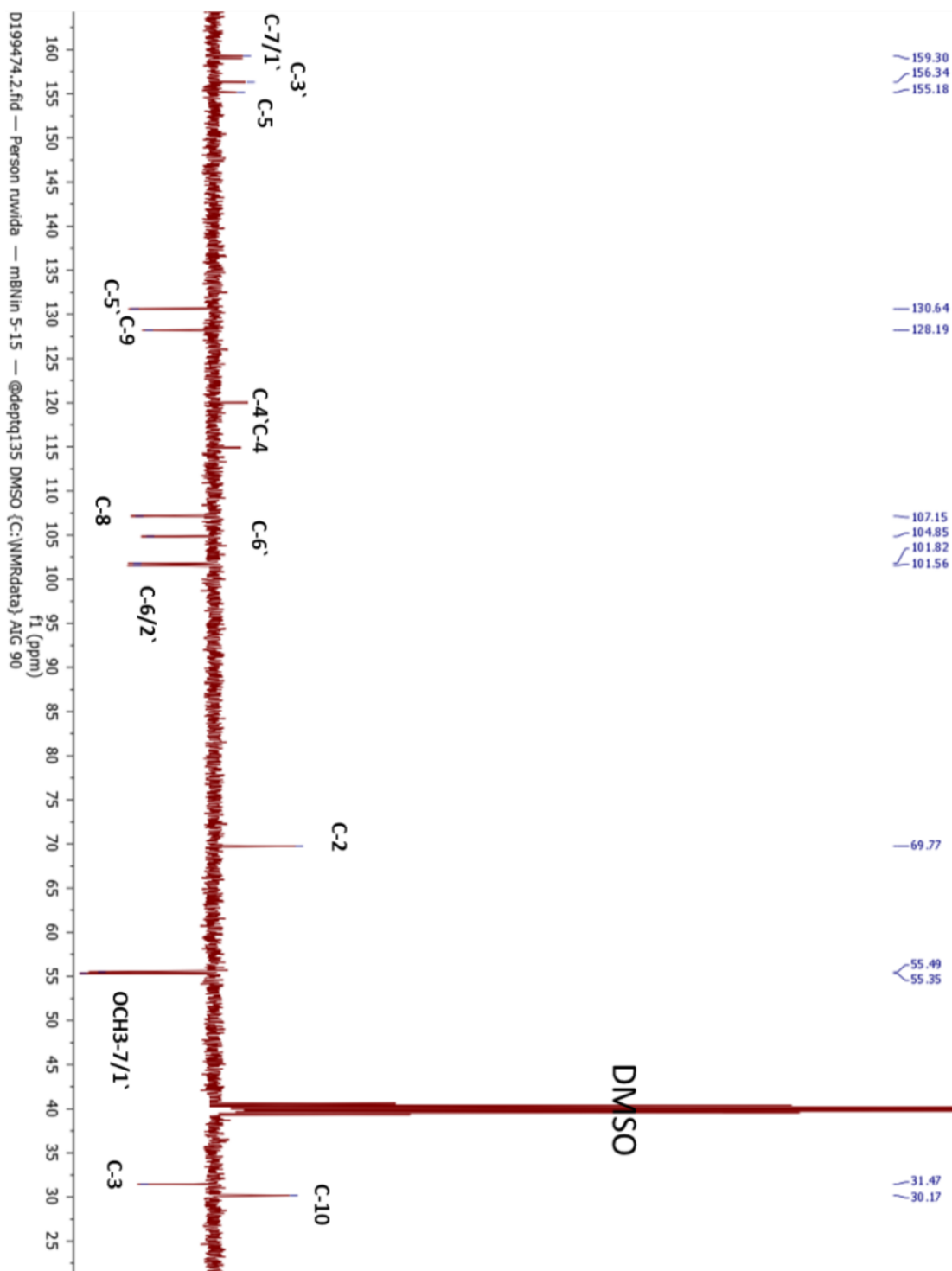


Figure 5-6: DEPT 135 ^{13}C NMR spectrum (100 MHz) of Riverinol in DMSO- d_6 .

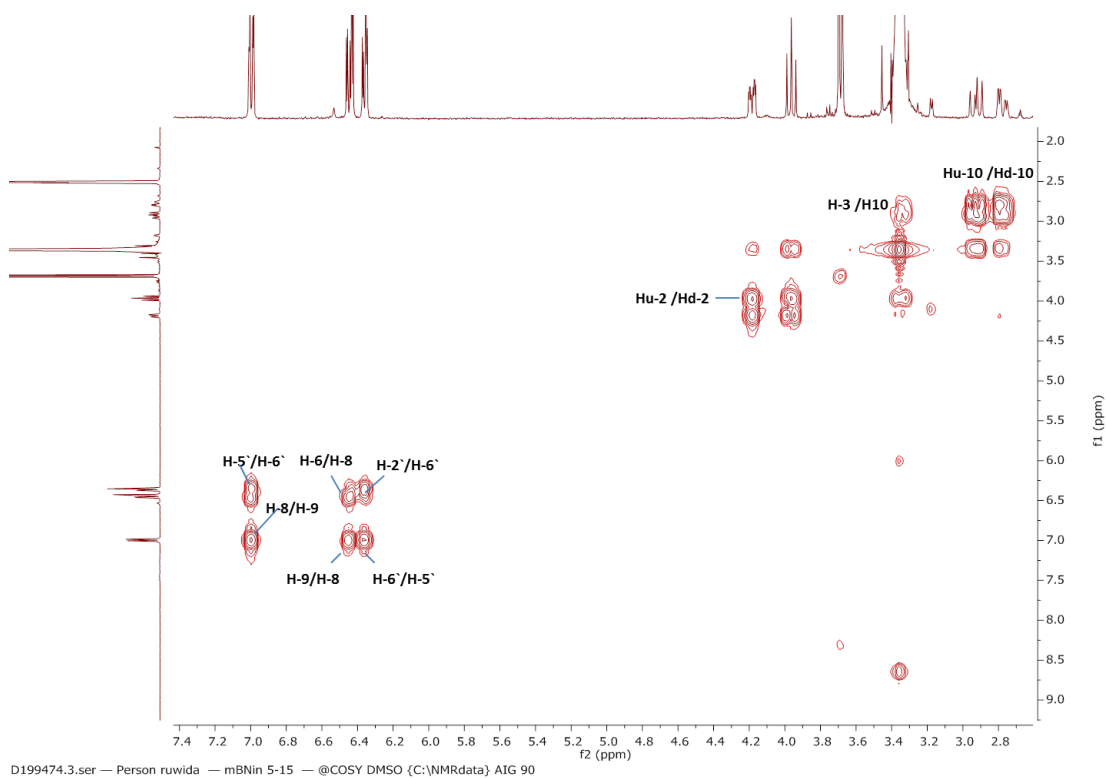


Figure 5-7: COSY spectrum (400 MHz) of Riverinol in DMSO- d_6 .

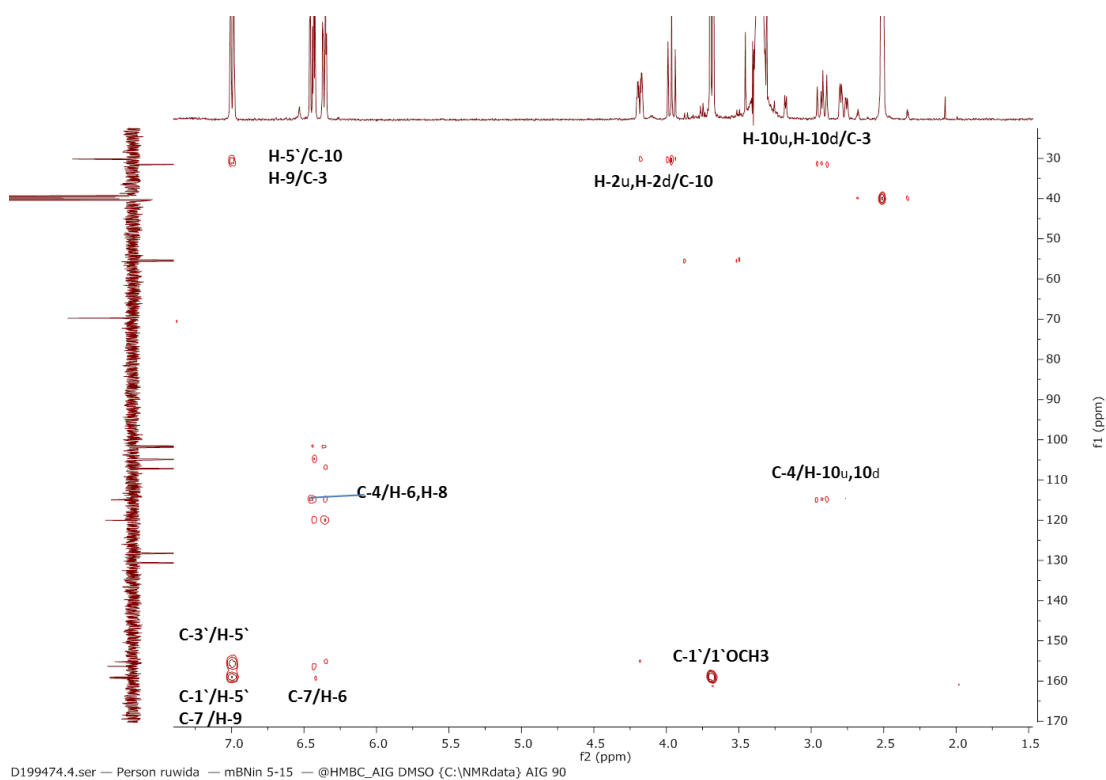


Figure 5-8: HMBC spectrum (400 MHz) of Riverinol in DMSO- d_6 .

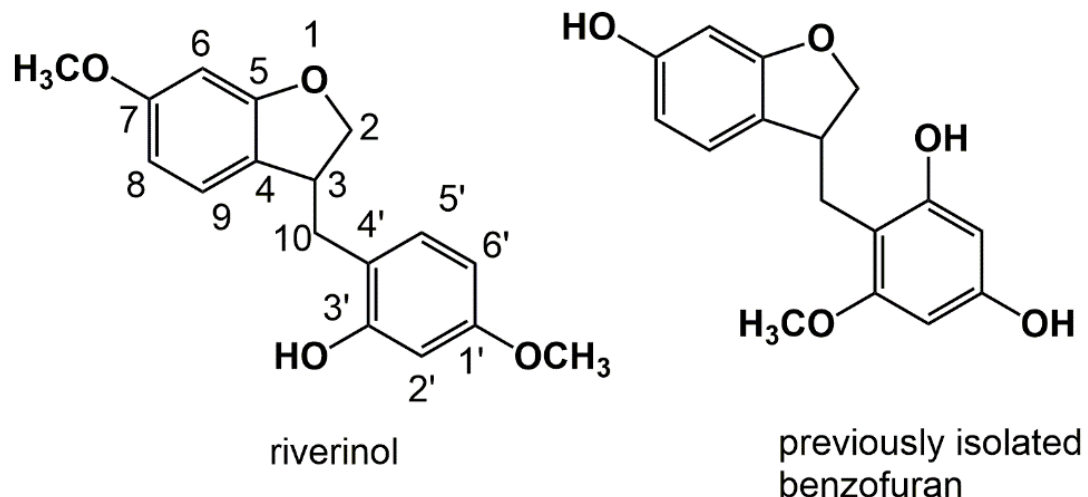


Figure 5-9: Numbered structure of Riverinol (6) for structure elucidation purposes, and a closely related dihydrobenzofuran previously isolated (Han *et al.*, 2008).

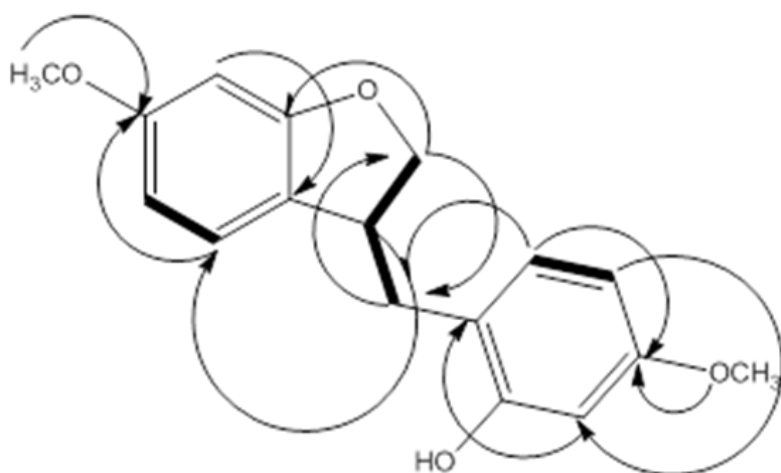


Figure 5-10: Key HMBC (\rightarrow) and COSY (\dashrightarrow) correlation for Riverinol.

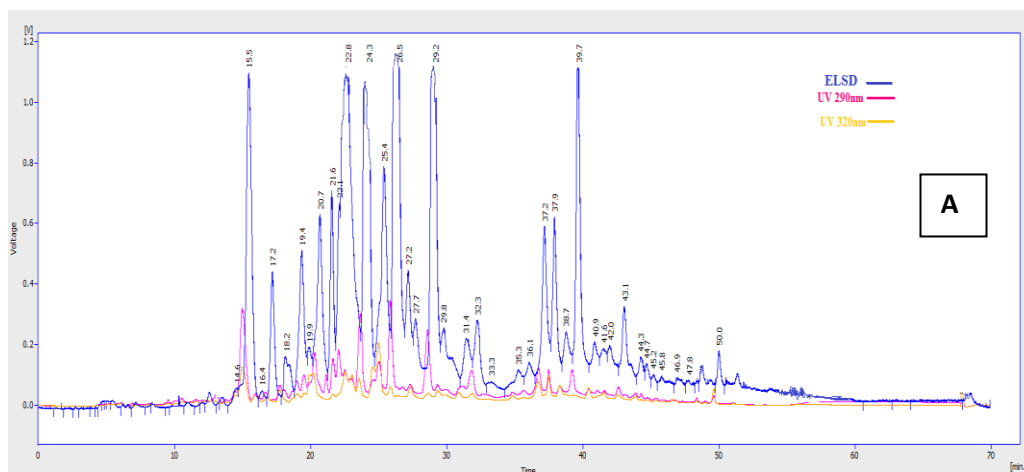
Table 5-1: ^1H NMR (400 MHz) and ^{13}C NMR (100 MHz) data of new benzofuran in DMSO- d_6 . Hd downfield and Hu=upfield partner of geminal proton pair.

Position	Chemical shift δ ppm ^1H (mult, J Hz)	Chemical shift δ ppm ^{13}C	COSY ($^1\text{H} - ^1\text{H}$)	HMBC ($^1\text{H} - ^{13}\text{C}$)
1	-	-	-	-
2	4.18, 1H _d (ddd, 10.4, 3.5, 1.9) 3.96, 1H _u (t, 10.4, 5.2)	69.8	H2 _u , H3, H10 _u , H2 _d , H3	C10
3	3.35, 1H, (m)	31.5	H10 _d , H10 _u , H 2 _d , H2 _u	C9, C10, C4'
4	-	114.9	-	-
5	-	155.2	-	-
6	6.43, 1H (d, 2.4)	101.5	-	C4, C5, C7, C8, 7-OCH ₃
7	-	159.0	-	-
7-OCH ₃	3.70, 3H, (s)	55.4	-	C7
8	6.46, 1H, (dd, 8.2, 2.4)	107.2	-	C4, C6, C7, 7-OCH ₃
9	6.99, 1H, (d, 8.2)	128.2	H8, H6	C5, C7
10	2.79, 1H _u , (ddd, 15.5, 5.6, 1.9) 2.95 1H _d (dd, 15.5, 10.8)	30.2	H10 _u , H3	C2, C3, C4, C4', C5'
1'	-	159.3	-	-
1'-OCH ₃	3.68, 3H, (s)	55.5	-	C1'
2'	6.35, 1H, (d, 2.6)	101.8	-	C1', C4'
3'	-	156.4	-	-
3'-OH	9.6, OH, (s)	-	-	C4'
4'	-	120.0	-	-
5'	7.01, 1H, (d, 8.5)	130.6	H5', H6'	C1', C3'
6'	6.37, 1H, (dd 8.5, 2.6)	104.9	H5', H6'	C2', C4'

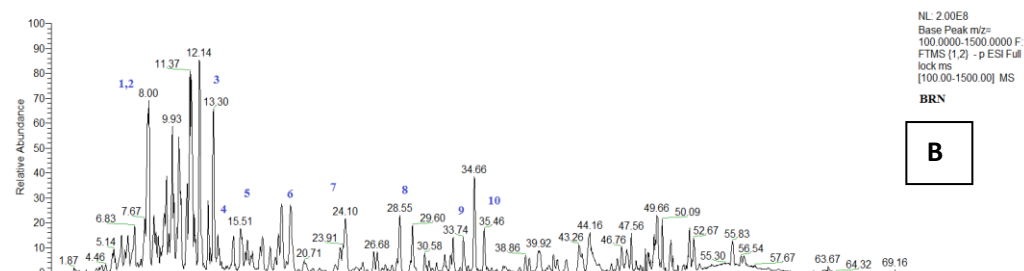
5.3.3 HPLC-UV-ELSD and HPLC- MS Profiling of RSN and BRN

HPLC-UV-ELSD and HPLC-MS analysis of RSN and BRN showed rich chromatographic responses **Figure 5-11** with the combination of the ELSD and the UV detector (290 and 320 nm), suggesting the absence of ELSD-only responsive compounds such as terpenes and fats. Many compounds were common between the two samples but with different relative abundances which are listed along with the elucidated (above) or partially elucidated structures (discussed below). Like Brazilian red propolis, the Nigerian red propolis contained liquiritigenin (**2**) vestitol (**4**), and medicarpin (**5**) which are probably collected from *Dalbergia ecastophyllum* (Piccinelli *et al.*, 2011).

The Nigerian sample also contains retusapurpurins; **Figure 5-12** shows the ESI spectra and an extracted ion trace corresponding to two retusapurpurin isomers, which are abundant in RSN and BRN, and they are responsible for the red colour of the propolis and have only been recorded in *Dalbergia* species. There are a number of *Dalbergia* species found in West Africa (Saha *et al.*, 2013) thus, there is a degree of similarity between Nigerian red and Brazilian red propolis based on the compounds found in *Dalbergia* species discussed above.

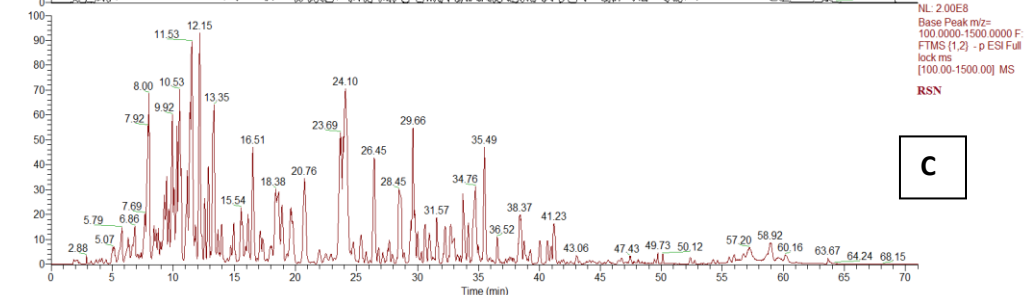


BRN 18/04/2015 22:07:20



NL: 2.00E8
Base Peak m/z= 100.0000-1500.0000 F
FTMS (1.2) - p ESI Full
lock ms
[100.00-1500.00] MS

BRN



NL: 2.00E8
Base Peak m/z= 100.0000-1500.0000 F
FTMS (1.2) - p ESI Full
lock ms
[100.00-1500.00] MS

RSN

Figure 5-11: A HPLC-ELSD-UV chromatogram of BRN; **B** is the negative LC-HR-ESIMS ion mode chromatogram for BRN and **C** is negative HR-ESIMS ion mode chromatogram for RSN.

However, there were also compounds either isolated and fully characterized or putatively identified by mass spectrometry, in the Nigerian samples that have not been reported to be present in Brazilian red propolis, and these included: the fully

characterized compounds propolin D (**9**), 6- and 8-prenylnarigenin (**7**, **8**) and macarangin (**10**).

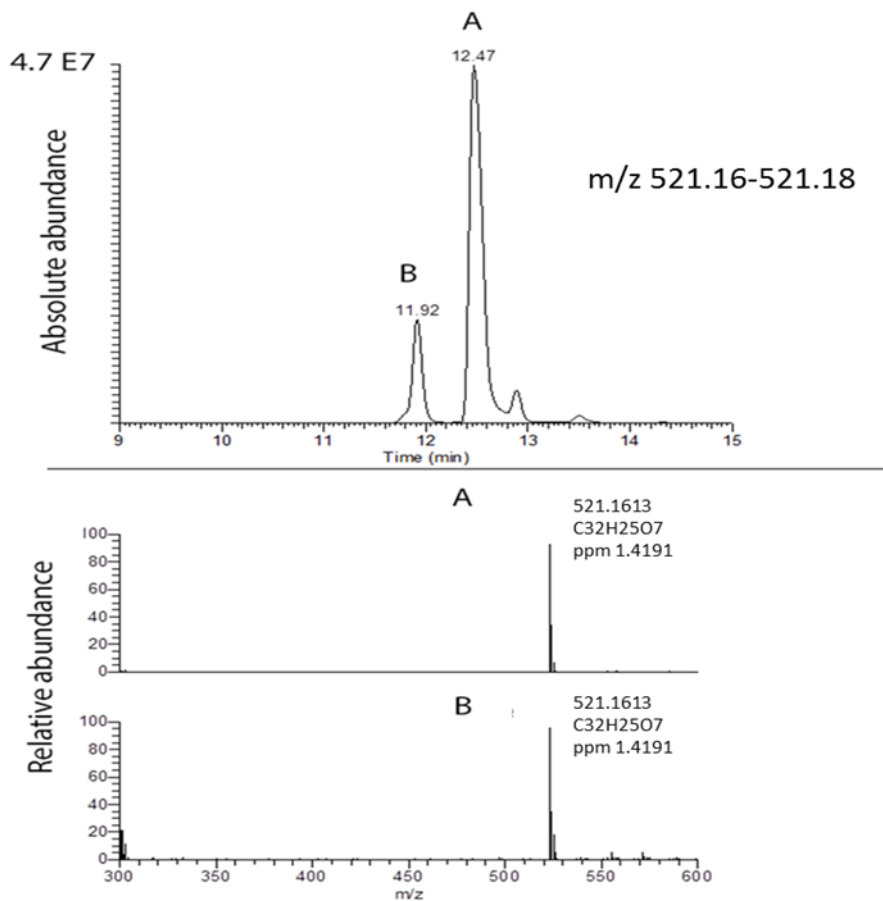


Figure 5-12: Extracted ion trace and negative ion spectra for Retusapurpurins.

In addition, there were many other abundant compounds in many cases related to the compounds isolated and characterized by NMR. The high-resolution mass spectra were generally accurate to within 2 ppm of the proposed formula which means that it is possible to be confident of the elemental composition assigned and indeed the hits in DNP database are all isomers of the proposed compositions. **Table-S15** in Appendix summarizes the elemental compositions for the top 200 compounds by

mean abundance in the samples. For many of the listed elemental compositions > 100 isomers can be found in the DNP database. The mass spectra of some of the characteristic compounds are discussed in detail below, and are referred to as **Unknowns 1–18**. Where MS³ data are reported for the base peak in the MS² spectrum.

Unknown 1: t_R 9.3 min. ESI-MS (negative mode), $[M - H]^-$ m/z 331.0822 (composition C₁₇H₁₅O₇, Δ -0.139 ppm, 184 matches in DNP). BRN/RSN 1.047. MS² m/z 316.0589 (100) (C₁₆H₁₂O₇, Δ -0.155 ppm), m/z 301.0357 (7) (C₁₅H₉O₇, Δ 1.11 ppm), m/z 151.0039 (Δ 1.5 ppm) (C₇H₃O₄, Δ 1.37 ppm). MS³ m/z 301.0354 (100) (C₁₅H₇O₆, Δ -0.180 ppm). Possibly dimethyl quercetin with methylation of the hydroxyl groups in ring B since the small ion at m/z 151.0039 indicates a dihydroxylated A ring.

Unknown 2: t_R 10.3 min. ESI-MS (negative mode), $[M - H]^-$ m/z 285.0765 (composition C₁₆H₁₃O₅, Δ 0.537 ppm, 225 matches in DNP). Not in RSN. MS² m/z 270.0356 (5) (C₁₅H₁₀O₅, Δ 0.81 ppm), m/z 267.0664 (61) (C₁₆H₁₁O₄, Δ 0.37 ppm), m/z 257.0819 (100) (C₁₅H₁₃O₄, Δ 0.03 ppm). MS³ m/z 242.0583 (100) (C₁₄H₁₀O₄, Δ -0.44 ppm), m/z 239.0716 (21) (C₁₆H₁₁O₃, Δ 1.14 ppm). Consistent with a methylated pterocarpin but fragmentation pattern does not match data reported previously (Piccinelli *et al.*, 2011) for pterocarpins in Brazilian red propolis.

Unknown 3: t_R 9.9 min. ESI-MS (negative mode), $[M - H]^-$ m/z 285.0765 (composition C₁₆H₁₃O₅, Δ -0.024 ppm, 225 matches in DNP). BRN/RSN (0.623). MS² m/z 270.0357 (9) (C₁₅H₁₀O₄, Δ 1.03 ppm), m/z 257.0821 (18) (C₁₅H₁₃O₄, Δ 0.964 ppm), m/z 241.0871 (100) (C₁₅H₁₃O₃, Δ 0.26 ppm), m/z 226.0638 (25)

(C₁₄H₁₀O₃, Δ 1.27 ppm), *m/z* 163.004 (19) (C₈H₃O₄, Δ 0.79 ppm), *m/z* 109.0295 (12) (C₆H₅O₂, Δ 0.25 ppm). MS³ *m/z* 226.0637 (100) (C₁₄H₁₀O₃, Δ 0.87 ppm). Consistent with a methylated pterocarpin but fragmentation pattern does not match data reported previously (Piccinelli *et al.*, 2011) for pterocarpins in Brazilian red propolis.

Unknown 4: *t_R* 23.7 min ESI-MS (negative mode), [M - H]⁻ *m/z* 423.1817 (composition C₂₅H₂₇O₆, Δ - 2.84 ppm, 137 matches in DNP). Ratio BRN/RSN 0.158. Putative identification geranylated or diprenylated flavanoid. MS² *m/z* 287.1285 (100) (C₁₇H₁₉O₄, Δ -1.192 ppm). The fragment at *m/z* 287.1285 indicates the presence of a geranyl or two prenyl groups in the A ring; the base peak in the MS³ spectrum for this ion was at *m/z* 243.1391 has the formula C₁₆H₁₉O₂ (Δ -0.234 ppm) corresponding to a loss of CO₂.

Unknown 5: *t_R* 32.9 min. ESI-MS (negative mode), [M - H]⁻ *m/z* 423.1817 (Composition C₂₅H₂₇O₆, -0.17 ppm, 137 matches in DNP). BRN/RSN 0.461. Unknown 5 is an isomer of propolin D but does not give any diagnostic MS² fragments since it loses CO to give a base peak at *m/z* 395.1861 (C₂₄H₂₇O₅, Δ -0.679 ppm). The MS³ spectrum of this base peak is more informative, yielding a peak at *m/z* 351.1961 due to loss of CO₂ and this ion appears to undergo another loss of C₇H₆ (approximating to benzyl) to give the base peak at *m/z* 261.1493 (C₁₆H₂₁O₃, Δ -1.08 ppm). There is also a fragment at *m/z* 287.1286 (C₁₇H₁₉O₄, Δ -1.088 ppm) suggesting that unknown 5 also has a geranyl or two prenyl groups in ring A.

Unknown 6: *t_R* 29.6 min. ESI-MS (negative mode), [M - H]⁻ *m/z* 407.1868 (composition C₂₅H₂₇O₅, Δ -2.5 ppm, 135 matches in DNP). BRN/RSN 0.289. MS² *m/z* 287.1282 (100) (C₁₇H₁₉O₄, Δ -1.3 ppm). The fragment *m/z* 287.1282 indicates the presence of the geranyl/prenyl groups in the A ring; *m/z* 119.0502 (0.8) (C₈H₇O,

Δ -0.657 ppm) indicates one hydroxyl group in ring B. Putative identification geranylated flavanoid.

Unknown 7: t_R 33.7 min. ESI-MS (negative mode), $[M - H]^-$ m/z 491.2445 (Composition $C_{30}H_{35}O_6$, Δ - 1.83 ppm, 36 matches in DNP). BRN/RSN 0.340. Unknown 7 is related to propolin D but carries an additional prenyl group. The base peak in the MS^2 spectrum of unknown is at m/z 219.0663 (100) ($C_{12}H_{11}O_4$, Δ 0.447 ppm) indicating substitution in ring A with two hydroxyl groups and a prenyl group and the additional geranyl group is in ring B as indicated by a fragment at m/z 271.1706 (15) ($C_{18}H_{23}O_2$, Δ 0.762 ppm).

Unknown 8: t_R 24.1 min ESI-MS (negative mode), $[M - H]^-$ m/z 353.1025 (Composition $C_{20}H_{17}O_6$, Δ -1.562 ppm, 160 matches in DNP). BRN/RSN 0.246. MS^2 m/z 335.0926 (68) ($C_{20}H_{15}O_6$, Δ 0.397 ppm), m/z 298.0584 (77) ($C_{16}H_{10}O_6$, Δ -0.549 ppm), m/z 269.0457 (100) ($C_{15}H_9O_5$, Δ 0.644 ppm). Possibly prenylated flavanoid where loss of C_4H_7 - might indicate loss of part of a prenyl chain.

Unknown 9: t_R 12.2 min. ESI-MS (negative mode), $[M - H]^-$ m/z 267.0666 (Composition $C_{16}H_{11}O_4$, Δ 1.26 ppm, 96 matches in DNP). BRN/RSN 0.893. MS^2 m/z 252.0429 (100) ($C_{15}H_8O_4$, Δ 0.21 ppm). MS^3 m/z 223.0403 (100) ($C_{14}H_7O_3$, Δ 0.903 ppm), m/z 208.0532 (83) ($C_{14}H_8O_2$, Δ 0.972 ppm) m/z 135.009 (2) ($C_7H_3O_3$, Δ 0.761 ppm). Isomer of methylchrysin with single hydroxy in ring A and methoxy in ring B.

Unknown 10: t_R 7.9 min. ESI-MS (negative mode), $[M - H]^-$ m/z 315.0875 ($C_{17}H_{15}O_6$, Δ 0.294 ppm, 176 matches in DNP). BRN/RSN 1.269. MS^2 m/z 297.0766 (100) ($C_{17}H_{13}O_5$, Δ 0.249 ppm), m/z 287.0926 (88) ($C_{16}H_{15}O_5$, Δ 0.324

ppm). MS³ m/z 282.0553 (100) (C₁₆H₁₀O₅, Δ 0.324 ppm). Possibly dimethyl flavonoid.

Unknown 11: t_R 18.9 min. ESI-MS (negative mode), [M - H]⁻ m/z 539.1702 (C₃₂H₂₇O₈, Δ -1.81 ppm, 5 matches in DNP) Ratio BRN/RSN 1.22. MS² 283.0977 (100) (C₁₇H₁₅O₄, Δ 0.699 ppm), m/z 255.0664 (75) (C₁₅H₁₁O₄, Δ 0.501 ppm), m/z 240.0431 (32) (C₁₄H₈O₄, Δ 1.262 ppm). MS³ m/z 268.0742 (100) (C₁₆H₁₂O₄, Δ 0.421 ppm). The molecule fragments into two halves of similar molecular weight suggesting an isoflavonoid dimer such as related to the daljanelins which are found in *Dalbergia* species (Saha *et al.*, 2013).

Unknown 12: t_R 11.4 min. ESI-MS (negative mode), [M - H]⁻ m/z 273.0773 (C₁₅H₁₃O₅, Δ 1.76 ppm, 217 matches in DNP) Ratio BRN/RSN 1.23. MS² m/z 163.0400 (100) (C₉H₇O₃, Δ -0.475 ppm), m/z 109.0294 (56) (C₆H₅O₂, Δ -0.94 ppm). The molecule forms two main fragments suggesting a dihydroxybenzene bonded to caffeic acid.

Unknown 13: t_R 10.5 min. ESI-MS (negative mode), [M - H]⁻ m/z 283.0632 (C₁₆H₁₁O₅, Δ 0.61 ppm, 165 matches in DNP) Ratio BRN/RSN 0.99. MS² m/z 268.0337 (100) (C₁₅H₈O₅, Δ -0.006 ppm). MS³ m/z 224.0480 (100) (C₁₄H₈O₃, Δ 0.57 ppm), m/z 135.0089 (3) (C₇H₃O₃, Δ 1.29 ppm). Isomer of methyl galangin with one hydroxyl group in ring A.

Unknown 14: t_R 49.7 min. ESI-MS (negative mode), [M - H]⁻ m/z 601.3528 (C₃₈H₄₉O₆, Δ 1.035 ppm, 41 matches in DNP). Ratio BRN/RSN 14.1. Putative identification polyisoprenylated benzophenone isomer of guttiferone A. The fragments in the MS² spectra were consistent with those observed previously although shifted by *ca* 2 amu since the previous data were obtained in positive ion

mode (Piccinelli *et al.*, 2011). MS² m/z 465.3363 (100) (C₃₁H₄₅O₃, Δ -2.04 ppm) which is consistent with loss of the dihydroxybenzoyl group from this molecule. Piccinelli *et al.* (2011) observed this ion in positive ion mode at m/z 467 and attributed it to the loss of a geranyl chain which has the same mass as the dihydroxy benzophenone moiety, in the current case it is clear from the accurate mass data that the loss is due to loss of dihydroxy benzophenone as described previously (Yang *et al.*, 2010). An ion at m/z 423.3258 (C₂₉H₄₃O₂, Δ -2.39 ppm) is consistent with cracking across the ring bearing the dihydroxy benzophenone moiety. An ion at m/z 409.1657 (observed by Piccinelli *et al.* 2011, at m/z 411 but not interpreted) (C₂₄H₂₅O₆, Δ 0.116) would be consistent with a structure such as oblongifolin A where a geranyl group is substituted onto the bicyclononane ring. These proposed fragmentations are illustrated in **Figure 5-13** using oblongifolin A as the example.

Unknown 15: t_R 50.8 min. ESI-MS (negative mode), [M - H]⁻ m/z 601.3544 (C₃₈H₄₉O₆, Δ -2.45 ppm, 41 matches in DNP). Not found in RSN. The MS² spectrum has the same fragment at m/z 465.3362 as **Unknown 14** but does not have an ion at m/z 409.16. However, a corresponding loss occurs from the ion at m/z 465.3362 in the MS³ spectrum of **Unknown 15** resulting in an ion at m/z 273.1491 (100) (C₁₇H₂₁O₃, Δ -1.74 ppm) suggesting that this molecule also has a geranyl tail attached. Loss of the geranyl tail itself from the ion at m/z 465.3362 is also observed giving rise to an ion at m/z 327.1960 (20) (C₂₁H₂₇O₃, Δ - 1.8 ppm).

Unknown 16: t_R 52.7 min. ESI-MS (negative mode), [M - H]⁻ m/z 669.4147 (C₄₃H₅₇O₆, Δ -2.08 ppm 11 matches in DNP). Ratio BRN/RSN 11.1. The MS² spectrum gives a base peak at m/z 533.3981 (C₃₈H₅₃O₃, Δ -1.48 ppm) showing the same loss of dihydroxybenzophenone as was seen for **Unknowns 14** and **15**. The

spectrum also has a small ion at m/z 477.2266 ($C_{29}H_{33}O_6$, -3.44 ppm) which indicates the loss of a fragment containing the geranyl tail as was observed for **Unknowns 14** and **15**.

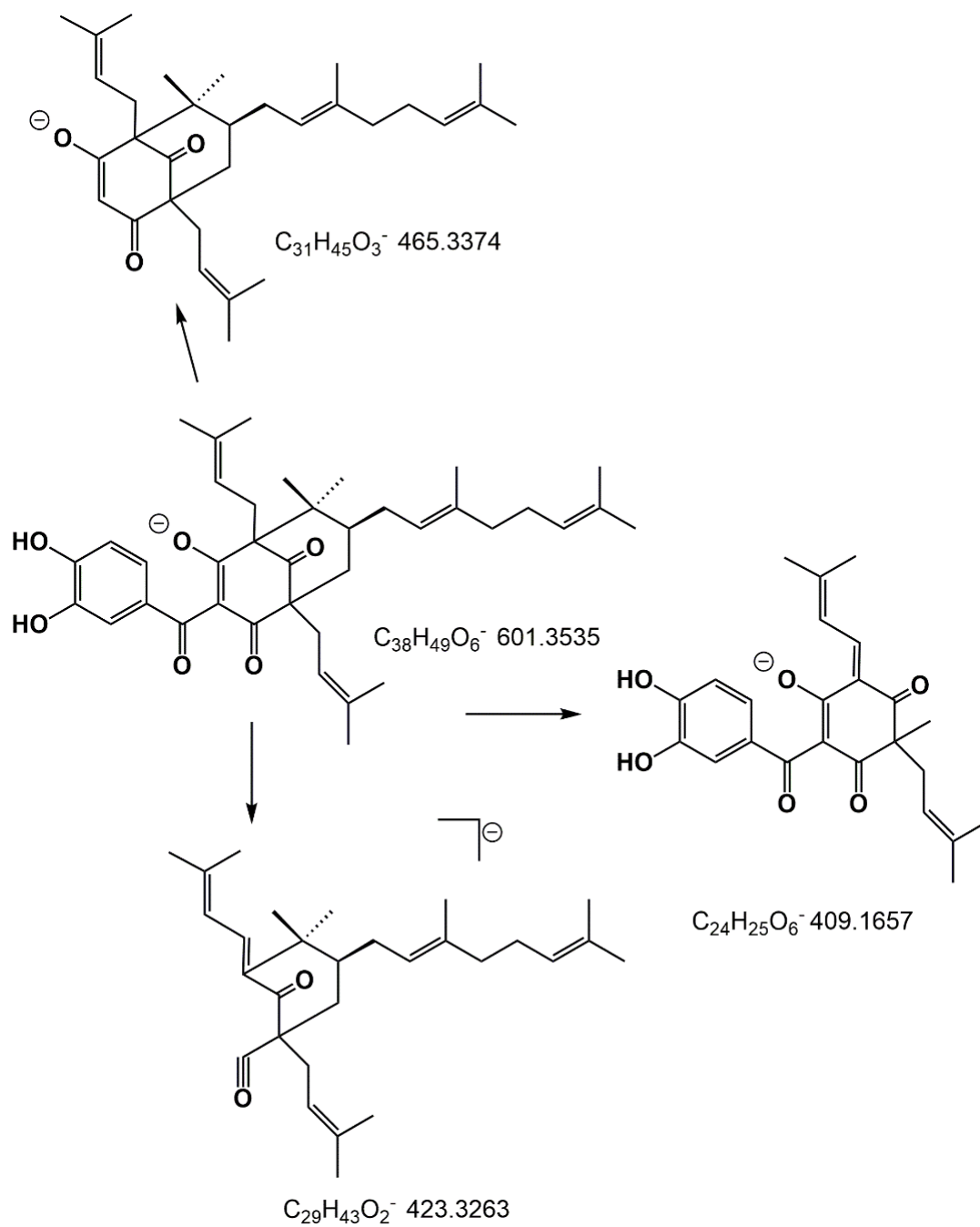


Figure 5-13: MS² fragmentation of a polyprenylated benzophenone illustrated for oblongifolin A.

Unknown 17: t_R 38.4 min. m/z 515.3158 ESI-MS (negative mode), $[M - H]^-$ ($C_{34}H_{43}O_4$ Δ -1.71 ppm 3 matches in DNP) Ratio BRN/RSN 0.1. Only one of the DNP matches is naturally occurring since two of the matches are polyprenylated benzophenones which were methylated during isolation. Thus the unique match is to schweinfurthin C which is a digeranylated stilbene isolated from *Macaranga schweinfurthii* (Beutler *et al.*, 1998). However, more recently further isomers of this formula, denticulatains A and B, not listed in DNP, have been isolated from *Macaranga denticulata* which are diterpene/stilbenes (Yang *et al.*, 2015). The MS² spectrum for **Unknown 17** gave the following major ions: m/z 445.2390 (3) ($C_{29}H_{33}O_4$, Δ -2.05 ppm), m/z 405.2791 (95) ($C_{28}H_{37}O_2$, Δ -2.4 ppm), m/z 379.1915 (4) ($C_{24}H_{27}O_4$, Δ -0.31 ppm), m/z 309.1131 (11) ($C_{19}H_{17}O_4$, -0.43 ppm), m/z 255.0660 (91) ($C_{15}H_{11}O_4$, -1.4 ppm), m/z 253.0504 (66) ($C_{15}H_9O_4$, -0.84 ppm), m/z 241.0503 (100) ($C_{14}H_9O_4$, -1.295 ppm). From the fragmentation pattern, it seems likely that **Unknown 17** is one of the denticulatains. The diterpene moiety is attached to one of the rings making it possible to lose an unmodified dihydroxybenzene ring to give the fragment at m/z 405.2791. A proposed fragmentation pattern accounting for the major fragments is shown in **Figure 5-14** using denticulatain A as an example. **Figure 5-14** also shows the major fragments derived from the m/z 241.0503 ion in the MS³ spectrum. Macarangin (**10**) which was isolated in pure form from the BRN propolis was also isolated from *M. vedeliana* (Hnawia *et al.*, 1990), thus it seems likely that the diterpene stilbene was obtained from a *Macaranga* species. There are several minor isomers of **Unknown 17** present in the extract and one of these has a spectrum that fits more with the digeranylated structure of schweinfurthin C since the ion at m/z 405.2791 is absent from the MS² spectrum and

ions at m/z 377.1754 (100) ($C_{24}H_{25}O_4$, Δ -1.014 ppm) and m/z 241.0506 ($C_{14}H_9O_4$, Δ -0.261 ppm) result from successive losses of geranyl chains.

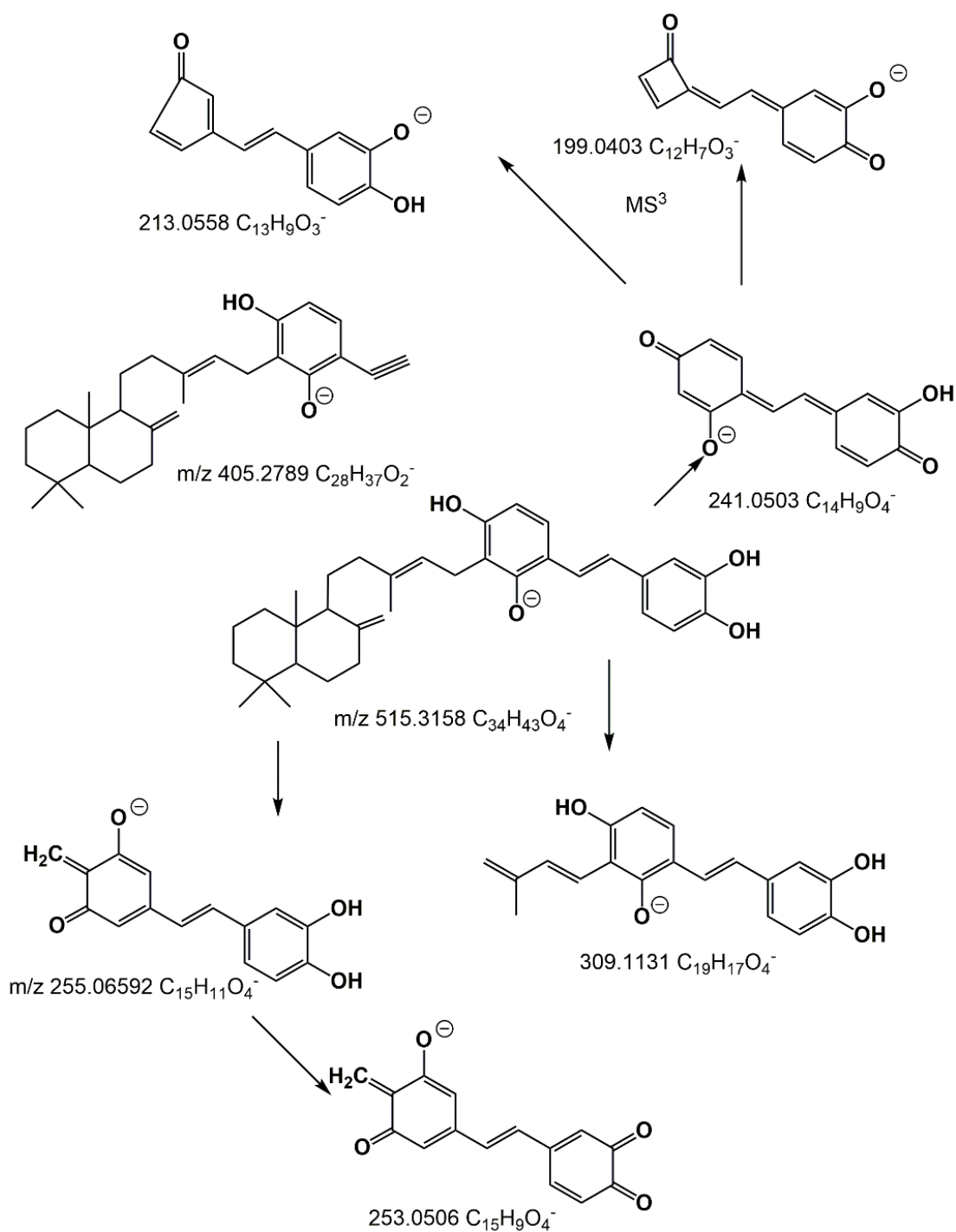


Figure 5-14: Proposed MS² and MS³ fragmentation of denticulatain A.

Unknown 18: t_R 34.6 min. ESI-MS (negative mode), $[M - H]^-$ m/z 447.2536 ($C_{29}H_{35}O_4$, Δ -1.031 ppm, 9 matches in DNP). BRN/RSN 0.366. MS² m/z 391.19220 (30) ($C_5H_{27}O_4$, Δ 1.83 ppm), m/z 377.1765 (100) ($C_{24}H_{25}O_4$, Δ 1.63 ppm), m/z 309.1137 (70) ($C_{19}H_{17}O_4$, Δ 1.44 ppm), m/z 241.0511 (18) ($C_{14}H_9O_4$, Δ 2.07 ppm). The compound has fragments in common with **Unknown 17**, suggesting a sesquiterpene stilbene adduct.

As can be seen from **Table-S15** in page 265 there are many other abundant compounds in the propolis samples that have yet to be characterized.

5.3.4 Bioassay results

Preliminary screening of both crude extracts, fractions and pure compounds were performed *in vitro* to determine their activity against the bloodstream form of *Trypanosoma brucei brucei* using an AlamarBlue assay as previously described in section 2.6.1. Initially the tests were carried out at three concentrations of 20 $\mu\text{g/mL}$, 10 $\mu\text{g/mL}$, 5 $\mu\text{g/mL}$ and the results obtained are presented in **Table 5-2**. Crude samples and some pure compounds were further investigated according to protocol in section 2.6.2 and results are shown in **Table 5-3**. Some bioassay results are listed in **Table 5.4** and will be discussed in detail in section 5.3.5.

Table 5-2: Anti-trypanosomal activity, of crude extracts, fractions obtained from reversed phase chromatography of EEP of RSN on Grace, fractions from CC of BRN, and purified compounds. Highlighted cells indicates high activity, * fractions were subjected for further purification. MIC expressed in $\mu\text{g/mL}$ in case of crudes and fractions and in μM for pure compounds.

Sample code	20 $\mu\text{g/mL}$	10 $\mu\text{g/mL}$	5 $\mu\text{g/mL}$	MIC ($\mu\text{g/mL}$)
	% of control T.b. S427			
Crudes				
RSN	9.9	15.7	6.7	1.56
BRN	3.5	-0.4	-	-
Fractions from reverse phase Grace of RSN				
RSN-R1	81.6	94.7	102.0	-
RSN-R2	-4.0	8.1	88.2	-
RSN-R3	-13.1	-11.1	37.2	-
RSN-R4	-6.6	-6.3	39.9	50
RSN-R5	-11.4	-9.5	28.1	-
RSN-R6	-11.2	-12.7	-3.4	-
RSN-R7	-7.9	-6.7	6.7	-
RSN-R8	-5.6	-4.0	73.1	-
RSN-R9	-1.8	-3.5	-1.1	-
RSN-R10	-3.4	-3.8	-2.1	-
RSN-R11	-4.1	-3.8	-1.2	-
RSN-R12	-2.0	-1.2	-0.5	-
RSN-R15	-4.6	-2.8	1.7	-
RSN-R16	-0.9	-1.0	7.6	-
RSN-R18	-1.6	-0.3	63.3	-
RSN-R19	24.6	77.9	98.3	-
RSN-R20	-0.6	-1.2	2.4	-
BRN0	103.1	99.0	97.1	-

BRN1	102.8	101.0	101.1	-
BRN2	100.4	101.0	101.8	-
BRN3	99.8	100.4	99.3	-
BRN5*	-2.6	18.0	85.3	-
BRN6	-3.4	13.4	88.4	-
BRN7	-3.3	-2.3	34.0	-
BRN8	-8.0	-5.8	-1.7	-
BRN9*	-0.9	-0.8	59.4	-
BRN10	-1.0	-1.4	19.8	-
BRN11	-0.5	11.7	86.3	-
BRN12	2.3	70.0	96.2	-
BRN13	3.8	93.7	99.6	-
BRN14	103.3	95.9	101.2	-
Some purified compounds				
Medicarpin	-	-	-	11.5
pinocembrin	1.2	2.4	76.5	48.8
Riverinol (RSN-R13)	0.6	-1.2	9.3	43.7
Propolin D (RSN-R14)	-5.7	-4.7	-1.8	7.4
Macarangi (RSN-R17)	-0.4	-0.9	6.7	-
Suramin	(+ control) MIC= 0.125 μ M			

The activities of the two crude extracts, fractions, and the pure compounds were all tested against *T. brucei*. The crude extracts, and some fractions were more active than the isolated compounds, suggesting either that the most active compounds had not been isolated or that mixtures of components together were acting synergistically.

Some isolated compounds like medicarpin, Propolin d showed a relatively strong antitrypanosomal activity with MIC= 11.5 and 7.4 μ M respectively. both

pinocembrin and riverinol demonstrated a moderate activity with MIC of 48.8 and 43.7 μM .

Table 5-3: EC₅₀ values (n=3) against three strains of *T. bruciae*: Lister 427 wild-type, AQP2-KO and B48. Averages and SEM are given for n= 3. Resistance factor (RF) is the ratio of EC₅₀ for resistant strain over WT. Unpaired t-test compared EC₅₀ values of each resistant strain versus WT. Units are in µM except for crude RSN, BRN, where the EC₅₀ value is given in µg/mL. Data were provided by Harry P. De Koning from Glasgow University.

Sample	Tbs427WT			B48			aqp2/aqp3 null				
	EC ₅₀	SEM		EC ₅₀	SEM	RF	t-Test	EC ₅₀	SEM	RF	t-Test
RSN	4.2	0.04		3.9	0.16	0.92	0.13	4.4	0.26	1.05	0.46
BRN	6.9	0.3		7.2	0.3	1.04	0.58				
Riverinol	58.0	0.24		16.4	1.83	0.28	<0.001	23.1	1.52	0.40	<0.001
Calycosin	35.2	0.44		52.1	1.61	1.48	0.05	26.1	0.32	0.74	0.01
Vestitol	30.5	0.10		37.8	0.66	1.23	0.05	29.8	0.14	0.97	0.18
8-prenyl Naringenin	17.9	0.10		20.9	0.18	1.15	0.01	19.1	0.06	1.05	0.05
6-Prenyl Naringenin	33.5	0.34		40.3	0.33	1.20	0.01	30.6	0.18	0.91	0.05
Macarangin	18.5	0.10		24.2	2.56	1.31	0.40	15.4	0.05	0.83	<0.001
Pentamidine	0.0023	0.0002		0.51	0.04	224.78	<0.001	0.071	0.002	31.08	<0.001

Table 5-3 shows more detailed testing that was carried out for some of the compounds against a wild type strain and against two resistant strains. The compounds showed strong antitrypanosomal activity with EC_{50} values against a standardized strain ranging from 4.2 $\mu\text{g/mL}$ for the crude RSN to 58 μM for the new benzofuran (Riverinol), confirming the exceptionally high activity of the unpurified fraction. Of the purified compounds, 8-prenylnarigenin was the most active at $17.9 \pm 0.1 \mu\text{M}$ but several other compounds including macarangin displayed very similar activities. In order to assess the potential for cross-resistance with current drugs of the diamidine and melaminophenylarsenical classes, the compounds were tested on the multi-drug resistant (MDR) strains B48, and aqp2/aqp3 null in parallel. Pentamidine, was used as a control drug, was 31-fold ($P=5.3\text{E-}6$) and 224-fold ($P=0.00028$) less active against B48 and aqp2/aqp3 null, respectively. In contrast, none of the fractions or compounds tested displayed a substantially reduced sensitivity to the MDR strains, with the resistance factors not exceeding 1.5-fold, establishing that the activity of these phytochemicals is not dependent on the same drug transporters that mediate uptake of the currently used drugs (De Koning, 2008).

5.3.5 Chemometric modelling of RSN fractions with regard to anti-trypanosomal activity.

As discussed above the fractions and crudes were more active than the isolated compounds, and this is clear in case with fraction GRP 11 obtained from normal phase chromatography of EEP of RSN that was more active than the crude material but the individual components isolated from GRP11 were less active than the crude material. Therefore, in order to target the compound responsible for high activity, chemometric modelling was performed on LC-MS data of fractions.

MIC results of anti-trypanosomal activity were determined for individual fractions from normal phase Grace chromatography for the EEP of RSN, section 5.2.2, as well as crude extract and are listed in **Table 5-4** below. Most of fractions demonstrated high to very high activity, MIC values higher than 10 µg/mL were considered as not active samples and were not tested.

Table 5-4: MIC and percentage of yields of fractions from Grace normal phase chromatography of EEP of RSN. Highlighted cells indicated high activity. GRP11 was chosen for further purification. MP (mobile phase). MIC in ($\mu\text{g/mL}$).

Sample	%Yield	MP Hex:EtOAc	<i>Trypanosoma brucei brucei</i> S427 % of control			MIC $\mu\text{g/mL}$
			20 $\mu\text{g/mL}$	10 $\mu\text{g/mL}$	5 $\mu\text{g/mL}$	
GRP6	1.9	80:20	0.2	39.8	90.9	not active
GRP7b	3.2	80:20	21.0	59.7	94.2	not active
GRP8	1.2	80:20	3.1	10.3	48.0	not active
GRP11	23.5	60:40	8.9	13.4	6.3	0.78
GRP12	4.2	60:40	5.3	5.0	64.5	not active
GRP13	4.6	60:40	8.0	13.7	64.1	not active
GRP14	1.7	60:40	8.3	11.5	38.1	not active
GRP15	4.1	60:40	9.8	8.0	21.9	not active
GRP16	1.2	60:40	11.2	8.7	10.8	not active
GRP17	4.8	60:40	10.8	12.7	9.9	0.78
GRP18	2.85	40:60	8.3	17.2	12.4	not active
GRP19	4.4	40:60	12.5	14.0	7.6	1.56
GRP20	1.9	40:60	12.5	22.1	8.8	1.56
GRP21	1.38	40:60	11.1	20.0	6.1	0.78
GRP22	5.4	40:60	7.0	5.0	2.7	0.78
GRP24	4.0	0:100	9.4	6.4	3.6	≤ 0.2
GRP25	2.8	0:100	9.8	5.8	8.1	1.56
GRP26	5.9	0:100	6.2	5.7	21.3	not active
CRP (crude)	800 mg		9.9	15.7	6.7	1.56

LC-MS data of all fractions were splitted into positive and negative data sets, negative data were processed by MZ-mine2.14, and files was transferred to SIMCA-P14 as in section 2.3.2.1.

Hierarchical Clustering analysis (HCA) produced a dendrogram shown in **Figure 5-15** which divided the fractions into three groups: green Group1 (very active), plum Group3 (not active) except GRP11, and blue Group2 (mixed activity). In order to investigate and predict the biomarkers that might be responsible for activity within these fractions, groups 1, 3 were chosen for simplicity. Orthogonal Partial Least Squares- discriminant analysis (OPLS-DA) score plot were constructed and it clearly discriminates between active and non active fractions **Figure 5-16**, corresponding S-plot **Figure 5-17** The loading points in the S-plot refer to the m/z values LC-MS. The extreme ends of the S-plot show variables of high magnitude and high reliability for differentiation between active and non-active compounds; the highlighted variables in the left bottom quadrant (red) are the biomarkers that are correlated to high anti-trypanosomal activity, while the top right red show low activity.

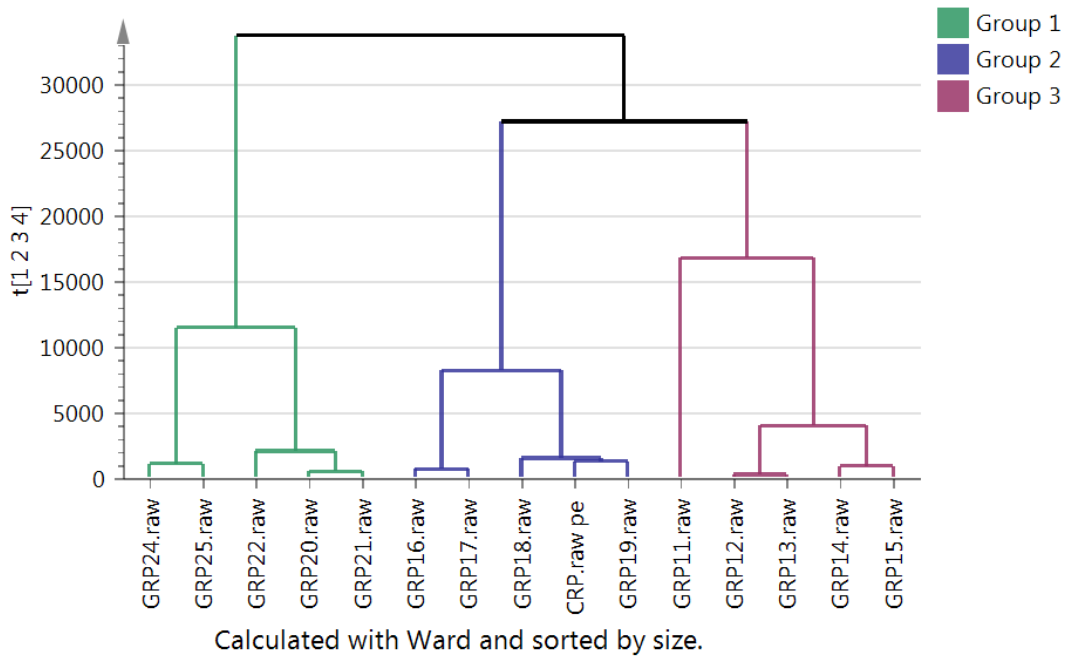


Figure 5-15: Hierarchical Clustering analysis (HCA), the dendrogram above shows observations clustered into three groups. X-axis fractions observations and y-axis hows similarity index. The higher the similarity index the more between-groups variability, and the smaller the similarity index the higher similarity within groups.

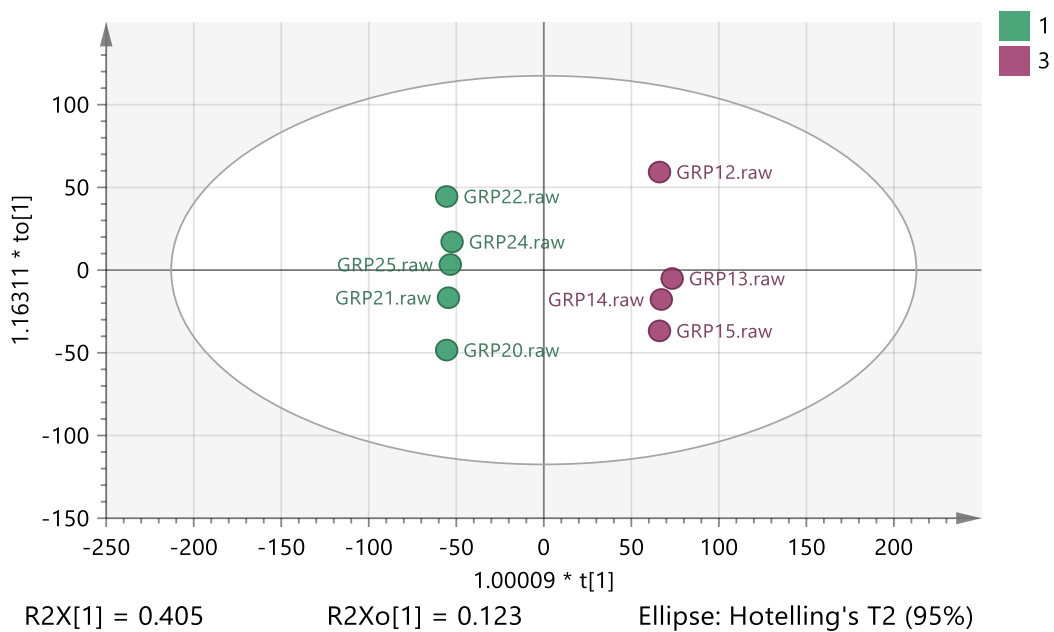


Figure 5-16: OPLS-DA score plot for fractions group1 (green) active fractions and group 2 (plum) inactive fractions.

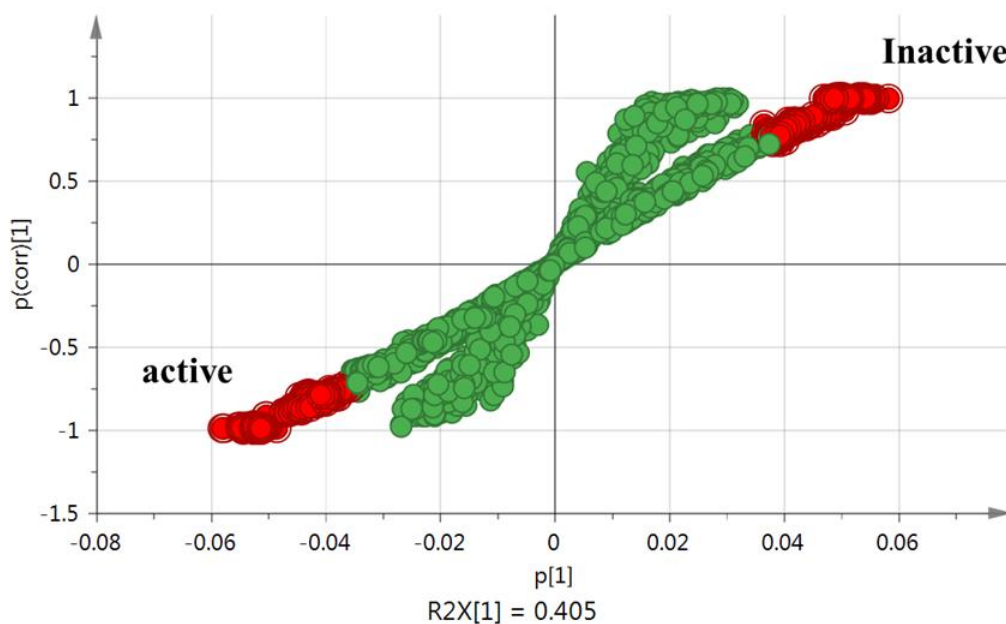


Figure 5-17: An S-plot showing putative biomarkers that were identified as contributing significantly to good activity.

The masses of potential anti-trypanosomal compounds were searched against the DNP database. As shown in **Table 5-5** the source of these compounds was variable with various plant origins *Kadsura*, *Shorea*, *Dalbergia*, *Garcinia*. The latter two genera are well-known to be a rich source of bioactive prenylated benzophenones, xanthenes, triterpenes, and bioflavonoids and many other compounds in Brazilian and Cuban red propolis. Nymphaeol B, Macarangaflavanone A have been isolated before in Taiwan propolis, they are prenylated and geranylated flavonoids and have been reported to have various anti-microbial activities. By comparing **Table 5-5** with **Table-S15** in appendix that presents most abundant components in crude extracts we can conclude that the compounds in active fractions with higher activity than crude were not dominant in crude itself.

Table 5-5: List of potential anti-trypanosomal compounds extracted from the S-plot and searched in the DNP in house database.

<i>m/z</i>	<i>t_R</i> (min)	Elemental composition	Name	Botanical source
681.27	28.6	C ₄₀ H ₄₂ O ₁₀	Pentahydroxydihydragarofuran	<i>Celastrus paniculatus</i>
679.291	36.4	C ₄₁ H ₄₄ O ₉	Unknown	-
665.275	32.4	C ₄₀ H ₄₂ O ₉	Salvia bisclerodane B	<i>Salvia wagneriana</i>
649.28	34.9	C ₄₀ H ₄₂ O ₈	Excelsa octaphenol	<i>Chlorophora excels</i>
643.145	8.9	C ₃₄ H ₂₈ O ₁₃	Unknown	-
639.187	20.9	C ₃₆ H ₃₂ O ₁₁	Deacylkadsulignan C	<i>Kadsura heteroclite</i>
635.178	5.2	C ₃₃ H ₃₂ O ₁₃	Unknown	-

631.218	24.0	C ₃₅ H ₃₆ O ₁₁	Calyflorenone B	<i>Calycopteris floribunda</i>
631.182	7.9	C ₃₄ H ₃₂ O ₁₂	Hemsleyanoside F	<i>Shorea hemsleyana</i>
627.187	12.2	C ₃₅ H ₃₂ O ₁₁	2, Dihydroxybenzyl ; 2(Benzoylglucopyranoside)	<i>Homalium longifolium</i>
627.15	8.9	C ₃₄ H ₂₈ O ₁₂	Shorealactone	<i>Shorea hemsleyana</i>
625.208	20.7	C ₃₆ H ₃₄ O ₁₀	Hexahydroxylignan	<i>Myrianthus arboreus</i>
623.191	30.9	C ₃₆ H ₃₂ O ₁₀	Octahydrox2,2cyclo lignan	<i>Kadsura angustifolia</i>
615.187	22.2	C ₃₄ H ₃₂ O ₁₁	Heteroclitin E; 8, Epoxide, benzoyl	<i>Kadsura heteroclite</i>
607.182	10.9	C ₃₂ H ₃₂ O ₁₂	Candinol C	<i>Heracleum candicans</i>
601.208	25.3	C ₃₄ H ₃₄ O ₁₀	Singueanol I	<i>Cassia singueana</i>
599.192	33.0	C ₃₄ H ₃₂ O ₁₀	Calycopterone	<i>Calycopteris floribunda</i>
595.088	7.1	C ₃₂ H ₂₀ O ₁₂	Unknown	-
587.193	24.0	C ₃₃ H ₃₂ O ₁₀	Occidentalol I	<i>Cassia occidentalis</i>
585.177	10.5	C ₃₃ H ₃₀ O ₁₀	Santalin Y	<i>Pterocarpus santalinus</i>
583.161	9.0	C ₃₃ H ₂₈ O ₁₀	Amentoflavone	Garcinia
579.333	38.4	C ₃₅ H ₄₈ O ₇	Schweinfurthin A	<i>Macaranga schweinfurthii</i>
571.124	5.7	C ₃₁ H ₂₄ O ₁₁	Daphnodorin G	<i>Daphne genkwa</i>
569.109	5.9	C ₃₁ H ₂₂ O ₁₁	Morelloflavone	Garcinia
567.129	8.1	C ₃₂ H ₂₄ O ₁₀	Amentoflavone	Garcinia
539.135	8.0	C ₃₁ H ₂₄ O ₉	Floribundiquinone A; 3Demethoxy	<i>Berchemia floribunda</i>

537.191	34.4	C ₃₃ H ₃₀ O ₇	Dracoflavan B1	<i>Daemonorops spp</i>
533.327	41.4	C ₃₄ H ₄₆ O ₅	Quaesitol; Me ether	<i>Garcinia quaesita</i>
525.192	30.5	C ₃₂ H ₃₀ O ₇	Kurzichalcolactone A	<i>Cryptocarya obovata</i>
523.176	29.6	C ₃₂ H ₂₈ O ₇	Daljanelin D	<i>Dalbergia nitidula</i>
511.27	35.2	C ₃₀ H ₄₀ O ₇	Longipedlactone A	<i>Kadsura coccinea</i>
507.181	34.6	C ₃₂ H ₂₈ O ₆	Dracoflavan B1; Deoxy, dMe	<i>Daemonorops spp.</i>
507.166	13.9	C ₂₈ H ₂₈ O ₉	Rocagloic acid	<i>Aglaia odorata</i>
503.134	18.3	C ₂₈ H ₂₄ O ₉	Unknown	-
475.14	27.2	C ₂₇ H ₂₄ O ₈	Guangsangon L	<i>Morus macroura</i>
441.192	25.2	C ₂₅ H ₃₀ O ₇	Nymphaeol B	Taiwan propolis
425.197	34.1	C ₂₅ H ₃₀ O ₆	Macarangaflavanone A	Taiwan propolis
405.098	17.2	C ₂₃ H ₁₈ O ₇	Melatinone	<i>Dalbergia melanoxylon</i>
387.108	10.8	C ₂₀ H ₂₀ O ₈	Hexahydroxyflavone	Leguminosae
385.093	14.0	C ₂₀ H ₁₈ O ₈	Dehydrodiferulic acids	Gramineae
375.109	7.4	C ₁₉ H ₂₀ O ₈	Abruquinone A	<i>Abrus precatorius</i>
373.129	10.7	C ₂₀ H ₂₂ O ₇	Pentamethoxyflavanone	Many plant spp.
371.113	18.0	C ₂₀ H ₂₀ O ₇	Pentahydroxyisoflavone	Leguminosae
359.077	11.5	C ₁₈ H ₁₆ O ₈	Hexahydroxyisoflavone	<i>Garcinia nervosa</i>
349.093	10.9	C ₁₇ H ₁₈ O ₈	Erythrostominone	<i>Gnomonia erythrostoma</i>
347.041	8.2	C ₁₆ H ₁₂ O ₉	Heptahydroxyflavone	<i>Eriocaulon ligulatum</i>
343.082	9.5	C ₁₈ H ₁₆ O ₇	Pentahydroxyisoflavone	<i>Dalbergia parviflora</i>
315.051	4.2	C ₁₆ H ₁₂ O ₇	Pentahydroxyflavone	<i>Dalbergia odorifera</i>
305.067	4.9	C ₁₅ H ₁₄ O ₇	Hexahydroxyflavan	Many plant spp.

301.036	8.3	C ₁₅ H ₁₀ O ₇	Pentahydroxyflavone	Many plant spp.
297.077	11.2	C ₁₇ H ₁₄ O ₅	Maackiain	<i>Pterocarpus santalinus</i> ; Cuban propolis
275.056	4.0	C ₁₄ H ₁₂ O ₆	Pentahydroxybenzophenone	<i>Garcinia multiflora</i>
269.046	5.3	C ₁₅ H ₁₀ O ₅	Galangin	<i>Platymiscium praecox</i>

5.4 Discussion

It would seem that Nigerian red propolis is very similar to Brazilian red propolis. Nigerian propolis is rich in isoflavonoid compounds that have a very restricted distribution in the plant kingdom and occur almost exclusively in legumes (Leguminosae family) (Silva *et al.*, 2008), along with isoflavans such as liquiritigenin, medicarpin. The latter have been previously isolated from Cuban and northern Brazilian red propolis, which originates largely from *Dalbergia ecastophyllum* resin (Piccinelli *et al.*, 2005). The Nigerian red propolis, according to LC-MS profiling, also contains prenylated benzophenones that are typically found in Brazilian and Cuban propolis and originate from Clusiaceae species (Yuliar *et al.*, 2013; Yang *et al.*, 2010); in Nigeria a likely source would be the African mangosteen (*Garcinia livingstonei*).

Nigerian propolis also contains prenylated benzophenones that have been previously isolated from Cameroonian propolis (Al Mutairi *et al.*, 2014) as well as geranylated flavonoids that have been isolated before from Japanese propolis collected from Okinawa and also from Pacific propolis collected from the Solomon Islands

(Kumazawa *et al.*, 2007; Raghukumar *et al.*, 2010). The origin of the geranylated flavonoids has not thus far been identified. Macarangiin has previously been isolated from Kenyan propolis and was reported to originate from two *Macaranga* species: the Asian *M. denticulata* and the New Caledonian *M. vedeliana* (Petrova *et al.*, 2010). Prenyl naringenins have not been reported before in propolis and have only been reported as occurring in hops (Jung *et al.*, 1990).

The strong anti-protozoal activity of red propolis appears to be an almost constant feature of the material and strongly suggests that bees collect the material to protect themselves against protozoal attack. The best known protozoal parasite of bees is *Crithidia bombi* which infects bumble bees (Schluns *et al.*, 2010) and this flagellated kinetoplastid is a quite close relative of the human pathogen *T. brucei*. Isolated compounds and fractions be tested against *Crithidia* but results not provided yet.

Within the series of compounds isolated there is a strong indication that the more lipophilic compounds such as medicarpin which only has one hydroxyl group, or propolin D which has a lipophilic geranyl group are the more active anti-trypanosomal compounds. Quite small alterations in structure appear to produce a marked difference in anti-trypanosomal activity with 8-prenyl naringenin being more active than its isomer 6-prenyl naringenin.

Propolis can be collected in large quantities and thus has good potential for treating protozoal infections at an intermediate technology level appropriate for developing countries.

CHAPTER SIX

PROFILING AND PURIFICATION OF

PROPOLIS FROM SOUTH AFRICA

6 PROFILING AND PURIFICATION OF PROPOLIS FROM SOUTH AFRICA

6.1 Introduction

During the preliminary investigations on anti-trypanosomal activity of African propolis, it was found that an ethanolic extract of a sample collected from Kwa Zulu Natal, South Africa **Figure 6-1** (coded: D46SA) exhibited high anti-trypanosomal activity (MIC: 6.25 $\mu\text{g/mL}$) in a bioassay test. The chemical analysis showed that it was different from other South African samples; it mainly consisted of different diterpenoid acids which are the characteristic chemical components in the propolis from the eastern Mediterranean regions (Zhang *et al.*, 2014). As a result, this sample was selected for detailed chemical profiling and subsequent successive fractionation and purification using various chromatographic techniques including HPLC and flash chromatography in order to isolate and purify the active compound(s) present in this sample.



Figure 6-1: Map of South Africa and collection site of (D46SA) Propolis (<http://bigpictureofthebible.com/south-africa-mission>).

6.2 Profiling of crude propolis sample (D46SA)

The ethanolic extract was first profiled by ELSD, LC-HRMS, NMR and GC-MS techniques, using the same methods described in section 2.3.

HPLC-UV-ELSD of the crude sample showed clearly that it contained mostly compounds with no UV-absorbing activity, that could be terpenoids or fats or any other compounds without chromophores, however, at retention times of 20 and 38 min. UV active compounds were detected but with low intensities **Figure 6-2**.

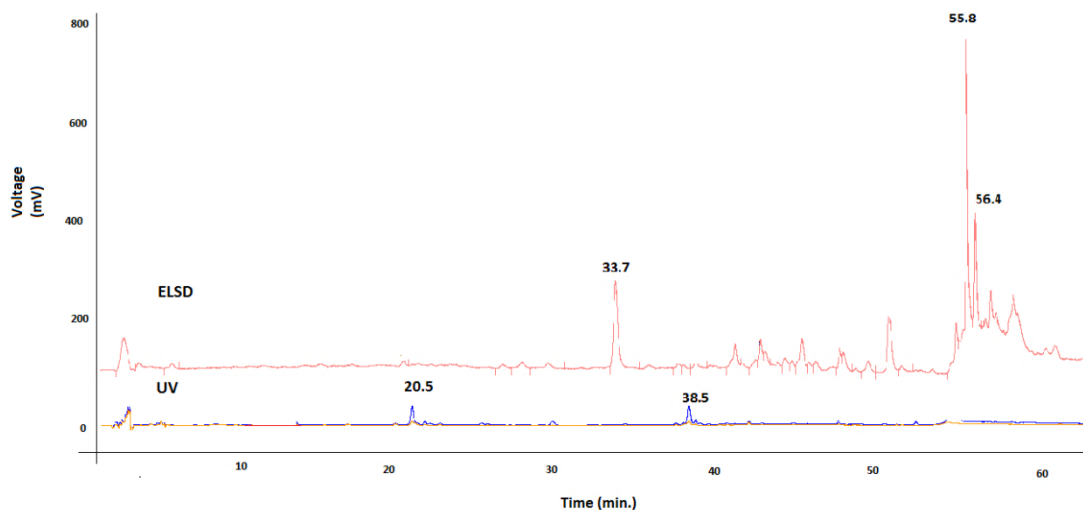


Figure 6-2: Chromatogram of HPLC-UV-ELSD of crude D46SA, red line ELSD response, blue and yellow are UV responses at 290 nm and 320 nm respectively. Experimental conditions in section 2.3.1

NMR was initially employed to determine the general nature of components in the crude sample. The spectra displayed strong responses for aliphatic protons. The major signals in the spectra could be referred to alkene protons, which would be associated with terpenoids. Interpretation proved the presence of oleic acid, which was confirmed by comparison with the literature see **Figure 6-3**, a clear multiplet at δ 5.35 referred to two vicinal protons at C9/C10 characteristic for oleic acid. Therefore, during subsequent extraction and purification stages, many steps were undertaken in order to remove fats as shown in **Scheme I** on page 179. A few signals detected by the NMR of the crude sample referred to phenolic compounds but with intensities less than those of the terpenoids.

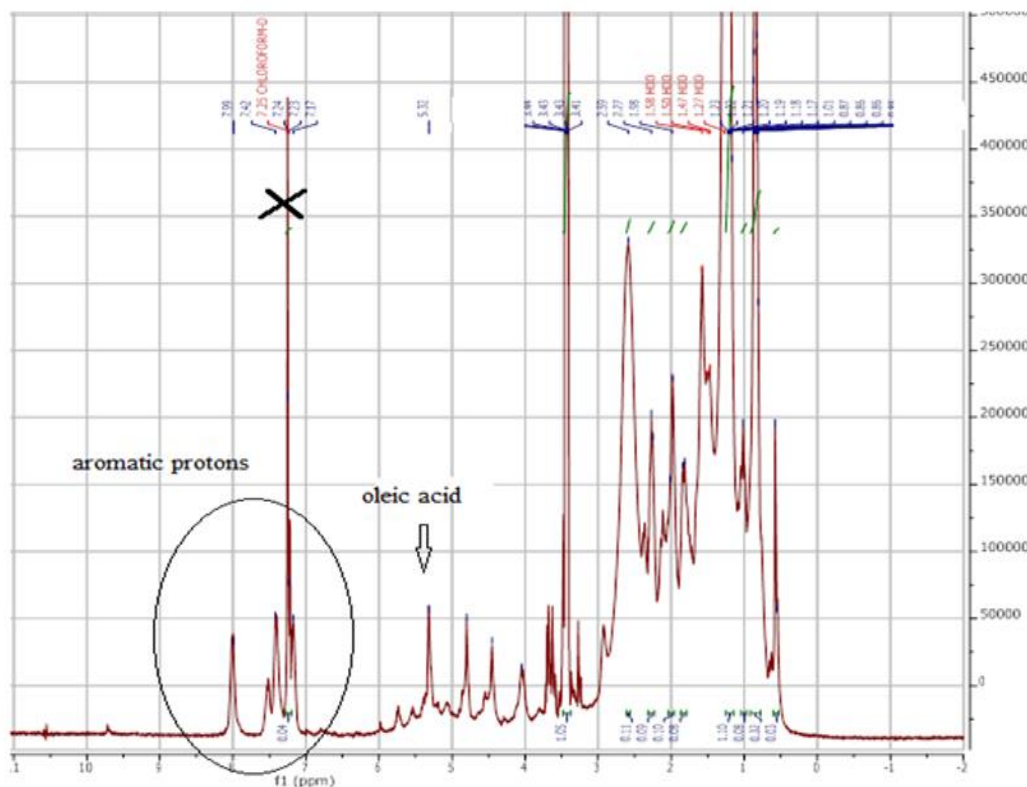


Figure 6-3: ¹H NMR spectrum (400 MHz, in CDCl₃) of crude D46SA showing mainly aliphatic protons, oleic acid and some phenolic compound(s) with lower intensities.

Analysis by GC-MS, chromatogram shown in **Figure 6-4** exhibited a large number of peaks related to non-polar volatile compounds as shown in **Table 6-1**. Some compounds were partially characterized by comparing their electron impact spectra with those found in the NIST library with similarity score higher than 800.

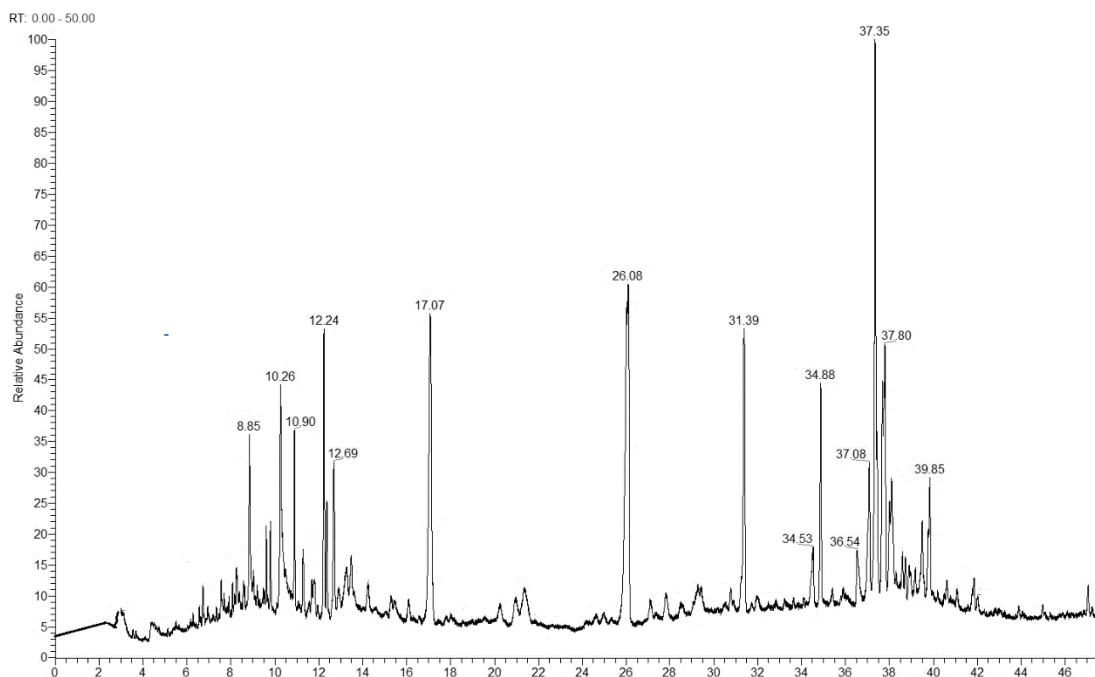


Figure 6-4: GC chromatogram of D46SA. Experimental condition in section 2.3.3.

Table 6-1: Compounds extracted from NIST library with Similarity score higher than 800.

t_R (min.)	Compound	Mwt.	Formula
8.9	Estra-1,3,5(10)trien-17-ol	256	C ₁₈ H ₂₄ O
9.6	5a'-Cholestan-3a'-ol,2-methylene	400	C ₂₈ H ₄₈ O
10.3	Oleic acid	282	C ₁₈ H ₃₄ O ₂
12.2	Wax(2,6,0,15tetramethylheptadecane)	296	C ₂₁ H ₄₄
12.4	Ferruginol	286	C ₂₀ H ₃₀ O
12.7	Totarol	286	C ₂₀ H ₃₀ O
26.1-37.4	Wax (long chain alkane), 2-methyleicosane	296	C ₂₁ H ₄₄
39.9	Cis 11-Eicosenoic acid	310	C ₂₀ H ₃₈ O ₂

Based on a previous study performed by Kasote *et al.*, which carried out chemical profiling and chemometric analysis of 39 propolis samples collected from different sites in South Africa including Western, Northern, Eastern Cape, Free State, North West, Kwa Zulu Natal and Gauteng state, it was reported that the common types of propolis contained 15 marker phenolic compounds. These compounds were identified by UPLC-PDA-Qtof-MS/MS and included two phenolic acids (caffeic acid and *p*-coumaric acid) along with 13 flavonol compounds (Kasote *et al.*, 2014). In the D46SA sample, LC-MSⁿ was an effective and comprehensive tool that identified the marker flavonoid compounds but phenolic acids were absent in this sample.

The LC-MS chromatogram of the crude D46SA sample was complex and contained many peaks with different intensities **Figure 6-5**. The data were processed manually to identify all major peaks, 13 of which were identified as shown in **Table 6-2**, by comparing their exact masses and fragments produced on LC-MSⁿ. The identified major peaks were identical with the flavonols identified in Saleh *et al.*'s study that used standard chemicals and was run using the same instrument used in this research (Saleh *et al.*, 2015), thus this propolis seemed like a typical poplar propolis.

Another five unknown compounds were detected to be major in this sample, their RDB (relative double bond) numbers were low, suggesting terpenoid compounds except for compound D as illustrated in **Figure 6-7**, they were searched in DNP and identified as shown in **Table 6-3**.

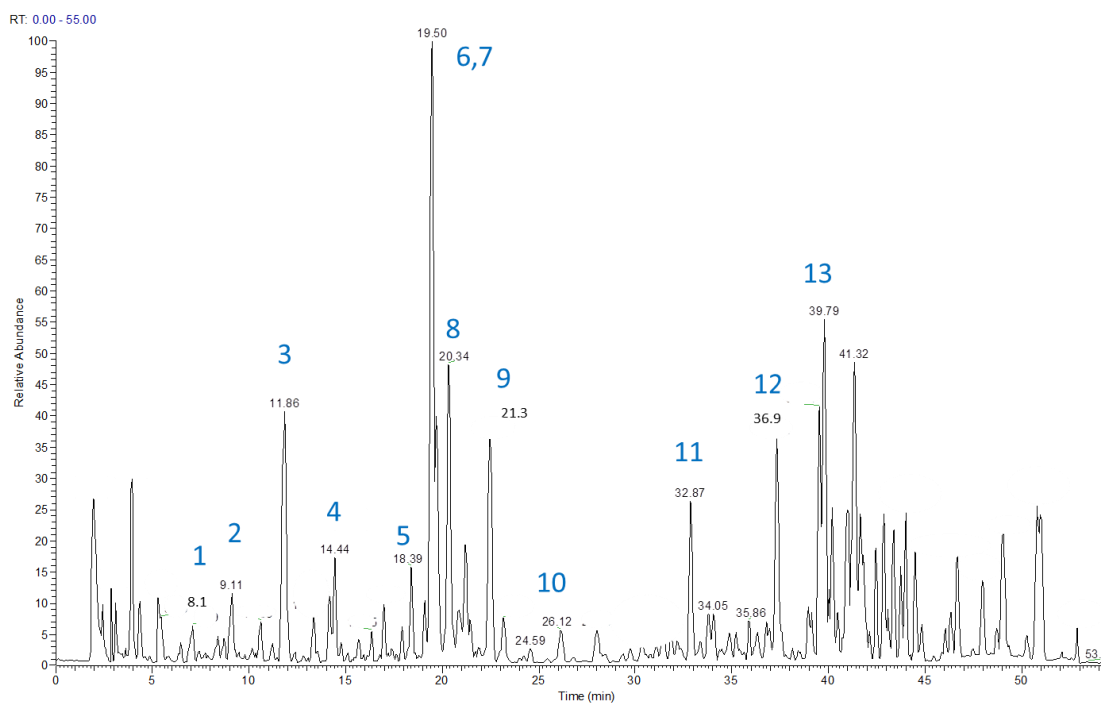
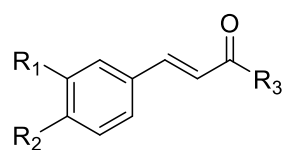


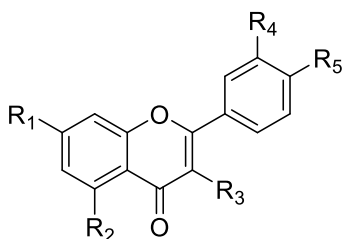
Figure 6-5: TIC chromatogram of crude D46SA. Experimental condition as in section 2.5.2.

Table 6-2: Putative identification of flavonols and other major components of the crude sample D46SA.

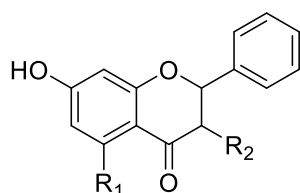
No. of peak	t _R (min.)	Elemental composition	m/z	Name
1	8.1	C ₁₅ H ₁₀ O ₇	301.0359	Quercetin
2	9.1	C ₁₆ H ₁₄ O ₅	285.0769	Pinobanksin-5- methyl ether
3	11.9	C ₁₅ H ₁₂ O ₅	271.0612	Pinobanksin
4	14.1	C ₁₆ H ₁₂ O ₅	283.0614	Galangin 5-methyl ether
5	18.4	C ₁₅ H ₁₀ O ₄	253.0505	Chrysin
6	19.4	C ₁₅ H ₁₂ O ₄	255.0663	Pinocebrin
7	19.7	C ₁₅ H ₁₀ O ₅	269.0453	Galangin
8	20.3	C ₁₇ H ₁₄ O ₆	313.072	Pinobanksin -3- <i>O</i> -acetate
9	21.4	C ₁₆ H ₁₂ O ₅	283.0614	Tectochrycin
10	26.1	C ₁₈ H ₁₆ O ₆	327.0875	Pinobanksin 3- <i>O</i> -propionate
11	32.9	C ₁₉ H ₁₈ O ₆	341.1033	Pinobanksin3- <i>O</i> - butyrate or isobutyrate
12	36.9	C ₂₀ H ₂₀ O ₆	355.1189	Pinobanksin 3- <i>O</i> -pentanoate or 2-methylbutyrate
13	40.0	C ₂₁ H ₂₂ O ₆	369.1347	Pinobanksin 3- <i>O</i> -hexanoate



Caffeic acid R1= OH, R2= OH, R3= OH
 p-Coumaric acid R1= H, R2= OH, R3= OH



Quercetin R1=OH, R2=OH, R3=OH, R4=OH, R5=OH
 Chrycin R1=OH, R2=OH, R3=H, R4=H, R5=H
 Tectochrysin R1=OCH3, R2=OH, R3=OH, R4=H, R5=H
 Galangin R1=OH, R2=OH, R3=OH, R4=H, R5=H
 Galangin-5-methyl ether R1=OH, R2=OCH3, R3=OH, R4=H, R5=H



Pinocembrin R1=OH, R2=H
 Pinobanksin R1=OH, R2=OH
 Pinobanksin-5- methyl ether R1=OCH3, R2=OH
 Pinobanksin -3-O-acetate R1=OH, R2=OCOH3
 Pinobanksin 3-O-propionate R1=OH, R2=OCOC2H5
 Pinobanksin3-O- butyrate R1=OH, R2=OCOC3H7
 Pinobanksin 3-O-pentanoate R1=OH, R2=OCOC4H9
 Pinobanksin-3-O-hexanoate R1=OH, R2=OCOC5H11

Figure 6-6: Structures of the previously reported South African propolis marker compounds were all identified except phenolic acids caffeic and *p*-Coumaric acid.

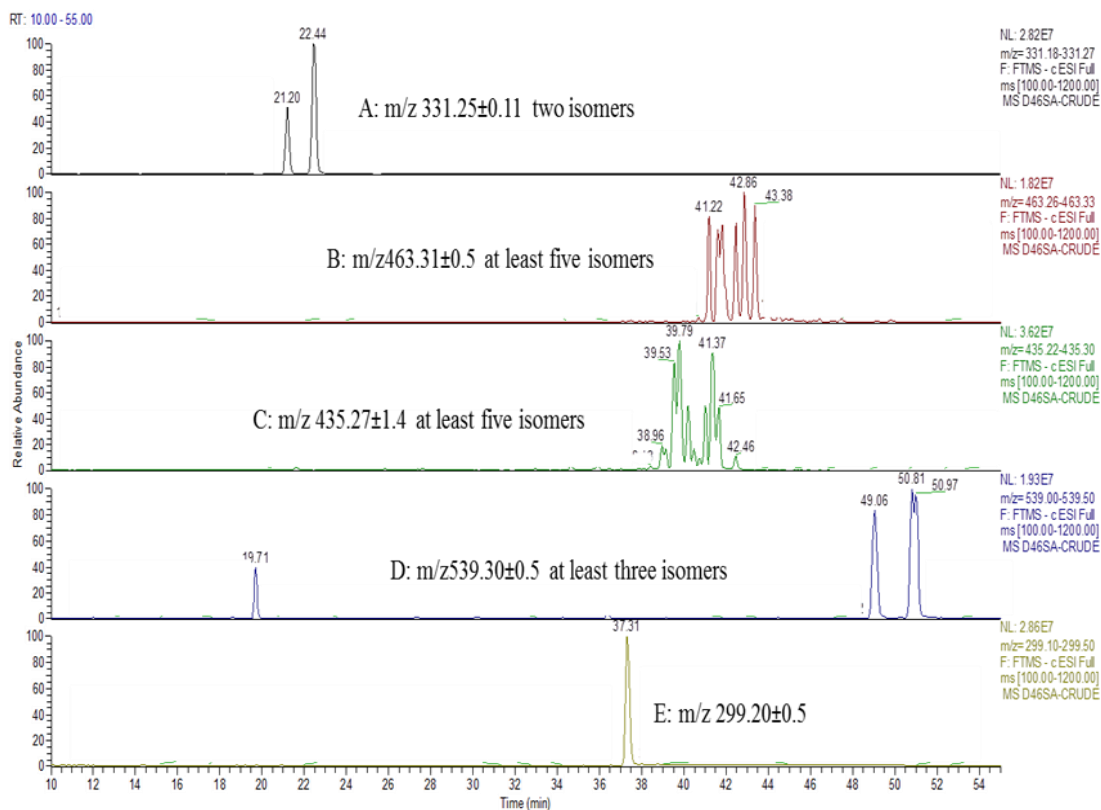


Figure 6-7: Extracted ion traces of the main unknown compounds in the crude D46SA extract.

Table 6-3: Elemental compositions, exact mass and fragmentation of five abundant unknown compounds in the crude extract of D46SA. The chemical names in red are possible identities searched in DNP.

Compound	t _R (min)	[M-H] ⁻	Formula	RDB	LC-MS ²
Unknown A Trihydroxyoctadecanoic acid	22.4	331.2490	C ₁₈ H ₃₆ O ₅ 2 isomer	1.5	253.05(C ₁₅ H ₉ O ₄) 271.06(C ₁₅ H ₁₁ O ₅)
Unknown B Ecdysone	41.2	463.3064	C ₂₇ H ₄₄ O ₆ 42 isomers	6.5	313.23(C ₁₈ H ₃₃ O ₃)
Unknown C 3,8,13,17-Tetrahydroxyprenyl 15,11-labdadiol	39.5	435.2747	C ₂₅ H ₄₀ O ₆ 23 isomers	6.5	313.23(C ₁₈ H ₃₃ O ₄) 321.24(C ₂₀ H ₃₃ O ₃)
Unknown D Globostellatic acid A	50.8	539.3013	C ₃₂ H ₄₄ O ₇ 10 isomers	11.5	417.26(C ₂₅ H ₃₇ O ₅) 424.42(C ₂₈ H ₅₆ O ₂)
Unknown E Dehydroabietate; 1-hydroxy 8,11,11-triaabietatriene	37.3	299.2019	C ₂₀ H ₂₈ O ₂ 163 isomers	7.5	227.11(C ₁₅ H ₁₅ O ₂) 283.17(C ₁₉ H ₂₃ O ₂) 269.15(C ₁₈ H ₂₁ O ₂) 241.12(C ₁₆ H ₁₇ O ₂)

6.3 Extraction and fractionation of propolis sample D46SA

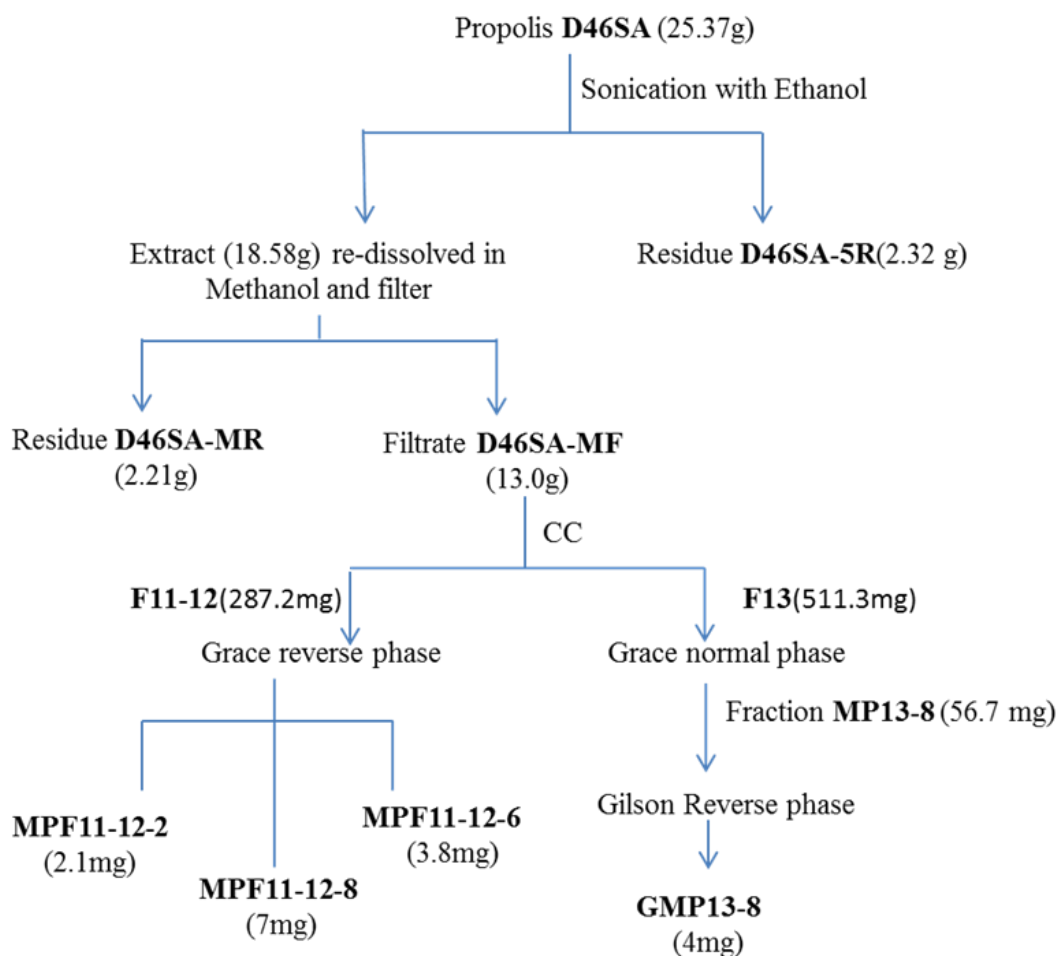
As already stated above, the crude sample was rich in fats, which usually interrupt the separation and identification of other components in a sample. Thus, additional steps

were added in the extraction protocol as shown in **Scheme I**, by including a polar solvent methanol in order to remove fats.

The sample (25.4 g) was extracted with 900 mL (3×300) of ethanol with sonication and macerated overnight, and filtered through a filter paper. The extract was dried under vacuum in a rotatory evaporator with a temperature not exceeding 60 °C, and the resultant gum was mixed with methanol and then filtered to produce a filtrate coded D46SA-MF (13.0 g) and residue coded D46SA-MR (2.2 g). All of these were tested against trypanosomes and from the results obtained, bioassay guided fractionation was carried out to obtain progressively more active extracts. As shown in **Table 6-4**, D46SA-MF had the highest weight and strongest bioactivity and therefore it was chosen for further fractionation.

Table 6-4: Summary for the weights and anti-trypanosomal activity obtained from D46SA extracts. Highlighted cells indicate high activity.

Extract code	Yield (g)	Inhibition of <i>T. b. brucei</i> % of control (20 µg/mL)	Inhibition of <i>T. b. brucei</i> % of control (10µg/mL)
D46SA-MF	13.0	-0.7	-1.6
D46SA-MR	2.2	-1.7	15.9
D46SA-5R	2.3	69.3	66.4



Scheme I: Isolation of compounds from the Ethanolic extract of D46SA propolis.

As shown in the scheme, D46SA-MF (13.0 g) was fractionated by silica open column chromatography using a gradient of hexane:ethyl acetate:methanol, resulting in 36 fractions which were monitored by ELSD, and pooled to produce 13 separate fractions. All these were tested against trypanosomes and *M. marinum*, and fractions F13, F11-12, demonstrated high activities. The active fractions revealed the presence of UV absorbing moieties in the HPLC-ELSD chromatograms and since they had a relatively high weight, they were chosen to be purified for further studies.

Table 6-5: Summary of the weights and anti-trypanosomal activity of the fractions of D46SA-MF obtained from CC. Fractions in pink were isolated and identified. The highlighted cells indicate high activity.

Fraction number	Yield (mg)	Inhibition of <i>T. b. brucei</i>		
		20 µg/mL	10 µg/mL	5 µg/mL
D46SA-04	27.2	104.0	100.0	101.7
D46SA-58	352.2	105.6	101.1	101.4
D46SA-910	291.4	40.5	95.5	99.0
D46SA1112	287.2	2.1	39.6	89.4
D46SA-13	511.3	-0.4	8.9	82.2
D46SA-1416	383.0	2.9	2.5	84.8
D46SA-1719	852.5	3.0	0.6	0.7
D46SA-2021	753	1.3	-1.6	-0.6
D46SA-2225	901	0.2	-2.1	-1.3
D46SA-2627	282.7	0.5	-0.7	-1.5
D46SA-2831	331.5	0.1	-2.4	42.1
D46SA-3233	937.2	0.4	26.0	86.8
D46SA3436	645.0	1.3	25.9	99.6

For further purification, **Fraction 13** was first dry loaded and run on the Grace® system in normal phase mode using a pre-packed silica column (24g) and ethyl acetate (A) and hexane (B) as mobile phases. The gradient conditions were starting from 100% hexane, up to 100% of ethyl acetate for 78 minutes, at a flow rate of 12mL/min. As shown on the chromatogram produced in **Figure 6-8**, the UV absorbing moiety was targeted and collected.

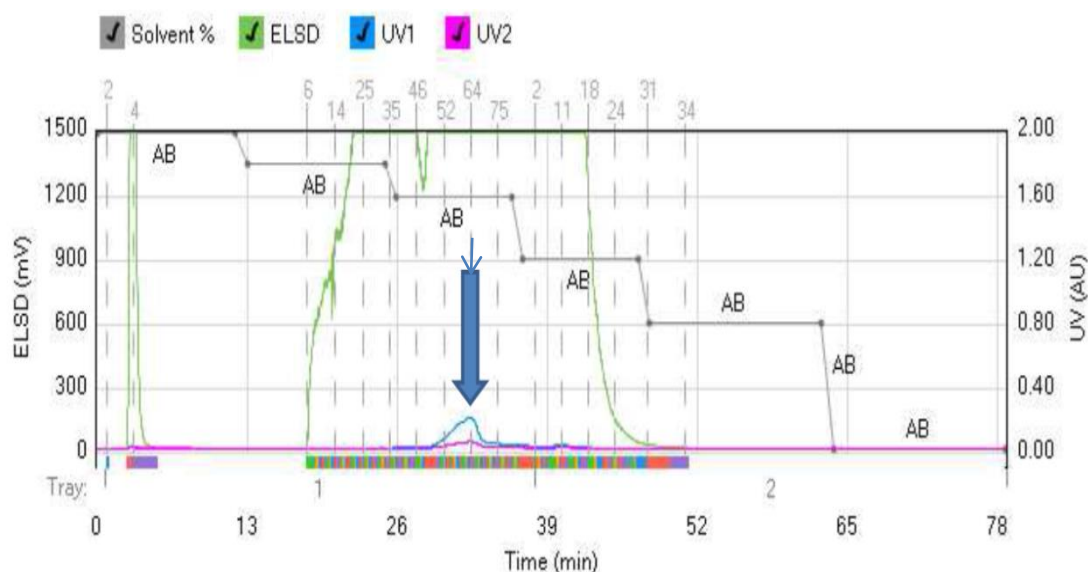
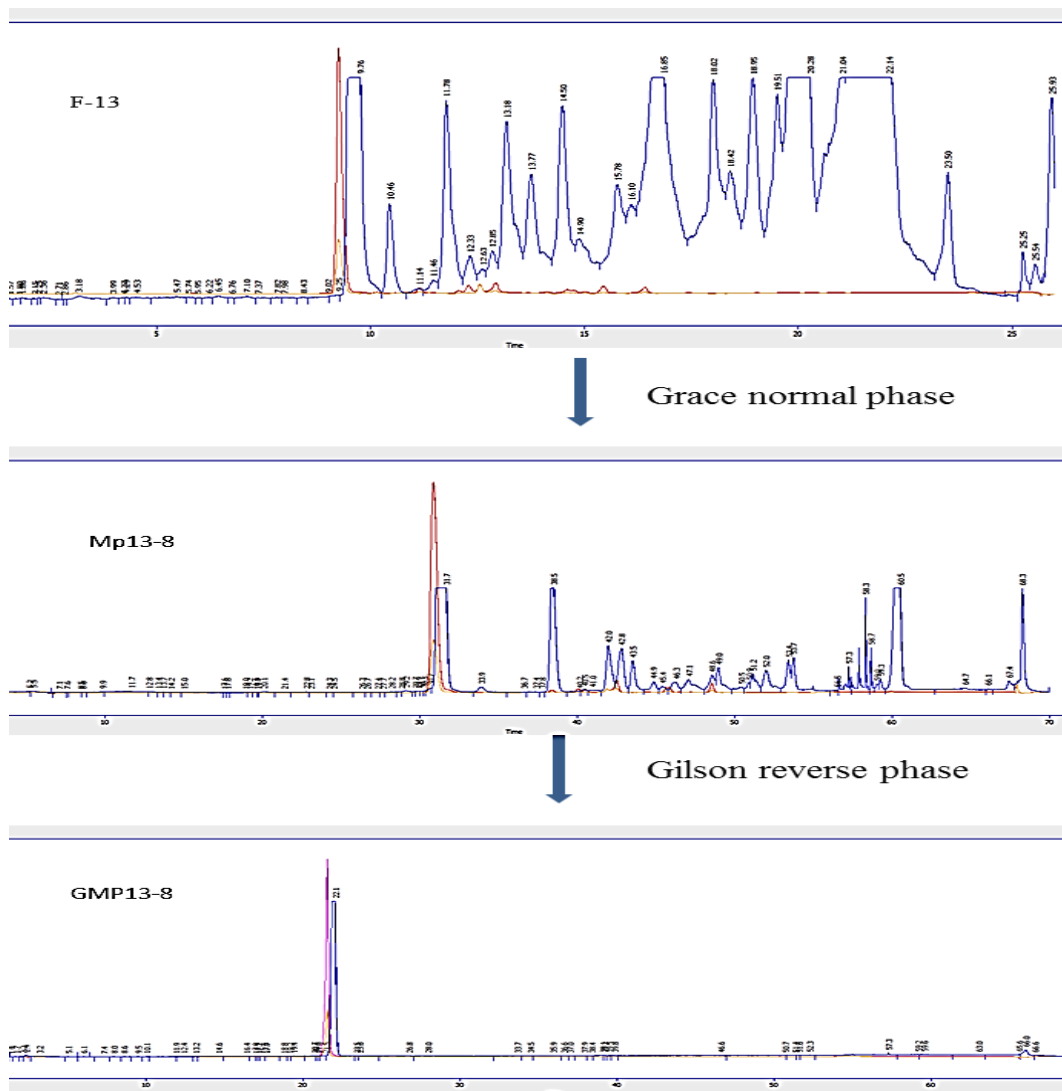


Figure 6-8: Chromatogram of F13 on the Grace® system revealing the targeted UV absorbing compound (blue arrow).

Fractionation with normal phase chromatography on the Grace® did not sufficiently separate the compounds as expected. This was verified when fraction MP13-8 from the Grace® was run on the HPLC-ELSD and found not to be pure, but rather showed a complex chromatogram (Scheme II, middle). Therefore an isocratic method was developed by HPLC-UV-ELSD for fraction MP13-8, and was transferred to Gilson

semi-preparative system using a reversed phase ACE5-C18 column (250×10 mm i.d.) as specified in section 2.4.3, and eluted with 50:50 acetonitrile:water. The flow rate was scaled up from 0.3 mL/min to 4.5 mL/min, and a pure fraction of GMP13-8 was obtained as seen in scheme II below. Chemical structure elucidation was performed by 1D and 2D NMR and then compared with the literature.

F11-12 (250.0 mg) was purified using the Grace Reveleris system in reversed phase mode using a C18 (12 g) column. Initially the method was developed on an analytical scale the HPLC-ELSD and an isocratic method with 50:50 acetonitrile:water was employed in a 30 min run on the MPLC system and at a flow rate of 12mL/min. This led to isolation of three fractions MPF11-12-2 (2.1 mg), MPF11-12-6 (6.7 mg) and MPF11-12-8 (7.0 mg) as pure compounds. The purity profiles of these three fractions were tested on HPLC-ELSD. Their structures were elucidated using 1D and 2D NMR spectroscopy.



Scheme II: Showing the UV/ELSD Chromatograms during purification steps obtained on an ACE C18 column (150 x 3 mm, 3 μ m) as described in 2.3.1.

6.3.1 Characterization of GMP13-8 and MPF11-12-2 as Pinocembrin

The two fractions each contained a peak which appeared on LC-MS as a major component at 19.4 min. The negative mode HRESI-MS data for GMP13-8 showed the base ion $[M-H]^-$ at m/z 255.0663 with an elemental composition of $C_{15}H_{12}O_4$ relative double bond (RDB= 10.5). The fragmentation pattern was discussed earlier in section 5.3.1. 1H , ^{13}C NMR data were consistent with those previously reported for Pinocembrin (Press *et al.*, 1990) as shown in **Table -S8** in appendix, $[\alpha]_D +108$ (c 1.00, Methanol).

6.3.2 Characterization of MPF11-12-6 as Acetylimbricatolic acid (labdane type diterpene).

MPF11-12-6 was isolated as a colourless oil. On the HPLC-UV-ELSD, this compound showed only ELSD signals, with a peak at 46.4 min. **Figure 6-9**. Its specific optical rotation was measured to be $[\alpha]_D^{25} +33$ (c 1.00, Chloroform). The negative mode HRESI-MS data for MPF11-12-6 showed a quasi-molecular ion $[M-H]^-$ at m/z 363.2536, with an elemental composition of $C_{22}H_{36}O_4$ (RDB=5.5). On analysis by LC-MS² the fragments formed 304.2020(100), ($C_{20}H_{32}O_2$, Δ 1.20 ppm), and at 276.2025 (60), ($C_{18}H_{28}O_2$, Δ 2.01. ppm)

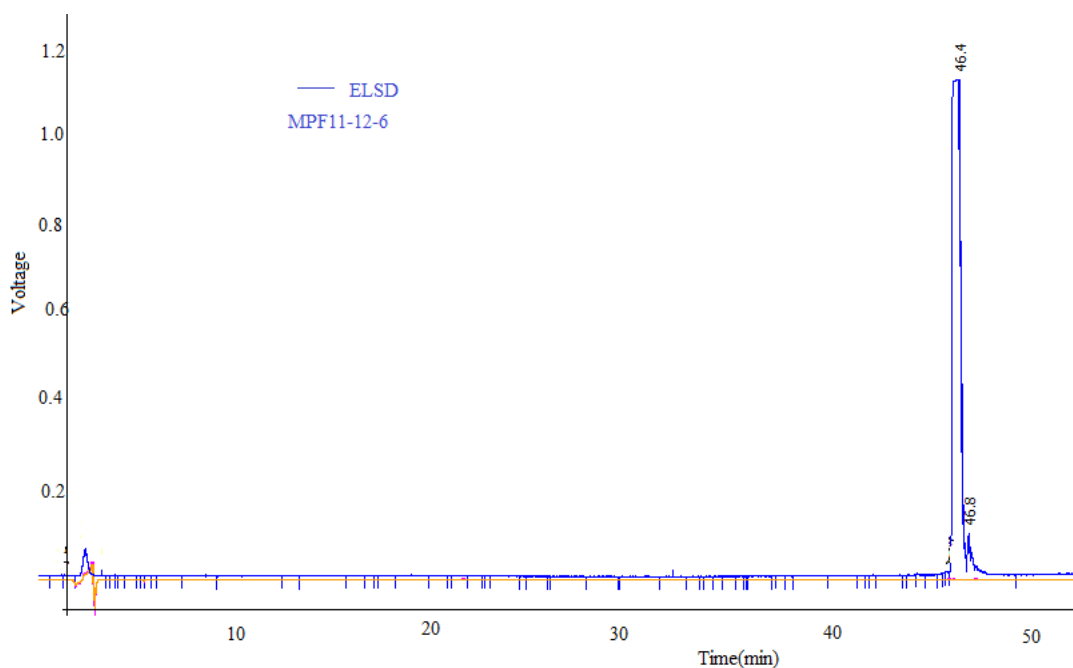


Figure 6-9: Chromatogram of MPF11-12.6 on the analytical HPLC ELSD system.

$^1\text{H-NMR}$ **Figure 6-11A**, **Table 6-6** shows the presence of two singlet large signals at 4.83, 4.47 suggesting an exomethylene, four singlets for methyls at δ 0.87 (3H), δ 0.55 (3H), δ 1.11 (3H), and δ 1.97(3H). The latter was a methyl of an acetyl group and therefore was deshielded.

$^{13}\text{C NMR}$ **Figure 6-11B**, **Table 6-6** revealed the presence of 4 methyl groups, 10 methylene groups, three methines, one exomethine and 5 quaternary carbons. Two carbonyl groups were clear in HMBC. In the HMBC spectrum, the exomethylene protons (H-17) at δ 4.83 showed 3J correlations to a methylene at δ 38.7 ppm(C-7) and a methine at δ 56.3 ppm (C-9). The methyl at δ 1.11 (H-19) 3J coupled to quaternary carbons at δ 178.5 (C-18) of the carboxylic acid while the other methyl at 1.97(H-OAc) 3J coupled to quaternary carbon at 170(15-AOc). The methyl proton at δ 0.55

(Me-20) showed 3J correlations to the carbon at $\delta 39.0$ (C-1) and $\delta 56.3$ (C-9). The signal at $\delta 0.87$ (Me-16) 2J correlated to the carbons at $\delta 30.3$ (C-13) $\delta 35.9$ (C-12), and carbon at $\delta 35.1$ (C-14). Based on the above data, MPF11-12-6 was identified as acetylimbricatolic acid in agreement with a previously reported dehydrogenated form of the structure called acetoxisocupressic acid (Cheng *et.al.*,1989). The two structures are shown in **Figure 6-10**.

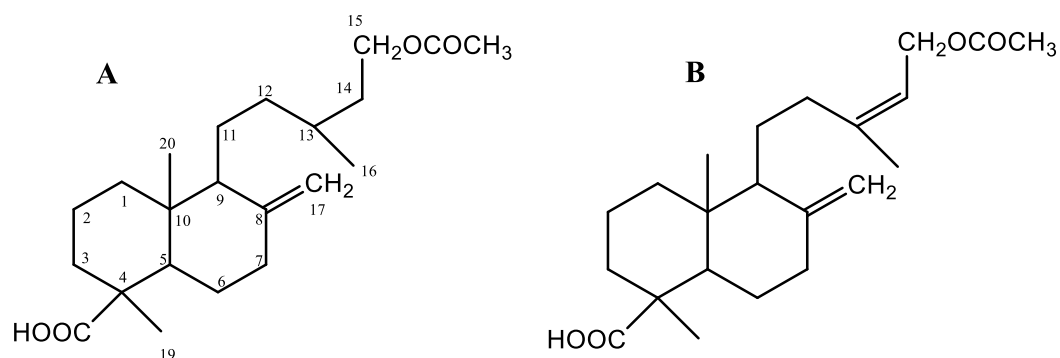


Figure 6-10: A- Structure of acetylimbricatolic acid and B- Structure of 15-acetyl isocupressic acid.

Table 6-6: ^1H (400 MHz) and ^{13}C NMR (100 MHz) data of MPF11-12-6 in DMSO- d_6 .

Position	Chemical shift δ ppm ^1H (mult, J Hz)	Chemical shift δ ppm ^{13}C
1	1.04, 1.80 (<i>m</i>)	39.0 (CH_2)
2	1.78, 1.43 (<i>m</i>)	20.2 (CH_2)
3	1.00, 2.01(<i>m</i>)	38.1 (CH_2)
4	-	43.0 (C)
5	1.28,1H,(<i>d</i> ,2.8)	55.7 (CH)
6	1.89, 1.75(<i>m</i>)	26.4 (CH_2)
7	2.33,1H,eq(<i>m</i>), 1.8,1H,ax(<i>m</i>)	38.7 (CH_2)
8	-	148.2(C)
9	1.54,1H (<i>m</i>)	56.3 (CH)
10	-	39.7 (C)
11	1.32 (<i>m</i>),1.47 (<i>m</i>)	20.9 (CH_2)
12	0.92 (<i>m</i>), 1.37(<i>m</i>)	35.9 (CH_2)
13	1.46 (<i>m</i>)	30.3 CH
14	1.59 (<i>m</i>),1.35 (<i>m</i>)	35.1 CH_2
15	4.00 (<i>m</i>)	62.6 CH_2
16	0.87,3H (<i>s</i>)	20.0 CH_3
17	4.83, 1H (<i>d</i>) 4.47,1H,(<i>d</i>)	106.5(CH_2)
18	-	178.5(C)
19	1.11,3H(<i>s</i>)	29.2 (CH_3)
20	0.55,3H(<i>s</i>)	13.0 (CH_3)
15-OAc	-	170.0 (C)
	1.97,3H(<i>s</i>)	21.2 (CH_3)

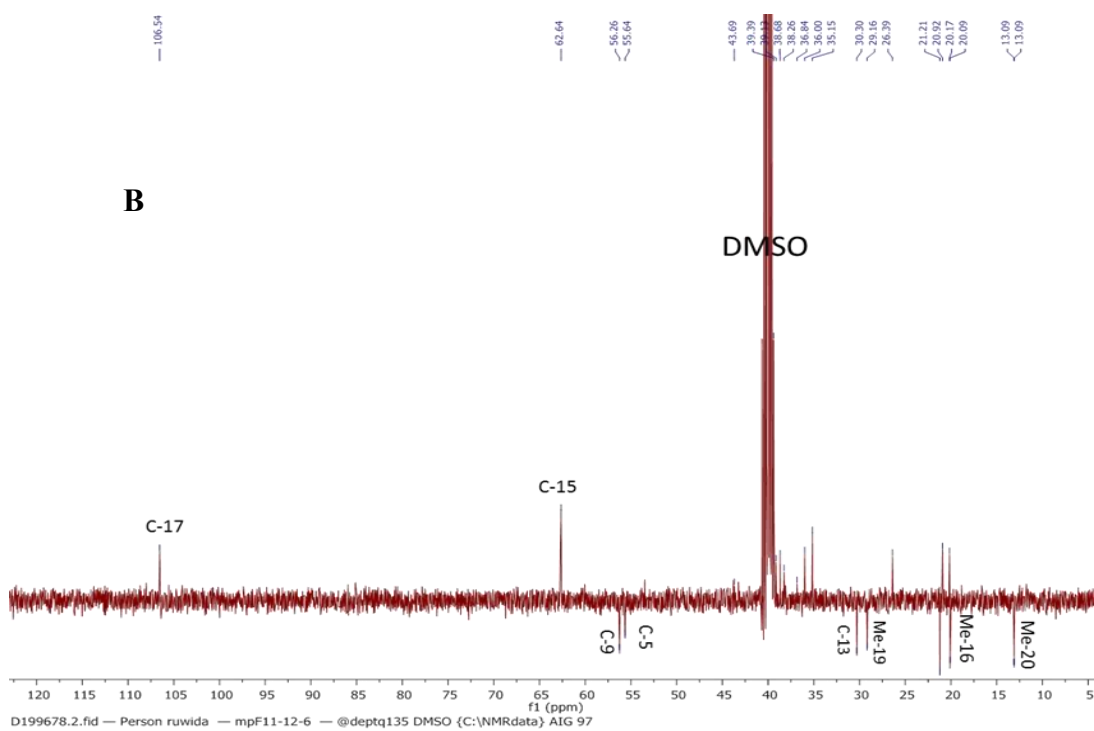
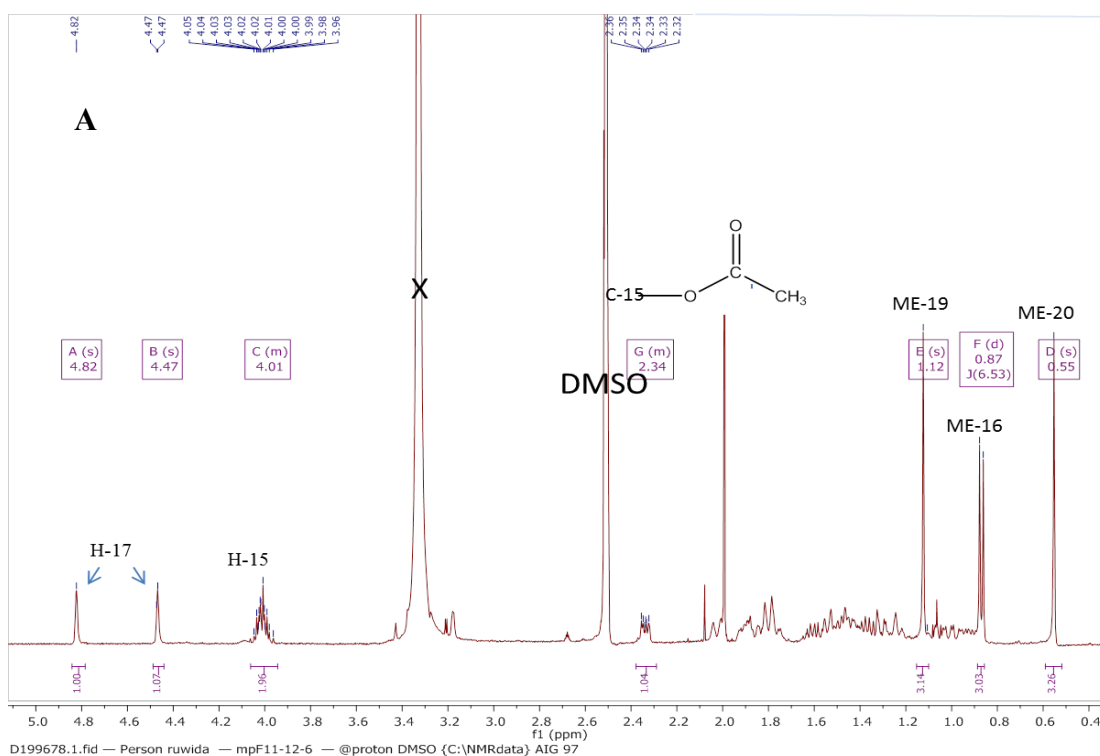


Figure 6-11: A ^1H NMR spectrum (400 MHz) and B DEPT 135 ^{13}C NMR (100 MHz) of MPF11-12-6 in DMSO- d_6 , X denotes for solvent.

Labdane diterpenes have been isolated before in Brazilian type propolis as acetylisocupressic acid which had originated from buds of *Baccharis dracunculifolia*, and studies have shown it has hepatoprotective and anti-*Helicobacter pylori* activity (Banskota *et al.*, 2001). This type of diterpene, along with other diterpenes, is considered as a marker of Mediterranean type propolis (Popova *et al.*, 2010).

6.3.3 Characterization of MPF11-12-8 as (-)-Pimara-8(14), 15-dien-19-oic acid.

MPF11-12-8 was isolated as colourless needles; its purity was confirmed by HPLC ELSD **Figure 6-12**. The compound eluted in the retention time range of 51.0–52.4 min., with only ELSD response and the absence of UV absorptivity at both 290 and 320 nm strongly suggested terpenoids or a non-phenolic compound. Its specific optical rotation $[\alpha]_D$ was -12° (c 1.00, Chloroform).

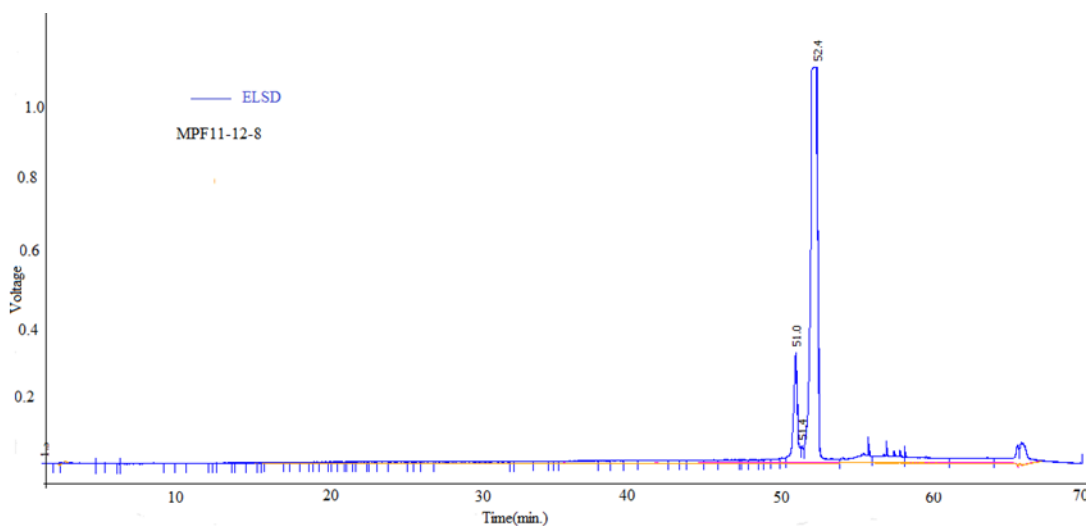


Figure 6-12: ELSD Chromatogram of MPF11-12.8 on ELSD.

The negative mode HRESI-MS data for MPF11-12-8 showed a quasi-molecular ion $[M-H]^-$ at m/z 301.2169, at the same retention time as observed on ELSD, and with an elemental composition of $C_{20}H_{30}O_2$ (RDB=6.5). From LC-MS² the main fragment observed at m/z 273.68(100) was indicative of loss of -CO from the carboxylic acid group.

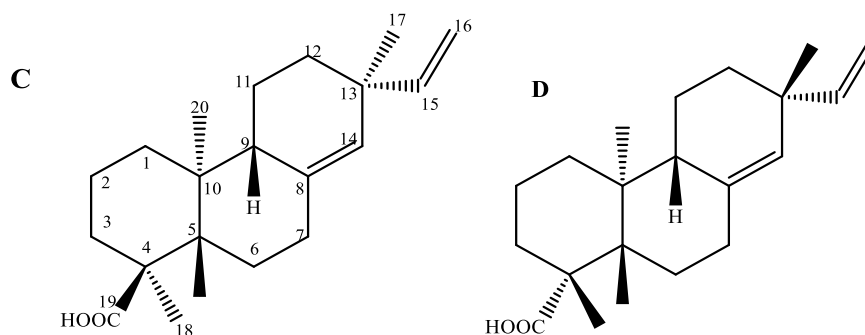


Figure 6-13: Structure of two isomers **C** pimaric acid, **D** (-)-pimara-8(14), 15-dien-19-oic acid.

The 1H NMR spectrum **Figure 6-14E**, **Table 6-7** displayed olefinic protons at δ 5.21 ppm (1H, *s*) and δ 5.76 ppm (1H, *dd*) with *J* values of 17.3 Hz and 10.7 Hz respectively, and two protons of methylene at 4.87, 1H (*q*, 1.6), 4.92, 1H (*dd*, with *J* values at 10.5, 1.7), and three methyl groups at δ 0.78 (*s*), δ 1.09 (*s*) and δ 1.01 (*s*). Some other signals were also detected at δ 1.84 (1H, *dd*, *J*=12.3, 2.6 Hz), δ 1.98 (1H, *dt*, *J*=12.9, 7.4 Hz), δ 2.20 (1H, *ddd*, *J*=13.9, 4.7, 2.0 Hz) and with the aid of the HMBC experiment they were identified.

The ^{13}C NMR spectrum in **Figure 6-14F**, showed three methyls at δ 26.4, δ 17.5, δ 15.3, two methylenes at δ 110.9 ppm (C-16), δ 148.8 ppm (C-15), and olefinic carbon at 129.0 ppm (C-14) and two signals referred to $-\text{CH}$ at 49.0 ppm and 50.5 ppm referred to (C-5,C9) respectively. With the aid of the HMBC experiment, the presence of five quaternary carbons were also established with signals as shown in **Table 6-7**; one of them referred to a carboxylic acid at 180.0 ppm (C-19).

The above NMR results were greatly consistent with previous reports for (-)-Pimara-8(14), 15-dien-19-oic acid previously isolated from the root of *Aralia cordata* Thunb (Araliaceae). It has been used as a traditional Chinese medicine for rheumatism, and the two isomers are pimaric acid and (-) - pimara-8(14), 15 diene-19-oic acid **Figure 6-13**. It showed significant antibacterial activity and inhibitory activity of Cyclooxygenases COX1, COX2 which are involved in inflammation (Dang *et al.*, 2005). These diterpenes were isolated before from Mediterranean propolis and are considered as markers for propolis from these regions (Velikova *et al.*, 2000).

Table 6-7: ^1H (400 MHz) and ^{13}C NMR (100 MHz) data of MPF11-12-8 in DMSO- d_6 .

Position	Chemical shift δ ppm ^1H (mult, J Hz)	Chemical shift δ ppm ^{13}C
1	1.69, 1.08 (m)	38.4 CH_2
2	1.61, 1.48m (m)	18.6 CH_2
3	1.67, 1.5(m)	37.0 CH_2
4	-	46.7 C
5	1.84,1H,(dd, 12.3,2.6)	49.0 CH
6	1.34, 1.18(m)	24.8 CH_2
7	1.98,1H(dt12.9,7.43), 2.20,1H(ddd,13.9,4.7,2.0)	35.5 CH_2
8	-	136.5C
9	1.75,1H(m)	50.5 CH
10	-	37.8 C
11	1.5 (m)	18.3 CH_2
12	1.34, 1.42(m)	34.4 CH_2
13	-	37.5 C
14	5.21, 1H(s)	129.0 CH
15	5.76,1H (dd,17.3,10.7)	148.8 CH
16a	4.87,1H(q,1.6), 4.92,1H(dd,10.5,1.7)	110.9 CH_2
16b		
17	1.01,3H(s)	26.4 CH_3
18	1.09,3H(s)	17.5 CH_3
19	-	180.0 C
20	0.78,3H(s)	15.3 CH_3

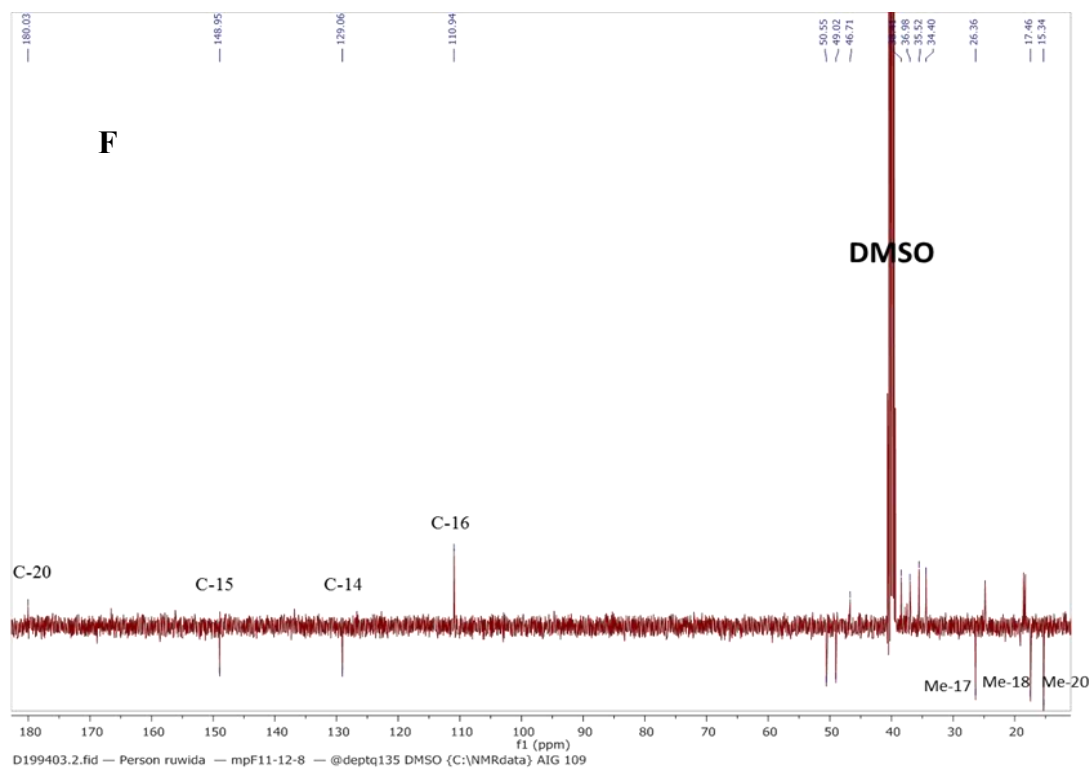
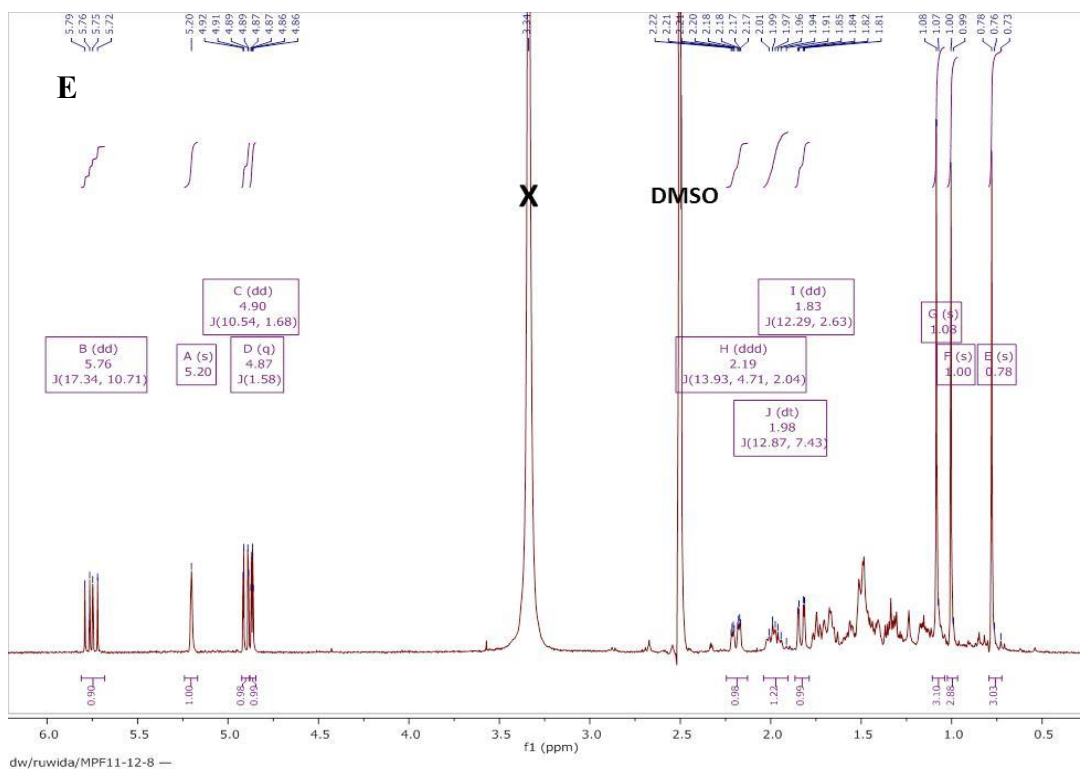


Figure 6-14: E- ^1H NMR spectrum (400 MHz), F- DEPT ^{13}C NMR spectrum (100 MHz) of MPF11-12-8 in DMSO-d_6 , X denotes the solvent peak.

6.4 Anti-trypanosomal activity

The preliminary screening of the fractions and crude extracts of the D46SA sample shown in **Table 6-4**, **Table 6-5** were carried out in order to determine their biological activity *in vitro* against *T. brucei brucei* using the Alamar Blue 96-well microplate assay as explained in section 2.6.1. Some of these fractions (F13 and F11-12) which showed high potency were chosen for further purification to isolate the bioactive components. The three isolated pure compounds showed moderate potency against *T. brucei brucei* when further screened to determine their minimum inhibitory concentrations in this organism **Table 6-8**. These MIC values were compared to that of suramin as a positive control with an MIC of 0.125 μM .

Table 6-8: MIC values in μM of pure compounds when tested against *T. brucei brucei*

Compound	MIC in <i>T. brucei brucei</i> (μM)
Pinocembrin	48.8
MPF11-12-8	41.4
MPF11-12-6	137.3
Suramin	0.125

6.5 Discussion

Although South Africa has an active bee-keeping community, and propolis production is considered to be additional income for the South African beekeepers, where low capital minimum labour input are involved, there is a rarity of scientific research on the biological properties and chemistry of locally produced propolis. This is unexpected as numerous websites claim that South African propolis is a widely valued health product. Few studies on anti-oxidant, antimicrobial and anti-inflammatory activities of South African propolis have been documented (Kumazawa *et al.*, 2004; Toit *et al.*, 2009). These studies along with our previous study on propolis from different African countries have reported that South African propolis mostly contains different types of phenolic compounds similar to temperate region poplar propolis, and samples collected from KwaZulu-Natal in South Africa were rich in diterpenoid acids, characteristic of propolis from eastern Mediterranean regions which derives in part from Cypress trees.

The results from this research approved the presence of 13 characteristic flavonol markers that have been reported previously in detailed chemical profiling of 39 South African samples collected from different regions, using chemometric approaches (Kasote *et al.*, 2014). Their presence was confirmed by LC-MS² and comparing the fragments produced with literature. The results showed the absence of two phenolic acids, caffeic acid and *p*-coumaric acid. Profiling by GC-MS and NMR techniques was helpful for understanding the general nature of components of the crude sample and proved the high content of terpenoid-wax and fat in this South

African propolis, this helped in the development of a suitable method for extraction and purification.

The diterpenic profile in sample D46SA was close to that of Mediterranean propolis especially from Maltese propolis and propolis from South-Eastern Greece. The later displayed significant similarity to the profile of the resin of *C. sempervirens* (*Cupressaceae* family), suggesting that this could be the source of this sample.

Fractionation of this sample led to isolation of one flavonol, pinocembrin, and two diterpenic acids; acetylimbricatolic acid, and (-)-pimara-8(14), 15-dien-19-oic acid. Their structures were fully elucidated by 1D-2D NMR. And data were consistent with literature.

Anti-trypanosomal activity was also reported for crude and fractions from silica gel and for purified compounds for the first time, even though South Africa is one of the regions most threatened by sleeping sickness disease (Surveillance & Malaria, 2004). The fractions seem to have activity higher than that of the purified compounds and the crude itself. This suggests a synergistic effect of components of the fractions. However, the compounds responsible for most of the activity have yet to be isolated.

CHAPTER SEVEN
GENERAL DISCUSSION

7 GENERAL DISCUSSION

Propolis is a resinous substance that bees collect from plants in order to seal up gaps in their hives and they also use it as an anti-infective agent to prevent infection of the hive by microorganisms—social immunity and is widely used by humans as an ingredient of nutraceuticals, over-the-counter preparations and cosmetics. Its chemical composition is highly variable and complex and varies by geographic location, climatic zone and local flora. The understanding of the chemical information of propolis is important with respect to quality control and standardization purposes. Also, if the propolis type is new and unexplored, it may contain new valuable bioactive compounds. Propolis has been studied for its biological activity for many years and there is an increasing interest in it as a source of new drugs.

Human African trypanosomiasis is a serious public health issue in Africa, since it threatens thousands of people there, readily available drugs have limited efficacy and serious adverse effects. Thus, the priorities in tropical medicine researches are the identification and characterization of parasite-specific biomolecules. Discovery of novel anti-trypanosomal medicines has led to many researchers across the world seeking solutions from naturally occurring substances.

Based on a previous study, a sample collected from Nigeria demonstrated strong anti-trypanosomal activity, and characteristic chemical composition. Therefore, the present study focused on that area in Africa and investigated chemical composition and biological activity of twelve propolis samples collected from eight different regions in Nigeria, trying to chemically characterize samples, and investigate

biological activity against *Trypanosoma brucei*, the causative agent of sleeping sickness, and two genetically modified strains, that are pentamidine resistant. In addition, activity against *Crithidia fasciculata* was tested.

Chemical profiling was carried out using many instrumental methods including: high performance liquid chromatography (HPLC) coupled to different detectors such as evaporative light scattering detector (ELSD), ultraviolet detection (UV), and high resolution mass spectrometry (HRMS); gas chromatography mass spectrometry (GC-MS), and NMR. This provided an overall picture of most of the components in propolis samples, regardless of their nature, ionizability or volatility. All the techniques proved that composition of Nigerian propolis samples varies widely and can be divided into two groups according to geographical origin; which were Southern propolis samples rich in UV absorbing compounds like flavonoids, phenolic compounds or central propolis containing mainly non-UV absorbing triterpenoids, waxes and fats.

Samples coded RSN, BRN, CCN, ION and UDN from Southern Nigeria demonstrated the highest activity against *T.brucei* and *C.fasiculata* **Table 3-2**. The activity against *C.fasiculata* supports the idea that the bees may collect propolis to protect from infection by *Crithidia* species, which are known to be pathogens of bees, and are quite closely related to *T.brucei*. The extracts were active against both the standard strain of *T.brucei* and two isolates which displayed a degree of resistance against pentamidine.

Principal components analysis (PCA) of the processed LC-MS data collected demonstrated uniqueness in the chemical composition of four samples collected from

the southern part of Nigeria which were also were highly active against *Trypanosoma brucei* as shown in **Table3-2**.

A dereplication study on the LC-MS data of these samples was performed using partial least squares modelling in order to identify the compounds responsible for high levels of antitrypanosomal activity and this pointed towards denticulatain isomers as being most strongly associated with the anti-trypanosomal activities.

The study proceeded with four active samples collected from three regions in Southern Nigeria in more detail, by using an optimized medium pressure chromatographic technique to fractionate and purify them, and attempt to isolate the component(s) responsible for the activity. Several compounds from different classes including diterpenes, flavonoids, prenylated flavonoids, pterocarpan, phenolics, xanthenes, triterpenes, and fatty acid were isolated and structurally elucidated by 1D-2D NMR and LC-MSⁿ.

HPLC-ELSD-UV was effectively utilized to test purity and to develop method for purification of targeted compounds in crude extracts or fractions from open-column chromatography.

Sample UDN collected from Ugelli/Delta fractionation led to isolation of three isomers of prenylated xanthenes, (1,3,7-trihydroxy-2,8-di-(3-methylbut-2-enyl)xanthone), (1,3,7-trihydroxy-4,8-di-(3-methylbut-2-enyl)xanthone), and previously undescribed xanthone named 1,7-dihydroxy-8(3-methylbut-2-enyl)-3(3-methylbut-2-enyloxy) xanthone. Structures were elucidated by 1D-2D NMR, and LC-MSⁿ, closely related compounds of prenylated xanthenes were isolated before in

propolis from Thai stingless bees collected from mangosteen orchards (Vongsak *et al.*, 2015).

Bioassay tests showed that prenylated xanthenes isolated from UDN sample were more active than crude itself with EC₅₀ ranging from 3.9-14.7 μ M. In addition, the differences in substitution dramatically effect their activity as showed in **Table 7-1**.

Three triterpenes were purified from sample ION collected from Ijebu-Ode/Ogun two cycloartanes, ambonic and mangiferonic acids, and a mixture of α Amyrin with mangiferonic acid as (1:3), their NMR spectra were compared with the literature. All of them demonstrated a moderate inhibitory activity against trypanosomes **Table 7-2** with MIC values of 39.5, 25.5 and 20.9 μ M respectively.

Two samples collected from River state Nigeria in different time, has a different appearance being red in color were investigated in detail and compared to Brazilian propolis which is considered as a golden standard for propolis samples. By comparing fragments produced by LC-MSⁿ Nigerian red propolis was found to be very similar to Brazilian red propolis being rich in isoflavonoids compounds collected mainly from legumes such as *Dalbergia ecastophyllum*. Ten phenolic compounds were purified, One isoflavanone, Calycosin (**1**); two flavanones, liquiritigenin (**2**) and pinocembrin (**3**); an isoflavan, vestitol (**4**); a pterocarpan, medicarpin (**5**); two prenylflavanones, 6-prenylnaringenin(**7**) and 8-prenylnaringenin (**8**) ; and two geranyl flavonoids, propolin D (**9**) and macarangin (**10**). The tenth component was characterized as a previously undescribed dihydrobenzofuran 3-(2-hydroxy-4-methoxybenzyl)-6-methoxy-2,3-dihydrobenzofuran (**6**) named Rivernol for simplicity. Other eighteen compounds were structurally elucidated by LC-MSⁿ.

The isolated compounds were tested against *Trypanosoma brucei* and displayed moderate to high activity **Table 5-2, Table 5-3**. Some of the compounds tested had similar activity against wild type *T. brucei* and two strains displaying pentamidine resistance. Within the series of compounds isolated there is a strong indication that the more lipophilic compounds such as medicarpin which only has one hydroxyl group, or propolin D which has a lipophilic geranyl group are the more active anti-trypanosomal compounds. Quite small alterations in structure appear to produce a marked difference in anti-trypanosomal activity with 8-prenyl naringenin being more active than its isomer 6-prenyl naringenin.

The sample collected from Kwa Zulu Natal, South Africa demonstrated a strong antitrypanosomal activity and profiling revealed that it contained mainly flavonols and diterpenic acids, two of which as acetylimbricatolic acid and (-)-pimara-8(14), 15-dien-19-oic acid and one flavonol pinocembrin purified but were less active than crude itself with MIC values ranging from 41.4-137.3 μM .

In conclusion, the proposed HPLC method, based on the use of UV, ELSD and MS and, MS/MS data, allowed the identification of multiple compounds, including phenolic acids and flavonoids, in ethanolic extracts of propolis, and helped in the development methods for isolation of target compounds to be transferred to MPLC. These methods have to be validated in agreement with ICH guidelines for comprehensive multi-component analysis of propolis samples.

CHAPTER EIGHT

CONCLUSION AND FUTURE WORK

8 CONCLUSION AND FUTURE WORK

Overall, this work proved the variability in propolis composition and biological activity even when collected from same area. It has revealed new propolis constituents which possess biological activity and has confirmed the presence of some interesting compounds which could be employed as lead compounds for new drug discovery. The major work remaining on the Nigerian propolis samples would be to isolate the denticulatain isomers which appear to be responsible for the highest anti-trypanosomal activity.

It is essential for biologically active compounds to demonstrate their mode of action or interaction with identified or target pathways in the body or cell. These new demands for bioactivity imposed new approaches and strategies like metabolomics to be employed in modern drug discovery programs.

The active compounds must show selective cytotoxicity to diseased cells or microorganisms only while not affecting normal cells therefore cytotoxicity tests should be performed to test selectivity in order to improve safety and reduce the side effects.

Since there is a shortage of literature available on the study of African propolis, the use of statistical tools for clustering the data from LC-MS is useful and could be used to profile the different types of African propolis, and to make a library for matching samples. Other techniques such as LC-MS(n) could be included in future work as an aid for structure elucidation and dereplication of new target compounds.

There are many more exciting samples in Africa which could be isolated, characterised and tested and this research will certainly be continued.

9 References

- Abd El Hady, F. K., & Hegazi, A. G. (2002). Egyptian propolis: 2. Chemical composition, antiviral and antimicrobial activities of East Nile Delta propolis. *Zeitschrift Fur Naturforschung - Section C Journal of Biosciences*, 57(3–4), 386–394.
- Abu-Mellal, A., Koolaji, N., Duke, R. K., Tran, V. H., & Duke, C. C. (2012). Prenylated cinnamate and stilbenes from Kangaroo Island propolis and their antioxidant activity. *Phytochemistry*, 77, 251–259.
- Alcolea, P. J., Alonso, A., Garcí'a -Tabares, F., Torano, A., & Larraga, V. (2014). An insight into the proteome of *Crithidia fasciculata* choanomastigotes as a comparative approach to axenic growth, peanut lectin agglutination and differentiation of *Leishmania* spp. promastigotes. *PLoS ONE*, 9(12), 1–26.
- Al-Massarani, S. M., El Gamal, A. A., Al-Musayeib, N. M., Mothana, R. A., Basudan, O. A., Al-Rehaily, A. J., Maes, L. (2013). Phytochemical, antimicrobial and antiprotozoal evaluation of *Garcinia Mangostana* pericarp and α -mangostin, its major xanthone derivative. *Molecules*, 18(9), 10599–10608.
- Almutairi, S., Eapen, B., Chundi, S. M., Akhalil, A., Siheri, W., Clements, C., Edrada-Ebel, R. (2014). New anti-trypanosomal active prenylated compounds from African propolis. *Phytochemistry Letters*, 10(1), 35–39.

- Almutairi, S., Edrada-Ebel, R., Fearnley, J., Igoli, J. O., Alotaibi, W., Clements, C. J., Watson, D. G. (2014). Isolation of diterpenes and flavonoids from a new type of propolis from Saudi Arabia. *Phytochemistry Letters*, 10(December), 160–163.
- Alqarni, A. S., Rushdi, A. I., Owayss, A. a., Raweh, H. S., El-Mubarak, A. H., & Simoneit, B. R. T. (2015). Organic Tracers from Asphalt in Propolis Produced by Urban Honey Bees, *Apis mellifera* Linn. *Plos One*, 10(6), e0128311.
- Araújo, A. S., da Rocha, L. L., Tomazela, D. M., Sawaya, A. C. H. F., Almeida, R. R., Catharino, R. R., & Eberlin, M. N. (2005). Electrospray ionization mass spectrometry fingerprinting of beer. *The Analyst*, 130(6), 884–889.
- Arias, M. C., & Sheppard, W. S. (2005). Phylogenetic relationships of honey bees (Hymenoptera:Apinae:Apini) inferred from nuclear and mitochondrial DNA sequence data. *Molecular Phylogenetics and Evolution*, 37(1), 25–35.
- Assegid, G., & Lamprecht, I. (1997). Microcalorimetric investigations on the influence of propolis on the bacterium *micrococcus luteus*. *Thermochimica Acta*, 290(2), 155–166.
- Awale, S., Shrestha, S. P., Tezuka, Y., Ueda, J. Y., Matsushige, K., & Kadota, S. (2005). Neoflavonoids and related constituents from Nepalese propolis and their nitric oxide production inhibitory activity. *Journal of Natural Products*, 68(6), 858–864.
- Bacchi, C. J. (1993). Resistance to clinical drugs in African trypanosomes. *Parasitology Today*, 9(5), 190–193.

Bacchi, J., Lambros, C., Goldberg, B., Hutner, S. H., & de Carvalho, G. D. (1974). Susceptibility of an insect *Leptomonas* and *Crithidia fasciculata* to several established antitrypanosomatid agents. *Antimicrobial Agents and Chemotherapy*, 6(6), 785–790.

Bagag, a, Giuliani, a, & Laprévote, O. (2008). Atmospheric pressure photoionization mass spectrometry of oligodeoxyribonucleotides. *European Journal of Mass Spectrometry* (Chichester, England), 14(2), 71–80.

Baker, N., Glover, L., Munday, J. C., Aguinaga Andres, D., Barrett, M. P., de Koning, H. P., & Horn, D. (2012). Aquaglyceroporin 2 controls susceptibility to melarsoprol and pentamidine in African trypanosomes. *Proceedings of the National Academy of Sciences*, 109(27), 10996–11001.

Bankova, V. (2005). Recent trends and important developments in propolis research. *Evidence-Based Complementary and Alternative Medicine : eCAM*, 2(1), 29–32.

Bankova, V., Christov, R., Kujungiev, A., Marcucci, M. C., & Popov, S. (1995). Chemical composition and antibacterial activity of Brazilian propolis. *Zeitschrift Fur Naturforschung. Teil C: Biochemie, Biophysik, Biologie, Virologie*, 50(3–4), 167–172.

Bankova, V., Marcucci, M. C., Simova, S., Nikolova, N., Kujungiev, a., & Popov, S. (1996). Antibacterial diterpenic acids from Brazilian propolis. *Zeitschrift Fur Naturforschung Section C - Journal of Biosciences*, 51(5–6), 7–10.

- Bankova, V., Popova, M., Bogdanov, S., & Sabatini, A.-G. (2002). Chemical Composition of European Propolis: Expected and Unexpected Results. *Zeitschrift Für Naturforschung C*, 57(5–6).
- Bankova, V. S., De Castro, S. L., & Marcucci, M. C. (2000). Propolis: recent advances in chemistry and plant origin. *Apidologie*, 31, 3–15.
- Banskota, A. H., Tezuka, Y., Prasain, J. K., Matsushige, K., Saiki, I., & Kadota, S. (1998). Chemical constituents of Brazilian propolis and their cytotoxic activities. *Journal of Natural Products*, 61(7), 896–900.
- Banskota, a H., Tezuka, Y., Adnyana, I. K., Ishii, E., Midorikawa, K., Matsushige, K., & Kadota, S. (2001). Hepatoprotective and anti-Helicobacter pylori activities of constituents from Brazilian propolis. *Phytomedicine: International Journal of Phytotherapy and Phytopharmacology*, 8(1), 16–23.
- Barrett, M. P., Boykin, D. W., Brun, R., & Tidwell, R. R. (2007). Human African trypanosomiasis: pharmacological re-engagement with a neglected disease. *British Journal of Pharmacology*, 152(8), 1155–1171.
- Barrett, M. P., Burchmore, R. J. S., Stich, A., Lazzari, J. O., Frasch, A. C., Cazzulo, J. J., & Krishna, S. (2003). The trypanosomiasis. *Lancet*, 362(9394), 1469–1480.
- Beutler, J. A., Shoemaker, R. H., Johnson, T., & Boyd, M. R. (1998). Cytotoxic geranyl stilbenes from *Macaranga schweinfurthii*. *Journal of Natural Products*, 61(12), 1509–1512.
- Braithwaite A & Smith FJ. (1996). *Chromatographic methods*. (5th edition).

Breitmaier, E. (2002). *Structure Elucidation By NMR In Organic Chemistry: A Practical Guide*. (8 edition).

Bridges, D. J., Gould, M. K., Nerima, B., Mäser, P., Burchmore, R. J. S., & de Koning, H. P. (2007). Loss of the high-affinity pentamidine transporter is responsible for high levels of cross-resistance between arsenical and diamidine drugs in African trypanosomes. *Molecular Pharmacology*, 71(4), 1098–1108.

Bro, R., & Smilde, A. K. (2014). Principal component analysis. *Analytical Methods*, 6(9), 2812.

Burdock, G. a. (1998). Review of the biological properties and toxicity of bee propolis. *Food and Chemical Toxicology: An International Journal Published for the British Industrial Biological Research Association*, 36(4), 347–63.

Cantarelli, M. Á., Camiña, J. M., Pettenati, E. M., Marchevsky, E. J., & Pellerano, R. G. (2011). Trace mineral content of Argentinean raw propolis by neutron activation analysis (NAA): Assessment of geographical provenance by chemometrics. *LWT - Food Science and Technology*, 44(1), 256–260.

Castaldo, S., & Capasso, F. (2002). Propolis, an old remedy used in modern medicine. *Fitoterapia*, 73 Suppl 1, S1-6.

Chen, C.-N., Weng, M.-S., Wu, C.-L., & Lin, J.-K. (2004). Comparison of Radical Scavenging Activity, Cytotoxic Effects and Apoptosis Induction in Human Melanoma Cells by Taiwanese Propolis from Different Sources. *Evidence-Based Complementary and Alternative Medicine : eCAM*, 1(2), 175–185.

Claridge TDW. (2006). *High-resolution NMR techniques in organic chemistry*. (Second edition). Netherlands.

Coggshall, W. and Morse, S.A. (1984). *Beewax: production, harvesting, processing, and product*. Wicwas press, Ithaca. NY .USA.

Conte, J. E., Upton, R. a, & Lin, E. T. (1987). Pentamidine pharmacokinetics in patients with AIDS with impaired renal function. *The Journal of Infectious Diseases*, 156(6), 885–90.

Coustou, V., Besteiro, S., Rivière, L., Biran, M., Biteau, N., Franconi, J.-M., Bringaud, F. (2005). A mitochondrial NADH-dependent fumarate reductase involved in the production of succinate excreted by procyclic *Trypanosoma brucei*. *The Journal of Biological Chemistry*, 280(17), 16559–70.

Crane, E. (1988). *Beekeeping: Science, Practice and World Resources*. London: Heinemann.

Cross, G. A. M. (1978). Antigenic variation in trypanosomes. *proc.R.Soc.Lond*, 202(B), 55–72.

Cruz-Vega, D., Verde-Star, M. J., Salinas-Gonzalez, N. R., Rosales-Hernandez, B., Estrada-Garcia, I., Mendez-Aragon, P., Castro-Garza, J. (2009). Review of pharmacological effects of *Glycyrrhiza radix* and its bioactive compounds. *Zhongguo Zhong Yao Za Zhi = Zhongguo Zhongyao Zazhi = China Journal of Chinese Materia Medica*, 22(April 2008), 557–559.

Cunha, I. B. D. S., Salomão, K., Shimizu, M., Bankova, V. S., Custódio, A. R., Astro, L. D. C., Arcucci, M. (2004). Antitrypanosomal Activity of Brazilian Propolis from *Apis mellifera*. *Pharmaceutical Society of Japan*, 52(5), 602–604.

Da Silva, F. C., Favaro-trindade, C. S., De Alencar, S. M., Thomazini, M., & Balieiro, J. C. C. (2011). Physicochemical properties , antioxidant activity and stability of spray-dried propolis. *Journal of Apiprodukt and Apimedical Science*, 3(2), 94–100.

Dang, N. H., Zhang, X., Zheng, M., Son, K. H., Chang, H. W., Kim, H. P., Kang, S. S. (2005). Inhibitory constituents against cyclooxygenases from *Aralia cordata* Thunb. *Archives of Pharmacal Research*, 28(1), 28–33.

de Campos, R. O., Paulino, N., da Silva, C. H., Scremin, A., & Calixto, J. B. (1998). Anti-hyperalgesic effect of an ethanolic extract of propolis in mice and rats. *J Pharm Pharmacol*, 50(10), 1187–1193.

de Koning, H. P. (2008). Ever-increasing complexities of diamidine and arsenical crossresistance in African trypanosomes. *Trends in Parasitology*, 24(8), 345–349.

de Koning, H. P., & Jarvis, S. M. (2001). Uptake of pentamidine in *Trypanosoma brucei brucei* is mediated by the P2 adenosine transporter and at least one novel, unrelated transporter. *Acta Tropica*, 80(3), 245–250.

Delespaux, V., & de Koning, H. P. (2007). Drugs and drug resistance in African trypanosomiasis. *Drug Resistance Updates*, 10(1–2), 30–50.

Dharmaratne, H. R. W., Sotheeswaran, S., Balasubramaniam, S., & Reisch, J. (1986). Xanthenes from roots of three calophyllum species. *Phytochemistry*, 25(8), 1957–1959.

Du, X., Bai, Y., Liang, H., Wang, Z., Zhao, Y., Zhang, Q., & Huang, L. (2006). Solvent effect in ¹H NMR spectra of 3'-hydroxy-4'-methoxy isoflavonoids from *Astragalus membranaceus* var. *mongholicus*. *Magnetic Resonance in Chemistry: MRC*, 44(7), 708–12.

Dutra, R. P., De Barros Abreu, B. V., Cunha, M. S., Batista, M. C. A., Torres, L. M. B., Nascimento, F. R. F., Guerra, R. N. M. (2014). Phenolic acids, hydrolyzable tannins, and antioxidant activity of geopropolis from the stingless bee *Melipona fasciculata* Smith. *Journal of Agricultural and Food Chemistry*, 62, 2549–2557.

Fairlamb, A. H. (2003). Chemotherapy of human African trypanosomiasis: Current and future prospects. *Trends in Parasitology*, 19(11), 488–494.

Fairlamb, A. H., Henderson, G. B., Bacchi, C. J., & Cerami, A. (1987). In vivo effects of difluoromethylornithine on trypanothione and polyamine levels in bloodstream forms of *Trypanosoma brucei*. *Molecular and Biochemical Parasitology*, 24(2), 185–191.

Falcão, S. I., Vale, N., Cos, P., Gomes, P., Freire, C., Maes, L., & Vilas-Boas, M. (2014). In vitro evaluation of Portuguese propolis and floral sources for antiprotozoal, antibacterial and antifungal activity. *Phytotherapy Research*, 28(3), 437–443.

- Fang, Jim-Min, Hsu, K., & Cheng, Y. (1989). terpenoids leaves of calocedrus. *Phytochemrstry*, Vol 28(4), 1173–1175.
- Friebolin, H. (2011). *Basic One- and Two-dimensional NMR Spectroscopy* (5th ed.).
- Gavaghan, C. L., Wilson, I. D., & Nicholson, J. K. (2002). Physiological variation in metabolic phenotyping and functional genomic studies: Use of orthogonal signal correction and PLS-DA. *FEBS Letters*, 530(1–3), 191–196.
- Ghaly, M. F., Ezzat, S. M., & Sarhan, M. M. (1998). Use of propolis and ultrariseofulvin to inhibit aflatoxigenic fungi. *Folia Microbiologica*, 43(2), 156–60.
- González, M., Gómez, M. I., Tereschuk, M. L., & Molina, A. (2009). Thermal stability of propolis from Tucumán, Argentina. *Journal of Apicultural Research*, 48(4), 270–278.
- Greenaway, W., May, J., Scaysbrook, T., & Whatley, F. R. (1991). Identification by Gas Chromatography-Mass Spectrometry of 150 Compounds in Propolis. *Z. Naturforsch.*, 46c, 111–121.
- Gressler, L. T., Da Silva, A. S., Machado, G., Dalla Rosa, L., Dorneles, F., Gressler, L. T.,Monteiro, S. G. (2012). Susceptibility of Trypanosoma evansi to propolis extract in vitro and in experimentally infected rats. *Research in Veterinary Science*, 93(3), 1314–7.
- Grunberger, D., Banerjee, R., Eisinger, K., Oltz, E. M., Efros, L., Caldwell, M., Nakanishi, K. (1988). Preferential cytotoxicity on tumor cells by caffeic acid phenethyl ester isolated from propolis. *Experientia*, 44(3), 230–232.

Haberkorn, A., Harder, A., & Greif, G. (2001). Milestones of protozoan research at Bayer. *Parasitology Research*, 1060–1062.

Han H-Y, Wang X-H, Wang N-L, Ling M-T, Wong Y-C, Y. X.-S. (2008). Lignans Isolated from *Campylotropis hirtella* (Franch .) Schindl . Decreased Prostate Specific. *Journal of agricultural and food chemistry*, 6928–6935.

Hans jorg Part, S. P. (2011). *Industrial Scale Natural Products Extraction* (1st ed.). Wiley.

Hashimoto, T., Aga, H., Tabuchi, A., Shibuya, T., Chaen, H., Fukuda, S., & Kurimoto, M. (1998). Anti-*Helicobacter pylori* compounds in Brazilian propolis. *生藥學雜誌*, 52(6), 518–520.

Havsteen B. (1983). Flavonoids, a class of natural products of high pharmacological potency. *Biochemical Pharmacology*, 32(7), 1141–1148.

Hawking, F. (1940). Concentration of Bayer 205 (Germanin) in Human Blood and Cerebrospinal Fluid After Treatment. *Transaction of the Royal Society of Tropical Medicine and Hygiene*, 34(1), 37–52.

Heby, O., Persson, L., & Rentala, M. (2007). Targeting the polyamine biosynthetic enzymes: a promising approach to therapy of African sleeping sickness, Chagas' disease, and leishmaniasis. *Amino Acids*, 33(2), 359–366.

Heftmann, E. (1992). Chromatography: Fundamentals and application of chromatography and related differential migration methods. (5th ed.). *Journal of Chromatography Library*; 51A and 51B. Elsevier.

Hegazi, A. G. (1978). Propolis an overview.

Hernández, I. M., Fernandez, M. C., Cuesta-Rubio, O., Piccinelli, A. L., & Rastrelli, L. (2005). Polyprenylated benzophenone derivatives from Cuban propolis. *Journal of Natural Products*, 68(6), 931–4.

Hnawia, E., Thoison, O., Guéritte-Voegelein, F., Bourret, D., & Sévenet, T. (1990). A geranyl substituted flavonol from *Macaranga vedeliana*. *Phytochemistry*, 29(7), 2367–2368.

Hoet, S., Pieters, L., Muccioli, G. G., Habib-Jiwan, J. L., Opperdoes, F. R., & Quetin-Leclercq, J. (2007). Antitrypanosomal activity of triterpenoids and sterols from the leaves of *Strychnos spinosa* and related compounds. *Journal of Natural Products*, 70(8), 1360–1363.

Hostettmann K. and Terreaux C. (1996). Medium-Pressure Liquid chromatography pp. 3296–3303.

Hou, A., Fukai, T., Shimazaki, M., Sakagami, H., Sun, H., & Nomura, T. (2001). Benzophenones and Xanthenes with Isoprenoid Groups from *Cudrania*. *Journal of natural product*, 65–70.

Hu, Q., Noll, R. J., Li, H., Makarov, A., Hardman, M., & Graham Cooks, R. (2005). The Orbitrap: a new mass spectrometer. *Journal of Mass Spectrometry*, 40(4), 430–443.

Huang, S., Zhang, C.-P., Wang, K., Li, G., & Hu, F.-L. (2014). Recent Advances in the Chemical Composition of Propolis. *Molecules*, 19, 19610–19632.

Hübschmann, H. J. (2008). *Handbook of GC/MS: Fundamentals and Applications*, (3), 1–719.

Hughes, R. J., Croley, T. R., Metcalfe, C. D., & March, R. E. (2001). A tandem mass spectrometric study of selected characteristic flavonoids. *International Journal of Mass Spectrometry*, 210–211, 371–385.

Ito, J., Chang, F. R., Wang, H. K., Park, Y. K., Ikegaki, M., Kilgore, N., & Lee, K. H. (2001). Anti-AIDS agents. 48.(1) Anti-HIV activity of moronic acid derivatives and the new melliferone-related triterpenoid isolated from Brazilian propolis. *Journal of Natural Products*, 64(10), 1278–81.

Jefferies, P. R. (1978). Constituents of propolis. *Specialia*, 30(1973), 157–158.

Jung J. H., Patarapanich, C., Pummangura, S., & Chaichantipyuth, C. (1990). bioactive constituents. *Phytochemistry*, 29(5), 1667–1670.

Kardar, M. N., Zhang, T., Coxon, G. D., Watson, D. G., Fearnley, J., & Seidel, V. (2014). Characterisation of triterpenes and new phenolic lipids in Cameroonian propolis. *Phytochemistry*, 106, 156–63.

Kasote, D., Suleman, T., Chen, W., Sandasi, M., Viljoen, A., & Van Vuuren, S. (2014). Chemical profiling and chemometric analysis of South African propolis. *Biochemical Systematics and Ecology*, 55, 156–163.

Katajamaa, M., & Orešič, M. (2005). Processing methods for differential analysis of LC/MS profile data. *BMC Bioinformatics*, 6, 179.

Krell, R. (1996). *Value-added products from beekeeping*. FAO Agricultural Services Bulletin 4 Food and Agriculture Organization of the United Nations, (12th ed.). Rome.

Krol, W., Scheller, S., Czuba, Z., Matsuno, T., Zydowicz, G., Shani, J., & Mos, M. (1996). Inhibition of neutrophils' chemiluminescence by ethanol extract of propolis (EEP) and its phenolic components. *Journal of Ethnopharmacology*, 55(1), 19–25.

Kujungiev A., Tsvetkova, I., Serkedjieva, Y., Bankova, V., R.Christov, & Popov, S. (1999). Antibacterial, antifungal and antiviral activity of propolis of different geographic origin. *J Ethnopharmacol*, 64(64), 235–240.

Kumazawa, S., Hamasaka, T., & Nakayama, T. (2004). Antioxidant activity of propolis of various geographic origins. *Food Chemistry*, 84(3), 329–339.

Kumazawa, S., Ueda, R., Hamasaka, T., Fukumoto, S., Fujimoto, T., & Nakayama, T. (2007). Antioxidant prenylated flavonoids from propolis collected in Okinawa, Japan. *Journal of Agricultural and Food Chemistry*, 55(19), 7722–5.

Li, F., Awale, S., Tezuka, Y., & Kadota, S. (2008). Cytotoxic constituents from Brazilian red propolis and their structure-activity relationship. *Bioorganic and Medicinal Chemistry*, 16(10), 5434–5440.

Li, F., Awale, S., Zhang, H., Tezuka, Y., Esumi, H., & Kadota, S. (2009). Chemical constituents of propolis from Myanmar and their preferential cytotoxicity against a human pancreatic cancer cell line. *Journal of Natural Products*, 72(7), 1283–7.

Lloyd S., Joseph K., J. D. (2010). *Introduction to modern liquid chromatography*, (Third edition).

Loibner H & Seidl G. (1997). A low-cost medium pressure liquid chromatography for preparative system. *Chromatographia*, 12(9), 600–604.

Ma, C., Li, G., Zhang, D., Liu, K., & Fan, X. (2005). One step isolation and purification of liquiritigenin and isoliquiritigenin from *Glycyrrhiza uralensis* Risch. using high-speed counter-current chromatography. *Journal of Chromatography A*, 1078(1–2), 188–192.

Makarov, A., Denisov, E., Lange, O., & Horning, S. (2006). Dynamic Range of Mass Accuracy in LTQ Orbitrap Hybrid Mass Spectrometer. *Journal of the American Society for Mass Spectrometry*, 17(7), 977–982.

Marcucci, M. (1995). Propolis: chemical composition, biological properties and therapeutic activity. *Apidologie*, 26(2), 83–99.

Martos, I., Cossentini, M., Ferreres, F., & Tomasbarberan, F. a. (1997). Flavonoid composition of Tunisian honeys and propolis. *Journal of Agricultural and Food Chemistry*, 45(8), 2824–2829.

Matsuno, T. (1995). A new clerodane diterpenoid isolated from propolis. *Zeitschrift Fur Naturforschung - Section C Journal of Biosciences*, 50(1–2), 93–97.

Mcintosh, H., Olliaro, P., Mcintosh, H., & Olliaro, P. (2010). Artemisinin derivatives for treating severe malaria (Review) Artemisinin derivatives for treating severe malaria, (2).

Milena P. Popovaa, Vassya S. Bankovaa, Stefan Bogdanovb, Iva Tsvetkovac, Christo Naydenskic, Gian Luigi Marcazzand, A.-G. S. (2007). Original article Chemical characteristics of poplar type propolis of different geographic origin. *pidologie*, 38, 306–311.

Mirzoeva, O. K., & Calder, P. C. (1996). The effect of propolis and its components on eicosanoid production during the inflammatory response. *Prostaglandins Leukotrienes and Essential Fatty Acids*, 55(6), 441–449.

Mirzoeva, O. K., Grishanin, R. N., & Calder, P. C. (1997). Antimicrobial action of propolis and some of its components: the effects on growth, membrane potential and motility of bacteria. *Microbiological Research*, 152(3), 239–46.

Nakahara, K., Roy, M. K., Ono, H., Maeda, I., Ohnishi-Kameyama, M., Yoshida, M., & Trakoontivakorn, G. (2003). Prenylated Flavanones Isolated from Flowers of *Azadirachta indica* (the Neem Tree) as Antimutagenic Constituents against Heterocyclic Amines. *Journal of Agricultural and Food Chemistry*, 51, 6456–6460.

Negri, G., Marcucci, M. C., Salatino, A., & Salatino, M. L. F. (1998). Hydrocarbons and monoesters of propolis waxes from Brazil. *Apidologie*, 29(4), 305–314.

Nui, S. I., Himamura, Y. S., Asuda, S. M., Hirafuji, K. S., Oli, R. T. M., & Umazawa, S. K. (2012). A New Prenylflavonoid Isolated from Propolis Collected in the Solomon Islands. *Bioscience. Biotechnology. Biochemistry*, 76(5), 1038–1040.

Paulino, N., Dantas, A. P., Bankova, V., Longhi, D. T., Scremin, A., de Castro, S. L., & Calixto, J. B. (2003). Bulgarian propolis induces analgesic and anti-inflammatory

effects in mice and inhibits in vitro contraction of airway smooth muscle. *Journal of Pharmacological Sciences*, 93(3), 307–313.

Pépin, J., & Milord, F. (1994). The treatment of human African trypanosomiasis. *In Advances in parasitology* (Vol. 33, pp. 1–47).

Petrova, A., Popova, M., Kuzmanova, C., Tsvetkova, I., Naydenski, H., Muli, E., & Bankova, V. (2010). New biologically active compounds from Kenyan propolis. *Fitoterapia*, 81(6), 509–14.

Phillips, M. A., Coffino, P., & Wang, C. C. (1987). Cloning and sequencing of the ornithine decarboxylase gene from *Trypanosoma brucei*. Implications for enzyme turnover and selective difluoromethylornithine inhibition. *Journal of Biological Chemistry*, 262(18), 8721–8727.

Piccinelli, A. L., Lotti, C., Campone, L., Cuesta-Rubio, O., Campo Fernandez, M., & Rastrelli, L. (2011). Cuban and Brazilian red propolis: botanical origin and comparative analysis by high-performance liquid chromatography-photodiode array detection/electrospray ionization tandem mass spectrometry. *Journal of Agricultural and Food Chemistry*, 59(12), 6484–91.

Piccinelli AL, Campo Fernandez M, Cuesta-Rubio O, Marquez Hernandez I, De Simone F, R. L. (2005). Isoflavonoids Isolated from Cuban Propolis. *Journal of Agricultural and Food Chemistry*, 9010–9016.

Pietta, P. G., Gardana, C., & Pietta, a M. (2002). Analytical methods for quality control of propolis. *Fitoterapia*, 73 Suppl 1, S7-20.

Pluskal, T., Castillo, S., Villar-Briones, A., & Oresic, M. (2010). MZmine 2: modular framework for processing, visualizing, and analyzing mass spectrometry-based molecular profile data. *BMC Bioinformatics*, 11(1), 395.

Popova, M. P., Chinou, I. B., Marekov, I. N., & Bankova, V. S. (2009). Terpenes with antimicrobial activity from Cretan propolis. *Phytochemistry*, 70(10), 1262–1271.

Popova, M. P., Graikou, K., Chinou, I., & Bankova, V. S. (2010). GC-MS profiling of diterpene compounds in mediterranean propolis from Greece. *Journal of Agricultural and Food Chemistry*, 58(5), 3167–3176.

Popova, M. P., S.Bankova, V., Bogdanov, S., Tsvetkovac, I., Naydenskic, C., Marcazzand, G. L., & Sabatini, A.-G. (2007). Chemical characteristics of poplar type propolis of different geographic origin. *Apidologie*, 38, 306–311.

Popova M, Bankova V, Naydensky Ch, Tsvetkova I, K. A. (2004). Comparative study of the biological activity of propolis from different geographic origin: a statistical approach. *Macedonian Pharm Bull*, 50, 9–14.

Poulin, R., Lu, L., Ackermann, B., Bey, P., & Pegg, a. E. (1992). Mechanism of the irreversible inactivation of mouse ornithine decarboxylase by alpha difluoromethylornithine. Characterization of sequences at the inhibitor and coenzyme binding sites. *Journal of Biological Chemistry*, 267(1), 150–158.

Priotto, G., Kasparian, S., Mutombo, W., Ngouama, D., Ghorashian, S., Arnold, U., Kande, V. (2009). Nifurtimox-eflornithine combination therapy for second-stage

African Trypanosoma brucei gambiense trypanosomiasis: a multicentre, randomised, phase III, non-inferiority trial. *The Lancet*, 374(9683), 56–64.

Raghukumar, R., Vali, L., Watson, D., Fearnley, J., & Seidel, V. (2010). Antimethicillin-resistant Staphylococcus aureus (MRSA) activity of “pacific propolis” and isolated prenylflavanones. *Phytotherapy Research*, 24(8), 1181–7.

Räz, B., Iten, M., Grether-Bühler, Y., Kaminsky, R., & Brun, R. (1997). The Alamar Blue assay to determine drug sensitivity of African trypanosomes (T.b. rhodesiense and T.b. gambiense) in vitro. *Acta Tropica*, 68(2), 139–47.

Righi, A. a., Alves, T. R., Negri, G., Marques, L. M., Breyer, H., & Salatino, A. (2011). Brazilian red propolis: Unreported substances, antioxidant and antimicrobial activities. *Journal of the Science of Food and Agriculture*, 91(13), 2363–2370.

Rodenko, B., van der Burg, A. M., Wanner, M. J., Kaiser, M., Brun, R., Gould, M., Koomen, G.-J. (2007). 2,N6-Disubstituted Adenosine Analogs with Antitrypanosomal and Antimalarial Activities. *Antimicrob. Agents Chemotherapy*, 51(11), 3796–3802.

Rubio, O. C., Cuellar Cuellar, a, Rojas, N., Castro, H. V, Rastrelli, L., & Aquino, R. (1999). A polyisoprenylated benzophenone from Cuban propolis. *Journal of Natural Products*, 62(7), 1013–5.

Saha, S., Shilpi, J. A., Mondal, H., Hossain, F., Anisuzzman, M., Mahadhi Hasan, M., & Cordell, G. A. (2013). Ethnomedicinal, phytochemical and pharmacological profile of the genus Dalbergia L . (Fabaceae). *Phytopharmacology*, 4(2), 291–346.

Salatino, A., Teixeira, É. W., Negri, G., & Message, D. (2005). Origin and Chemical Variation of Brazilian Propolis. *Evidence-Based Complementary and Alternative Medicine*, 2(1), 33–38.

Saleh, K., Zhang, T., Fearnley, J., & Watson, D. G. (2015). A Comparison of the Constituents of Propolis from Different Regions of the United Kingdom by Liquid Chromatography-high Resolution Mass Spectrometry Using a Metabolomics Approach. *Current Metabolomics*, 3, 42–53.

Salituro, G.M. and Duresne, C. (1998). Isolation by low pressure column chromatography. In Cannell, R.J.P. (Ed). *Natural Products Isolation* (pp. 111–140). Humana Press Inc, Totowa, NJ.

Salomão, K., Dantas, A. P., Borba, C. M., Campos, L. C., Machado, D. G., Aquino Neto, F. R., & De Castro, S. L. (2004). Chemical composition and microbicidal activity of extracts from Brazilian and Bulgarian propolis. *Letters in Applied Microbiology*, 38(2), 87–92.

Salomão Kelly, M., D. S. E., Henriques-Pons, A., & Barbosa, Helene S. De Castro, S. L. (2011). Brazilian green propolis: Effects in vitro and in vivo on *Trypanosoma cruzi*. *Evidence-Based Complementary and Alternative Medicine*, 2011.

Sanpa, S., Popova, M., Bankova, V., Tunkasiri, T., Eitssayeam, S., & Chantawannakul, P. (2015). Antibacterial Compounds from Propolis of *Tetragonula laeviceps* and *Tetrigona melanoleuca* (Hymenoptera: Apidae) from Thailand. *PloS One*, 10(5), e0126886.

Sawaya, a. C. H. F., Palma, a. M., Caetano, F. M., Marcucci, M. C., Da Silva Cunha, I. B., Araujo, C. E. P., & Shimizu, M. T. (2002). Comparative study of in vitro methods used to analyse the activity of propolis extracts with different compositions against species of *Candida*. *Letters in Applied Microbiology*, 35, 203–207.

Schluns, H., Sadd, B. M., Schmid-Hempel, P., & Crozier, R. H. (2010). Infection with the trypanosome *Crithidia bombi* and expression of immune-related genes in the bumblebee *Bombus terrestris*. *Developmental and Comparative Immunology*, 34(7), 705–709.

Scott, A. G., Tait, A., & Turner, C. M. R. (1996). Characterisation of cloned lines of *Trypanosoma brucei* expressing stable resistance to MelCy and suramin. *Acta Tropica*, 60, 251–262.

Seidel, V., Peyfoon, E., Watson, D.G., Fearnley, J. (2008). Comparative study of the antibacterial activity of propolis from different geographical and climatic zones. *Phytotherapy Research*, 22, 1256–1263

Sforcin, J. M., Fernandes, a., Lopes, C. a M., Bankova, V., & Funari, S. R. C. (2000). Seasonal effect on Brazilian propolis antibacterial activity. *Journal of Ethnopharmacology*, 73(1–2), 243–249.

Shapiro, T. a, & Englund, P. T. (1990). Selective cleavage of kinetoplast DNA minicircles promoted by antitrypanosomal drugs. *Proceedings of the National Academy of Sciences of the United States of America*, 87(3), 950–954.

- Siheri, W., Igoli, J. O., Gray, A. I., Nascimento, T. G., Zhang, T., Fearnley, J., Watson, D. G. (2014). The isolation of antiprotozoal compounds from Libyan propolis. *Phytotherapy Research*, 28(12), 1756–1760.
- Silva, M S S; Citó, A M G L; Chaves, M H; Lopes, J. A. D. (2005). Triterpenóides tipo cicloartano de própolis de Teresina - PI. *Química Nova*, 28(5), 801–804.
- Silva, B. B., Rosalen, P. L., Cury, J. a, Ikegaki, M., Souza, V. C., Esteves, A., & Alencar, S. M. (2008). Chemical composition and botanical origin of red propolis, a new type of brazilian propolis. *Evidence-Based Complementary and Alternative Medicine : eCAM*, 5(3), 313–6.
- Silva, M. S. S., De Lima, S. G., Oliveira, E. H., Lopes, J. a D., Chaves, M. H., Reis, F. a M., & Citó, a. M. G. L. (2008). Anacardic acid derivatives from brazilian propolis and their antibacterial activity. *Eletica Quimica*, 33(3), 53–58.
- Simpson, L. (1986). Kinetoplast DNA in trypanosomid flagellates. *International Review of Cytology*.
- Smyth J.D. (1994). *Introduction to animal parasitology* (The third edition).
- Stevens, J. A. N. F., Ivancic, M., Hsu, V. L., & Deinzer, M. A. X. L. (1997). prenylflavonoids from humulus lupulus. *Phytochemistry*, 44(8), 3–6.
- Stoyanova, R., & Brown, T. R. (2001). NMR spectral quantitation by principal component analysis. *NMR in Biomedicine*, 14, 271–277.
- Sundar, S. (2001). Drug resistance in Indian visceral leishmaniasis. *Tropical Medicine and International Health*, 6(11), 849–854.

Surveillance, C. D., & Malaria, R. B. (2004). Using Climate to Predict Infectious Disease Outbreaks : A Review. English, 1–55.

Toit, K. Du, Buthelezi, S., & Bodenstein, J. (2009). Anti-inflammatory and antibacterial profiles of selected compounds found in South African propolis. *South African Journal of Science* ,470–472.

Toreti, V. C., Sato, H. H., Pastore, G. M., & Park, Y. K. (2013). Recent progress of propolis for its biological and chemical compositions and its botanical origin. *Evidence-Based Complementary and Alternative Medicine*, 2013.

Tosi, B., Donini, A., Romagnoli, C., & Bruni, A. (1996). Antimicrobial activity of some commercial extracts of propolis prepared with different solvents. *Phytotherapy Research*, 10(4), 335–336.

Uksamrarn, S. S., Omutiban, O. K., Atananukul, P. R., Himnoi, N. C., Artpornmatulee, N. L., & Uksamrarn, A. S. (2006). Cytotoxic Prenylated Xanthenes from the Young Fruit of *Garcinia mangostana*. *Chem. Pharm. Bull*, 54(March).

Valcic, S., Montenegro, G., Mujica, a M., Avila, G., Franzblau, S., Singh, M. P., Timmermann, B. N. (1999). Phytochemical, morphological, and biological investigations of propolis from Central Chile. *Zeitschrift Für Naturforschung. C, Journal of Biosciences*, 54(5–6), 406–16.

Vansterkenburg, E. L. M., Coppens, I., Wilting, J., Bos, O. J. M., Fischer, M. J. E., Janssen, L. H. M., & Opperdoes, F. R. (1993). The uptake of the trypanocidal drug

suramin in combination with low-density lipoproteins by *Trypanosoma brucei* and its possible mode of action. *Acta Tropica*, 54(3–4), 237–250.

Velikova, M., Bankova, V., Sorkun, K., Houcine, S., Tsvetkova, I., & Kujumgiev, A. (2000). Propolis from the Mediterranean region: chemical composition and antimicrobial activity. *Z Naturforsch [C]*, 55(9–10), 790–793.

Vickerman, K. (1985). Developmental cycles and biology of pathogenic trypanosomes. *British Medical Bulletin*, 41(2), 105–114.

Vongsak, B., Kongkiatpaiboon, S., Jaisamut, S., Machana, S., & Pattarapanich, C. (2015). In vitro alpha glucosidase inhibition and free-radical scavenging activity of propolis from Thai stingless bees in mangosteen orchard. *Brazilian Journal of Pharmacognosy*.

Wallace, L. J. M., Candlish, D., & De Koning, H. P. (2002). Different Substrate Recognition Motifs of Human and Trypanosome Nucleobase Transporters: SELECTIVE UPTAKE OF PURINE ANTIMETABOLITES. *Journal of Biological Chemistry*, 277(29), 26149–26156.

Watson, J.T. & Sparkman, O. D. (2007). *Introduction of Mass Spectrometry: Instrumentation, Applications and Strategies for Data Interpretation*. (4th Eds). John Wiley & Sons Ltd,.

Wilawan mahabusarakam, P. W. (1987). Chemical constituents of garcznza mangostana. *Journal of Natural Products*, 50(3), 474–478.

Wollenweber, E., & Buchmann, S. L. (1997). Feral honey bees in the Sonoran Desert: Propolis sources other than Poplars (*Populus* spp.). *Zeitschrift Für Naturforschung. C, Journal of Biosciences*, 52c, 530–535.

Word, K. (1993). phytochemical evidence for the botanical origin of tropical propolis from venezuela, *Phytochemistry* 34(1), 191–196.

WHO. 2016. Trypanosomiasis, human African sleeping sickness, Factsheet 259 [Online]. [Accessed 15-2-2016].

Yang, D.-S., Li, Z.-L., Wang, X., Yan, H., Yang, Y.-P., Luo, H.-R., Li, X.-L. (2015). Denticulatains A and B: unique stilbene–diterpene heterodimers from *Macaranga denticulata*. *RSC Adv.*, 5(18), 13886–13890.

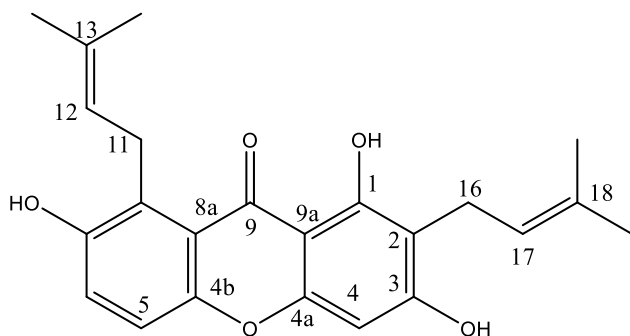
Yang, H., Figueroa, M., To, S., Baggett, S., Jiang, B., Basile, M. J., Kennelly, E. J. (2010). Benzophenones and biflavonoids from *garcinia livingstonei* fruits. *Journal of Agricultural and Food Chemistry*, 58(8), 4749–4755.

Yuliar, Manjang, Y., Ibrahim, S., & Achmad, S. A. (2013). Phenolic Constituents from the Tree Barks of *Garcinia cf cymosa* and their Antibacterial Activities. *Malaysian Journal of Fundamental and Applied Sciences*, 9(3), 115–118.

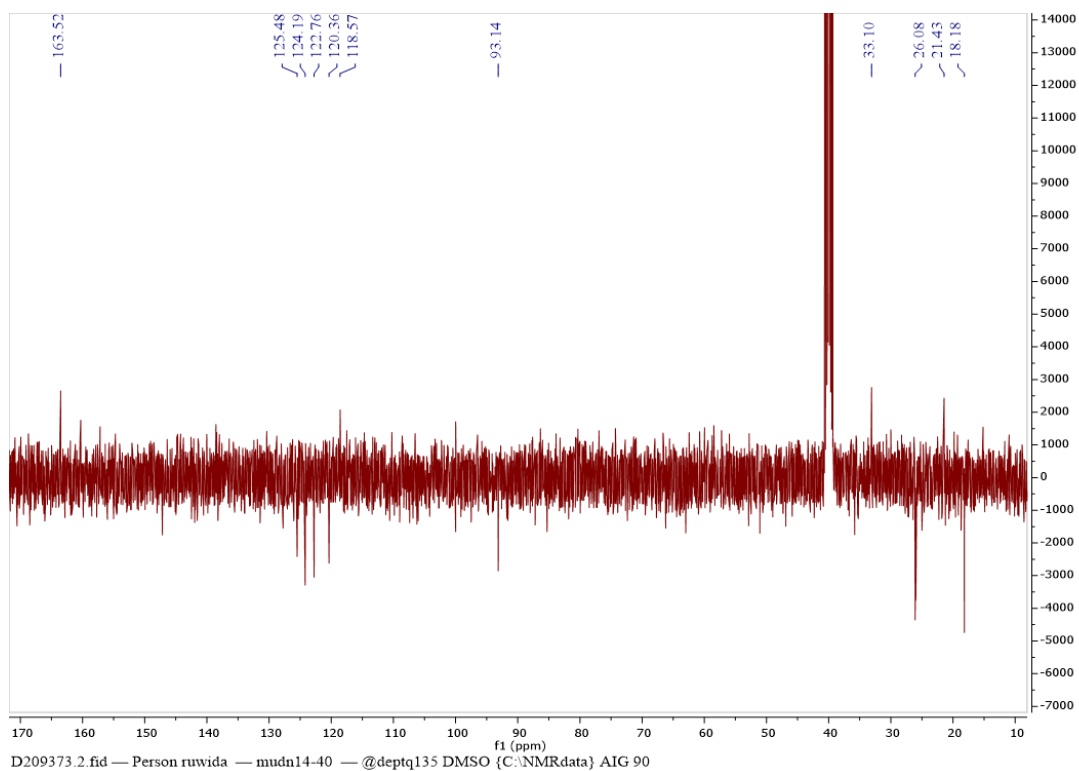
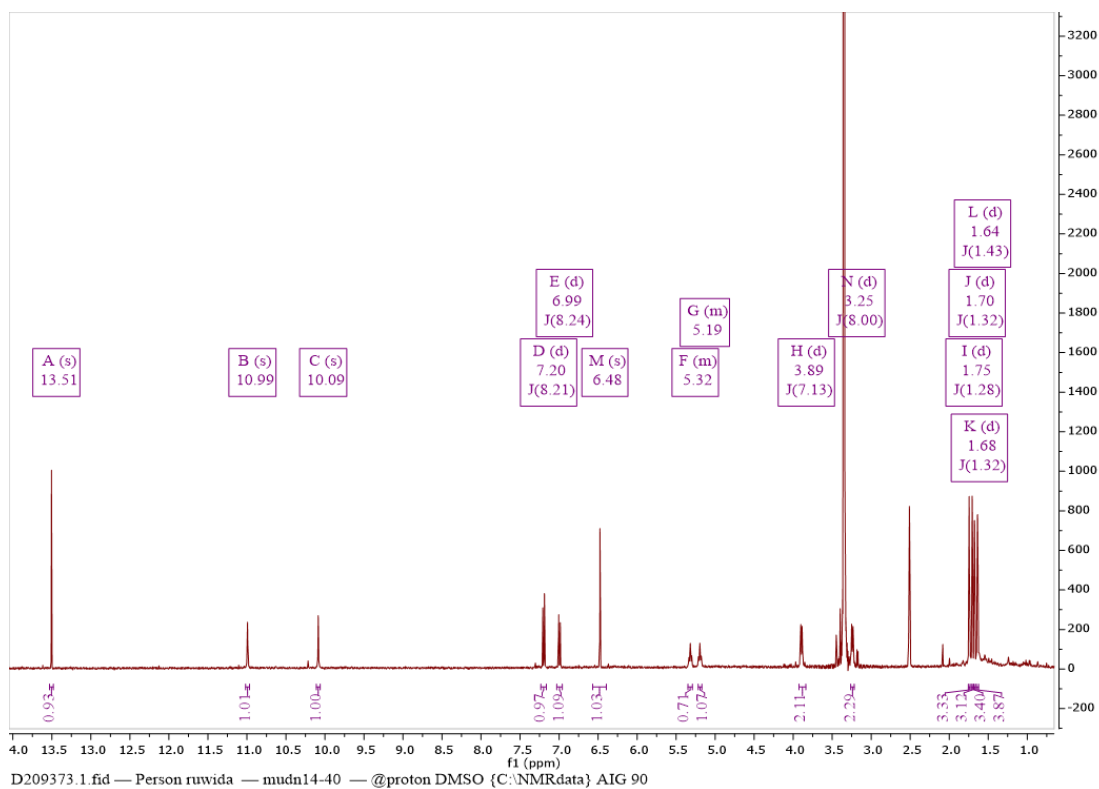
Zhang, T., Omar, R., Siheri, W., Al Mutairi, S., Clements, C., Fearnley, J., Watson, D. (2014). Chromatographic analysis with different detectors in the chemical characterisation and dereplication of African propolis. *Talanta*, 120, 181–90.

10 Appendix

Table- S1: NMR data for compound Mudn14-40(1,3,7-trihydroxy-2,8-di-(3-methylbut-2-enyl)xanthone).

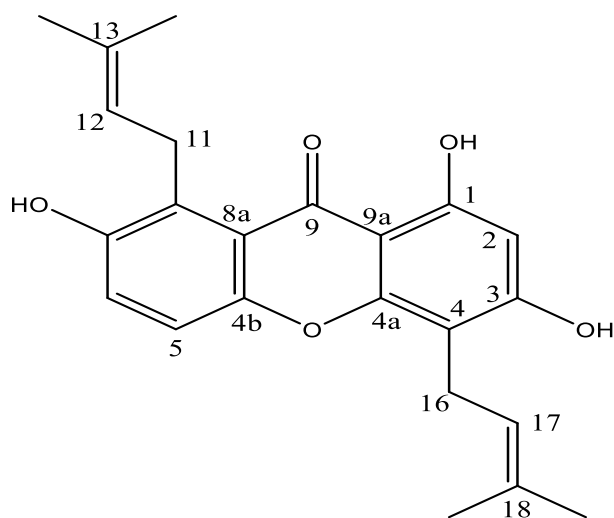


Position	^1H δ ppm (mult, <i>J</i>)	^{13}C δ ppm
1	-	160.0(C)
2	-	110.1(C)
3	-	163.3(C)
4	6.48, 1H (s)	93.0(CH)
4a	-	154.7(C)
4b	-	146.3(C)
5	6.99, 1H (d,8.2)	125.5(CH)
6	7.20, 1H (d,8.2)	120.3(CH)
7	-	144.6(C)
8	-	132.5(C)
8a	-	118.6(C)
9	-	191.1(C)
9a	-	102.5(C)
10	-	-
11	3.89, 2H (d,7.2)	33.1(CH ₂)
12	5.32, 1H (br.t)	124.2(CH)
13	-	131.4 (C)
14	1.70, 3H (s)	18.3(CH ₃)
15	1.68, 3H (s)	26.0(CH ₃)
16	3.25, 2H (d, 8.0)	21.6(CH ₂)
17	5.19, 1H (br.t)	122.9(CH)
18	-	130.7(C)
19	1.64, 3H (s)	26.1(CH ₃)
20	1.75, 3H (s)	18.3(CH ₃)
1-OH	13.51, 1H (s)	-



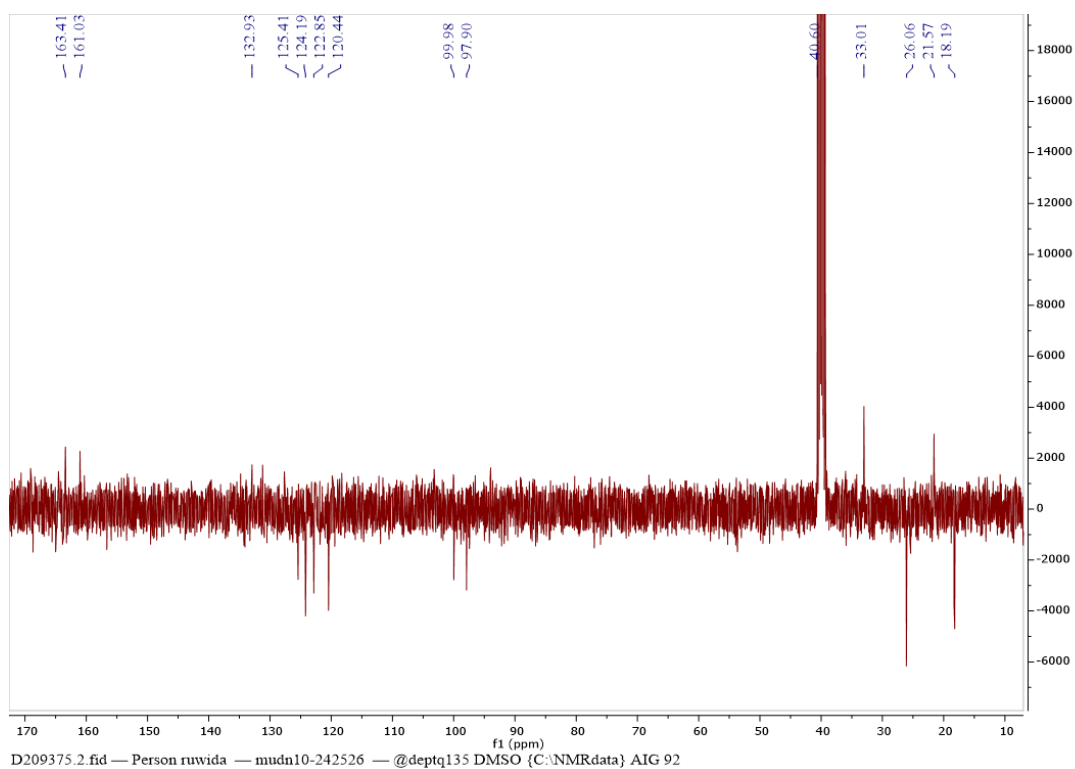
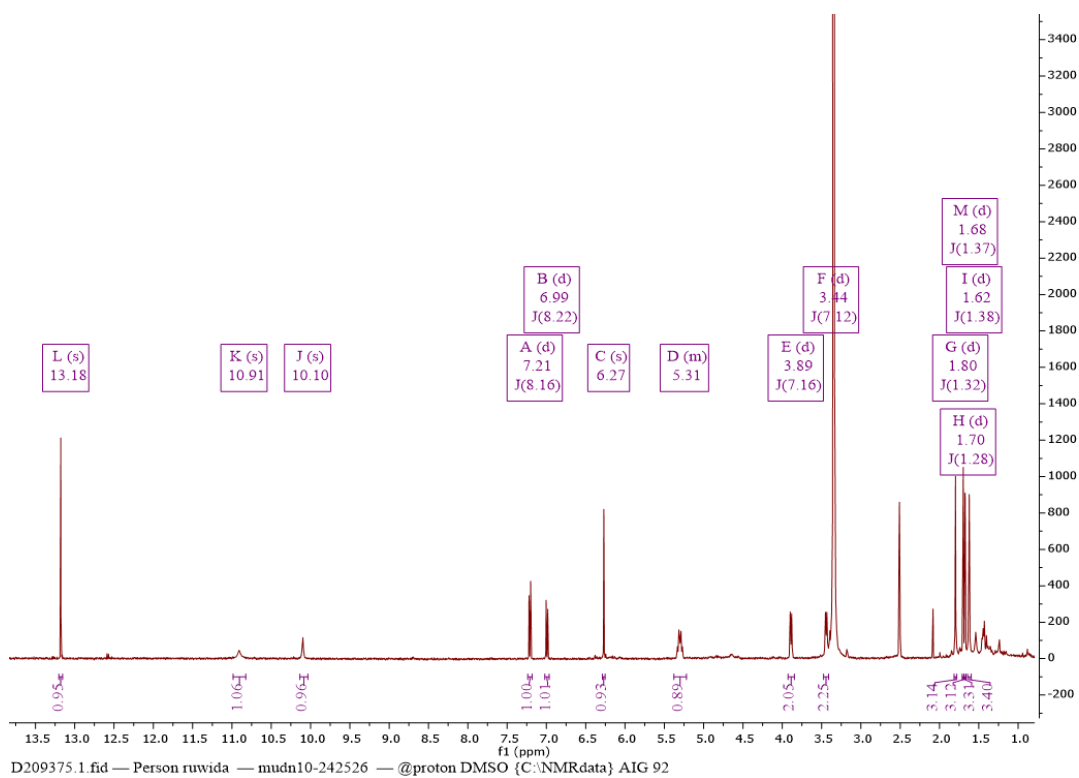
Appendix- 1: ^1H NMR (400 MHz, DMSO- d_6), and ^{13}C (100 MHz, DMSO- d_6) of Mudn14-40.

Table- S2: NMR data for compound Mudn10-242526(1,3,7-trihydroxy-4,8-di-(3-methylbut-2-enyl)xanthone).



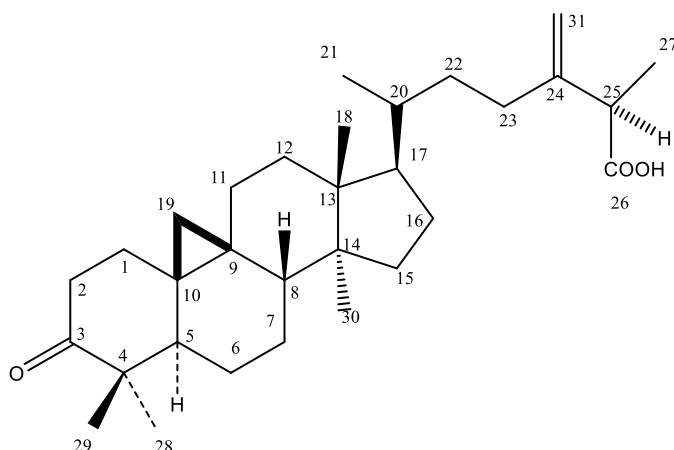
Position	^1H δ ppm (mult, <i>J</i>)	^{13}C δ ppm
1	-	161.0 (C)
2	6.27, 1H (s)	97.6 (CH)
3	-	163.2 (C)
4	-	106.0 (C)
4a	-	153.7 (C)
4b	-	146.8 (C)
5	6.99, 1H (d, 8.2)	125.4 (CH)
6	7.21, 1H (d, 8.2)	120.5 (CH)
7	-	145.0 (C)
8	-	132.7 (C)
8a	-	118.3 (C)
9	-	190.9 (C)
9a	-	103.2 (C)
10	-	-
11	3.89, 2H (d, 7.1)	33.04 (CH ₂)
12	5.31, 1H (m)	124.1 (CH)
13	-	131.9 (C)
14	1.70, 3H (s)	18.3 (CH ₃)
15	1.67, 3H (s)	26.08 (CH ₃)
16	3.45, 2H (d, 7.1)	21.53 (CH ₂)
17	5.29, 1H (m)	122.67 (CH)

18	-	133.4 (C)
19	1.80,3H (s)	18.8(CH3)
20	1.62,3H (s)	26.5(CH3)
1-OH	13.18,1H (s)	-
3-OH	10.92,1H (s)	-
7-OH	10.01,1H (s)	-



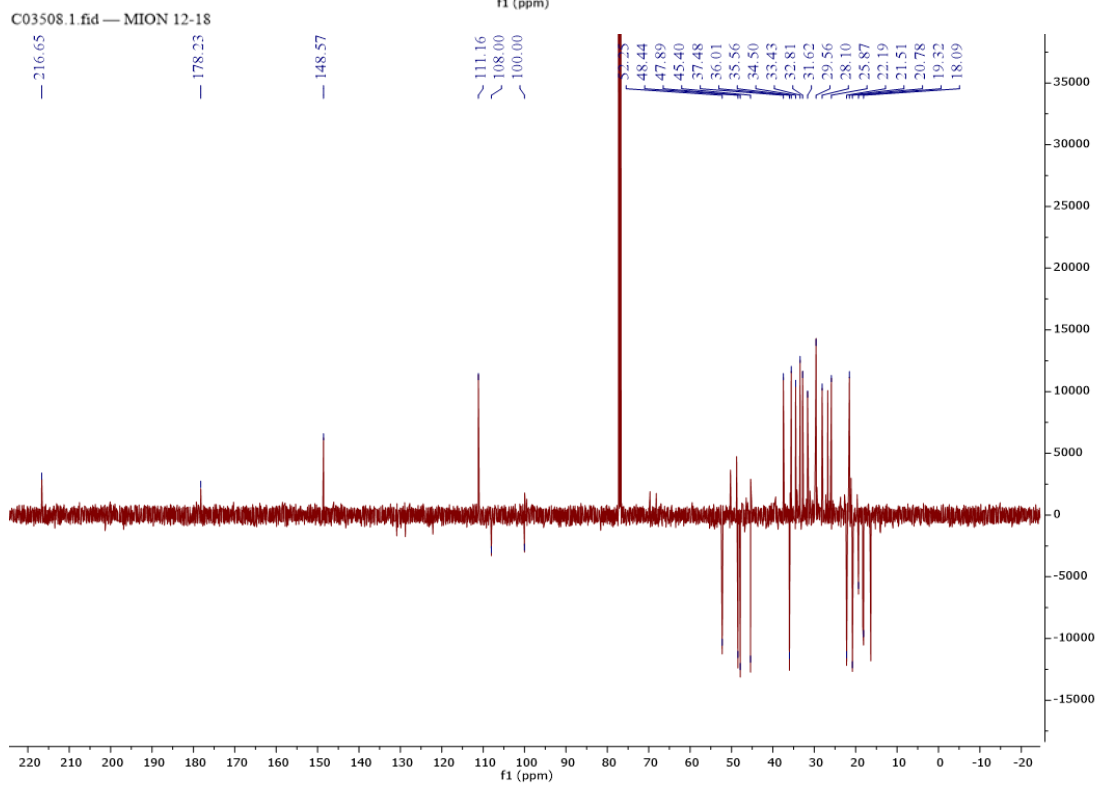
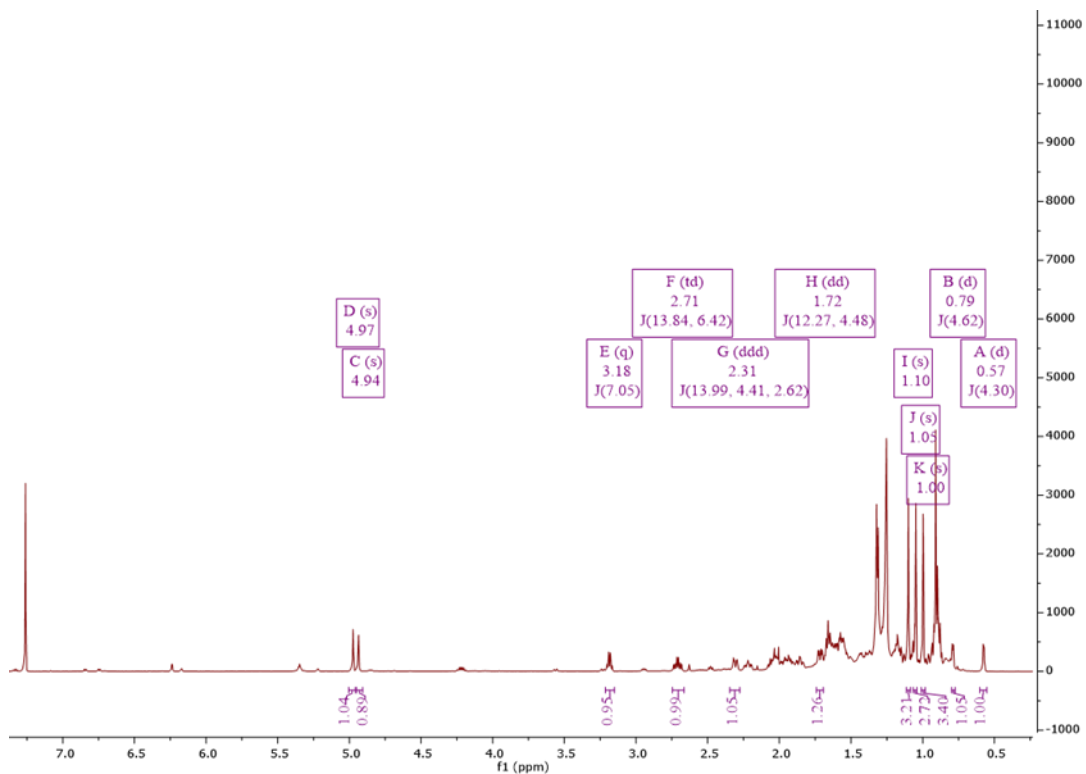
Appendix- 2: ^1H NMR (400 MHz, DMSO- d_6), and ^{13}C (100 MHz, DMSO- d_6) of Mudn14-242526.

Table- S3 : NMR data for compound Mion12-18 (ambonic acid).



position	^1H δ ppm (mult, <i>J</i>)	^{13}C δ ppm
1	1.88,1.57,2H (m)	33.4(CH ₂)
2	2.34, 1H (ddt, 14.0, 4.4, 2.6) 2.74,1H (td, 13.9, 6.4)	37.5(CH ₂)
3	-	219.6(C)
4	-	50.2(C)
5	1.74,1H (dd,12.3,4.5)	48.4(CH)
6	1.57,1.61,2H (m)	21.5(CH ₂)
7	1.95,2H (m)	28.1(CH ₂)
8	1.62,1H (m)	47.9(CH)
9	-	21.05(C)
10	-	25.9(C)
11	1.40, 2H (m)	25.9(CH ₂)
12	1.69,2H (m)	32.8(CH ₂)
13	-	45.3(C)
14	-	48.7(C)
15	1.35,2H (m)	35.6(CH ₂)
16	1.19, 1.22,2H (m)	26.7(CH ₂)
17	1.64,1H (m)	52.3(CH)
18	1.02,3H (s)	18.1(CH ₃)
19	0.82,1H (d,4.2) 0.60,1H (d,4.3)	29.5(CH ₂)

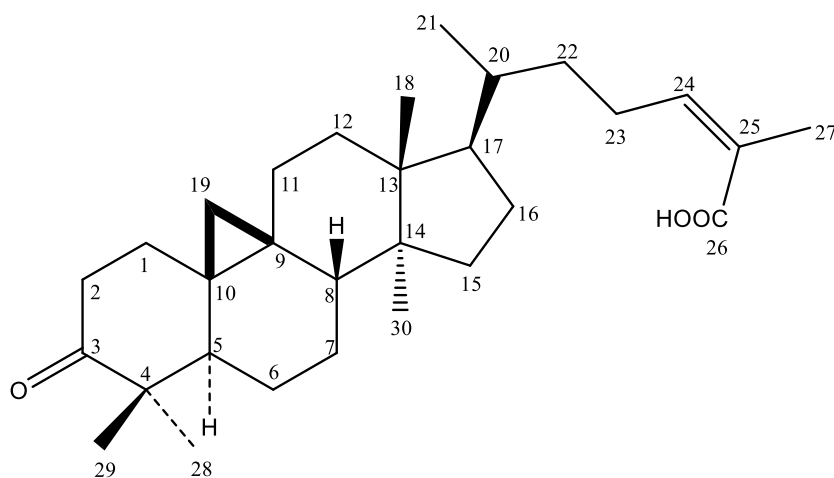
20	1.46,1H (m)	36.0(CH)
21	0.93,3H (d,7.1)	18.3(CH3)
22	1.65,1.20, 2H (m)	34.7(CH2)
23	2.25,1H (ddd, 15.7, 11.4, 4.8) 2.08,1H (t ,7.8)	31.6(CH2)
24	-	148.5(C)
25	3.21, 1H (q,7.0)	45.4(CH)
26	-	178(C)
27	1.35,3H (d,7.0)	16.4(CH3)
28	1.13,3H (s)	20.8(CH3)
29	1.08,3H (s)	22.2(CH3)
30	1.03,3H (s)	18.3(CH3)
31	4.9,1H (brs) 5.0,1H (brs)	111.1(CH2)



Appendix- 3: ¹H NMR (400 MHz, CDCl₃), and ¹³C (100 MHz, CDCl₃) of Mion12-

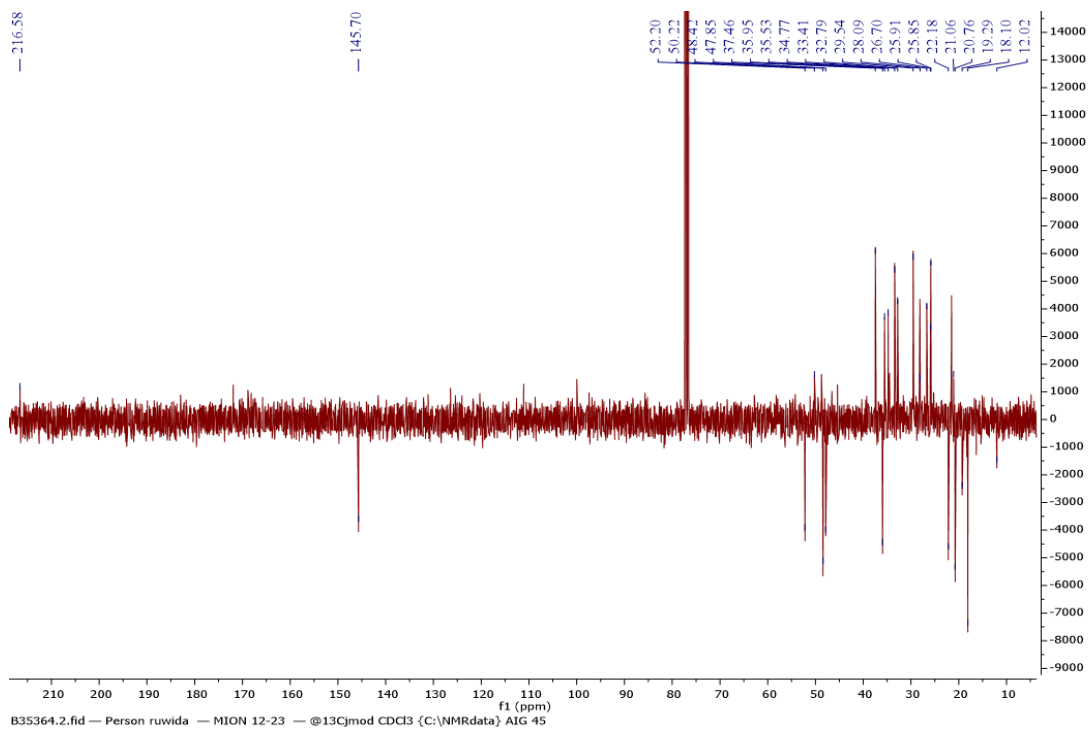
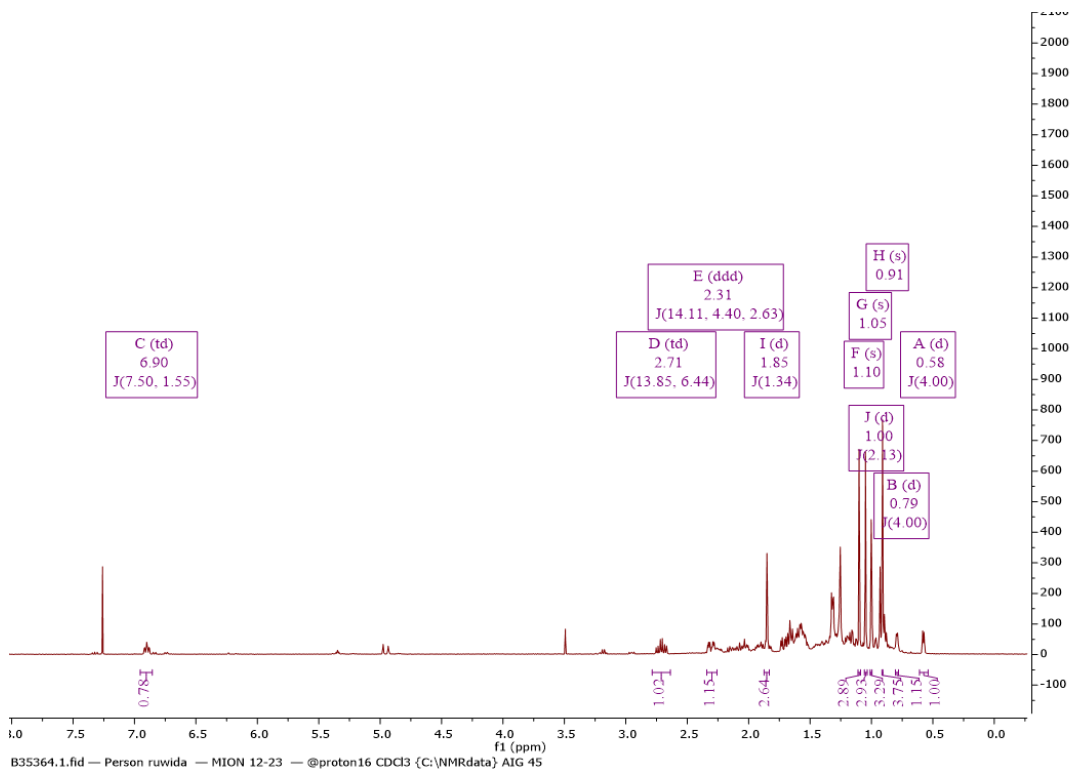
18.

Table- S4: NMR data for compound Mion12-23(mangiferonic acid).



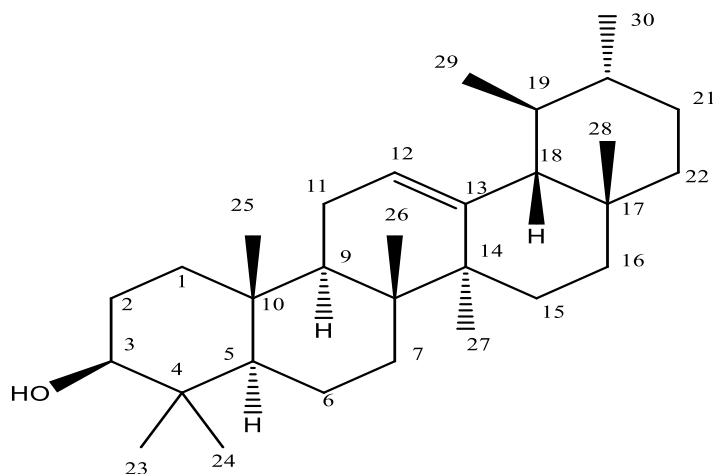
Position	^1H δ ppm (mult, <i>J</i>)	^{13}C δ ppm
1	1.88,1.57,2H (m)	33.4(CH ₂)
2	2.72,1H (ddd,13.9, 6.4) 2.32,1H (ddd,14.1, 4.4, 2.6)	37.4(CH ₂)
3	-	216.7(C)
4	-	50.2(C)
5	1.72 (m)	48.4(CH)
6	1.56,1H (m), 1.65,1H (m)	21.4(CH ₂)
7		25.9(CH ₂)
8	1.58,1H (m)	47.8(CH)
9	-	21.0(C)
10	-	25.9(C)
11	2.05,2H (m)	26.6(CH ₂)
12	1.66, 2H (m)	32.7(CH ₂)
13	-	45.4(C)
14	-	48.7(C)
15	1.32,2H (m)	35.5(CH ₂)
16	1.92,2H (m)	28.1(CH ₂)
17	1.61,1H (m)	52.2(CH)
18	1.01,3H (s)	18.1(CH ₃)
19	0.58,1H (d, 4) 0.80,1H (d, 4)	29.5(CH ₂)

20	1.46,1H (m)	35.9(CH)
21	1.01,3H (d,2.13)	18.1(CH ₃)
22	1.17,2H (m)	34.7(CH ₂)
23	2.15,2H (m)	25.8(CH ₂)
24	6.90,1H (td,7.5,1.55)	145.7(CH)
25	-	126.7(C)
26	-	171.9(C)
27	1.86,3H (s)	12.0(CH ₃)
28	1.06,3H (s)	22.1(CH ₃)
29	1.11,3H (s)	20.8(CH ₃)
30	0.92,3H (s)	19.2(CH ₃)



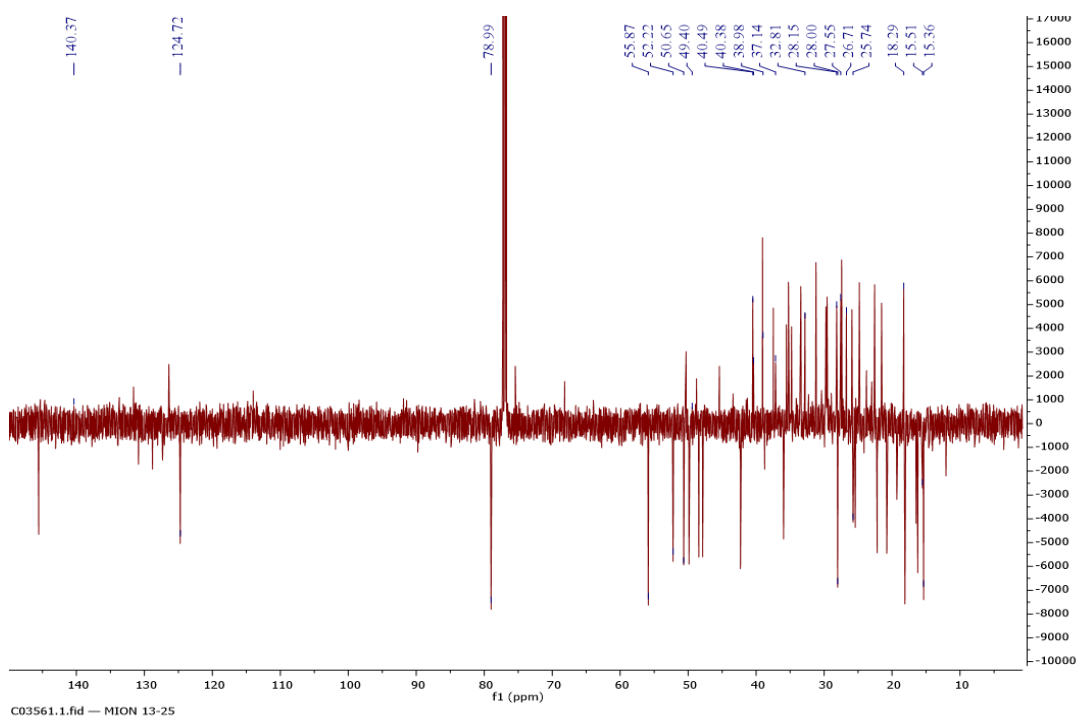
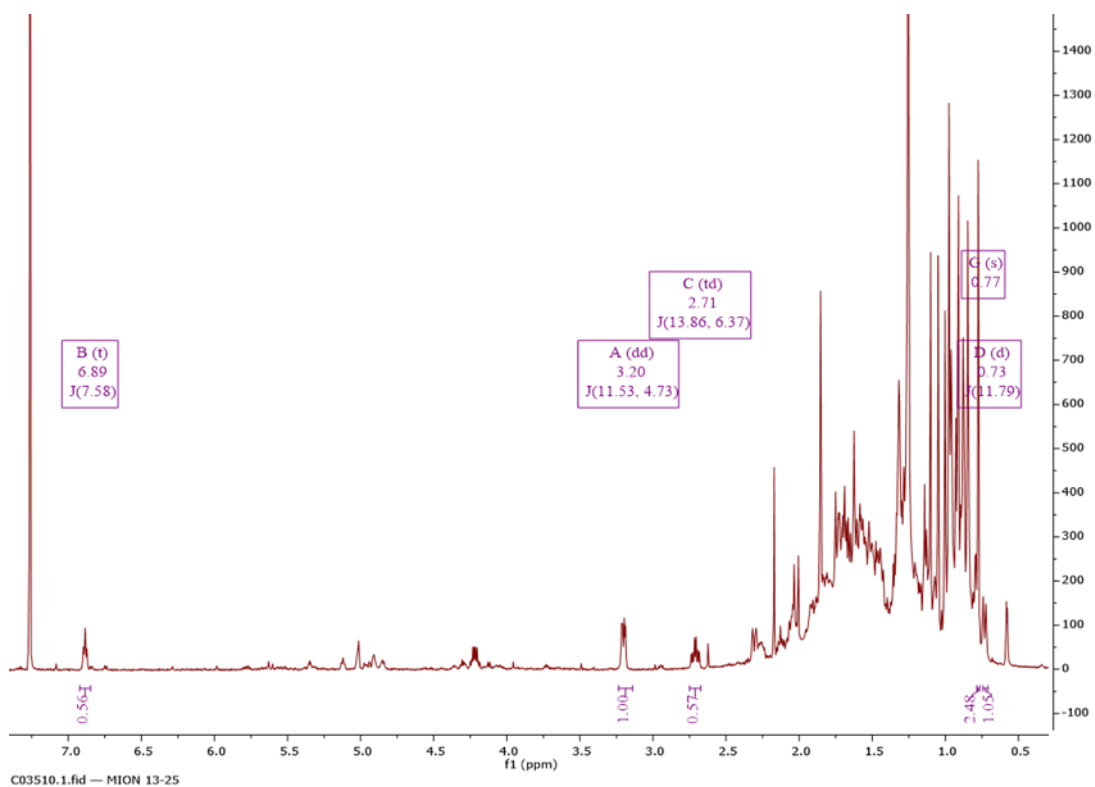
Appendix- 4: ^1H NMR (400 MHz, CDCl_3), and ^{13}C (100 MHz, CDCl_3) of Mion12-

23.

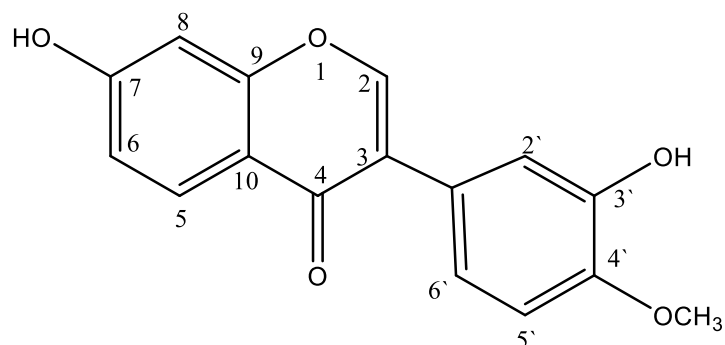
Table- S5: NMR data for compound Mion13-25 (α amyryn in mixture)

Position	^1H δ ppm (mult, J)	^{13}C δ ppm
1		38.9(CH ₂)
2		27.5(CH ₂)
3	3.23,1H (dd, 4.7, 11.5)	78.8(CH)
4	-	38.8(C)
5	0.75,1H (d,11.7)	55.7(CH)
6	1.46,1.55,2H (m)	18.3(CH ₂)
7	1.69,1.70,2H (m)	32.78(CH ₂)
8	-	40.36(C)
9	1.39,1H (s)	50.5(CH)
10	-	37.5(C)
11	2.06	23.01(CH ₂)
12	5.14,1H (t, 3.6)	124.7(CH)
13	-	140.6(C)
14	-	49.3(C)
15	1.5, 2H (m)	28.15(CH ₂)
16	2.06,2H (m)	26.9(CH ₂)
17	-	33.4(C)
18	1.63,1H (m)	52.23(CH)
19		39.15
20		39.21
21	1.66,2H (m)	32.8(CH ₂)
22	1.512H (m)	40.5(CH ₂)
23	1.00,3H (s)	28.0(CH ₃)

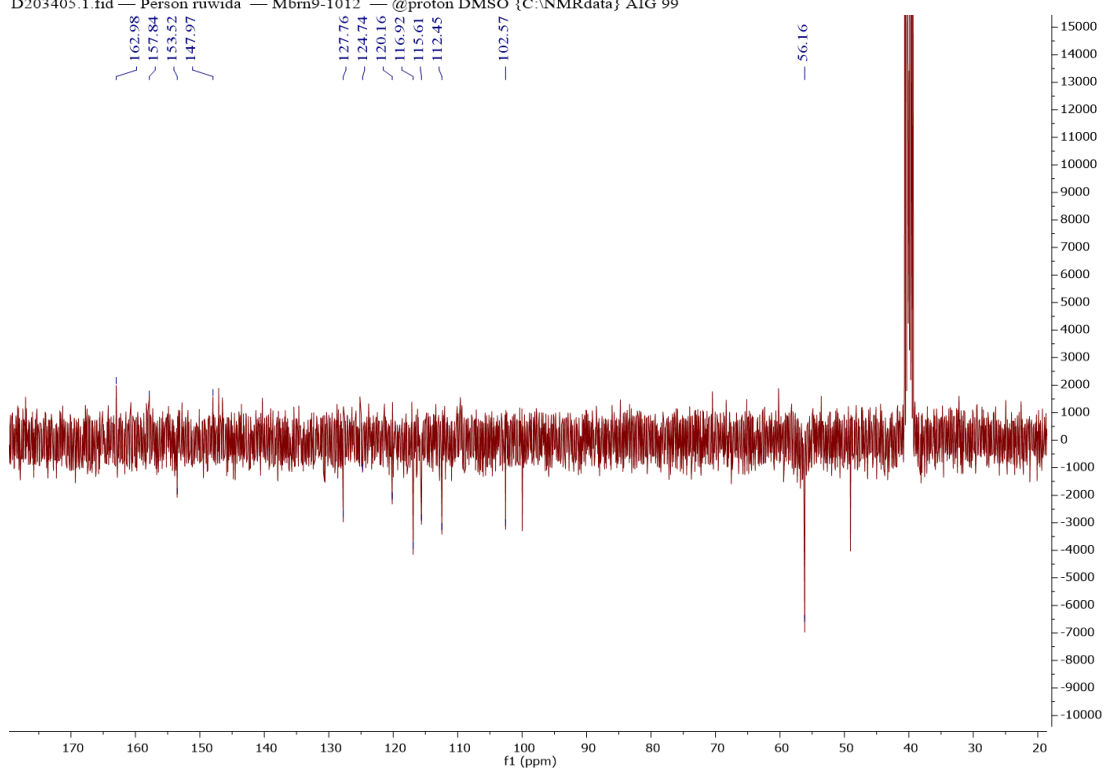
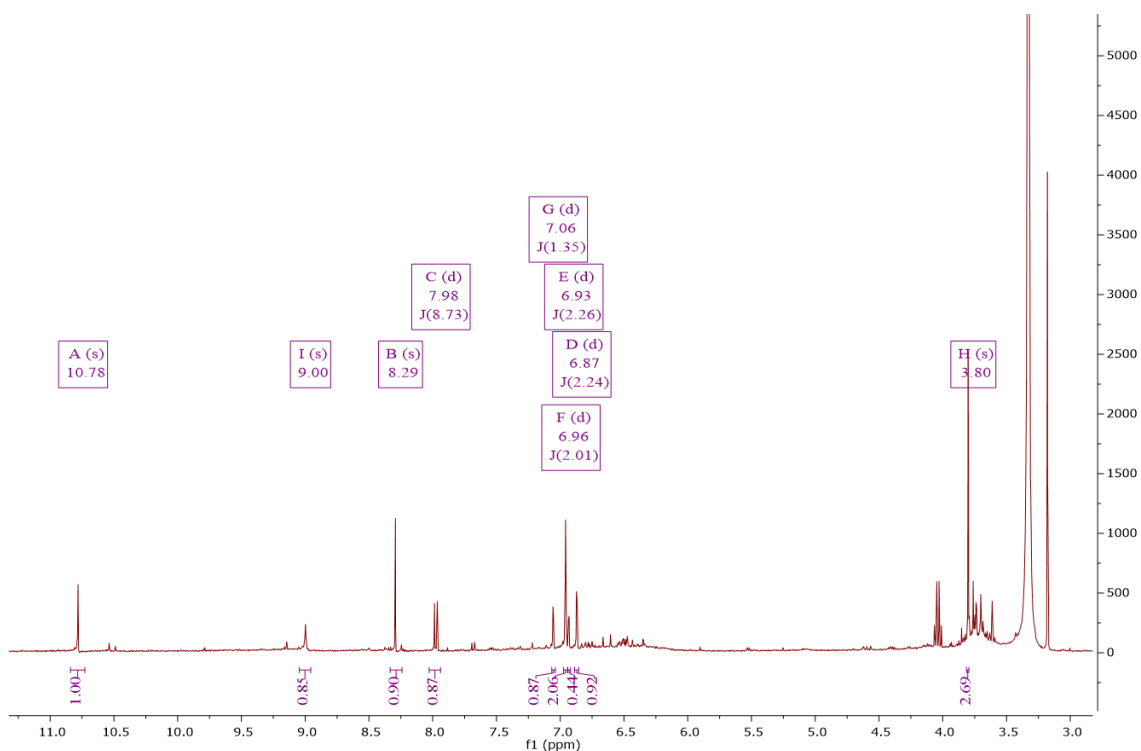
24	0.80,3H (s)	15.4(CH3)
25	0.87,3H (s)	15.5(CH3)
26	1.07,3H (s)	15.8(CH3)
27	1.03,3H (s)	26.0(CH3)
28	0.94,3H (s)	28.1(CH3)
29	1.03,3H (s)	33.3(CH3)
30	1.13,3H (s)	20.8(CH3)



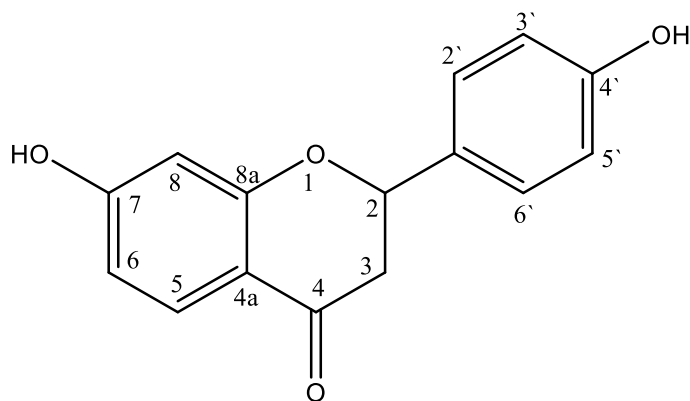
Appendix- 5: ^1H NMR (400 MHz, CDCl_3), and ^{13}C (100 MHz, CDCl_3) of Mion13-25.

Table- S6: NMR data for compound **1** (calycosin)

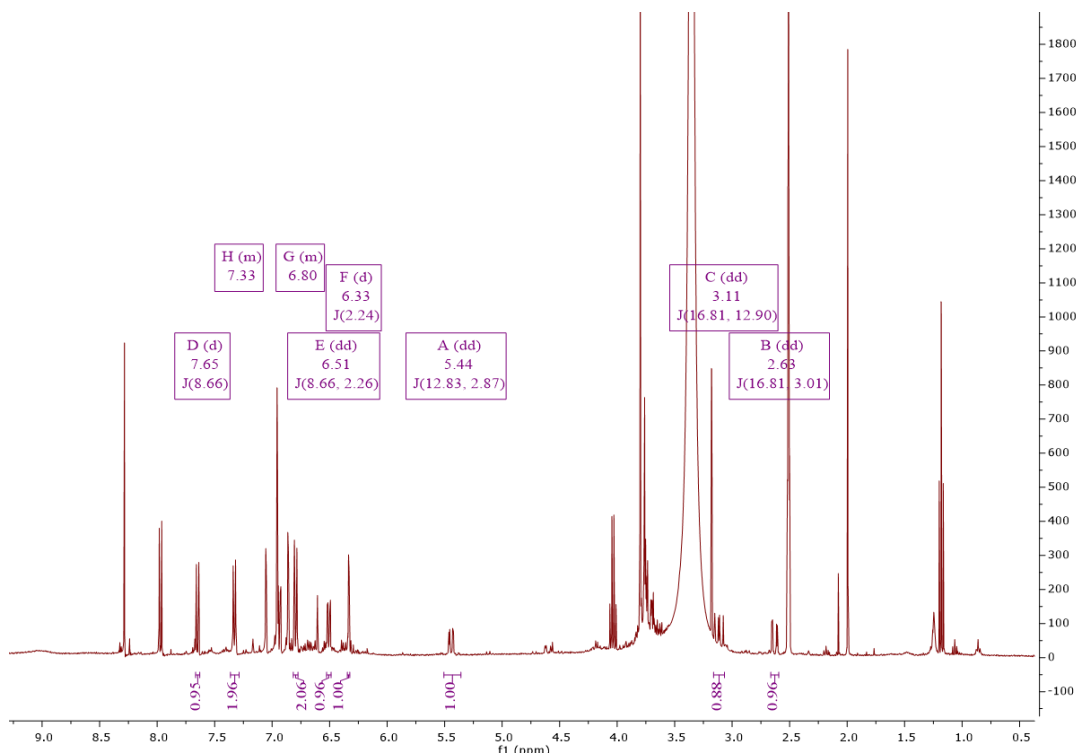
position	Chemical shift δ ppm ¹ H (mult, <i>J</i> Hz)	Chemical shift δ ppm ¹³ C
1	-	-
2	8.29, 1H (s)	153.3(CH)
3	-	125.1(C)
4	-	174.7(C)
5	7.98, 1H (d, 8.7)	127.7(CH)
6	6.93, 1H (d, 2.3)	115.6(CH)
7	-	163.0
8	6.85, 1H (d, 2.2)	102.2(CH)
9	-	157.5(C)
1'	-	124.1(C)
2'	7.06, 1H (d, 1.4)	116.8(CH)
3'	-	146.0(C)
4'	-	147.9(C)
5'	6.96, 1H (d, 2.0)	112.4(CH)
6'	6.96, 1H (d, 2.0)	120.1(CH)
7-OH	10.82, 1H (s)	-
3'-OH	9.02, 1H (s)	-
4'-OCH₃	3.75 (s)	56.12(CH ₃)



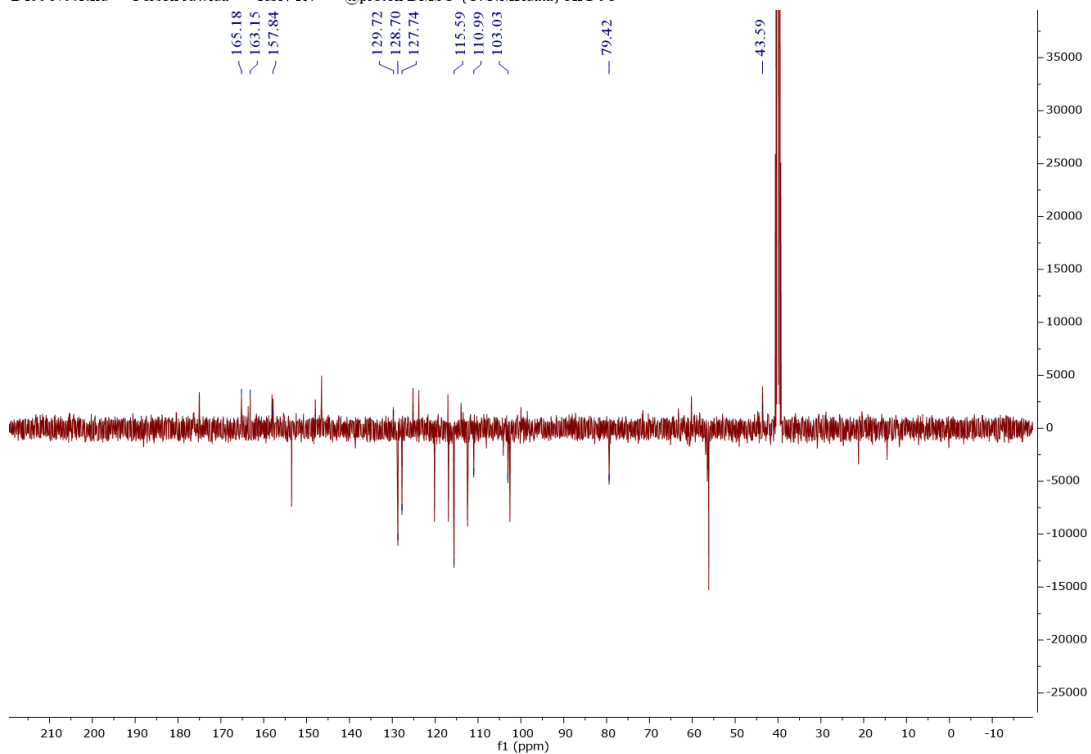
Appendix- 6: ^1H NMR (400 MHz, DMSO- D_6), and ^{13}C (100 MHz, DMSO- D_6) of **1** (calycosin).

Table- S7: NMR data for compound **2** (Liquiritigenin).

Position	Chemical shift δ ppm ^1H (mult, J Hz)	Chemical shift δ ppm ^{13}C
1	-	-
2	5.45, 1H (dd, 12.8, 2.9)	79.4(CH)
3	3.11, 1H (dd, 16.8, 12.9) 2.64, 1H (dd, 16.8, 3.0)	43.7(CH ₂)
4	-	190.8(C)
4a	-	113.9 (C)
5	7.65, 1H (d, 8.7)	129.0(CH)
6	6.51, 1H (dd, 8.7, 2.3)	110.0(CH)
7	-	163.5(C)
8	6.33, 1H (d, 2.2)	103.0(CH)
8a	-	165.1(C)
1'	-	129.0(C)
2'	7.33, 1H (m)	128.6(CH)
3'	6.78, 1H (m)	115.6(CH)
4'	-	158.0
5'	6.78, 1H (m)	115.6(CH)
6'	7.33, 1H (m)	128.7(CH)
7-OH	10.56, 1H (s)	-
4'-OH	9.65, 1H (s)	-



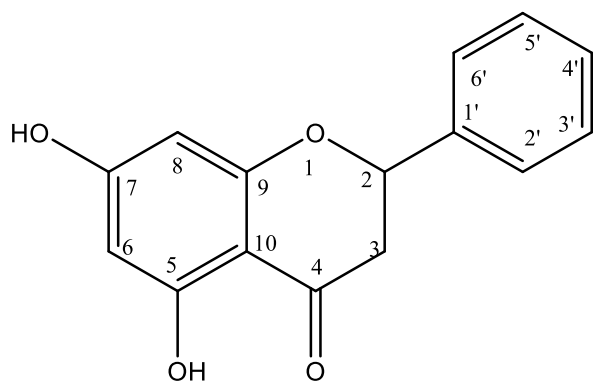
D199679.1.fid — Person ruwida — RSN-R4 — @proton DMSO {C:\NMR\data} AIG 98



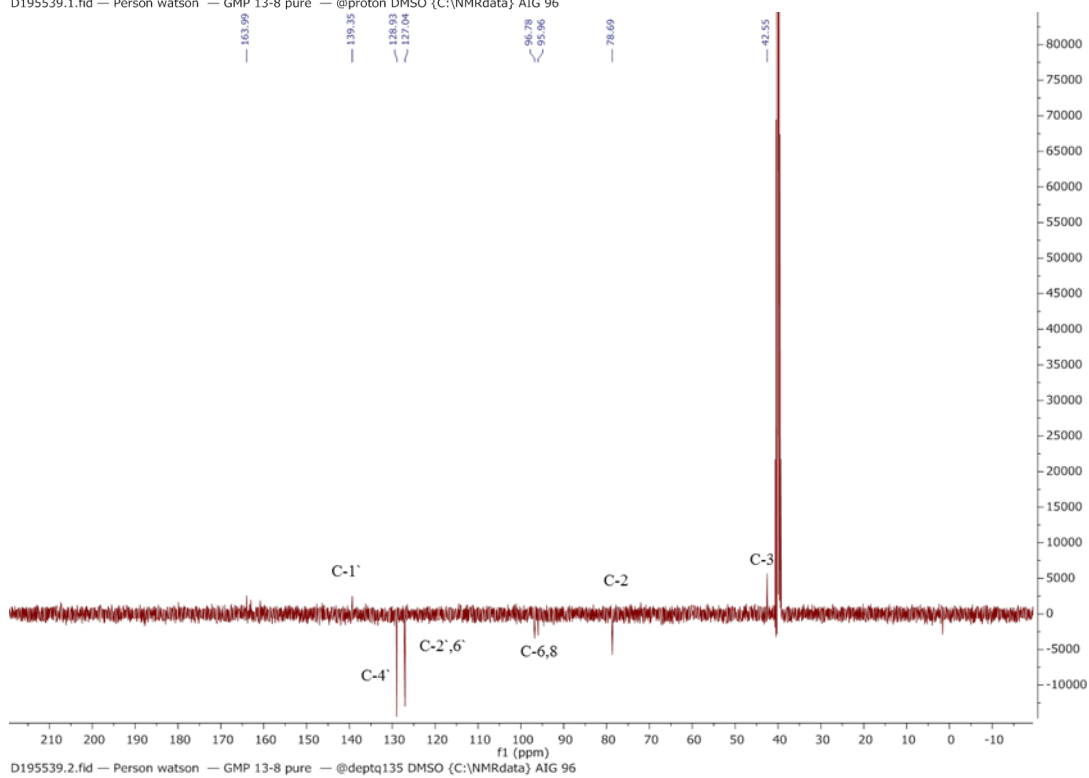
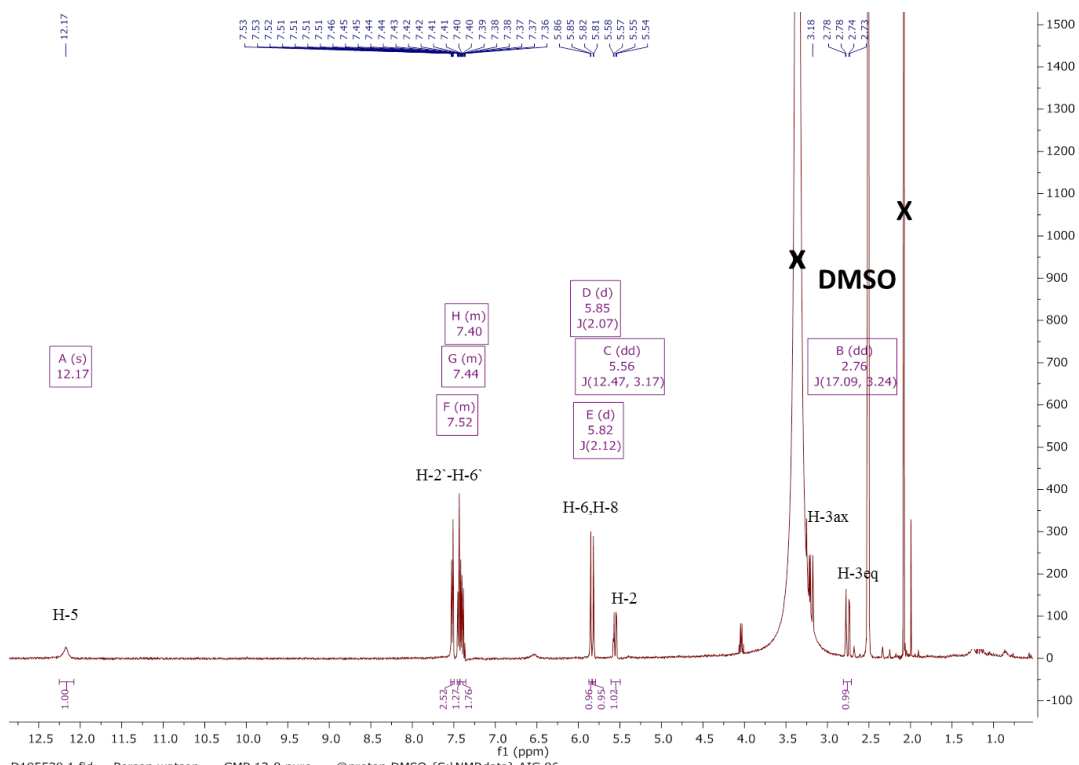
D199679.2.fid — Person ruwida — RSN-R4 — @deptq135 DMSO {C:\NMR\data} AIG 98

Appendix- 7: ^1H NMR (400 MHz, DMSO-d_6), and ^{13}C (100 MHz, DMSO-d_6) of **2** (Liquiritigenin).

Table- S8 : NMR data for compound **3** (Pinocembrin).

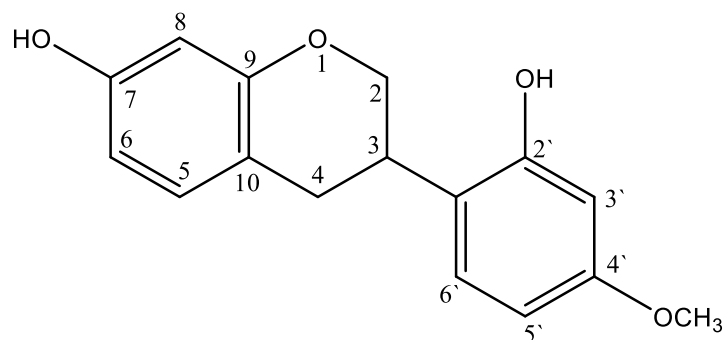


Position	Chemical shift δ ppm 1H (mult, <i>J</i> Hz)	Chemical shift δ ppm 13C
1	-	-
2	5.55, 1H (dd, 12.5, 3.2)	78.8(CH)
3-eq 3-ax	2.76, 1H (dd, 17.1, 3.2) 3.12, 1H (dd) overlapped with solvent	42.4(CH ₂)
4	-	196.0(C)
5	-	163.0(C)
6	5.82, 1H (d, 2.1)	96.7(CH)
7	-	167.3(C)
8	5.85, 1H (d, 2.1)	95.9(CH)
9	-	164.0(C)
10	-	101.0(C)
1'	-	139.1(C)
2'	7.50, 1H (m)	127.0(CH)
3'	7.41, 1H (m)	129.0(CH)
4'	7.43, 1H (m)	128.9(CH)
5'	7.41, 1H (m)	129.0(CH)
6'	7.50, 1H (m)	127.1(CH)
5-OH	12.17(s)	-

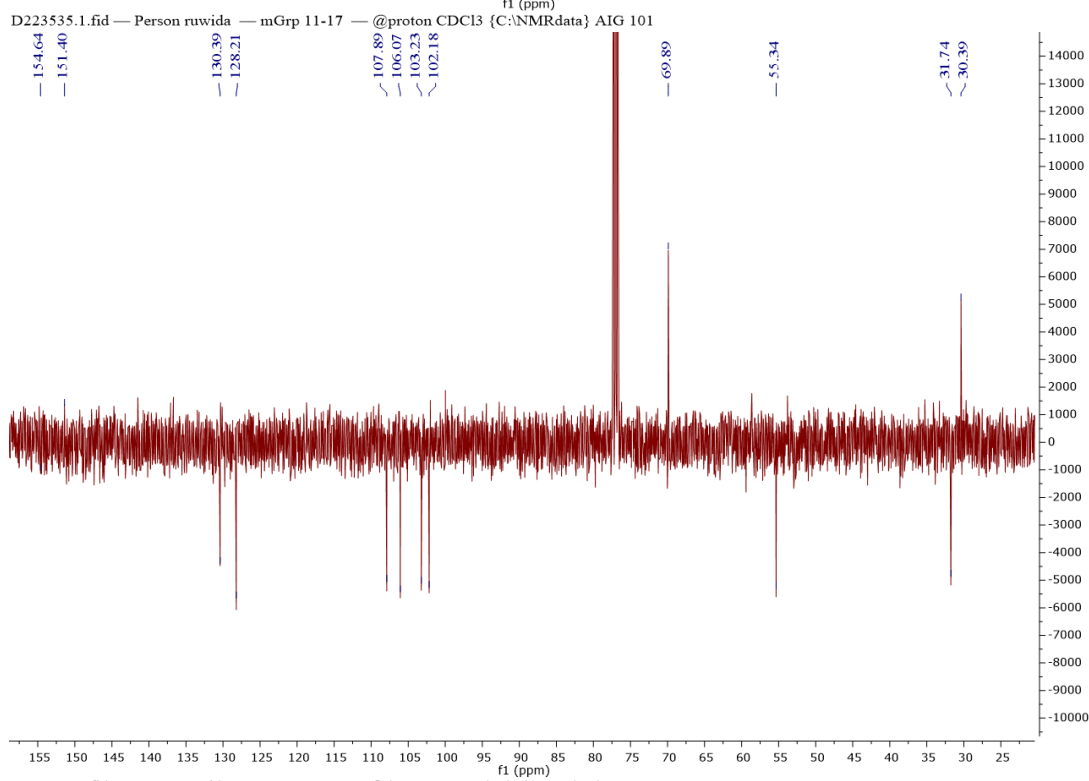
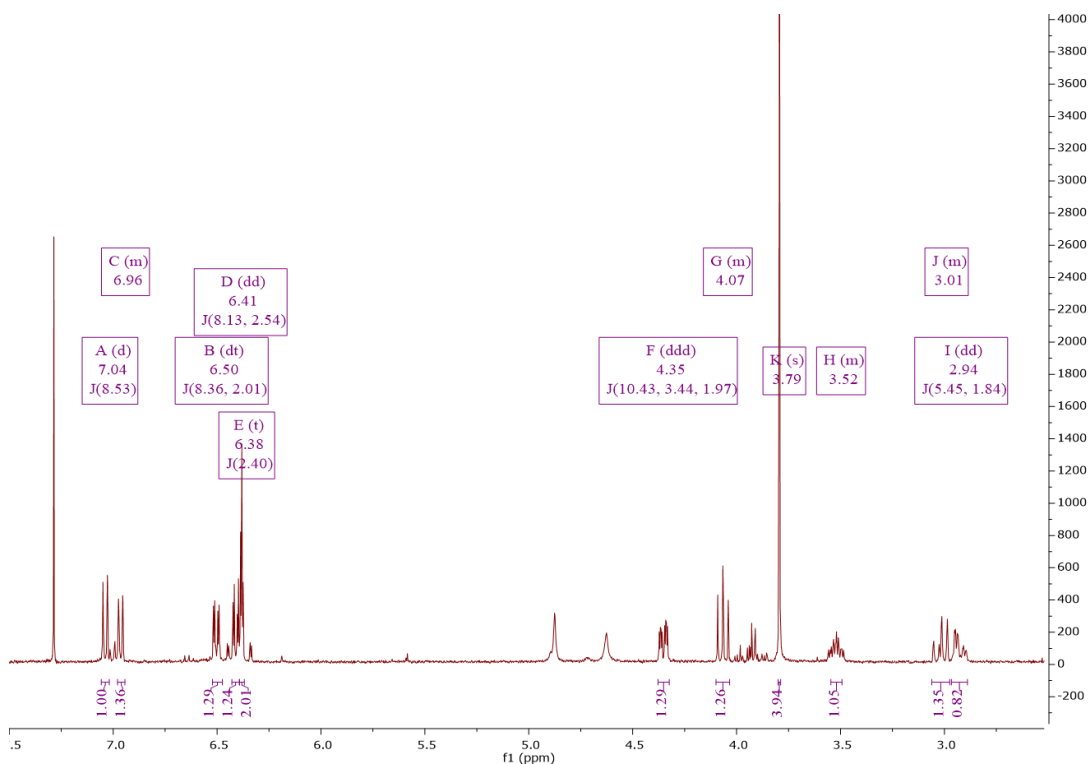


Appendix- 8: ^1H NMR (400 MHz, DMSO- d_6), and ^{13}C (100 MHz, DMSO- d_6) of **3** (Pinocembrin).

Table- S9: NMR data for compound **4** (Vestitol).

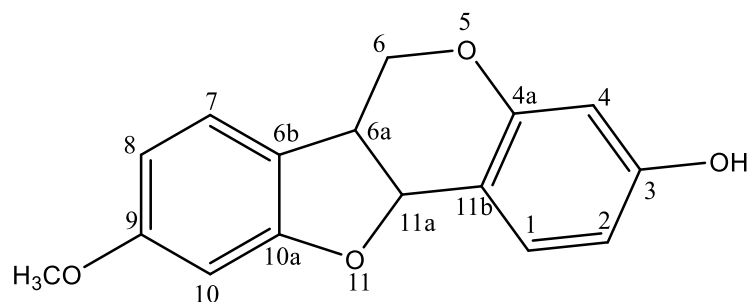


Position	Chemical shift δ ppm ^1H (mult, J Hz)	Chemical shift δ ppm ^{13}C
1	-	-
2	β 4.35, 1H (ddd, 10.4, 3.4, 2.0) α 4.04, 1H (m)	70.0(CH ₂)
3	3.50, 1H (m)	31.7(CH)
4	2.91, 1H (m), 3.0, 1H (m)	30.4(CH ₂)
5	6.96, 1H (m)	130.3(CH)
6	6.42, 1H (dd, 8.1, 2.5)	107.0(CH)
7	-	154.8(C)
8	6.38, 1H (overlapped with 3')	103.0(CH)
9	-	155.1(C)
10	-	119.9(C)
1'	-	119.1(C)
2'	-	153.9(C)
3'	6.38, 1H	102.3(CH)
4'	-	159.3(C)
4'-OCH₃	3.76, 3H (s)	55.3(CH ₃)
5'	6.5, 1H (dt, 8.4, 2.0)	105.8(CH)
6'	7.04, 1H (d, 8.5)	128.2(CH)

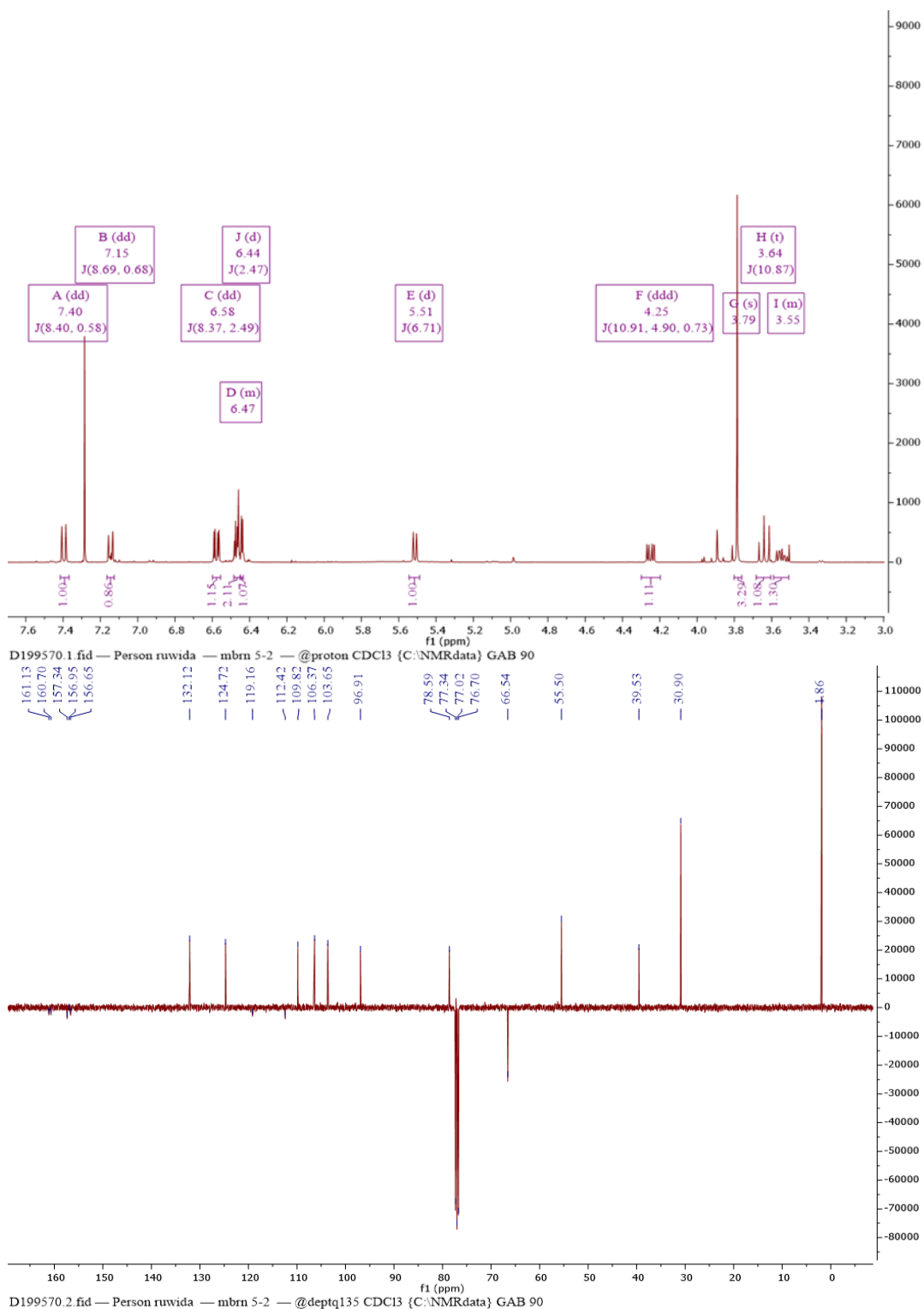


Appendix- 9: ¹H NMR (400 MHz, CDCl₃), and ¹³C (100 MHz, CDCl₃) of **4**

(Vestitol).

Table- S10 : NMR data for compound **5** (Medicarpin)

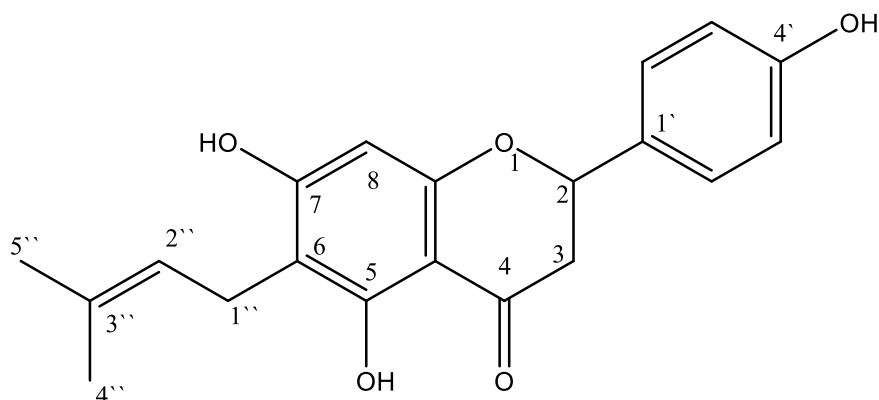
Position	Chemical shift δ ppm ^1H (mult, J Hz)	Chemical shift δ ppm ^{13}C
1	7.40, 1H (dd, 8.4, 0.6)	132.1(CH)
2	6.58, 1H (dd, 8.4, 2.5)	109.7(CH)
3	-	157.1(C)
4	6.44, 1H (d, 2.5)	103.6(CH)
4a	-	156.6(C)
5	-	-
6	4.24 α , 1H (ddd, 10.9, 4.9, 0.7) 3.62 β , 1H (t, 10.9)	66.5(CH ₂)
6a	3.57, 1H (m)	39.5(CH)
6b	-	119.2(C)
7	7.15, 1H (dd, 8.7, 0.7)	124.7(CH)
8	6.48, 1H (d, 2.27)	106.3(CH)
9	-	161.1(C)
9-OCH₃	3.79, 3H (s)	55.3(CH ₃)
10	6.46, 1H (m)	96.9(CH)
10a	-	160.7(C)
11	-	-
11a	5.51, 1H (d, 6.71)	78.5(CH)
11b	-	112.2(C)



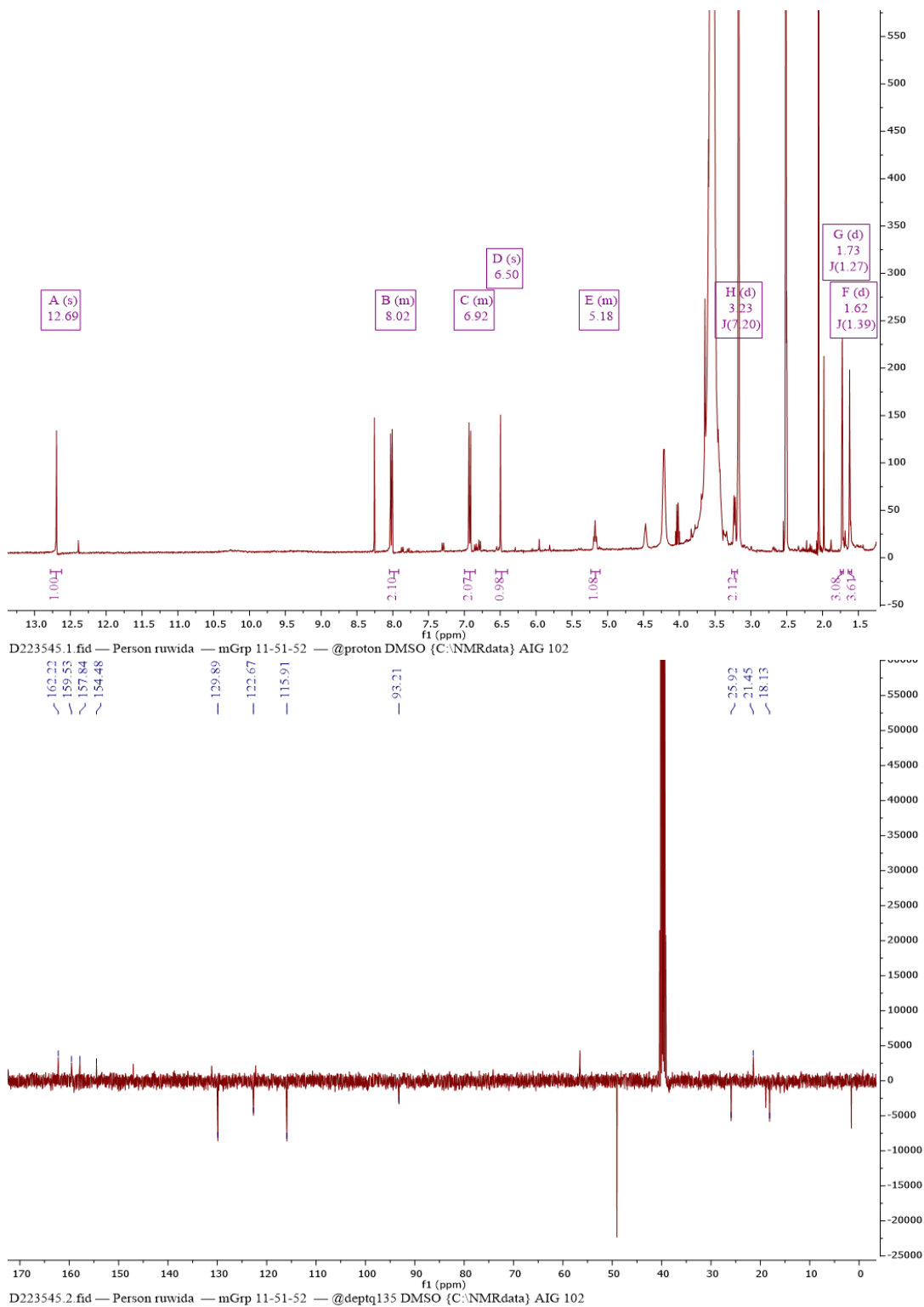
Appendix- 10 : ¹H NMR (400 MHz, CDCl₃), and ¹³C (100 MHz, CDCl₃) of **5**

(medicarpin)

Table- S11: NMR data for compound **7** (6-prenylnaringenin)

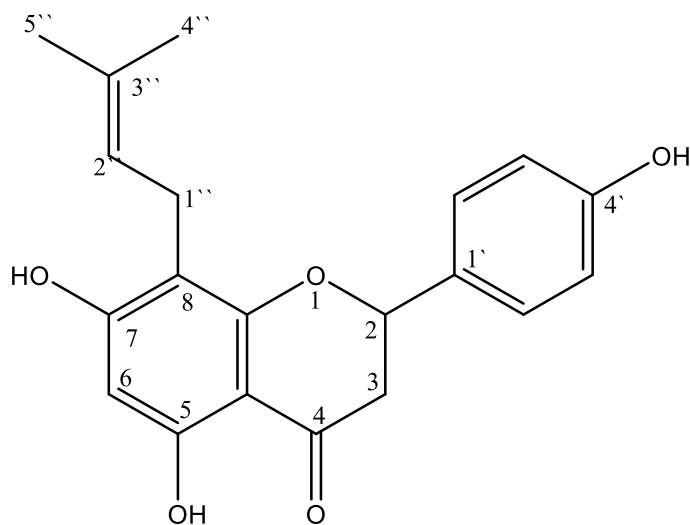


Position	Chemical shift δ ppm ^1H (mult, J Hz)	Chemical shift δ ppm ^{13}C
1	-	-
2		
3		
4	-	-
5	-	157.6(C)
6	-	110.8(C)
7	-	159.3(C)
8	6.5, 1H (s)	93.3(CH)
9	-	162.1(C)
10	-	103.1(C)
1'	-	122.3(C)
2'	8.02, 2H (m)	130.0(CH ₂)
3'	6.92, 2H (m)	115.3(CH ₂)
4'	-	154.0(C)
5'	6.92, 2H (m)	115.3(CH ₂)
6'	8.02, 2H (m)	130.0(CH ₂)
1''	3.22, 2H (brd, 7.21)	21.4(CH ₂)
2''	5.18, 1H (m)	122.4(CH)
3''	-	130.2(C)
4''	1.61, 3H (s)	25.4(CH ₃)
5''	1.69, 3H (s)	17.6(CH ₃)
5-OH	12.7, 1H (s)	-

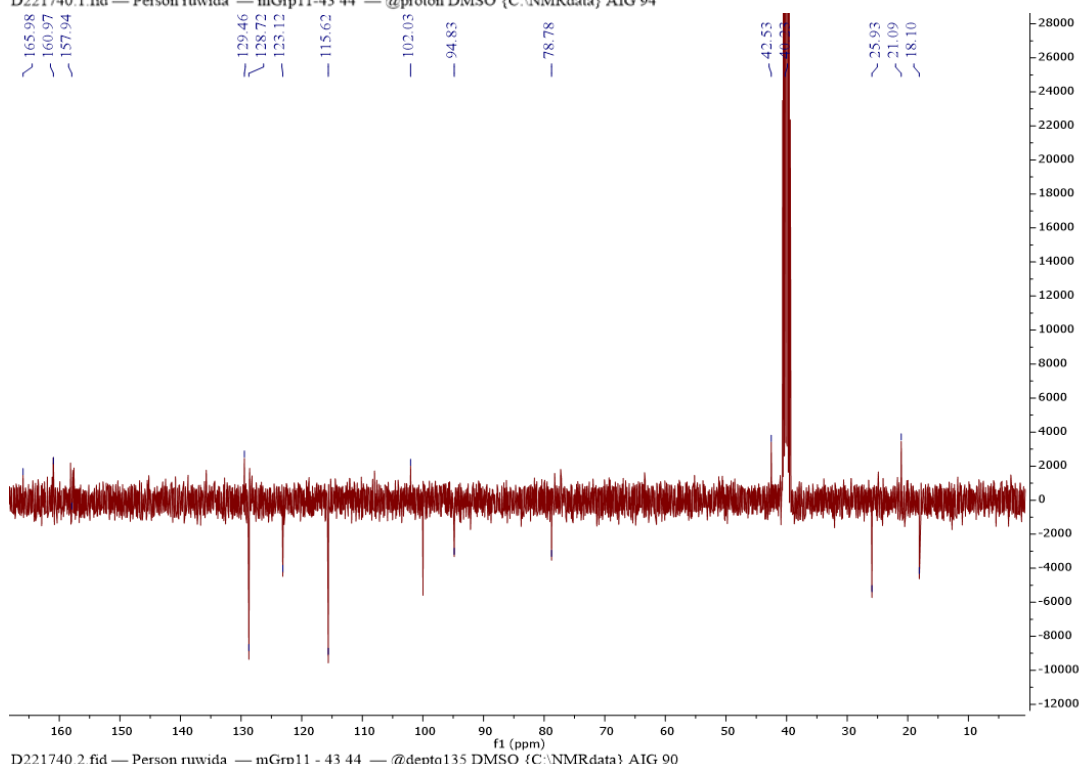
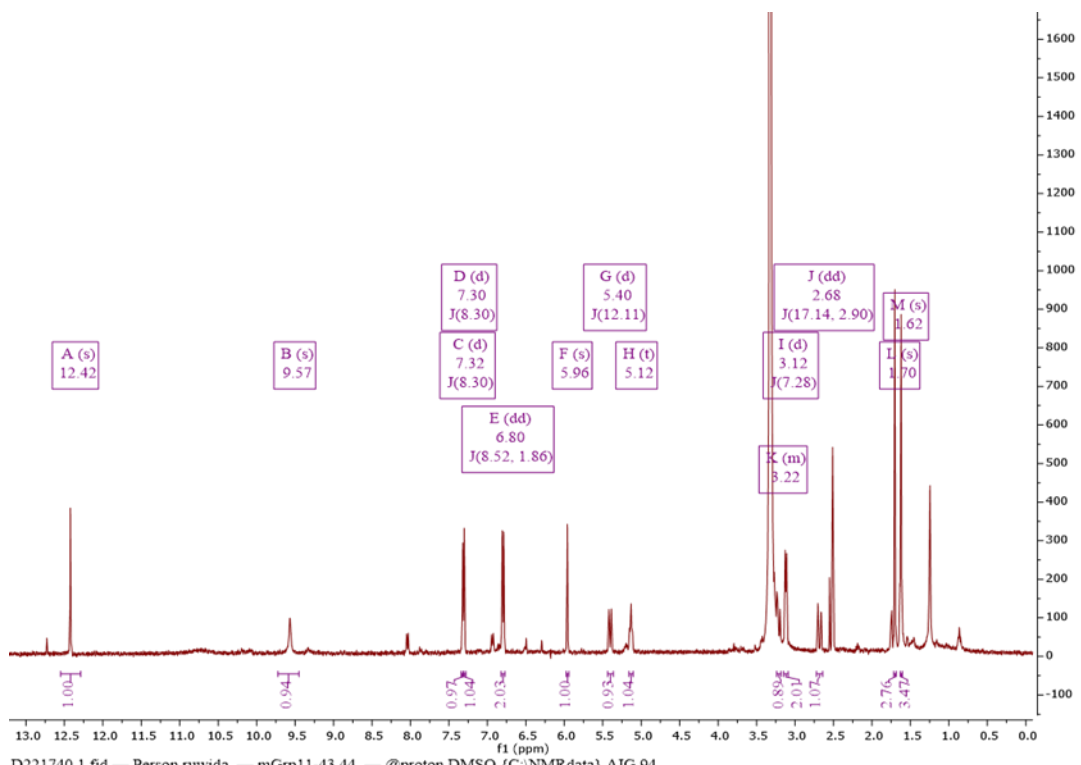


Appendix- 11: ¹H NMR (400 MHz, DMSO-d₆), and ¹³C (100 MHz, DMSO-d₆) of **7** (6-prenylnaringenin).

Table- S12: NMR data for compound **8** (8-prenylnaringenin).

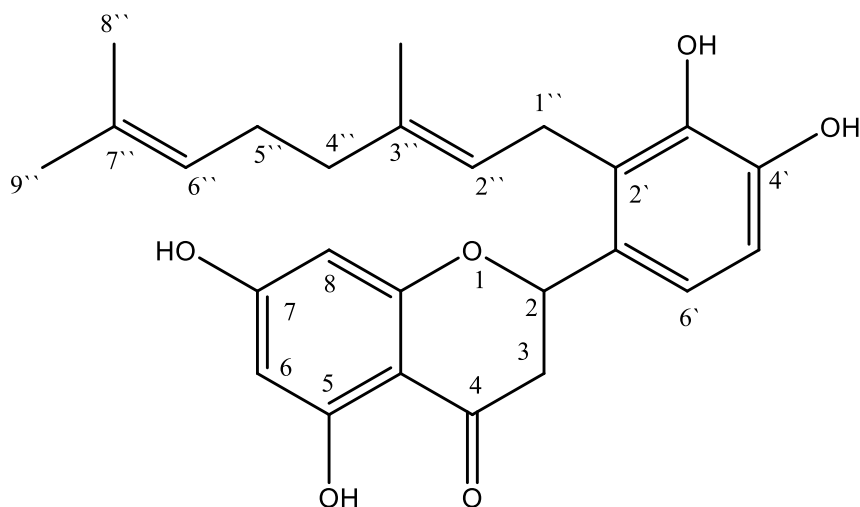


Position	Chemical shift δ ppm ^1H (mult, J Hz)	Chemical shift δ ppm ^{13}C
1	-	-
2	5.40, 1H (d, 12.4)	79.1(CH)
3	3.22ax, 1H (dd) 2.66,eq, 1H (dd, 17.3, 2.9)	42.5(CH ₂)
4	-	
5	-	160.6(C)
6	5.95, 1H (s)	94.6(1H)
7	-	163.0(C)
8	-	107.8(C)
9	-	
10	-	102.0(C)
1'		
2'	7.32, 2H (m)	128.7(CH ₂)
3'	6.79, 2H (dd, 8.5, 1.9)	115.5(CH ₂)
4'	-	157.7(C)
5'	6.79, 2H (dd, 8.5, 1.9)	115.5(CH ₂)
6'	7.32, 2H (m)	128.7(CH ₂)
1''	3.11, 2H (d, 7.3)	121.3(CH ₂)
2''	5.13, 1H (t, 7.8)	123.0(CH)
3''	-	130.1(C)
4''	1.64, 3H (s)	25.6(CH ₃)
5''	1.70, 3H (s)	18.3(CH ₃)
5-OH	12.42, 1H (s)	-



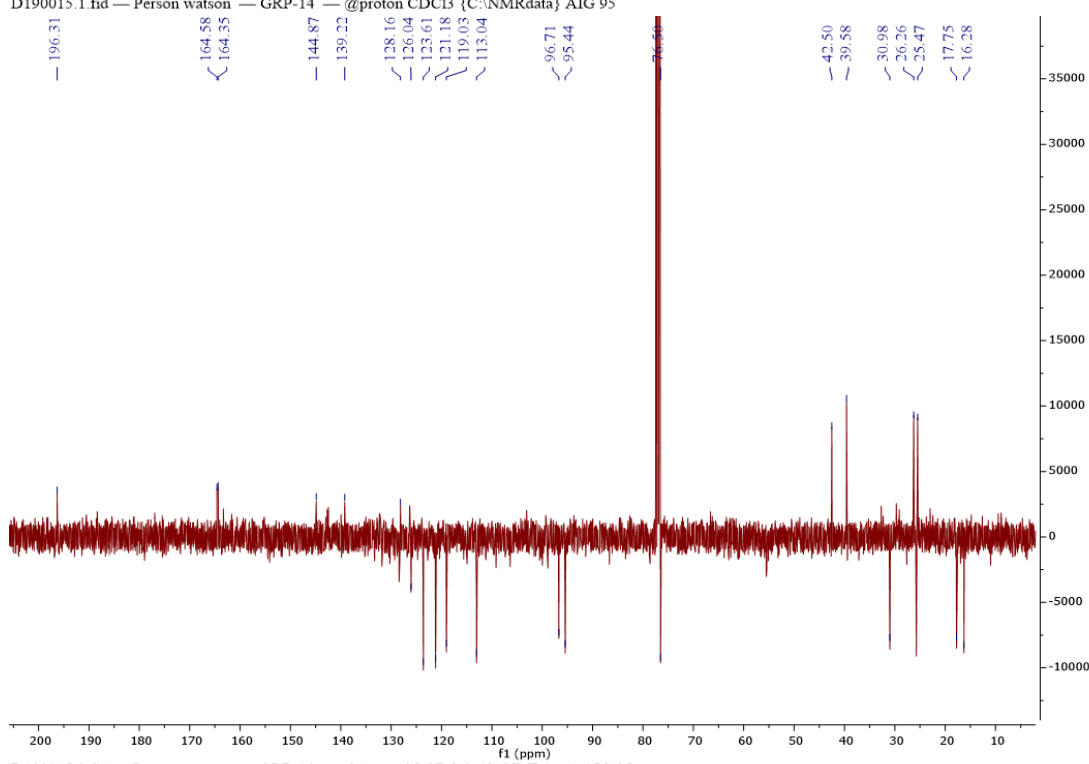
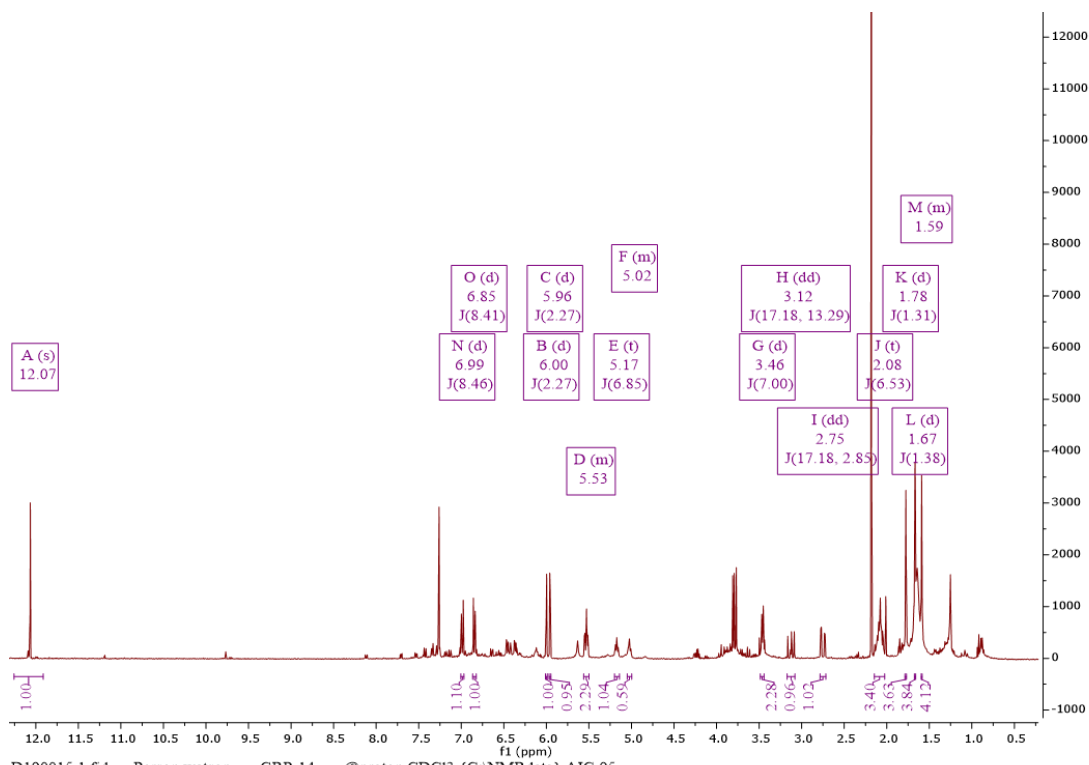
D221740.1.fid — Person ruwida — mGrp11-43 44 — @proton DMSO {C:\NMRdata} AIG 94
 D221740.2.fid — Person ruwida — mGrp11 - 43 44 — @deptq135 DMSO {C:\NMRdata} AIG 90
Appendix- 12: ¹H NMR (400 MHz, DMSO-d₆), and ¹³C (100 MHz, DMSO-d₆) of **8** (8-prenylharingenin).

Table- S13: NMR data for compound **9** (Propolin D).



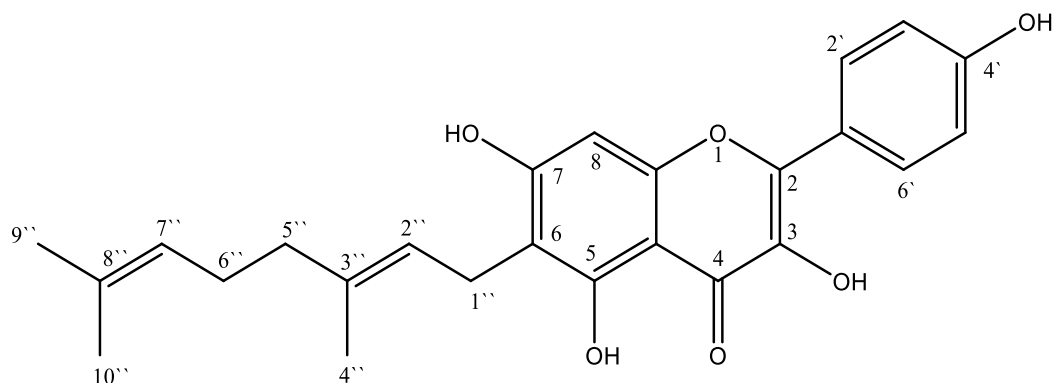
Position	Chemical shifts δ_{H} (mult, <i>J</i> Hz) in CDCl_3	δ_{C}
1	-	-
2	5.55, 1H (m)	76.5(CH)
3	2.77, 1H (dd, 17.2, 2.9) 3.15, 1H (dd, 17.2, 13.3)	42.5(CH ₂)
4	-	196.3(C)
5	-	164.7(C)
6	5.97, 1H (d, 2.3)	96.71(CH)
7	-	163.2(C)
8	6.02, 1H (d, 2.3)	95.4(CH)
9	-	163.3(C)
10	-	103.1(C)
1'	-	128.0(C)
2'	-	126.2(C)
3'	-	142.2(C)
4'	-	145.0(C)
5'	6.87, 1H (d, 8.4)	113.0(CH)
6'	7.01, 1H (d, 8.4)	119.0(CH)
1''	3.46, 2H (t, 7.0)	25.4(CH ₂)
2''	5.19, 1H (t, 6.8)	121.0(CH)
3''	-	139.2(C)
3''-CH₃	1.8, 3H (s)	16.3(CH ₃)
4''	2.1, 2H (m)	39.4(CH ₂)

5''	2.1, 2H (m)	26.2(CH ₂)
6''	5.04 ,1H (m)	123.7(CH)
7''	-	(C)
8''	1.61,3H (s)	17.8(CH ₃)
9''	1.69,3H (s)	25.8(CH ₃)
5-OH	12.09,1H (s)	-

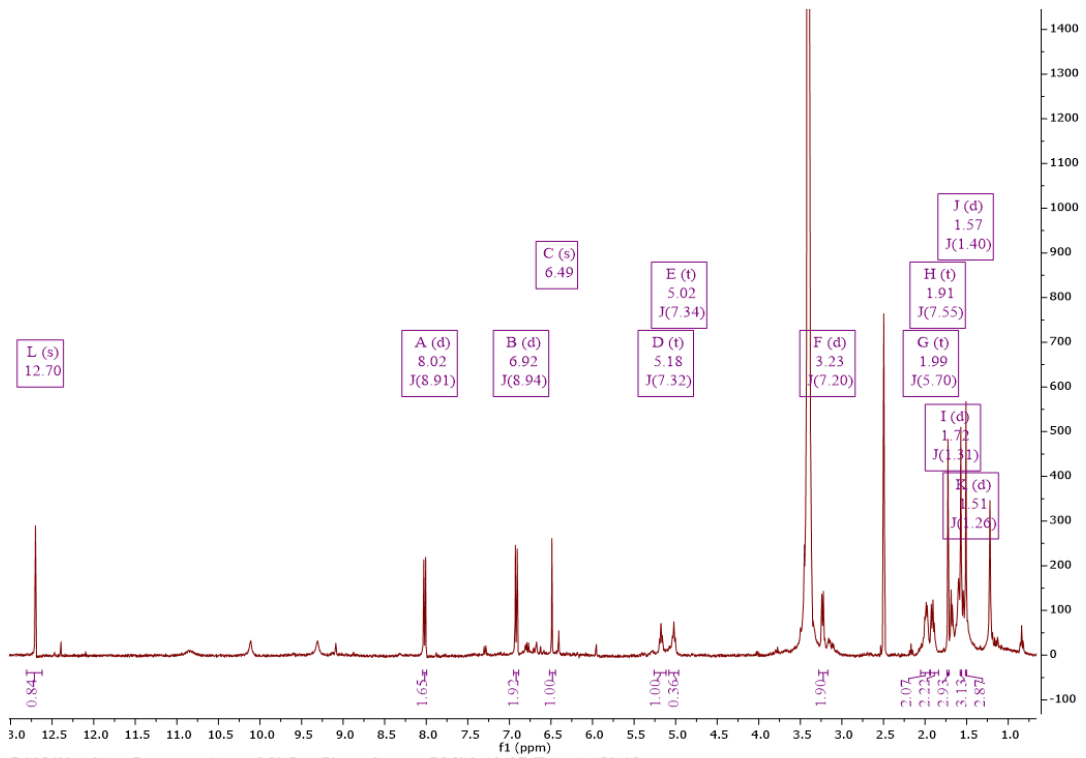


D190015.1.fid — Person watson — GRP-14 — @proton CDCl₃ {C:\NMRdata} AIG 95
 D190015.2.fid — Person watson — GRP-14 — @deptq135 CDCl₃ {C:\NMRdata} AIG 95
Appendix- 13: ¹H NMR (400 MHz, CDCl₃, and ¹³C (100 MHz, CDCl₃) of **9**
 (Propolin D).

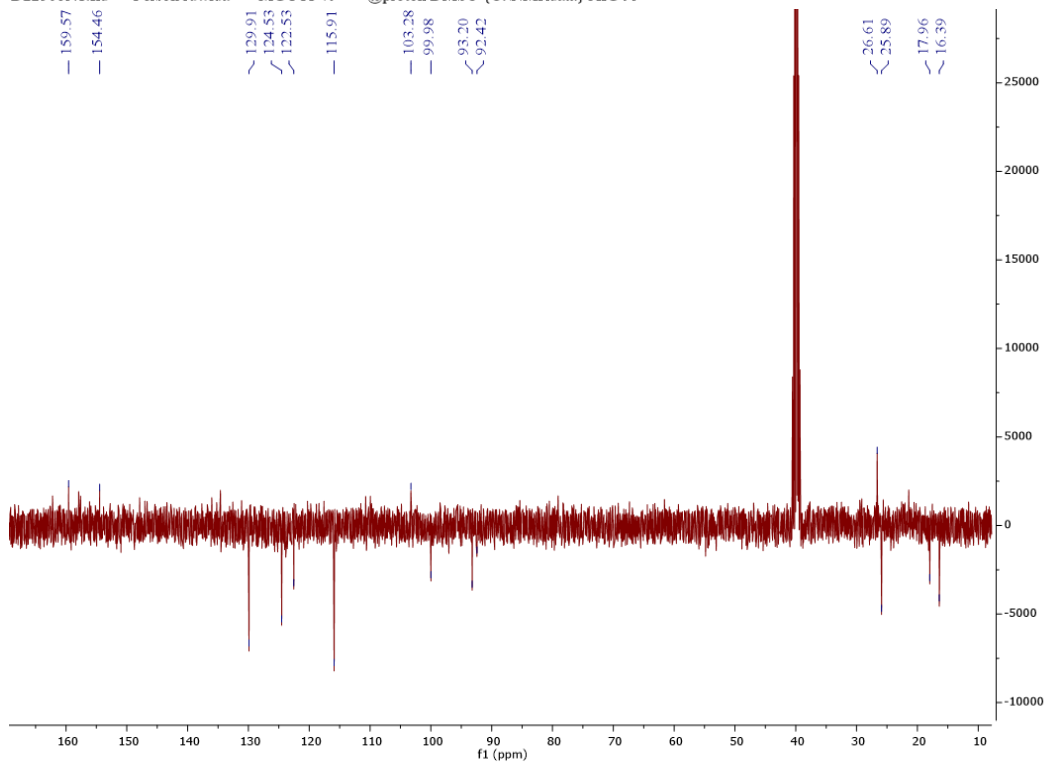
Table- S14: NMR data for compound **10** (Macarangin)



Position	Chemical shifts in DMSO -d ₆ δ_H (mult, J Hz)	δ_C
1	-	-
2	-	147.0(C)
3	-	
4	-	
5	-	157.7(C)
6	-	110.7(C)
7	-	162.1(C)
8	6.5, 1H (s)	93.1(CH)
9	-	154.2(C)
10	-	103.4(C)
1'	-	121.9(C)
2'	8.02 ,2H (d,8.9)	130.0(CH ₂)
3'	6.92, 2H (d,8.9)	115.9(CH ₂)
4'	-	159.4(C)
5'	6.92 ,2H (d,8.9)	115.9(CH ₂)
6'	8.02 ,2H (d,8.9)	129.9(CH ₂)
1''	3.24 ,2H (brd,7.2)	21.2(CH ₂)
2''	5.18,1H (t,7.3)	122.5(CH)
3''	-	134.2(C)
4''	1.74 ,3H (s)	16.3(CH ₃)
5''	1.93 ,2H (m)	39.5(CH ₂)
6''	2.00 ,2H (m)	26.6(CH ₂)
7''	5.03,1H (d,7.4)	124.5(CH)
8''	-	131.0(C)
9''	1.58 ,3H (s)	25.9(CH ₃)
10''	1.53 ,3H (s)	18.1(CH ₃)
5-OH	12.72 ,1H (s)	-



D225683.1.fid — Person ruwida — MG P11-79 — @proton DMSO {C:\NMRdata} AIG 95



D225683.2.fid — Person ruwida — MG P11-79 — @deptq135 DMSO {C:\NMRdata} AIG 95

Appendix- 14: ^1H NMR (400 MHz, DMSO- d_6), and ^{13}C (100 MHz, DMSO- d_6) of **10** (Macarangin).

Table- S15: Top 200 most abundant compounds in samples of red propolis from Rivers State Nigeria identified according to accurate mass by searching against DNP, red cell identified by MSⁿ, green identified by NMR. ARSN=compound absent in RSN sample.

<i>m/z</i>	Rt	Molecular formula	Name	Ratio BRN/RSN
285.077	9.9	C16H14O5	Methylated pterocarpin	0.6
353.104	24.1	C20H18O6	Prenylated flavonoid	0.2
267.067	12.2	C16H12O4	Methyl chrysin isomer	0.9
255.067	11.5	C15H12O4	Pinocembrin	0.7
315.088	7.9	C17H16O6	Dimethyl flavonoid	1.3
283.061	8.0	C16H12O5	Calycosine	0.9
539.172	18.9	C32H28O8	Biflavonoid	1.2
447.255	34.6	C29H36O4	Sesquiterpene stilbene	0.4
271.098	13.3	C16H16O4	Vestitol	0.7
273.077	11.4	C15H14O5	caffeic acid benzene diol ester	1.2
283.061	10.5	C16H12O5	Methyl galangin isomer	1.0
301.072	11.6	C16H14O6	5-Acetyl-3,4-dihydro-6,8-dihydroxy-3-(5-oxo-1,3-pentadienyl)-1H-2-benzopyran-1-one	0.8
423.182	23.7	C25H28O6	Geranylated or diprenylated flavanoid	0.2
423.182	28.6	C25H28O6	Propolin D	0.3
301.072	10.5	C16H14O6	5-Acetyl-3,4-dihydro-6,8-dihydroxy-3-(5-oxo-1,3-pentadienyl)-1H-2-benzopyran-1-one	0.9
339.124	23.9	C20H20O5	6-prenylnaringenin	0.2
331.083	9.5	C17H16O7	Dimethyl quercetin	1.0
271.062	10.0	C15H12O5	14(5->6)-Abeo-9,13-dihydroxy-1,5,7,9,11-furanoeremophilapentaen-14,15-olide	0.8
421.166	35.5	C25H26O6	Macarangin	0.3
407.187	29.6	C25H28O5	Geranylated or diprenylated flavanoid	0.3
331.083	11.2	C17H16O7	Abrunquinone A; (S)-form, 3',6-	0.9

			Bis(demethoxy), 6',8-dihydroxy	
313.072	8.4	C17H14O6	Aflatoxin B1; 1R-Alcohol	1.4
329.067	10.1	C17H14O7	2-Acetyl-1,3,6,8-tetrahydroxyanthraquinone; 1'R-Alcohol, 1'-Me ether	0.9
555.167	13.7	C32H28O9	Anhydrophlegmacin-9,10-quinone A1; Atropisomer, 2'-epimer, 10-deoxo	0.9
255.067	10.6	C15H12O4	14(5->6)-Abeo-9,13-dihydroxy-1,3,5,9- furanoeremophilatetraen-14-al	0.8
239.072	12.9	C15H12O3	14(5->6)-Abeo-9,13-dihydroxy-1,3,5,9- furanoeremophilatetraen-14-al; 13- Deoxy	0.7
379.192	26.4	C24H28O4	Angelicolide	0.2
439.177	20.7	C25H28O7	Abyssinoflavanone V	0.128
369.098	13.3	C20H18O7	1-Acetyl-2,4,5,7-tetrahydroxyanthraquinone; Tetra-Me ether	0.1
315.088	9.3	C17H16O6	8-(2-Acetoxy-3-methyl-1-oxo-2-butenyl)-7- methoxy-2H-1-benzopyran-2-one	1.0
353.104	16.5	C20H18O6	Acanthotoxin	0.2
601.354	49.7	C38H50O6	Polyprenylated benzophenone	14.1
369.098	18.4	C20H18O7	1-Acetyl-2,4,5,7-tetrahydroxyanthraquinone; Tetra-Me ether	0.2
299.056	7.8	C16H12O6	2-Acetyl-8-hydroxynaphtho[2,3-b]furan-4,9- dione; 7-Methoxy, Me ether	1.3
601.354	44.2	C38H50O6	Coccinone A	66.5
543.442	56.9	C35H60O4	3-(3,4-Dihydroxyphenyl)-2-propenoic acid; (E)-form, Hexacosyl ester	ARSN
273.077	6.8	C15H14O5	14(5->6)-Abeo-2,3-epoxy-9,14-dihydroxy- 5,9-furanoeremophiladien-1-one	1.1
239.072	19.8	C15H12O3	14(5->6)-Abeo-9,13-dihydroxy-1,3,5,9- furanoeremophilatetraen-14-al; 13- Deoxy	0.750
515.317	41.2	C34H44O4	Nemorosone; 7-Epimer, 4-Me ether	0.3
448.258	34.6	C24H37N2O6	Heliotropium europaeum Alkaloid	0.4
255.067	15.5	C15H12O4	14(5->6)-Abeo-9,13-dihydroxy-1,3,5,9- furanoeremophilatetraen-14-al	0.8
539.172	17.3	C32H28O8	2-(3,4-Dihydro-10-hydroxy-9-methoxy-1,3- dimethyl-1H-naphtho[2,3-c]pyran-5-	1.1

			yl)-1,8-dihydroxy-6-methyl-9,10-anthraquinone; 7'-Methoxy	
271.062	7.7	C15H12O5	14(5->6)-Abeo-9,13-dihydroxy-1,5,7,9,11-furanoeremophilapentaen-14,15-olide	1.0
355.119	18.6	C20H20O6	Abyssinone A; 1",2"-Dihydro, 2"-hydroxy	0.1
255.067	8.0	C15H12O4	Liquiritigenin	0.7
515.317	38.4	C34H44O4	Denticulatain	0.1
491.245	33.8	C30H36O6	Geranylated prenylated flavanoid	0.3
317.103	13.3	C17H18O6	5-Acetyl-2,3-dihydro-3-hydroxy-2-[1-(hydroxymethyl)ethenyl]benzofuran; (2R*,3R*)-form, Di-Ac	0.8
255.067	9.6	C15H12O4	14(5->6)-Abeo-9,13-dihydroxy-1,3,5,9-furanoeremophilatetraen-14-al	0.7
423.182	32.9	C25H28O6	Geranylated or diprenylated flavanoid	0.4
287.093	9.8	C16H16O5	14(5->6)-Abeo-1,2,6-trihydroxy-1,3,5(10)-furanoeremophilatrien-9-one; 1-Me ether	1.3
331.083	5.8	C17H16O7	Abruquinone A; (S)-form, 3',6-Bis(demethoxy), 6',8-dihydroxy	1.1
573.178	11.7	C32H30O10	3',3'''-Bis(2',4,4',6'-tetrahydroxydihydrochalcone); 4,4''-Di-Me ether	2.4
569.183	14.9	C33H30O9	Sanggenon B	0.9
571.162	13.4	C32H28O10	Candibirin A	1.7
271.061	5.2	C15H12O5	14(5->6)-Abeo-9,13-dihydroxy-1,5,7,9,11-furanoeremophilapentaen-14,15-olide	1.1
317.067	7.7	C16H14O7	4-Acetyl-6,8-dihydroxy-5-methyl-1H-2-benzopyran-1-one; Di-Ac	1.4
271.098	12.2	C16H16O4	14(5->6)-Abeo-9,13-dihydroxy-3,5,9-furanoeremophilatrien-14-al; 4?-form, 9-Me ether	0.8
299.056	6.3	C16H12O6	2-Acetyl-8-hydroxynaphtho[2,3-b]furan-4,9-dione; 7-Methoxy, Me ether	1.4
287.093	11.3	C16H16O5	14(5->6)-Abeo-1,2,6-trihydroxy-1,3,5(10)-furanoeremophilatrien-9-one; 1-Me	1.1

			ether	
569.183	15.6	C33H30O9	Sanggenon B	0.9
303.088	9.8	C16H16O6	Altersolanol A; 1,4-Dideoxy	1.2
299.056	12.1	C16H12O6	2-Acetyl-8-hydroxynaphtho[2,3-b]furan-4,9-dione; 7-Methoxy, Me ether	0.9
541.188	15.6	C32H30O8	4-(6',7-Dihydroxy-4'-methoxyisoflavan-3'-yl)-2',7-dihydroxy-4'-methoxyisoflavan	1.6
301.072	7.7	C16H14O6	5-Acetyl-3,4-dihydro-6,8-dihydroxy-3-(5-oxo-1,3-pentadienyl)-1H-2-benzopyran-1-one	0.7
539.172	15.9	C32H28O8	2-(3,4-Dihydro-10-hydroxy-9-methoxy-1,3-dimethyl-1H-naphtho[2,3-c]pyran-5-yl)-1,8-dihydroxy-6-methyl-9,10-anthraquinone; 7'-Methoxy	1.0
317.067	12.3	C16H14O7	4-Acetyl-6,8-dihydroxy-5-methyl-1H-2-benzopyran-1-one; Di-Ac	1.3
273.150	29.5	C17H22O3	Algoafuran	0.3
283.061	16.1	C16H12O5	Bauhiniastatin 1	0.9
424.185	23.7	C23H27N3O5	Cyclotryprostatin A; 13-Me ether	0.2
424.185	28.6	C23H27N3O5	Cyclotryprostatin A; 13-Me ether	0.3
255.103	17.1	C16H16O3	14(5->6)-Abeo-1,3,5,9-furanoeremophilatetraene-9,13-diol; 9-Me ether	0.6
299.056	10.6	C16H12O6	2-Acetyl-8-hydroxynaphtho[2,3-b]furan-4,9-dione; 7-Methoxy, Me ether	0.9
555.167	16.0	C32H28O9	Anhydrophlegmacin-9,10-quinone A1; Atropisomer, 2'-epimer, 10-deoxo	1.3
285.077	8.5	C16H14O5	2-Acetyl-1,8-naphthalenediol; Di-Ac	0.9
269.082	8.8	C16H14O4	14(5->6)-Abeo-9,13-dihydroxy-1,3,5,9-furanoeremophilatetraen-14-al; 9-Me ether	1.0
437.161	32.7	C25H26O7	Albanin C	0.4
285.077	9.1	C16H14O5	2-Acetyl-1,8-naphthalenediol; Di-Ac	1.1
619.365	39.9	C38H52O7	Garcimultiflorone C	ARSN
401.306	55.9	C26H42O3	12,16-Dihydroxy-20,24-dimethyl-25-nor-24-scalarane; (12?,16?)-form, 12-	5.794

			Ketone	
601.354	43.3	C38H50O6	Cocconone A	75.9
587.157	11.2	C32H28O11	Aurasperone A; 2,3-Dihydro, 2'-hydroxy	3.4
557.184	13.8	C32H30O9	Biscyclobin	1.8
507.239	29.8	C30H36O7	6,7-Dihydroxy-1,14-meliacadiene-3,16-dione; (6',7')-form, Di-Ac	0.1
355.119	12.6	C20H20O6	Abyssinone A; 1'',2''-Dihydro, 2''-hydroxy	0.1
269.082	14.0	C16H14O4	Medicarpin	0.3
571.198	13.6	C33H32O9	4-(6',7-Dihydroxy-4'-methoxyisoflavan-3'-yl)-2',7-dihydroxy-4'-methoxyisoflavan; (3R,4S,3''S)-form, 5'-Methoxy	1.00
587.194	13.5	C33H32O10	Dermocanarin 5	1.4
463.250	31.6	C29H36O5	3,9-Dihydroxy-16-kauren-19-oic acid; (ent-3'')-form, 3-Cinnamoyl	0.2
437.161	31.0	C25H26O7	Albanin C	0.3
283.061	8.7	C16H12O5	Bauhiniastatin 1	1.2
339.124	16.1	C20H20O5	8-prenylnaringenin	0.1
121.030	5.1	C7H6O2	Benzoic acid	1.1
583.162	18.6	C33H28O10	Amentoflavone; 2,2'',3,3''-Tetrahydro, 4',7,7''-tri-Me ether	7.4
287.056	14.9	C15H12O6	2-Acetyl-8-hydroxynaphtho[2,3-b]furan-4,9-dione; 7-Methoxy, 1''-alcohol	1.4
408.190	29.6	C23H27N3O4	Tacraline	0.3
285.077	15.9	C16H14O5	2-Acetyl-1,8-naphthalenediol; Di-Ac	0.9
307.075	13.3	C14H16N2O4S	Bisdethiobis(methylthio)gliotoxin; 3-De(methylthio), 5a,6-didehydro	0.9
373.275	52.4	C24H38O3	Dietrichequinone	6.7
601.354	46.8	C38H50O6	Cocconone A	
483.231	34.7	C18H36N4O11	Antibiotic NK 1012-3	0.6
557.183	13.1	C32H30O9	Biscyclobin	1.8
303.088	7.7	C16H16O6	Altersolanol A; 1,4-Dideoxy	1.4
299.093	17.1	C17H16O5	8-(2-Acetoxy-3-methyl-1,3-butadienyl)-7-methoxy-2H-1-benzopyran-2-one	1.7
459.159	28.6	C25H29ClO6	Antibiotic RP 1551-3; 2'',3''-Dihydro, 3''-hydroxy	0.4
423.182	25.4	C25H28O6	Arugosin A	0.1

463.250	22.5	C29H36O5	3,9-Dihydroxy-16-kauren-19-oic acid; (ent-3?)-form, 3-Cinnamoyl	0.1
147.045	6.4	C9H8O2	5-Benzofuranmethanol	1.0
257.082	11.2	C15H14O4	14(5->6)-Abeo-9,13-dihydroxy-3,5,9-furanoeremophilatrien-14-al	0.5
271.061	9.4	C15H12O5	14(5->6)-Abeo-9,13-dihydroxy-1,5,7,9,11-furanoeremophilapentaen-14,15-olide	0.9
269.082	12.8	C16H14O4	14(5->6)-Abeo-9,13-dihydroxy-1,3,5,9-furanoeremophilatetraen-14-al; 9-Me ether	0.2
553.188	28.4	C33H30O8	1,2-Diphenyl-3,4-bis(2,4,6-trihydroxybenzoyl)cyclobutane; (1?,2?,3?,4?)-form, 2''',2''',6'''-Tri-Me ether	3.1
440.180	20.7	C23H27N3O6	Tunichrome Mm 2	0.1
601.173	12.6	C33H30O11	Dahuribirin C	1.2
541.188	13.3	C32H30O8	4-(6',7-Dihydroxy-4'-methoxyisoflavan-3'-yl)-2',7-dihydroxy-4'-methoxyisoflavan	2.4
669.417	52.7	C43H58O6	Polyprenylated benzophenone	11.0
617.349	47.2	C38H50O7	Alphitexolide	
561.359	38.7	C36H50O5	24-Nor-4(23),22(29)-hopadiene-3,6,7-triol; (3?,6?,7?)-form, 7-(4-Hydroxybenzoyl)	0.04
383.114	24.7	C21H20O7	2-Acetyl-3-(3,4-dimethoxyphenyl)-3-hydroxy-2-methyl-5,6-methylenedioxyindenone	0.2
269.082	11.0	C16H14O4	14(5->6)-Abeo-9,13-dihydroxy-1,3,5,9-furanoeremophilatetraen-14-al; 9-Me ether	0.2
371.259	50.1	C24H36O3	2-Alkyl-5-hydroxy-4H-1-benzopyran-4-ones; 5-Hydroxy-2-pentadecyl-4H-1-benzopyran-4-one	7.9
557.183	12.0	C32H30O9	Biscyclobobin	1.6
407.187	35.4	C17H32N2O7S	Desalicetin	0.8
289.072	6.6	C15H14O6	14(5->6)-Abeo-2,3-epoxy-1,9,13-	1.2

			trihydroxy-5,7,9,11-furanoeremophilatetraen-14-al	
303.051	11.6	C15H12O7	Alphitonin	4.1
492.248	33.8	C28H35N3O5	Paraherquamide A	0.3
717.344	33.9	C46H46N4O4	Nordine	0.9
315.051	9.0	C16H12O7	2-Acetyl-1,3,6,8-tetrahydroxyanthraquinone; 1'R-Alcohol	1.0
301.072	7.1	C16H14O6	5-Acetyl-3,4-dihydro-6,8-dihydroxy-3-(5-oxo-1,3-pentadienyl)-1H-2-benzopyran-1-one	1.2
299.056	8.5	C16H12O6	2-Acetyl-8-hydroxynaphtho[2,3-b]furan-4,9-dione; 7-Methoxy, Me ether	2.2
375.291	56.7	C24H40O3	Amadannulen	4.5
151.040	5.7	C8H8O3	6-Acetyl-3-methyl-2H-pyran-2-one	1.0
317.067	9.3	C16H14O7	4-Acetyl-6,8-dihydroxy-5-methyl-1H-2-benzopyran-1-one; Di-Ac	1.1
301.072	5.7	C16H14O6	5-Acetyl-3,4-dihydro-6,8-dihydroxy-3-(5-oxo-1,3-pentadienyl)-1H-2-benzopyran-1-one	1.2
285.113	20.9	C17H18O4	Riverinol	0.9
309.054	6.8	C15H15ClO5	3-Chloro-8,9-dihydroxy-2-oxo-1(10),3,11(13)-guaiatrien-12,6-olide	1.0
379.192	18.6	C24H28O4	Angelicolide	0.1
553.188	25.0	C33H30O8	1,2-Diphenyl-3,4-bis(2,4,6-trihydroxybenzoyl)cyclobutane; (1?,2?,3?,4?)-form, 2''',2''',6'''-Tri-Me ether	1.7
315.051	6.1	C16H12O7	2-Acetyl-1,3,6,8-tetrahydroxyanthraquinone; 1'R-Alcohol	2.7
355.119	13.3	C20H20O6	Abyssinone A; 1'',2''-Dihydro, 2''?-hydroxy	0.1
585.359	47.6	C38H50O5	Dichapetalin B; 22-Deoxy, 11,12-dihydro	127.7
287.056	8.1	C15H12O6	2-Acetyl-8-hydroxynaphtho[2,3-b]furan-4,9-dione; 7-Methoxy, 1''?-alcohol	0.9
315.088	13.1	C17H16O6	8-(2-Acetoxy-3-methyl-1-oxo-2-butenyl)-7-methoxy-2H-1-benzopyran-2-one	1.6
299.056	5.3	C16H12O6	2-Acetyl-8-hydroxynaphtho[2,3-b]furan-4,9-dione; 7-Methoxy, Me ether	1.7

515.317	40.0	C34H44O4	Nemorosone; 7-Epimer, 4-Me ether	0.2
533.328	30.0	C34H46O5	Milbemycin IV; 7-Deoxy, 2,5,6,7-tetradehydro	0.1
459.159	33.0	C25H29ClO6	Antibiotic RP 1551-3; 2'',3''-Dihydro, 3''?-hydroxy	0.6
297.077	9.9	C17H14O5	2-[Bis(3,4-dihydroxyphenyl)methyl]furan	0.9
287.093	16.4	C16H16O5	14(5->6)-Abeo-1,2,6-trihydroxy-1,3,5(10)-furanoteremophilatrien-9-one; 1-Me ether	1.7
542.191	15.6	C23H34N3O10 P	Talopeptin	1.6
424.185	32.9	C23H27N3O5	Cyclotryprostatin A; 13-Me ether	0.5
572.165	13.4	C22H31N5O11 S	N-?-Alanyl-5-(S-glutathionyl)-3,4-dihydroxyphenylalanine	3.1
303.124	13.7	C17H20O5	Avicenol A	0.8
585.359	50.8	C38H50O5	Dichapetalin B; 22-Deoxy, 11,12-dihydro	59.3
585.178	16.0	C33H30O10	Candibirin E; 5'-Methoxy	1.4
533.328	30.7	C34H46O5	Milbemycin IV; 7-Deoxy, 2,5,6,7-tetradehydro	0.1
579.419	53.1	C41H56O2	Rhodopinol; 3,4-Didehydro, 20-aldehyde, 1-Me ether	ARSN
401.125	18.6	C21H22O8	Aloin; (10?)-form, 1''-Deoxy	0.1
421.166	33.0	C25H26O6	Albanin E	0.5
437.161	22.0	C25H26O7	Albanin C	0.1
307.075	11.8	C14H16N2O4S	Bisdethiobis(methylthio)gliotoxin; 3-De(methylthio), 5a,6-didehydro	0.6
541.177	18.9	C34H26N2O5	Gasabiimine	1.2
539.172	15.1	C32H28O8	2-(3,4-Dihydro-10-hydroxy-9-methoxy-1,3-dimethyl-1H-naphtho[2,3-c]pyran-5-yl)-1,8-dihydroxy-6-methyl-9,10-anthraquinone; 7'-Methoxy	0.7
585.177	17.7	C33H30O10	Candibirin E; 5'-Methoxy	2.8
515.317	43.1	C34H44O4	Nemorosone; 7-Epimer, 4-Me ether	0.0
469.187	32.9	C26H30O8	Ageratoriparin	0.6
391.096	18.6	C20H21ClO6	3-Chloro-8-hydroxy-2-oxo-1(10),3,11(13)-guaiatrien-12,6-olide; (5?,6?,8?)-form, 8-(2,3-Epoxy-2-	0.2

			methylbutanoyl)	
167.035	4.2	C8H8O4	3-Acetyl-4-hydroxy-6-methyl-2H-pyran-2-one	1.5
541.151	11.8	C31H26O9	Fredericamycin M1	1.4
670.420	52.7	C36H57N5O7	Arenamide A	15.0
317.103	12.2	C17H18O6	5-Acetyl-2,3-dihydro-3-hydroxy-2-[1-(hydroxymethyl)ethenyl]benzofuran; (2R*,3R*)-form, Di-Ac	0.6
555.167	10.9	C32H28O9	Anhydrophlegmacin-9,10-quinone A1; Atropisomer, 2'-epimer, 10-deoxo	1.1
383.244	38.9	C21H36O6	Betaenone D	2.2
383.114	18.0	C21H20O7	2-Acetyl-3-(3,4-dimethoxyphenyl)-3-hydroxy-2-methyl-5,6-methylenedioxyindenone	0.1
541.151	15.8	C31H26O9	Fredericamycin M1	2.6
553.151	26.7	C32H26O9	2',7-Dihydroxy-4'-methoxyflavone(3->5')-2',7-dihydroxy-4'-methoxyisoflavan	13.8
447.255	36.5	C29H36O4	3,28-Dihydroxy-24,30-dinor-1(10),3,5,7,20(29)-friedelapentaen-2-one; 28-Carboxylic acid, Me ester	0.000
527.221	33.7	C36H32O4	Juncus acutus Phenanthrene dimer 6	0.5
569.183	13.1	C33H30O9	Sanggenon B	0.6
585.177	14.4	C33H30O10	Candibirin E; 5'-Methoxy	0.9
585.178	12.6	C33H30O10	Candibirin E; 5'-Methoxy	1.1
445.239	39.2	C29H34O4	Artocarpol E	0.5
315.051	10.2	C16H12O7	2-Acetyl-1,3,6,8-tetrahydroxyanthraquinone; 1'R-Alcohol	0.5
603.152	9.7	C32H28O12	Protosappanin D	1.9
637.331	46.8	C39H46N2O6	Curine; (+)-form, O12-Me, N2,N2'-di-Me	ARSN
599.339	48.0	C38H48O6	Biyouxanthone A	ARSN
285.077	10.5	C16H14O5	Methylated pterocarpin	ARSN
465.265	23.3	C29H38O5	Chabrolonaphthoquinone B	1.4
553.151	13.2	C32H26O9	2',7-Dihydroxy-4'-methoxyflavone(3->5')-2',7-dihydroxy-4'-methoxyisoflavan	0.7
273.113	10.7	C16H18O4	2,2',6,6'-Biphenyltetrol; Tetra-Me ether	0.8
601.354	48.0	C38H50O6	Coccinone A	DIV/0
449.261	34.6	C19H38N4O8	Antibiotic SU2	0.4

617.167	10.8	C33H30O12	Cercosporin; 2',2''-Di-Ac	4.1
571.162	14.5	C32H28O10	Candibirin A	4.2
269.046	6.4	C15H10O5	2-Acetyl-8-hydroxynaphtho[2,3-b]furan-4,9-dione; Me ether	1.5
601.355	42.2	C38H50O6	Polyprenylated benzophenone	ARSN
601.173	13.2	C33H30O11	Dahuribirin C	3.2
555.167	20.8	C32H28O9	Anhydrophlegmacin-9,10-quinone A1; Atropisomer, 2'-epimer, 10-deoxo	DIV/0
572.202	13.6	C26H31N5O10	Roseoflavin; Tetra-Ac	1.0
599.193	25.5	C34H32O10	Bilinderone	1.7